Characterisation of the conserved and essential *wblE* gene in *Streptomyces venezuelae*

Lucas Nicholas Balis

Student No. 100082608

A thesis submitted in fulfilment of the requirements for the degree of Doctor of Philosophy at the University of East Anglia

February 2024

Abstract

The Wbl (WhiB-like) family of proteins is phyletically confined to the Actinobacteria where they primarily act as transcription factors. WblE is an ancient protein and its homologue WhiB1 is essential in *Mycobacterium tuberculosis*, but its function is unknown and before this work it had not been comprehensively studied in *Streptomyces* species. Using CRISPR-Cas9, this work confirms that WblE is an essential [4Fe-4S] protein that functions as a global transcription factor: Distinct from its relatives, ChIP-seq shows that WblE predominantly binds promoters of '*bld*' developmental genes; a characteristic that also pervaded Co-immunoprecipitation-MS (CoIP-MS) experiments. Importantly, WblE bound to the promoter of *dnaA*, the chromosomal replication initiator throughout development, which was confirmed *in vitro* by SPR; the response regulator MtrA, which also binds to the *dnaA* promoter, binds to the *wblE* promoter in a sequence-specific manner. This work posits that WblE is a major transcriptional activator of *dnaA*, which drives constitutive replication events in tight coordination with metabolism and the onset of development via other cell-cycle and developmental regulators, in addition to nitric oxide. Moreover, this alone could account for the essentiality demonstrated for *wblE* and its [4Fe-4S] cluster. CoIP-MS in tandem with bacterial two hybrid analysis shows that WblE mediates at least part of its function via a direct interaction with region 4.2 of σ^{HrdB}, akin to other WhiB-like proteins. However, a range of proteins with roles beyond transcription were consistently enriched and allude to a much broader functionality for the protein; this approach revealed at least one novel partner for WblE in *S. venezuelae* strain NRRL B-65442, that is conserved in the genus. These functions are discussed in the context of •NO signalling, WhiB-like cluster biochemistry and how this may link developmental signalling pathways that define *Streptomyces* spp. differentiation and the decision to initiate secondary metabolism.

(1) Recent publications have proposed the replacement of the current phyletic nomenclature 'Actinobacteria' with 'Actinomycetota' (Goodfellow, 2021). However, The Greek origin of '*myces*' (from '*mýkes*') distinctly refers to a branching growth pattern and does not befit a taxonomic title for this diverse bacterial phylum; moreover, this further obfuscates the distinction between the Phylum-level classification, the Actinomycetia class and the Actinomycetales order; *Actinobacteriota* would be more fitting. Thus, this doctoral thesis refers to the phylum with its original nomenclature.

Dedication

It's my honour to be able to dedicate this work to my grandparents Nancy and Brian Wood, and my mother Maxine Balis, who have guided my endless curiosity throughout my childhood and fostered my wild imagination into my adulthood. Years of fun, long conversations, hard conversations, laughs and adventures that I will forever hold close.

"I thank my God upon every remembrance of you"
Philippians 1:3 KJV

Acknowledgements

I would like to extend my eternal gratitude to my two supervisors, Professor Matt Hutchings and Professor Nick Le Brun. Their enthusiasm for my project, my findings and my success only compounded my love for the field and the strange bacteria which we study. The freedom I was given to explore my project combined with steady guidance and support is something for which I will be eternally grateful.

A special thanks to the members of the Le Brun and Hutchings labs, past and present: I have never felt more welcome and at ease; what a wonderful environment to develop my expertise. In particular to Doctors Rebecca Devine, Neil Holmes, and Jake Newitt. Everyday was a little brighter thanks to your kind words, guidance, support and entertaining my wild scientific theories. Sorry for always appearing over your shoulders to stare at your cool results.

My thanks extends to all the staff at the John Innes Centre and University of East Anglia. Notably, this includes Dr Gerhard Saalbach and Dr Carlo de Oliveira Martins from the proteomics department, Kim Findlay from the bioimaging department, Dr Clare Stevenson and Dr Julia Mundy from the biophysical department, and finally Dr Govind Chandra for his bioinformatics support.

Finally, to an eternal friend, Joshua Lewis - no matter how different the paths we end up taking are, nothing has really changed since we were children. Much of my wild imagination and ideas stem from my time with you.

Presentations given on the research documented in this thesis

(Poster) The annual Iron-Sulphur Meeting at Kings College London 2019

Publications arising during this doctoral work

Feeney M.A., Newitt J.T., Addington E., Algora-Gallardo L., Allan C., Balis L., Birke A.S., Castaño-Espriu L., Charkoudian L.K., Devine R., Gayrard D., Hamilton J., Hennrich O., Hoskisson P.A., Keith-Baker M., Klein J.G., Kruasuwan W., Mark D.R., Mast Y., McHugh R.E., McLean T.C., Mohit E., Munnoch J.T., Murray J., Noble K., Otani H., Parra J., Pereira C.F., Perry L., Pintor-Escobar L., Pritchard L., Prudence S.M.M., Russell A.H., Schniete J.K., Seipke R.F., Sélem-Mojica N., Undabarrena A., Vind K., van Wezel G.P., Wilkinson B., Worsley S.F., Duncan K.R., Fernández-Martínez L.T., Hutchings M.I., (2022). ActinoBase: tools and protocols for researchers working on Streptomyces and other filamentous actinobacteria. *Microbial Genomics*. Vol.8(7) : mgen000824 https://doi.org/10.1099%2Fmgen.0.000824

Contents

Chapter 1.

Introduction

1.1. The Actinobacteria

The Actinobacteria represent one of the dominant phyla in the bacterial domain and its members are notably ubiquitous throughout terrestrial and aquatic ecosystems. The exact point of their emergence from other bacterial phyla is ambiguous but they are demonstrably ancient (at least 2.3 billion years; Battistuzzi *et al*., 2004). Members almost universally conserve a Gram-positive cell wall and a higher genomic GC-content (51% to 75%), but also possess distinct 16S & 23S rDNA insertions which taxonomically differentiate them from other bacteria (Ventura et al., 2007). Many Actinobacteria demonstrate complex and highly specialised metabolic capabilities with a propensity to populate the microbiomes of higher eukaryotes as both the protagonists (such as the probiotic *Bifidobacterium* spp. or plant-symbiotic *Frankia spp.*) and antagonists (including the refractory human pathogens *Mycobacterium tuberculosis* & *M. leprae*); features that have cemented them as a focus of global research. An intriguing characteristic of the Actinobacteria is their innate pleomorphism, whereby distantly related taxa, across the phylum, exhibit complex developmental programs, uncharacteristic of most other bacteria. The most basic example of this being the branching, 'Y'-like rods of *Bifidobacterium* spp. (Husain et al., 1972), whereas the most extravagant example would be the multicellular growth exhibited by *Streptomyces* spp.

1.2. The *Streptomyces* genus

Streptomyces are thought to have emerged around 450 million years ago to fill a nutrient rich niche in the soil of terrestrial and aquatic environments, metabolising the complex carbohydrates accumulating from dead fungal and plant cell-walls. Most species are highly specialised metabolisers of (amino-)glycans, such as chitin or cellulose, allowing them to tap into some of the most abundant but largely inaccessible carbohydrates on the planet (Chater *et al*., 2010). Members of the genus conserve the Gram-positive cell wall and GC-rich (72.5%) genome that are typical of Actinobacteria but possess uncharacteristically large (7 – 12 Mbp) and linear chromosomes; a rare characteristic in the bacterial domain (Kirby, 2011). *Streptomyces* spp. are prolific producers of anti-neoplastic, and anti-microbial natural products, many of which are clinically applied and from which we source at least 60% of our current antibiotics; thus, highlighting their urgent medical importance.

1.2.1. Under Lock and Key: *Streptomyces* spp. Secondary Metabolism

The natural products of *Streptomyces* spp. and other microbes are commonly referred to as secondary or specialised metabolites and are encoded by groups of genes, clustered together on the genome, known as biosynthetic gene clusters (BGCs). These BGCs encode the core biosynthetic and tailoring enzymes required to make the molecules and also often encode transporters, immunity proteins and cluster-situated transcriptional regulators that control the expression of the BGC and compound export. As opposed to the cluster-situated regulators, global regulators (encoded *ex situ*) often integrate diverse environmental and metabolic signals with BGC expression and can play pivotal roles in ensuring appropriate expression. Whole genome sequencing from the early 2000s onwards revealed that these bacteria encode many more specialised metabolite clusters than are expressed under standard laboratory conditions, leading to the hypothesis that many BGCs are silent or cryptic (Bentley *et al*., 2002; Hoskisson & Seipke, 2020). Indeed, a recent genomic survey found that only 3% of BGCs have been matched to molecules, suggesting there are many new molecules and biosynthetic pathways waiting to be discovered (Gavriilidou *et al*., 2022). These BGCs can be identified in whole genomes using tools such as antiSMASH which searches for gene clusters based on homology to known classes; however, truly novel BGCs are hard to find (Blin et al., 2023). A major challenge also lies in activating the biosynthesis of molecules encoded by cryptic BGCs and there is no reliable method that can be applied to every BGC. Various techniques have been developed including cloning and heterologous expression, refactoring BGC elements (deleting repressors or overexpressing activators), manipulating global regulators and metabolism, adding chemical elicitors, or disrupting BGCs of known molecules to prevent rediscovery and, in some cases, activate the production of different antimicrobials (Olano et al., 2008; Sharma *et al*., 2021).

1.2.2. An Emerging Model Organism: *Streptomyces venezuelae*

The majority of our knowledge of *Streptomyces* biology originates from work on the model organisms *Streptomyces coelicolor* A3(2) and *Streptomyces griseus* NBRC 13350. However, in the last decade, *S. venezuelae*, has become favoured among laboratories studying *Streptomyces* development worldwide; the first isolate of *Streptomyces venezuelae*, originally named Burkholder no. A65, was collected from a mulched field near Caracas, Venezuela (Ehrlich et al., 1947). The strain was proposed to typify a new species, named *Streptomyces venezuelae* in relation to the location from which it was originally collected. Strain no. A65 was ultimately deposited in the American Type Culture Collection as the type-strain for this species (ATCC 10712; Ehrlich et al., 1948); it presents a morphologically ‘typical’ streptomycete with characteristic melanin production, which sporulates rapidly on solid media (3 days) with distinct,

loosely coiled aerial hyphae, in contrast to the tight coils of *S. coelicolor*. Although not a unique characteristic, *S. venezuelae* is also able to undergo a complete lifecycle in liquid culture, all within just 24 hours of growth (Glazebrook *et al*., 1990). Its genetic and metabolic flexibility make it tractable to a range of high throughput and microfluidic experimental methods that have proven invaluable in developmental studies (McCormick & Flärdh, 2012; Chater, 2016; Schlimpert *et al*., 2016; Schlimpert *et al*., 2017; Bush *et al*., 2022).

The work in this thesis uses the *Streptomyces venezuelae* strain NRRL B-65442 (John Innes Centre; Norwich, UK). Until recently, the ancestry of the NRRL B-65442 strain was not entirely certain but recent evidence has cemented NRRL B-65442 as a direct and close descendant of the ATCC 10712 (Caracas) strain, with 99.999% sequence identity across their 8.2 Mbp genomes and recently identified 158 Kbp plasmid (Gomez-Escribano *et al*., 2021). Interestingly, however, a point mutation in the FAD-dependant oxygenase involved in synthesis of the spore pigment (vnz_33525; *whiE-orfVIII*), grants this strain a charming, jade-green appearance, in contrast to its tan-grey pigmented ancestor ATCC 10712 (Gomez-Escribano *et al*., 2021). Orthologous *whiE* loci in different species are known to produce similar effects on the spore-pigment (Kelemen *et al*., 1998; Yu & Hopwood, 1995, Blanco *et al*., 1993). Remarkably, severely colour-blind members of the lab cannot easily distinguish the two *S. venezuelae* pigments, suggesting an innocent route of selection for the green pigment, *in vitro* (Personal Communications: Dr Neil Holmes, Dr Jake Newitt).

Streptomyces venezuelae was the first described species to manufacture the antimicrobial compound chloramphenicol (Ehrlich *et al*., 1947; Ehrlich *et al*., 1948; Smadel, 1949), which is now a staple of topical antimicrobial therapies and commonly used in eye drops to treat conjunctivitis (Sorsby *et al*., 1953). Nevertheless, the species boasts an additional 32 secondary metabolite BGCs, the majority of which remain cryptic and represent untapped metabolic potential; these are summarised in Table 1.1.

Table 1.1. The 33 anticipated *S. venezuelae* natural product BGCs identified after manual curation of an AntiSMASH v7.0 analysis of the NRRL B-65442 chromosome sequence, with strong reference to the similar table by Gomez-Escribano *et al*., (2021). The previously identified NRRL B-65442 BGCs, and their characterised products are highlighted in green; while not derived from NRRL B-65442, the products of BGC 6 ((+)-isodauc-8-en-11-ol – Rabe *et al*., 2015) and BGC 29 (Foroxymithine – Kodani *et al*., 2015) were determined from experiments with the ATCC 10712 strain and are highlighted in yellow.

BGC	BGC Type	start	end	BGC Product
1	Ectoine	237,110	247,526	Ectoine
2	Terpene	273,798	294,749	Geosmin
3	Type 1 & Type 3 PKS	519,875	549,437	Venemycin*
4	NRPS-like	554,017	582,919	Watasemycin*
5	Ripp (lanthipeptide)	613,767	629,532	-
6	Terpene	633,034	634,179	(+)-isodauc-8-en-11-ol
7	Ripp (lanthipeptide)	716,117	728,969	Venezuelin*
8	Indole	871,837	882,258	Arcyriaflavin*
9	NRPS-like	1,038,563	1,060,601	Chloramphenicol*
10	tRNA-dependent cyclodipeptide synthase	2,070,178	2,090,903	-
11	Siderophore	2,798,699	2,809,633	Desferrioxamine B
12	Ripp (lasso peptide)	3,410,820	3,433,179	Albusnodin
13	NRPS-like	4,408,114	4,450,353	-
14	Other	4,520,077	4,530,222	Gaburedins*
15	Melanin	5,001,915	5,010,131	-
16	Other	5,475,407	5,516,513	-
17	Ripp (thiopeptide)	5,525,842	5,558,923	-
18	Type 3 PKS	5,784,219	5,822,500	Flaviolin
19	Siderophore	5,872,827	5,885,289	-
20	Siderophore	5,938,343	5,952,704	-
21	Type 2 PKS	6,473,487	6,545,282	Jadomycin*
22	NRPS-like	6,673,724	6,714,283	-
23	NRPS-PKS	6,719,994	6,853,949	-
24	Terpene	7,020,609	7,045,713	Hopene
25	Ripp (Lanthipeptide)	7,061,572	7,084,199	SapB
26	Ripp (Bacteriocin)	7,127,295	7,138,149	Linocin M18
27	Type 2 PKS	7,403,744	7,476,256	Spore pigment
28	Melanin	7,482,101	7,492,490	Melanin
29	NRP Siderophore	7,704,299	7,757,163	Foroxymithine
30	Terpene	7,785,725	7,805,848	2-methylisoborneol
31	Type 3 PKS	7,943,145	7,984,236	Alkylresorcinol
32	Terpene	8,196,208	8,197,119	-
33	NRPS	8,208,224	8,212,381	-

1.3. *Streptomyces* Development

Streptomyces spp. are a marvel of prokaryotic development. Akin to fungi, and once mistaken as such, *Streptomyces* bacteria germinate from spores and grow as a saprophytic, vegetative mycelium which differentiates upon nutrient depletion or competition, ultimately undergoing a complex process of programmed cell death (PCD) and multicellular differentiation into chains of resilient spores (Figure 1.1). The organism presents a stark example of convergent evolution across domains, and teases with the possibility of novel biology, and new perspectives on traits originally considered purely eukaryotic. The factors responsible for controlling *Streptomyces* development form a complex cascade; the roles for developmentally important genes and their products are described in the following sections of this thesis.

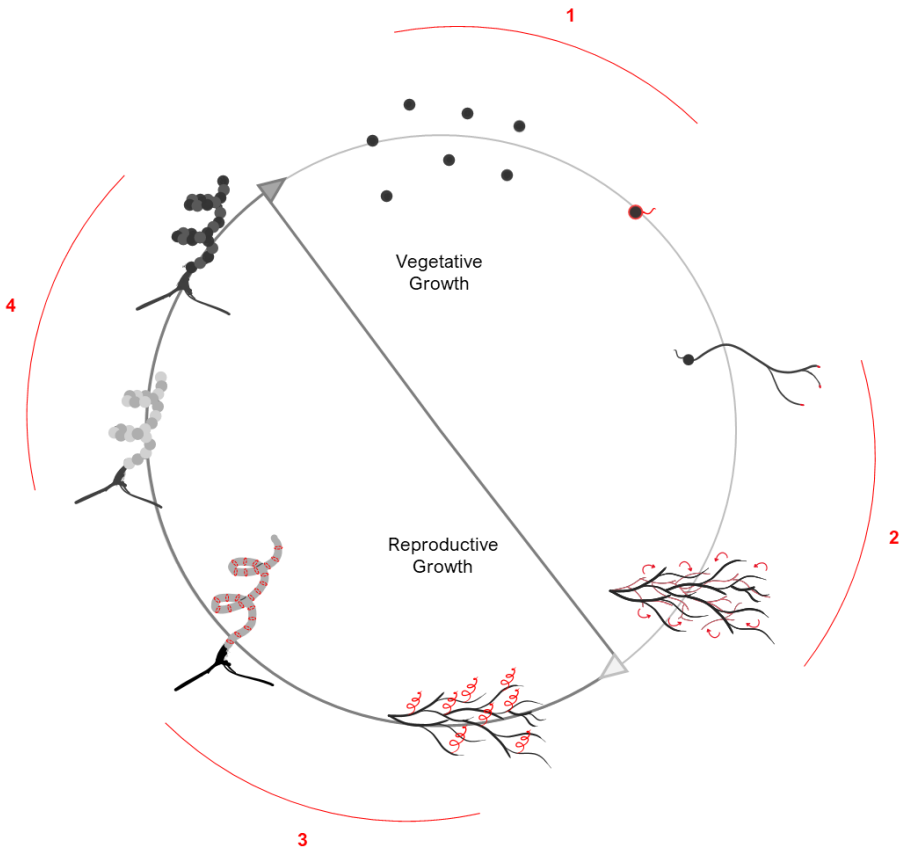

Figure 1.1. The key transitions in the developmental cycle of *Streptomyces* spp. (1) Germination; (2) exponential mycelial growth via tip extension preceding rounds of programmed cell death; (3) Aerial growth and placement of reproductive septa; (4) cell division and spore maturation. Red illustrations highlight certain key developmental transitions during these steps.

1.3.1. Germination

Streptomyces spores are small, hydrophobic and robust, withstanding heat, drought, radiation, and oxidative stress. An extensive trehalose matrix immobilises and stabilises pre-synthesised macromolecules necessary for a metabolic restart; the signals controlling this process only require water to initiate and are less-well understood. Nevertheless, spore germination comprises a succession of distinct steps: Spore-wall remodelling, swelling, and germ-tube emergence (Hardisson et al. 1978; Bobek *et al*., 2017).

Spore-wall remodelling is typified by a darkening of the cell-wall, resulting from ion exchange (Ca^{2+}, Mg^{2+}, Mn^{2+}, Zn^{2+} and Fe^{2+}) and an influx of water, as the hydrophobic coat is lost (Hardisson *et al*., 1978; Bobek *et al*., 2017). Subsequent cell-wall remodelling relies, at least in part, upon cAMP and the cAMP-receptor protein (Crp), which directly controls expression of *rpfA* and promotes germination. The lysozyme-like RpfA belongs to a class of resuscitation-promoting factors (Rpf) which mediate cell-wall remodelling by hydrolyzing the β-(1,4)-glycosidic bond between GlcNAc and MurNAc in the peptidoglycan (Telkov *et al*., 2006; Haiser *et al*., 2009). Congruent with this, Δ*cya* (adenylate cyclase) and Δ*crp* mutants maintain thick cell-walls and are defective in germination (Piette *et al*., 2005).

As the spore-wall undergoes accelerated remodelling, a dramatic drop in trehalose concentration accompanies a visually discernible swelling of the spore from osmotic water intake. During this period, the protective role of trehalose is inherited by protein chaperones that help proteins reobtain and maintain their functional conformations (Bobek *et al*., 2004). Arrays of chaperones: GroEL, Trigger factor, DnaK GrpE and CnoX (aka TrxA4) assist in the reactivation of the proteosynthetic apparatus (Bobek et al., 2004; Strakova et al., 2013a). Chaperones are constitutively present throughout the course of germination, indicating a vital role for their functions (Strakova et al., 2013a). Once the ribosomes have regained functionality, new proteins are translated from the immobilised mRNA stock (Strakova et al., 2013b) and chromosomal replication is engaged as germ-tubes emerge, designating the end of germination (Ruban-Osmialowska *et al*., 2006; Wolanski *et al*., 2011; Bobek *et al*., 2017).

1.3.2. Apical Growth and the Vegetative Mycelium

Typically, one or two germ tubes emerge from the germinating spore, and extend as a comprehensive, branching network across the substrate, secreting arrays of chitinolytic and cellulolytic enzymes, to aid nutrient acquisition, with motility derived from apical growth. In most morphologically primitive rod-shaped bacteria, such as *Bacillus* or *Escherichia* spp., new peptidoglycan is synthesised and incorporated into the lateral cell-walls. In *Streptomyces* spp., however, a multiprotein complex called the polarisome, targets cell-wall synthesis to the cell-

poles, mediating apical tip extension - a process shared by the actinomycetes, *Mycobacterium* and *Corynebacterium* spp. (Hammond *et al*., 2019; Joyce *et al*. 2012; Letek *et al*. 2008).

In *Streptomyces* spp., DivIVA (vnz_08495) is the principal component of the polarisome and it is essential for cell viability (Flärdh, 2003). The DivIVA protein acts as a hub for biosynthetic proteins which are necessary for cell-wall synthesis and development, but the protein also drives localisation of the unique Scy *(Streptomyces* cytoskeletal) protein which forms a scaffold for the recruitment of structural components of the cell, such as the intermediate filament-like protein, FilP (vnz_24950; Fuchino *et al*., 2013). Chromosomal replication is uniquely constitutive within hyphae, with segregation of daughter chromosomes coupled to tip extension by interactions between Scy and ParA, the chromosome-partitioning protein that organizes nucleoprotein complexes in conjunction with ParB bound to *parS* sites on the chromosome (Ditkowski *et al*. 2013; Donczew et al. 2016).

The vegetative mycelium invariably proceeds through two distinct and mutually exclusive cell-types, which are defined by their septal patterns. The initial vegetative mycelia (MI) which emerge from spores exhibit regular compartmentalisation by thin, non-divisive cross-walls thought to permit cell-to-cell communication. Alternating compartments of the MI mycelium undergo an initial round of PCD with surviving MI undergoing a transition to stage 2 (MII) hyphae, that rarely form cross-walls but are uniquely multinucleate and primed for reproductive differentiation (Yagüe *et al*., 2013). Very little is known about what controls these stages of development or the transition between them, although, disruption of antioxidant defences in *S. natalensis* caused development to stall at the MI stage (Beites *et al*., 2015).

The non-divisive cross-walls of the MI and MII hyphae are dependent on FtsZ; the tubulin homologue that typically mediates bacterial cell-division (McCormick *et al*., 1994; Santos-Beneit *et al*., 2014); the formation of these specialised septa is positively controlled by the *Streptomyces*-specific SsgA-like proteins (SALPs). SsgA localises at septation sites followed by the sequential recruitment of SsgB and FtsZ (Willemse *et al*., 2011) The SALPs are not the only novel proteins involved in the formation of septa, many others are recruited via diverse interactions. In particular, SepX appears to function during vegetative cross-wall formation by stabilising FtsZ (Bush *et al*., 2022; Cantlay *et al*., 2021).

In contrast to all studied bacteria, the *ftsZ* gene is dispensable for survival in *Streptomyces* spp. and is only required for reproductive differentiation and development (see following sections). This redundancy is further illustrated by the fact that other canonical cell division genes, such as *ftsI* and *ftsW*, are expendable for vegetative growth (McCormick *et al*., 1994; Santos-Beneit *et al*., 2014). Instead, it has been proposed that a novel re-sealing mechanism occurring at branch-sites in amorphogenic Δ*ftsZ* mutants, may partially complement the loss of *ftsZ*.

Overexpression of *divIVA* yields a striking hyper-branching phenotype, suggesting that the protein plays a determining role in branch-point selection, but the signals and mechanisms that precisely coordinate branching are only vaguely described (Hempel *et al*., 2008; Hempel *et al*., 2012; Santos-Beneit *et al*., 2014).

1.3.3. The Decision to Differentiate: The *bld* cascade

In 1967, Professor David Hopwood pioneered the research into *Streptomyces* development and genetics (Hopwood, 1967) whereby *Streptomyces coelicolor* mutants were generated via UV or chemical (*N*-methyl-*N'*-nitro-*N*-nitrosoguanidine) mutagenesis. A mutation denoted S48 conferred an inability to initiate differentiation or synthesise the pigmented antibiotics, actinorhodin and undecylprodigiosin (Hopwood, 1967). Further studies revealed a heterogeneous group of development genes, termed "bald" due to the soft and smooth appearance of the non-sporulating mutant colonies (Merrick, 1976). It is now known that bald (*bld*) genes and their products comprise a complex network that is intimately connected to metabolism by a range of small molecules and that this network coordinates the decision to initiate reproductive differentiation and secondary metabolism in MII hyphae.

The nucleotide second messenger cyclic (c-)di-GMP is ubiquitous amongst bacteria, where it coordinates diverse aspects of bacterial growth and behaviour, including motility, virulence, biofilm formation and cell cycle progression (Jenal *et al*., 2017). However, in *Streptomyces* spp. c-di-GMP is one of the major signals controlling the onset of multicellular differentiation and is by far the best-studied (Hull *et al*. 2012; Tschowri *et al*. 2014). The signal carried by c-di-GMP primarily effects morphogenesis via the master developmental repressor, BldD, which dimerises around a c-di-GMP tetramer, effecting repression of approximately 170 genes, with many known to function in or throughout reproductive growth and sporulation (Elliot *et al*. 2001; den Hengst *et al*. 2010; Tschowri *et al*. 2014; Schumacher *et al*., 2017). Hence, reproductive development is dependent on a sudden drop in the intracellular levels of c-di-GMP and collapse of the BldD-dimer. A unique but pivotal target of BldD is *bldA*, encoding the tRNA necessary for translation of the rare 'TTA' leucine codon (Leskiw *et al*., 1991), thus translationally gating the expression of UUA-containing transcripts until the onset of development.

Among the genes known to rely upon the TTA codon, *bldA* seems to exert the majority of its morphogenic influence via AdpA (aka BldH), a major global transcriptional activator of early developmental genes that amplifies this signal via a positive feedback loop with *bldA* (Higo *et al*., 2011). The null mutant phenotypes for *bldA* and *adpA* are similarly bald with impotent secondary metabolism, phenotypes which can be largely overcome by silently mutating the TTA codon in AdpA, to TTG (Takano *et al*., 2003). AdpA is an important activator of the developmental

regulator *ramR* (see section 1.3.4) but has also emerged as an important activator of proteases, including the conserved ClpXP system (essential in *Streptomyces* and *Mycobacterium* spp.), SgmA (extracellular M4 metallopeptidase), and the extracellular *Streptomyces* trypsin inhibitor (Sti); all of which have eminent, early developmental functions (Kato *et al*., 2002; Kim *et al*., 2008; Wolański *et al*., 2011). The oligopeptide importer BldK is believed to transduce an obscure, covalently modified peptide fragment (Bld261 or BldJ) potentially yielded from cleaved signal peptides of secreted proteins, as part of this pathway (Nodwell *et al*., 1996; Nodwell & Losick, 1998). Therefore, a significant portion of AdpA function may be the initiation of this proteolytic cascade. Nevertheless, AdpA coordinates this process with the repression of DNA replication, by competing with the replication initiator DnaA for binding to *oriC* (Wolański *et al*., 2012).

The universal and essential metabolite *S*-adenosylmethionine (SAM) is an important activator of AdpA translation (via *bldA*), secondary metabolism, and oligopeptide transporters, which include but are seemingly not limited to, BldK; indicating a significant role for SAM in this cascade, the details of which remain elusive (Okamoto *et al*., 2003; Huh *et al*., 2004; Park *et al*., 2005; Xu *et al*., 2008).

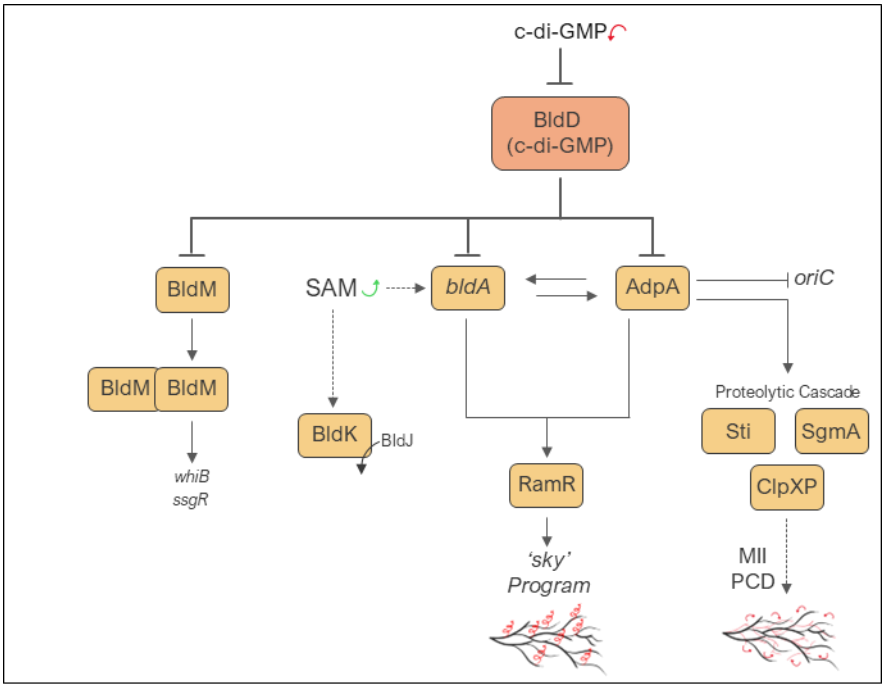

Figure 1.2. *Streptomyces* spp. 'bald' (*bld*) regulatory network, as described in Section 1.3.3, leading up to the initiation of MII mycelium programmed cell death (PCD) and the initiation of the the *sky* program (see Section 1.3.4). BldD-(c-di-GMP) acts as a global repressor of reproductive genes during vegetative growth, activating the cascade upon local drops in c-di-GMP concentrations. SAM concentrations affect expression of certain developmental genes. Arrows indicate activation, bars indicate repression; solid lines indicate direct effects, dotted lines indicate indirect or poorly described effects.

A curious feature of mutants in this cascade is their ability to be complemented by mere proximity to a wild-type strain (Willey *et al*., 1993). Complementation via related developmental mutants can also occur but this phenomenon exhibits a clear hierarchy, indicating that distinct extracellular cues are presented during development, and these are important checkpoints for developmental progression (Figure 1.3). Other proteins seemingly contribute to this cascade and are still necessary for early development, but the reason for their position in the cascade hierarchy is less-well defined, particularly as their functions are less-well understood and may involve indirect effects. This includes the BldG protein, an anti-sigma factor antagonist (ASA) similar to RsbV and SpoIIAA of *Bacillus subtilis* that dephosphorylate RsbW-like (SpoIIE) anti-sigma factors in order to activate alternative sigma factors. Phosphorylation-deficient BldG (Ser 57 to Ala) exhibits a similar phenotype to the null Δ*bldG* mutant, demonstrating the key role of phosphorylation in BldG function, at least in *S. coelicolor* (Bignell *et al*., 2000; Bignell *et al*., 2003). Uniquely, BldG seems to participate in a complex phosphorylation network that includes multiple RsbW/SpoIIE-like anti-sigma factor, pleiotropically influencing multiple σ-factors (Parashar *et al*., 2009; Takano et al., 2011; Sevcikova *et al*., 2020).

The atypical and orphan response regulator BldM is a signature *Streptomyces* protein (Chandra & Chater, 2014). In *S. coelicolor* BldM could not be phosphorylated in vitro, and a *bldM* allele with a D54A substitution in its conserved phosphorylation pocket restores sporulation to a Δ*bldM* mutant, highlighting the dispensable nature of phosphorylation for this response regulator (Molle & Buttner, 2000). However, this raises the question as to why BldM conserves 100% amino acid identity across all sequenced *Streptomyces* orthologues. During early development, BldM functions as an activator of at least 17 genes including the developmental regulators *ssgR* and *whiB* which control septation, as well as genes involved in the stringent response. BldM forms homodimers (BldM-BldM), and this is reflected in palindromic binding sites in the promoters of some target genes (Al-Bassam *et al*., 2014). However, these genes do not necessarily explain the Δ*bldM* phenotype or why a *S. venezuelae* Δ*bldM* mutant, constitutively produces the cryptic antibiotic venemycin (Thanapipatsiri *et al*., 2016; Al-Bassam *et al*., 2014).

Ultimately, these signals are believed to initiate a second major round of PCD that occurs throughout a significant population of the submerged (or overgrown on solid medium) MII mycelium, and which directly precedes aerial growth (Manteca *et al*., 2005 & 2008; Yagüe *et al*., 2012). The uptake of *N*-acetylglucosamine that is believed to originate from digested cell-walls, is an essential signal for development and antibiotic synthesis, which is transmitted in part by the global metabolic regulator, DasR (Rigali *et al*., 2006 & 2008). The similarly pivotal nature of GlcNAc (and presumably *S*-adenosylmethionine) metabolism in promoting development and secondary metabolism, raises the question of how these signals are precisely coordinated with the fall in c-di-GMP.

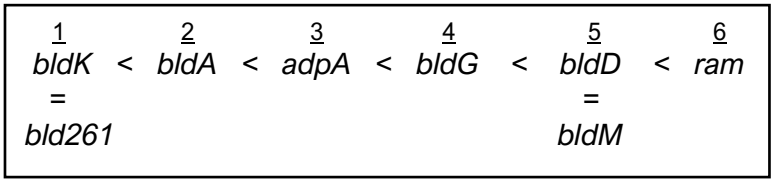

Figure 1.3. Extracellular complementation hierarchy. Where mutants in higher positions (higher numbers) can complement all of the lower mutants e.g., the *bld261* and *bldK* mutant is blocked at the beginning of the cascade and transduce none of the necessary signals, while *bldD* mutants produce these signals but do not couple this with the induction of aerial mycelium formation via activation of morphogenic surfactant *ram* operon (see section 1.3.4).

1.3.4. The Transition from MII to Aerial Hyphae: The *sky* pathway

The '*sky'* pathway was a term coined by Claessen *et al.* (2006) to describe the regulatory cascade governing the hydrophobic escape of MII aerial progenitors away from the vegetative mycelium; it has been extended here to include the subsequent differentiative cell division that yields a basal septum and the juvenile aerial hypha which eventually form the sub-apical stem compartment; a non-sporogenic, stalk-like structure enclosed between septa (Figure 1.4 - Kwak *et al*., 2001; Dalton *et al*., 2007; Fowler-Goldsworthy *et al*., 2011).

The hydrophobic escape of aerial progenitors is mediated by an array of secreted morphogenic surfactant proteins. Notably, *ramR* encodes the operonic regulator for *ramBASC* which resembles a lanthibiotic BGC and export system that are dependent on the elements of the extracellular proteolytic cascade. The product of *ramS* is post-translationally modified by RamC to form a cyclic peptide (SapB) that forms a hydrophobic film across progenitor cells. This peptide seemingly permits aerial growth but not differentiation in mutants of the extracellular cascade, demonstrating a premier role in the *sky* pathway (Willey *et al*., 1993; Tillotson *et al*., 1998; Claessen *et al*., 2006). On the other hand, the Chaplins (Chp) and Rodlins (Rdl) which cooperatively assemble as a hydrophobic sheath on aerial hyphae, are controlled by the extra cytoplasmic function $\sigma^{(BldN)}$ and its cognate anti-sigma factor (RsbN), themselves transcriptionally dependent on the activity of BldG and AdpA (Bibb *et al*., 2000 & 2012). It has been speculated that RsbN could respond to reduced surface tension, initially induced by SapB but ultimately driving a positive feedback loop that reinforces *chp*, *rdl* and *bldM* expression (Molle & Buttner, 2000; Schumacher *et al*., 2018). Nonetheless, σ^{BldN} is translated as a pro-peptide that must also be proteolytically processed to permit its activity (Bibb & Buttner, 2003; Schumacher *et al*., 2018). The alternative σ^{N} factor is activated, in turn, through an unclear mechanism that depends on the Chaplins; the transcription factor promotes expression of the hydrophobic cell-wall protein NepA, which promotes cell-wall integrity until the next germination event and enables the coordinated emergence of MII aerial progenitors (Dalton *et al*., 2007; De Jong *et al*., 2009).

Finally, a complex and asymmetric division event is driven by a unique [4Fe-4S] containing transcription factor, WblA, in part by repressing aspects of the *sky* cascade whilst activating later stage (white) developmental genes (section 1.3.5). Deletion of *wblA* specifically stalls development at this stage of growth, and yet *wblA* is expressed constitutively throughout growth, albeit from various promoters, suggesting that undiscovered transcriptional and post-transcriptional mechanisms could contribute to this phenotype; more details provided in section 1.4.2 (Fowler-Goldsworthy *et al*., 2011).

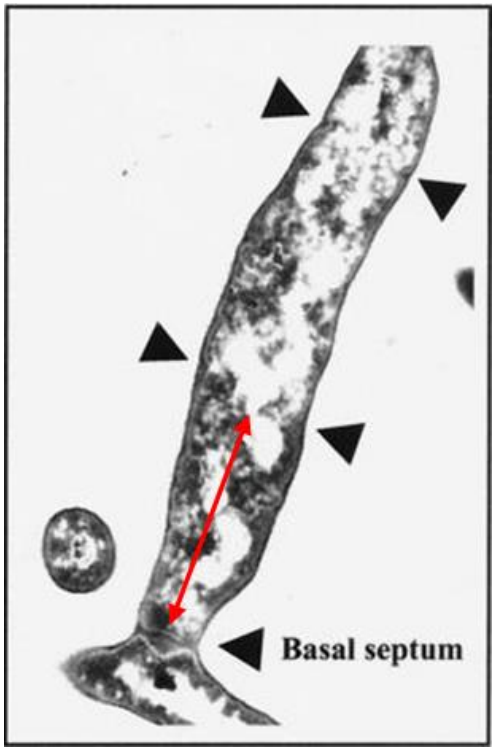

Figure 1.4. Transmission electron micrograph of a growing aerial hypha. Black arrows represent sporulation septa and the basal septum (labelled). The red arrow marks the position of the subapical stem which forms between the basal septum and the initial sporulation septum (Dalton *et al*., 2007). Figure adapted from that presented by Kwak *et al*. (2001).

1.3.5. Controlling Sporulation: The '*whi*' cascade

Apical growth of the new aerial hyphae is thought to predominantly utilise the same machinery present in the polarisome of their vegetative counterparts, but yield coiled hyphae that do not branch, indicative of regulatory and/or structural variations between these stages of growth. These aerial hyphae experience a coordinated cessation of growth and undergo a synchronous cell-division event concomitant with chromosomal segregation and condensation, resulting in abundant chains of unigenomic spores, coordinated by the FtsZ-dependent divisome. Synthesis of the thickened spore envelope is coordinated by a multiprotein complex known as the spore wall synthesizing complex (SSC) that includes the cytoskeletal Mre(BCDE) actin homologues (Vollmer 2019).

Genes whose mutants are defective in aerial (or reproductive) development are canonically referred to as 'white' (*whi*) genes, reflecting the presence of aerial hyphae but lack of the polyketide spore pigment that is characteristic of the final stages of reproductive development and sporogenesis (Figure 1.5). The eight membered *whiE*(*orfI-orfVIII*) locus encodes the spore pigment biosynthetic machinery but does not have an eminent developmental function. In contrast, the *whi* genes (*whiA*, *B*, *G*, *H*, *I*) all encode known or predicted (*whiD*), DNA-binding transcriptional regulators, whose developmental functions are described here (Flärdh & Buttner, 2009); expression of the *whiE* locus was greatly reduced or overall abolished in their respective mutants indicating a failure to reach maturation (Kelemen *et al*., 1998). Each of these has evidence for transcriptional activation by WblA, thus coordinating their activities with the end of the *sky* program, at least in *S. chattanoogensis* L10 and the deep-sea *S. somaliensis* SCSIO ZH66 (Yu et al., 2014; Huang et al., 2016).

The sigma factor WhiG belongs to the flagellar clade of sigma factors that are distinct from the other sigma factors described, the prototypical example being σ^{FliA} of enteric bacteria (Chater et al., 1989). *Streptomyces* WhiG appears to function as a dedicated activator of the developmental regulator genes *whiH* and *whiI*, through which WhiG peripherally affects the expression of more than 100 late-stage developmental genes (Gallagher *et al*., 2020). Consistent with a positive role for WhiG in sporulation, overexpression results in hyper-sporulating phenotypes (Gallagher *et al*., 2020). In *S. coelicolor*, *whiG* was shown to be constitutively expressed throughout the life cycle (Kelemen *et al*., 1996) where WhiG activity is controlled by a cognate anti-sigma factor, designated RsiG (Gallagher *et al*., 2020). The crystal structure of WhiG-RsiG revealed a c-di-GMP dimer that maintains the stability of the complex. Thus, WhiG is activated in response to a similar stimulus as BldD which, itself, represses WhiG, seemingly illustrating a staggered cascade dependent on a fall in c-di-GMP. (Tschowri *et al*., 2014; Schumacher *et al*., 2017; Gallagher *et al*., 2020). *S. coelicolor* Δ*whiG* mutants exhibit straight aerial hyphae without any sporulation septation or spore pigment formation (Mendez & Chater, 1987). In comparison, the

S. venezuelae Δ*whiG* mutant can (rarely) generate chains of immature spores, indicating subtle differences in function between species (Gallagher *et al*., 2020).

A primary target of σ^{WhiG} is *whiI*, another atypical response regulator which lacks key residues for phosphorylation (Aínsa *et al*., 1999; Tian et al., 2007). Point mutations in the abnormal phosphorylation pocket of WhiI only result in a lack of spore pigment formation, as opposed to the sporulation defects seen in null mutant strains (Tian *et al*., 2007). There are seemingly no genes significantly regulated by the independent activity of WhiI, which instead seems to function primarily as an auxiliary protein to adapt BldM binding specificity through heterodimerization (Al-Bassam *et al*., 2014). The BldM-WhiI complex directly binds the promoters of several known sporulation genes, including the *whiE* and *smeA-sffA* operons. The latter encodes an FtsK-like DNA pump (SffA) and it's membrane localising partner (SmeA) which function in DNA-transport at division sites (Ausmees *et al.*, 2007). WhiH, on the other hand, is a global transcriptional regulator of the GntR family, which regulates its own expression (Ryding *et al*., 1998; Persson *et al*., 2013). WhiH was shown to indirectly activate the expression of the dynamin-like genes *dynA* and *dynB*, the latter of which specifies a protein which interacts with SepX to form part of the sporulation-specific, FtsZ-dependent, divisome (Schlimpert *et al*., 2017; Bush *et al*., 2022).

The functions of WhiA and WhiB are interdependent on one another and are essential for the coordinated activation of *ftsZ*, cessation of apical growth that accompanies the assembly of Z-rings at future division sites. The WhiA protein is widespread throughout Gram-positive bacteria while WhiB is the founding member of a novel family of small, WhiB-like (Wbl) proteins of [4Fe-4S] binding regulators, which include WblA (Soliveri *et al*., 2000; Aínsa *et al*., 2000). Another Wbl protein WhiD, mediates the crucial final stages of spore formation and maturation, aiding the completion of the life cycle (Molle *et al*., 2000).

The pervasive nature of the WhiB-like proteins throughout *Streptomyces* multicellular development and secondary metabolism has made their functions of utmost interest. The following sections provide more detailed descriptions for the WhiB-like proteins and their roles in regulating aspects of multicellular differentiation and secondary metabolism in *Streptomyces* spp.

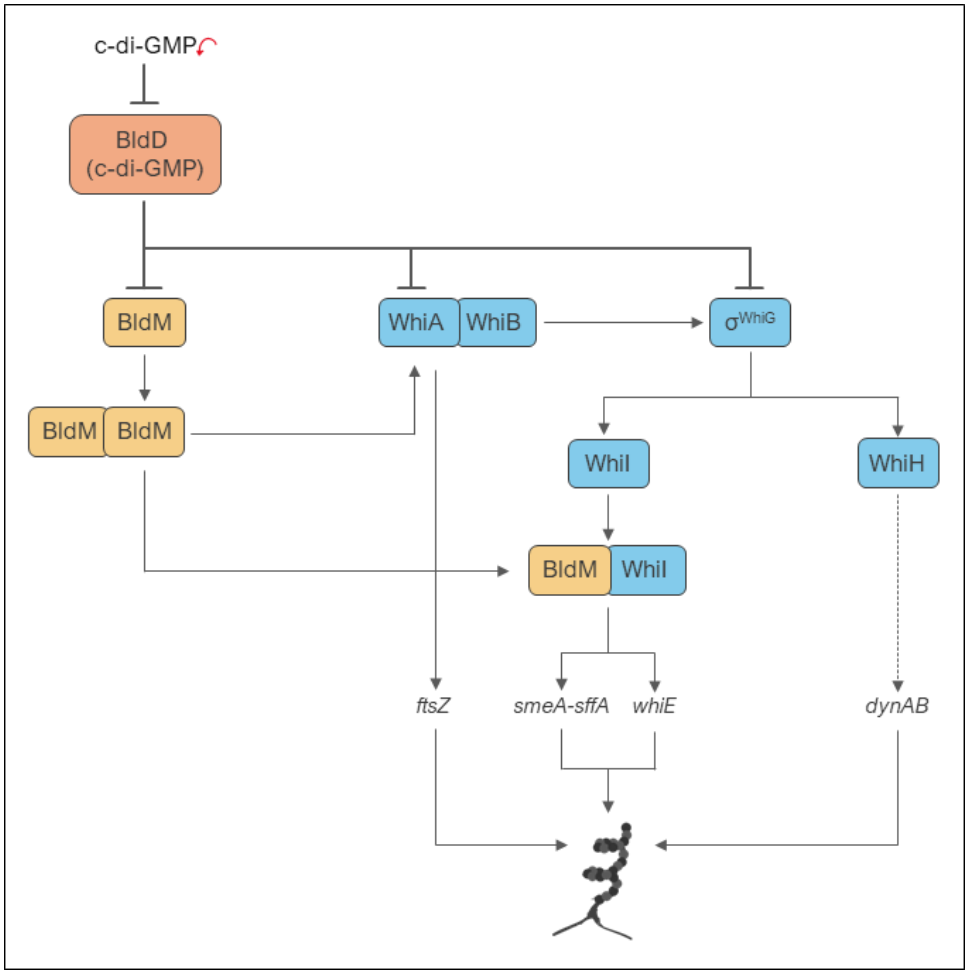

Figure 1.5. *Streptomyces* 'white' (*whi*) regulatory network, as described in Section 1.3.5, leading up to formation of mature spore chains. BldD-(c-di-GMP) acts as a global repressor of reproductive genes in the *whi* cascade, activating the pathway upon local drops in c-di-GMP concentrations. Arrows indicate activation, bars indicate repression; solid lines indicate direct effects, dotted lines indicate indirect or poorly described effects.

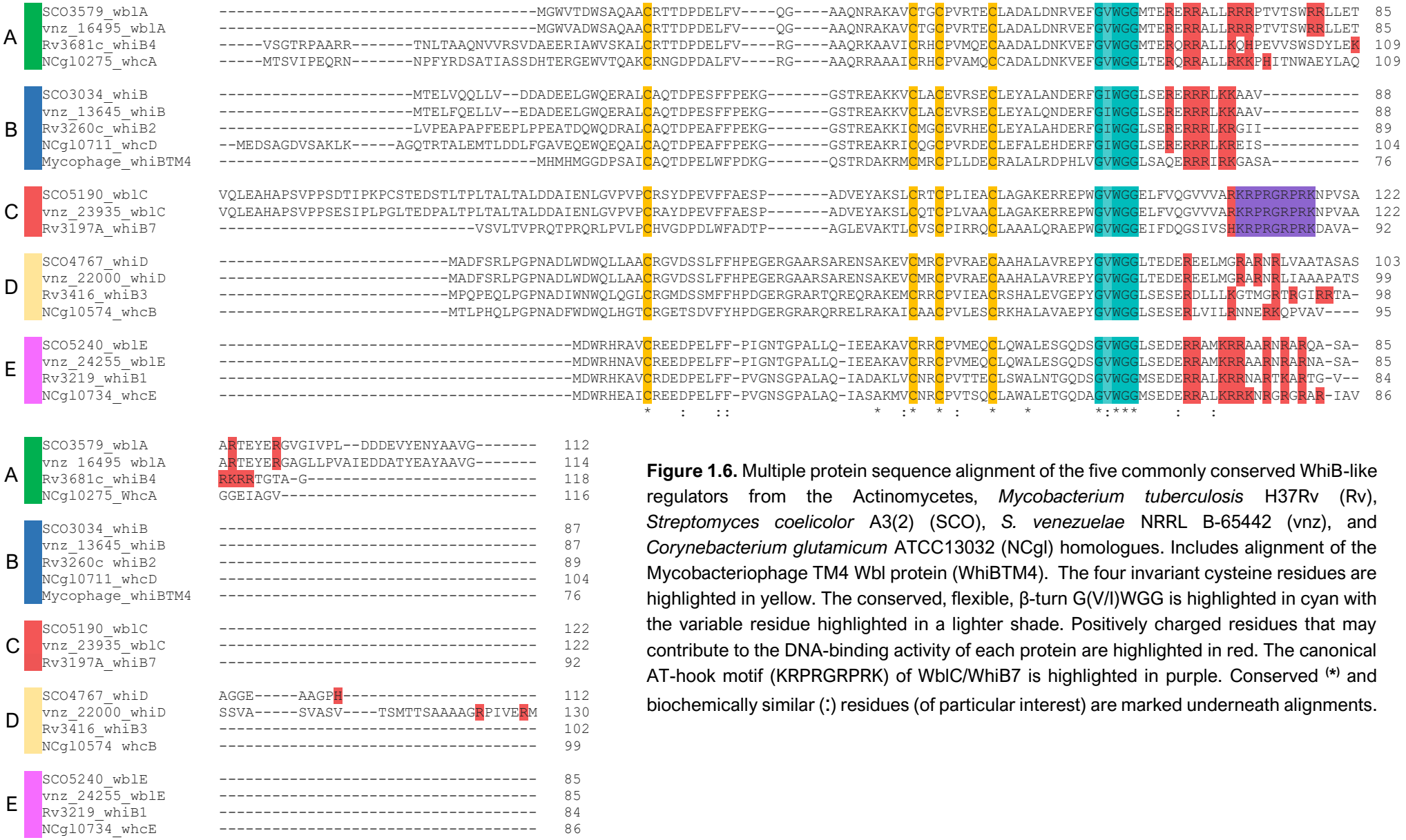

Figure 1.6. Multiple protein sequence alignment of the five commonly conserved WhiB-like regulators from the Actinomycetes, *Mycobacterium tuberculosis* H37Rv (Rv), *Streptomyces coelicolor* A3(2) (SCO), *S. venezuelae* NRRL B-65442 (vnz), and *Corynebacterium glutamicum* ATCC13032 (NCgl) homologues. Includes alignment of the Mycobacteriophage TM4 Wbl protein (WhiBTM4). The four invariant cysteine residues are highlighted in yellow. The conserved, flexible, β-turn G(V/I)WGG is highlighted in cyan with the variable residue highlighted in a lighter shade. Positively charged residues that may contribute to the DNA-binding activity of each protein are highlighted in red. The canonical AT-hook motif (KRPRGRPRK) of WblC/WhiB7 is highlighted in purple. Conserved (*) and biochemically similar (:) residues (of particular interest) are marked underneath alignments.

1.4. The WhiB-like Paradigm of Transcriptional Regulators

Among the first eight *bona fide* genomic loci identified as important for *Streptomyces*' sporulation, the *whiB* gene was unique, presenting a small protein of just 86 amino acids (in *S. coelicolor* and *S. venezuelae*) but with several features comparable to known transcription factors (Chater, 1972; Davis and Chater, 1992). This included a basic C-terminal alpha-helix, resembling a DNA-binding motif, and an amphipathic N-terminus which could potentially facilitate interactions with cognate partner-proteins or the core transcriptional apparatus (Davis and Chater, 1992). Most notably, four cysteine residues interspaced throughout the peptide alluded to the possibility that the gene-product may even coordinate a metal co-factor.

With improved sequencing and bioinformatic techniques, it has become apparent that WhiB defines a paradigm for a protein family, phyletically confined to the Actinobacteria, but specifically expanded within the *Actinomycetales* order (Soliveri *et al.*, 2000; Chandra & Chater, 2014; Averina *et al.*, 2012). *Streptomyces spp.* seem to carry at least seven *wbl* genes which are usually important for development and secondary metabolism, however their numbers vary significantly between species and many have undefined roles (Bush, 2018). In comparison, *Mycobacterium tuberculosis* is highly dependent on seven *wbl* genes (*whiB1-7*) for successful development, disseminative colonisation of the host, and virulence (Smith *et al*., 2010; Saini *et al*., 2012; Chawla *et al*., 2012 & 2018). *Corynebacterium spp*. conserve just four, and *Bifidobacterium* spp. just two, which seem to function more generally in response to heat and oxidative stress (Kim *et al*., 2005; Averina *et al.*, 2012; Bush, 2018).

Nevertheless, five archetypal WhiB-like proteins exist widely throughout the phylum and form sub-families which capture the majority of WhiB-like diversity. In *Streptomyces spp.* these paralogous genes are denoted: WblA, WhiB, WblC, WhiD and WblE (Bush, 2018; Soliveri *et al.*, 2000). Significant variation in peptide length (around 80 – 150 aa) and amino acid composition exists between each archetypal member, indicative of distinct cellular functions (Figure 1.6). However, each member maintains a predominantly alpha-helical structure which centres around a flexible β-turn (G(V/I)WGG) and a perfectly conserved 'Cys-X_n-Cys-X_2-Cys-X_5-Cys' (4Cys) motif, which ligates a [4Fe-4S] cluster (Crack *et al*., 2009). The role of the β-turn, however, remains enigmatic (Bush, 2018).

It has become well-established that multiple members of the Wbl family function as global regulators of gene expression via DNA-binding activity, which is commonly attributed to a [4Fe-4S] cluster-dependent interaction with the major Sigma factor, σ^{HrdB} (or σ^{A} in *Mycobacterium* spp.) which appears to constitute a common mechanism of action within the family (Lee *et al*., 2021; Lilic *et al*., 2021; Lilic *et al*., 2023; Khudair *et al*., 2017; Wan *et al*., 2020; Crack *et al*., 2009; Bush *et al*., 2016). To date, no comparable interaction has been demonstrated for any alternative

or ECF Sigma factor (Alhadlaq *et al*., 2021 & personal communications). Nevertheless, several non-sigma factor partner proteins have been identified for specific Wbl proteins but their evolutionary and physiological significance remains poorly explored, with the exception of WhiA (Aínsa *et al*., 2000; Lilic *et al*., 2023). Additional functions have been proposed such as disulphide reductase and chaperone activity, but these remain controversial or uncorroborated within the broader literature (Alam *et al*., 2007; Garg *et al*., 2007 & 2009; Alam & Agrawal, 2008; Crack *et al*., 2009; Konar *et al*., 2012; Park *et al*., 2016).

1.4.1. WhiB-like Redox Biochemistry: A Family of Redox Gas Sensors

The WhiD protein of *S. coelicolor* provided the first evidence that Wbl proteins bind a [4Fe-4S] cluster (Jakimowicz *et al.*, 2005). Importantly, subsequent work showed that the WhiB-like iron-sulphur clusters are dramatically more sensitive (x 10^4) to •NO than $O_2^{(-)}$ and are comparatively insensitive to the oxidants hydrogen peroxide or diamide. Up to 8[•NO] (on average) can rapidly bind a Wbl iron-sulphur cluster before it reacts, forming a dinitrosyl iron complex (Crack *et al.*, 2009 & 2010; Stewart *et al*., 2020). On the other hand, O_2-based degradation appears to be more gradual (Singh *et al*., 2007). Transcriptional analyses in *M. tuberculosis* also identified •NO and redox-stress as common inducers of WhiB1-7 transcription, indicating a role as redox-sensing regulators of the cell (Geiman *et al*., 2006; Larsson *et al*., 2012).

More recently, it has been demonstrated that both *M. tuberculosis* WhiB1 (Wan *et al*., 2019) and *S. venezuelae* WhiD (Stewart *et al*., 2020) are protected from oxygen-based cluster degradation *in vitro*, by interaction with a conserved histidine-proline motif in region 4 of the primary sigma factor (Figure 1.7), alluding to their potential roles as specific •NO-sensors of the cell. Moreover, there is growing evidence that the cluster-status (apo or holo) and the apo-cysteine oxidation states (oxidised, nitrosated or reduced) can influence DNA-binding capability and extend it beyond that of the principal σ-factor, at least *in vitro* (Singh *et al.*, 2009; Kudhair et al., 2017).

Intriguingly, certain Wbl proteins, including WhiB4, WhiB1, and WhiD have been shown to form dimeric or trimeric units under oxidative conditions. In the case of WhiB4, these complexes can oligomerise on DNA, eliciting topological changes *in vitro*, as determined by electron force microscopy (EFM; Chawla *et al*., 2018). It has been feasibly proposed, that the iron-sulphur cluster and perhaps the ligating cysteines, function in redox-switch mechanisms as seen in other [4Fe-4S] and cysteine-based sensors/regulators, but with an •NO-specific pathway (Munnoch *et al*., 2016), thus activating or repressing distinct responses under different redox conditions. Nonetheless, the specificity of Wbl [4Fe-4S] clusters for •NO and the propensity for apo-Wbls to oligomerise remains unresolved in the broader physiological context.

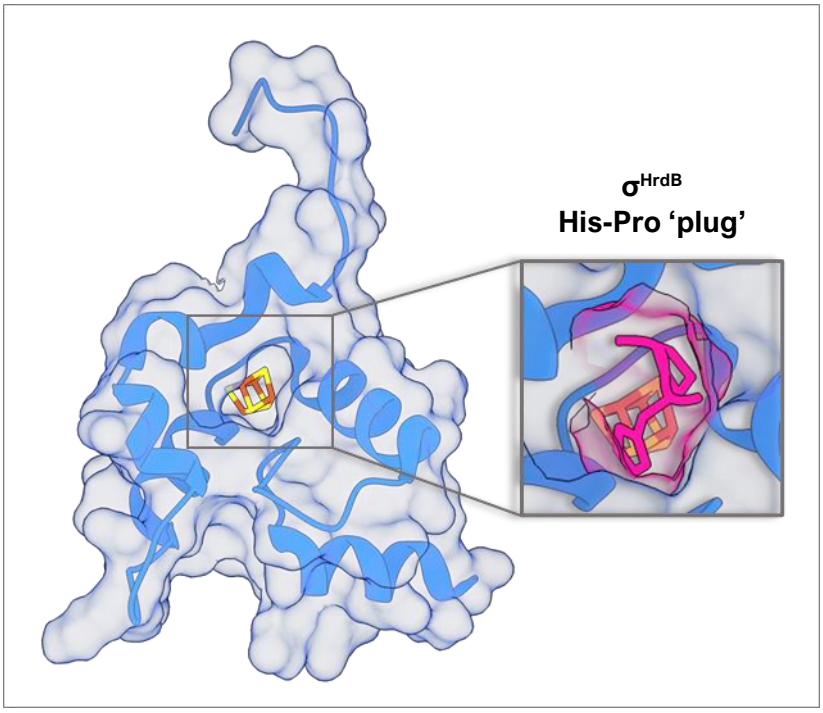

Figure 1.7. Cryo-EM Structure of WhiB (with WhiA, HrdB and the RNA polymerase hidden). Inset shows the HrdB 'Histidine-Proline plug' which forms a central interface for the HrdB-WhiB and HrdB-WhiB1 interactions (see section 1.4) and the other Wbl proteins.

1.4.2. WblA (WhiB4; WhcA) - *Streptomyces* (*Mycobacterium*; *Corynebacterium*)

Interspecies microarray analyses were the first to highlight the significance of the *wblA* gene-product as a pleiotropic down-regulator of both morphogenesis and antibiotic synthesis in *Streptomyces* species (Kang et al., 2007). Accordingly, *Streptomyces* mutants which overexpress *wblA* are unable to proceed beyond vegetative (*bld*) growth and exhibit reduced antibiotic production (Huang et al., 2017). On the other hand, Δ*wblA* mutants exhibit major transcriptional variations (183 genes upregulated and 103 downregulated) which accompany much more complex phenotypes. Scanning electron micrographs of Δ*wblA* mutants all similarly depict aerial hyphae which initiate but form long, spindle-like fibres, resembling a perpetuated sub-apical stem compartment (see '*sky* program' section 1.3.4. – Yu *et al.*, 2014; Rabyk *et al.*, 2011; Huang *et al.*, 2017; Fowler-Goldsworthy *et al.*, 2011). The *wblA* gene is also a direct target for repression by BldD (Makitrynskyy *et al.*, 2020) and activation by AdpA (Lee *et al*., 2013; Yu *et al*., 2014), two of the major global regulators of differentiation, indicative of a role in reproductive development.

In accordance with its developmental phenotype, major aspects of the *sky*-program were shown to be amongst the most severely dysregulated genes in Δ*wblA* mutants; this included the downregulation of the morphogenic surfactant chaplins (*chpADE),* and the structural protein NepA. Intriguingly, *whiA, whiB* and *whiGHI* genes are also among those commonly found to be

under-expressed in transcriptional analyses of *wblA* mutants and appear (directly or indirectly) dependent on WblA-mediated activation (Fowler-Goldsworthy *et al*., 2011; Yu *et al*., 2014; Huang *et al*., 2016; Rabyk *et al*., 2011). In contrast, WblA appears to function as an important repressor of *ramS* (SapB), *chpB* and the protease-inhibitor *sti*, specifically tailoring surfactant composition and, presumably, activating a proteolytic pathway during differentiation. Unfortunately, no *in vivo* DNA-binding data yet exists for WblA or its homologues. Nevertheless, despite its apparent role at such a distinct stage of growth, WblA is constitutively expressed from three developmentally regulated promoters (Fowler-Goldsworthy *et al*., 2011). Thus, *wblA* is important for coupling aspects of the *sky* and *whi* programs, which is specifically necessary for a distinct differentiative step.

Intriguingly, *Streptomyces* strains that possess a defective *wblA* gene also characteristically display temporal and spatial dysregulation of their secondary metabolism (Fowler-Goldsworthy *et al.*, 2011; Yu et al., 2014). Most evidence suggests that WblA globally represses secondary metabolite BGCs, via direct and indirect mechanisms. As such, its deletion and repression has been regularly and successfully employed as a novel method to both improve antibiotic synthesis and aid novel compound discovery (Noh *et al*., 2010; Nah *et al*., 2012; Huang *et al*., 2016; Wei *et al*., 2018). Although, in a unique case, *wblA* is indispensable for the activation of Natamycin biosynthesis in *Streptomyces chattanoogenesis* L10 (Yu *et al*., 2014).

1.4.2.1. Antioxi-don't: Conserved Antioxidant Repression by WblA

A curious effect of *wblA* deletion is the global induction of molecular antioxidants, an effect qualifiable by increased resistance to the oxidant diamide in solid *S. coelicolor* Δ*wblA* cultures and bolstered survival and virulence of *M. tuberculosis* Δ*whiB4*. Targeted real-time RT-PCR revealed that the expression of *S. coelicolor* superoxide dismutases, *sodF* and *sodF2* are notably enhanced in a Δ*wblA* genetic background (Kim *et al*., 2012). Deletion of *whiB4* in *M. tuberculosis* similarly relieves repression of multiple antioxidant defenses, including the major alkylhydroperoxidase *ahpC(D)*, which is a direct regulatory target of WhiB4 (Chawla *et al*., 2012). The same antioxidant repressing effect has been observed for *C. glutamicum* WhcA, implying that antioxidant repression is a conserved feature of orthologous function for this gene-product. In *S. coelicolor* and *C. glutamicum*, apo-WblA/WhcA conserves a cluster-independent interaction with the SpiA dioxygenase (Stress protein interacting with WblA). In *C. glutamicum*, SpiA seems to function antagonistically to WhcA's antioxidant repression, but the result is less obvious in *S. coelicolor* (Kim *et al*., 2012; Kim *et al*., 2013). The physiological significance of antioxidant repression during *Streptomyces* development and secondary metabolism is still unclear.

1.4.3. WhiB; WhiB2; WhcD

WhiB is the founding member of the WhiB-like family of proteins (Soliveri *et al*., 2000; Davis, 1992). The role of WhiB appears to be strictly reproductive with *Streptomyces* Δ*whiB* mutants failing to cease aerial growth; instead, cells keep growing and produce long aerial hyphae devoid of division septa and evidence of nucleoid condensation (Flärdh *et al*., 1999; Bush *et al*., 2013 & 2016; Lilic *et al*., 2023). It is understandable, therefore, that *whiB* is a key target of the developmental repressor BldD. The gene is also subject to dedicated repression by BldO (also thought to bind c-di-GMP), which specifies *whiB* expression to aerial growth, something that is reflected in its phenotype and expression patterns (Kormanec *et al.,* 1998; Yan *et al*., 2019; Bush *et al*., 2017). Deletion of *bldD*, *bldO*, or overexpression of *whiB*, produces similar hyper-sporulating mutants which have bypassed the development of aerial hyphae (Bush *et al*., 2017; Tschowri *et al.*, 2014). In *M. smegmatis*, *whiB2* gene depletion induces filamentous growth and reduces septation, while overexpression leads to hyper-septated cells with stunted growth, indicative of an analogous role for its product (Gomez & Bishai, 2000; Raghnunand & Bishai, 2006).

The phenotype of *S.coelicolor* Δ*whiB* mutants was noted to be nearly identical to those of another developmental mutant, Δ*whiA* (Aínsa *et al*., 2000) a consequence of the fact that WhiA and WhiB are interdependent transcription factors that interact to control expression of a shared set of target genes (Bush *et al*., 2013 & 2016). WhiA is a unique protein, representing an ancient fusion between an RNA polymerase sigma-factor and a LAGLIDADG Homing-Endonuclease (LHE) which has become domesticated and widespread throughout Gram-positive bacteria (Kaiser *et al*., 2009; Bush et al., 2013). Even so, the reason behind the acquisition of WhiA function by WhiB in Actinobacteria remains enigmatic.

In direct contrast to WhiB, WhiA is omnipresent throughout the life cycle and is encoded by one of a few, core developmental genes that are not directly regulated by BldD (den Hengst *et al*., 2010; Bush *et al*., 2013 & 2015). As such, the developmental function of WhiAB seems to be specified via WhiB (Bush *et al*., 2013, 2015 & 2016). No WhiB-independent function has yet been shown for WhiA in *Streptomyces* spp., but the regulatory WhiAB complex regulates over 120 genes and is a pivotal activator of *ftsZ* which satisfactorily explains the lack of division septa in *whiAB* mutants.

More recently, Cryo-EM was used to model *S. venezuelae* RNA polymerase bound to the tripartite σ^{HrdB}-WhiA-WhiB regulatory complex, at the *sepX* promoter (Lilic *et al*., 2023; Figure 1.8). WhiB makes non-specific contact with AT bases in the minor groove, adjacent to the -35 site, somewhat comparable to the function of eukaryotic TATA-binding proteins (TBP; Starr & Hawley, 1991). Intriguingly, WhiB forms two distinct hydrophobic interfaces with σ^{HrdB} and WhiA

which mediate an otherwise unsustainable tripartite interaction and demonstrates a unique scaffolding function for a Wbl protein, at the RNA polymerase (Lilic *et al*., 2023).

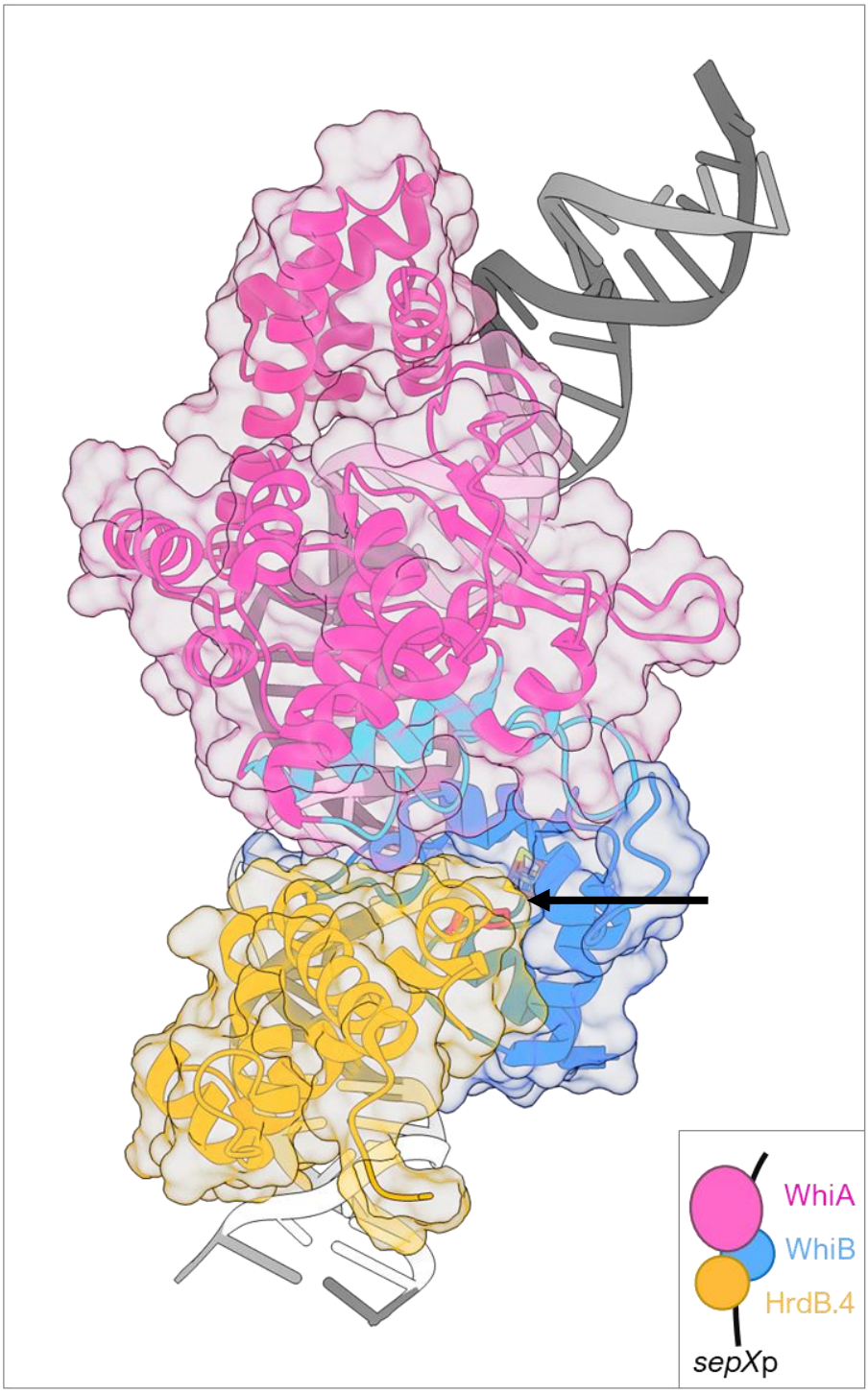

Figure 1.8. An aerial view of the Cryo-EM structure of WhiAB-σ^{HrdB}-RbpA-RpoABCZ at the modified *sepX* promoter (Lilic *et al*., 2023), specifically showing HrdB region 4 (yellow), WhiB (blue) and WhiA (pink) that are involved in the tripartite interaction. The histidine and proline residues critical for WhiB interaction with HrdB are visualised as pink sticks and indicated with an arrow, structural aspects of WhiA which come in close proximity to WhiB are highlighted in cyan. DNA is shown for reference. Developed from PDB:8DY9 (Lilic *et al*., 2023).

1.4.4. WblC (WhiB7)

1.4.4.1 WblC Controls Intrinsic Antibiotic Resistance

In contrast to acquired antibiotic resistance, which describes the horizontal transfer of resistance genes or spontaneous mutations in susceptibility genes, intrinsic antibiotic resistance refers to 'innate' resistance traits in bacteria, such as outer membrane impermeability and non-selective efflux channels. At sub-inhibitory concentrations, antimicrobial compounds can function as elicitors of intrinsic resistance via physiological reprogramming, relayed by diverse sensing and signalling mechanisms to mitigate the cellular damage exerted by antimicrobials (Jarlier & Nikaido, 1994; Davies *et al.*, 2006; Bernier & Surette, 2013).

The *wblC* (*whiB7*) gene encodes a large (123 aa in *S. venezuelae* and *S. coelicolor*) Wbl protein, generally observed only within the *Actinomycetales* order, and critical for the initiation of intrinsic multi-drug resistance mechanisms. Mutants which lack a functional copy of *wblC,* are unable to cope with antibiotic stress and exhibit elevated susceptibility, especially to translation-inhibiting antimicrobial compounds (Figure 1.9; Morris *et al.*, 2005; Ramón-García *et al.,* 2013). There appear to be remarkable similarities in the function of WblC/WhiB7 across the *Actinomycetales* genera and orthologues are apparently able to largely complement heterologous Δ*wblC*/*whiB7* mutant hosts but are likely to have species-specific targets (Ramón-García *et al.,* 2013).

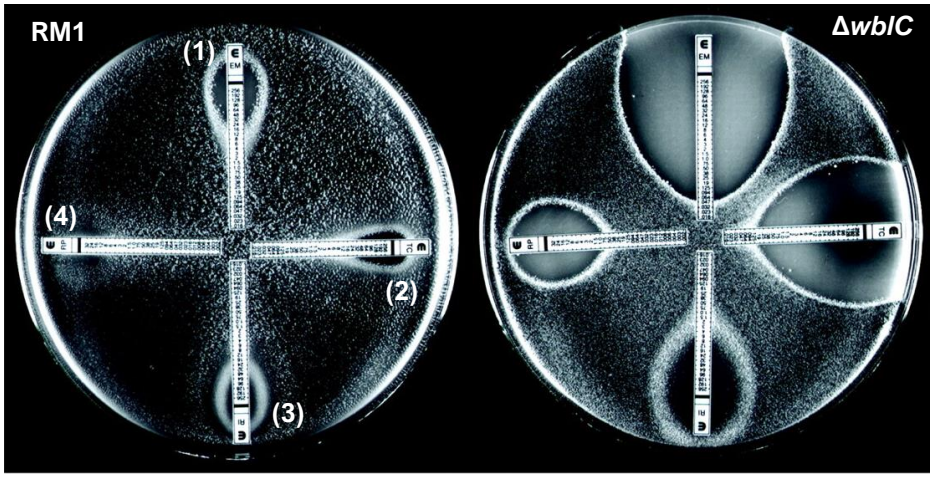

Figure 1.9. Comparative susceptibility fingerprints of wildtype *S. lividans* RM1 and an RM1 Δ*wblC* mutant, to a range of antibiotics applied via E-test strips: (1) Erythromycin (2) Tetracycline (3) Rifampicin (4) Quinupristin. Figure adapted from that published by Morris *et al.* (2005).

1.4.4.2. Ribosome-Mediated Attenuation of *wblC* Transcription

Upon exposure to sub-inhibitory concentrations of translation-inhibiting antibiotic (e.g. Tetracycline, Erythromycin, or Streptomycin), the transcription of *wblC* mRNA is markedly and rapidly enhanced by up to several orders of magnitude over controls (Geiman *et al.*, 2006; Burian *et al.*, 2012; Lee *et al.*, 2020). Antibiotic-dependent *wblC* induction is established by a ribosome-mediated transcription-attenuation (riboregulation) mechanism (Lee *et al.*, 2022). In short, an upstream (u)ORF (relative to *wblC*) acts to relay the translational state of the cell to a DNA-based Rho-Independent Terminator (RIT) within the promoter region of *wblC*, prematurely terminating transcription under translation-permitting conditions. Ribosomal stalling during uORF mRNA translation causes a change in the RIT's structure, forming an anti-terminator which promotes readthrough into *wblC*. This intriguing mechanism of gene regulation was first described for the Tryptophan biosynthetic operon, *trpL (EDCBA)*, of *Pseudomonas* (Yanofsky, 1981) but has become better defined as a key bacterial approach to ensure the necessary expression of resistance genes for translation-inhibiting compounds (Lovett *et al*., 1996; Dar *et al*., 2016; Wang *et al*., 2021). Nevertheless, the uORF-WblC system appears to be evolutionarily distinct from comparable systems (Lee *et al*., 2022).

1.4.4.3 Redox, Regulation and the Ribosome: WblC's Resistance Mechanisms

The first direct regulatory target of WblC to be determined in *Streptomyces* spp. was the *sigR-rsrA* operon, encoding the ECF sigma factor σ^R and its redox-sensitive anti-sigma factor, RsrA, which control the principal thiol stress response in Streptomyces (Paget *et al*., 1998). The standard SigR response auto-induces expression of a longer, but unstable, isoform of SigR from a SigR-dependent promoter (*sigR*p2), eliciting a rapid and transient response (Kim *et al*., 2009; Park *et al*., 2019). In contrast, in the presence of antibiotics, WblC mediates expression from a downstream and SigR-independent promoter, *sigR*p1, yielding a more stable isoform of SigR (SigR') and a prolonged stress response (Yoo *et al*., 2016). This function of WblC revealed thiol-oxidative stress as a previously unappreciated but deleterious consequence of translational inhibition.

More recently, *in vivo* ChIP-seq performed in the model organism *Streptomyces coelicolor*, under antibiotic-challenged conditions, indicated global binding of WblC to over 300 promoters. Comparable to WhiB, WblC targets an AT-rich region directly upstream of the -35 bp region of target promoters (Lee *et al.*, 2020), this is consistent with previous findings that WblC and its orthologues possess a canonical AT-hook motif (Bush et al., 2018; Figure 1.6). The Cryo-EM structure of *M. tuberculosis* WhiB7-σ^A complex bound to *whiB7*p has been solved and demonstrated binding within the minor-groove of DNA, a feature conserved by WhiB and also more generally by AT-hook proteins (Aravind & Landsman, 1998; Lilic *et al*., 2021 and 2023).

Understandably, many identified WblC targets in *S. coelicolor* encode proteins which could participate in antibiotic export, such as ABC and MFS-superfamily transporters (e.g. *CmlR2*, *Pep*) or various transferases, which may act to chemically inactivate translation-inhibiting compounds. Nevertheless, many of these genes have never been studied. More interestingly, WblC was found to regulate various ribosomal proteins, and deletion of *wblC* significantly altered ribosomal protein composition under antibiotic stress, as determined by mass spectroscopy. Thus, WblC controls adaptive regulation of ribosomal composition to promote translation under translation-inhibiting conditions and, consequently, create a feedback loop to maintain its own repression (Lee *et al*., 2020).

1.4.5. WhiD (WhiB3; WhcB)

Early micrographs of *S. coelicolor* Δ*whiD* mutants revealed morphological abnormalities in spore-chains, compared to the wild type, indicating a possible role in late-stage (stationary) growth and spore-maturation. Accordingly, WhiD appears to be specifically transcribed during late reproductive growth but the underlying molecular mechanisms defining its mutant phenotype remain unclear, and little work has since managed to clarify the *in vivo* function of WhiD in *Streptomyces* spp. (Molle *et al*., 2000). Nevertheless, all WhiD orthologues are associated with stationary growth (Lee *et al*., 2012; 2013). *Streptomyces* WhiD has served as an important model for the *in vitro* study of the iron-sulphur cluster and the interaction with σ^{HrdB}/σ^{A} (Section 1.4.1). Unique C-terminal domains mediate *in vitro* dimerisation of *S. venezuelae* WhiD, which may be important for its *in vivo* function (Stewart *et al.,* 2020).

The molecular roles for WhiB3 in *Mycobacterium* spp. are better described. The *whiB3* gene is specifically upregulated and required during starvation, hypoxia and ·NO stress encountered within macrophages (Singh *et al*., 2007; Saini *et al*., 2012). In accordance with this, *whiB3* is activated by the key pH- and nutritionally responsive regulators RegX3(SenX3), GlnR and PhoP(R), which have important roles in survival and virulence (Feng *et al*., 2018; You *et al*., 2019; Mahatha *et al*., 2020). In agreement with this, *whiB3* mutants are unable to cope with starvation or acid stress and exhibit attenuated virulence within murine models. Mutants also lose accumulation of the complex lipids, phthiocerol dimycocerosate (PDIM), polyacyltrehalose (PAT) and the sulfolipid (SL-1) which are important virulence components in pathogenic species. In part, this has been attributed to apo-oxidised (disulphide) WhiB3 binding to the promoter elements of *pks2* (SL-1) and *msl3* (PAT), encoding polyketide synthases, to activate their transcription (Singh *et al*., 2009).

Intriguingly, under defined redox stress, *whiB3* mutants lose the ability to accumulate triacylglycerol (TAG), a key aspect of mycobacterial development and the dormancy program,

but the mechanism behind *whiB3*-dependent TAG and PDIM accumulation remains unclear (Singh *et al*., 2009). The *whiB3* gene has been transcriptionally associated with dormant cells in *M. smegmatis* and draws a direct molecular parallel with its role in sporulation of *Streptomyces* spp. (Wu *et al*., 2016). As both *Streptomyces* and *Mycobacterium* spp. are uniquely oleaginous bacteria and accumulate TAG as an alternative energy source, the function of mycobacterial WhiB3 in lipid anabolism could indicate a comparable function in the *Streptomyces* homologue, although this remains to be determined experimentally.

1.4.6. An Enigma – WblE (WhiB1; WhcE)

The *wblE* gene of *Streptomyces* spp. and its orthologues in other actinomycetes remain enigmatic. Two independent attempts to disrupt *wblE* in *S. coelicolor* and *S. avermitilis*, using the homologous recombination-based 'ReDirect' technology, failed to yield mutants (Fowling-Goldsworthy, 2011; Liu *et al*., 2017). Meanwhile, large-scale transposition mutagenesis in *S. coelicolor* revealed a 2112 bp transpositional dead-zone (5,701,374 – 5,703,486 bp) which spanned the entirety of *wblE* and its preceding gene SCO5241 (*vnz_24260*), thus implying that the gene product is essential (Xu *et al*., 2017). This is comparable to *M. tuberculosis* where conditional *whiB1* knockouts are lethal to the cell (Smith *et al*., 2010). Nevertheless, varying evidence exists for the gene's importance throughout the wider Actinobacteria, such as in *Corynebacterium, Bifidobacterium* and *Gordonia* spp*.* where it can be deleted without lethality (Kim *et al*., 2005; Murarka *et al*., 2020). Intriguingly, *C. glutamicum* Apo-WhcE stably interacts with a Hydrophobe/Amphiphile-Efflux (HAE)-1 family transporter 'SpiE', but no identifiable homologue is present in either *Streptomyces* or *Mycobacterium spp.* suggesting that distinct functional differences do in fact exist (Park *et al*., 2016). To this end, *M. tuberculosis* WhiB1 and the glycogen branching enzyme GlgB1 undergo disulphide exchange, but the conservation and relevance of this interaction is poorly understood (Garg *et al*., 2009).

A central function for WblE in *Streptomyces* growth, development and secondary metabolism can be interpreted from the regulatory pathways that connect to the *wblE* gene (Figure 1.10). The redox sensor, Rex, controls aerobic respiration and haem biosynthesis in response to the NADH:NAD^+ ratio, but also directly represses *wblE* in *S. avermitilis*, suggesting a role for the gene product that is dependent on, or important for, aerobic growth (Brekasis & Paget, 2003; Liu *et al*., 2017). The expression of *wblE* also seems to be intimately connected with the extracellular environment via two conserved response regulators. MtrA (of the TCS MtrAB-LpqB) and AbrC3 (of the atypical TCS AbrC1-C2-C3), which both coordinate development and secondary metabolite synthesis in cooperation with their cognate histidine kinases. While AbrC3 positively influences *wblE* expression through an indirect mechanism, evidence suggests MtrA directly represses *wblE* by binding its promoter (Rico *et al*., 2014; Som *et al*., 2017a and 2017b).

The *wblE* gene is also directly repressed by the paralogous protein WblC (Section 1.4.4) and by the developmental regulator AdpA/BldH (Guyet et al., 2014). Unfortunately, no work has explored the physiological significance of these connections any further.

Intriguingly, preliminary evolutionary analysis using reciprocal and recursive BLASTp (Section 2.32.2) suggests that *wblE* is a contemporary representative of the most ancient WhiB-like ancestor in the databases; i.e. genera which possess only one WhiB-like protein are reciprocal best hits with WblE. Therefore studying WblE and its function has broader implications for WhiB-like biology and evolution.

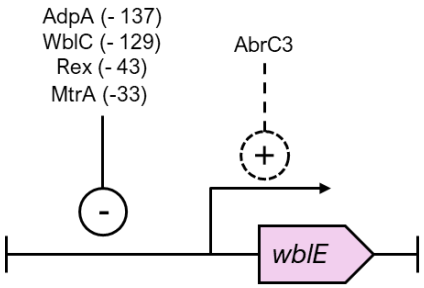

Figure 1.10. Transcription factors acting at the *wblE* promoter and whether they regulate *wblE* directly (solid line) or indirectly (dashed); and in a positive (+) or negative (-) manner. Predicted binding sites, relative to transcriptional start sites, are shown for regulators with evidence of direct binding to *wblE*p

1.4.7. Accessory Wbl Proteins

A common feature in many Actinomycetes is the presence of additional, unique *wbl* genes which often share similarity with the core paralogues described above but are poorly conserved across species and/or genera. Many accessory *wbl* genes are carried on plasmids, (e.g. *pvnz_37335* in *S. venezuelae*) which may therefore represent transmissible hubs for their evolution and expansion in Actinobacteria. Under standard growth conditions, Accessory *wbl* gene knockouts in *Streptomyces* spp. often lack clear phenotypes upon their deletion, indicating adaptive functions; *S. coelicolor* accessory Wbls (*wblH, I, J, K, L, M, N*) have each been deleted, but to no phenotypic avail, although, varying information exists for the importance of *wblI* in *S. lividans* TK24 (Fowler-Goldsworthy *et al.,* 2011; Yan *et al*., 2017). Another curious example is, WblP which represents a WhiB-like protein fused to a sigma factor and often carried on plasmids. *Mycobacterium* spp. also encodes *whiB5* and *whiB6* which are distinct from the archetypal genes or *Streptomyces* accessory *wbl* genes, but play demonstrably important roles in virulence and survival of *M. tuberculosis* (Casonato *et al*., 2012; Chen et al., 2016).

1.4.8. The WhiB-like Genesis Dilemma

As stated earlier, WhiB-like proteins are confined to the Actinobacteria; a curious exception is their presence in associated actino-bacteriophages (actinophages). Notably, *Mycophage* TM4 encodes WhiBTM4 (aligned in Figure 1.6), a homologue of WhiB which hijacks Mycobacterial development via *whiB2* repression, inhibiting cell-division but foregoing cell-death (Rybniker *et al.*, 2010). The distinct phylogenetic distribution of Wbl proteins between actinophages and the Actinobacteria nonetheless raises a chicken and egg dilemma for WhiB-like proteins. Did WhiB-like proteins evolve in Actinobacteria and transfer their genes to co-evolving bacteriophages, or did an early actinophage evolve specialised effectors which slipped into enemy hands?

1.5. Ancient Prosthetic Groups: Iron-Sulphur Clusters

Iron-sulphur clusters represent an ancient and versatile prosthetic group that likely emerged from abiogenic origins on early Earth (Bonfio *et al*., 2017; Jordan *et al*., 2021); a history that is reflected in their pervasive and often crucial roles (beyond regulation) in electron transport chains and as catalytic centres in core biosynthetic or catabolic enzymes, in all domains of life (Beinert *et al*., 1997). Most commonly, clusters are ligated by cysteine thiolates ($-RS^-$), like in Wbl proteins, although alternative residues such as histidine, aspartate and serine are less frequently reported (Crack *et al*., 2012, 2018). An array of stable Fe-S arrangements are documented to exist within proteins but the [4Fe-4S] and [2Fe-2S] cluster arrangements are the most common and are the only configurations with documented regulatory functions (Crack *et al*., 2018).

1.5.1. Cluster Assembly and Incorporation

The intracellular assembly of Fe-S clusters from free ferrous and/or ferric iron (Fe^{2+} / Fe^{3+}) and sulphide (S^{2-}) ions is prohibited due to their inherent reactivity. In order to circumvent the toxicity posed by these ions, organisms must employ dedicated intracellular cluster-assembly machinery. Within the prokaryotes, three distinct, multi-protein pathways have emerged: the ISC (Iron-sulphur cluster), SUF (Sulphur assimilation) and NIF (Nitrogen fixation) pathways. The machinery encoded by the *nif* genes maintain a largely specialised role in nitrogen-fixing bacteria, where it mediates the assembly of iron and sulphur into the simple [4Fe-4S], and complex [7Fe-9S-Mo-C] (FeMo-co) and [8Fe-7S] (P cluster) centres of Nitrogenase enzymes (Hu & Ribbe, 2011; Einsle & Rees, 2021). In contrast, the *isc* and *suf* operons are widespread and encode the machinery necessary for 'house-keeping' iron-sulphur cluster assembly (Roche *et al*., 2013); some species, such as *E. coli*, possess both. The SUF machinery, in particular, appears to function favourably under conditions of iron starvation or oxidative stress, and has thus been preferentially retained over the ISC-system in most aerobic Gram-positive bacterial species and pathogens, including *Streptomyces* and *Mycobacterium* spp. (Fontecave *et al*., 2005; Huet et *al*., 2005; Willemse et al., 2018; Cheng *et al*., 2020)

Each assembly system utilises a similar mechanism which varies predominantly in the machinery used (Roche *et al*., 2013). First, iron and sulphur must both be donated to the pathway; a cysteine-desulphurase (SufS) enables the use of the amino acid, L-cysteine, as a stable sulphur source, liberating and binding sulphur as a transient persulphide intermediate (R-SSH; S^0). The route for iron donation remains controversial but likely occurs via species-specific carrier proteins and via passive scavenging of labile Fe^{2+}. These elements are simultaneously loaded onto the SufB (or SufU) scaffolds, whereby electrons are donated via NADPH or ferredoxins

(Fdx), to bond persulphide sulphur (S^0) and iron(II). The specific maturation and transfer of the [Fe-S] cluster to apoproteins, is catalysed primarily by chaperone/co-chaperone-like ATPase systems, such as the $SufBC_2D$ complex, which drive conformational changes to facilitate rapid cluster transfer to client apo-proteins.

Each system also usually contains an A-type (e.g. SufA/IscA) carrier, which can receive mature [2Fe–2S] or [4Fe–4S] clusters from the $SufBC_2D$ machinery via three conserved Cys residues, before transferring them to client apoproteins. A-type carriers are expected to provide an important level of diversity and control in tailoring [Fe-S]-cluster delivery to a broad range of client proteins (Roche *et al*., 2013). In *E. coli*, A-type SufA, IscA and ErpA (for essential respiratory protein A) are essential for cluster biogenesis in the presence of oxygen or other electron acceptors, as well as during iron-depletion (Johnson *et al*., 2006a; Gupta *et al*., 2009; Loiseau *et al*., 2007; Vinella *et al*., 2009; Angelini *et al*., 2008).

In *S. venezuelae and S. coelicolor*, the putative house-keeping *sufTUSC(fdx)DBR* operon is situated at the vnz_07605 - vnz_07640 (SCO1919 - SCO1926) locus (Table 1.2). The only identifiable A-type carrier in the genus is a distantly encoded ErpA homologue (vnz_08915; SCO2161). Unfortunately, limited investigation has been undertaken on this system within *Streptomyces*, although the *suf* pathway in the related pathogen, *M. tuberculosis*, has been somewhat better characterised (Huet *et al*., 2005; Tripathi *et al*., 2022) and these systems are well conserved across the bacterial domain. Even so, it has not been adequately ascertained how Wbl proteins acquire their [4Fe-4S] cluster *in vivo* and the regeneration of Holo-Wbl proteins poses an interesting basis for control of Wbl-signalling and function.

Table 1.2. The *suf* operon of *S. venezuelae* (*S. ven*) and *S. coelicolor* (*S. coe*) and their predicted encoded components. Experimental evidence presently available for these assignments is provided in the right column: (1) Tripathi *et al*., 2022 (2) Cheng *et al*., 2020 (3) Willemse *et al*., 2018 (4) Loiseau *et al*., 2007.

S. ven	*S. coe*	Name	Function	Ref.
vnz_07605	SCO1919	SufT	Auxiliary factor	1
vnz_07610	SCO1920	SufU	U-type scaffold	-
vnz_07615	SCO1921	SufS	Cysteine desulphurase	-
vnz_07620	SCO1922	SufC	[Fe-S] Chaperone ATPase	-
vnz_07625	SCO1923	Fdx	[2Fe-2S] Ferredoxin	-
vnz_07630	SCO1924	SufD	[Fe-S] Chaperone assembly protein	-
vnz_07635	SCO1925	SufB	[Fe-S] Chaperone scaffold	-
vnz_07640	SCO1926	SufR	[Fe-S] Operon sensor-regulator	2, 3
vnz_08915	SCO2161	ErpA	A-type carrier protein	4

1.6. A molecular •NOmad: Nitric Oxide as a Signaling Molecule

The small, gaseous radical, nitric oxide (•NO), is an uncharged radical with a minimal dipole moment across its double bond which, together with its radical electron, yields a lipophilic character to the molecule. Consequently, •NO dissolves freely in both aqueous and hydrophobic environments, enabling its unimpeded diffusion through the cytoplasm *and* cell membrane, a feature that differentiates the molecule as a potent mediator of signals in biological systems. The signals generated by •NO can be transduced via direct or indirect pathways, within the cell.

Despite how nitric oxide is often portrayed, it is a relatively weak oxidant and is not capable of directly abstracting bis-allylic hydrogens from fatty acids (unlike •OH), an initiating step in the deleterious lipid peroxidation chain reaction. Nevertheless, •NO can directly *S*-nitrosylate metal centres, a signal seemingly sensed by the WhiB-like and NsrR proteins (Sections 1.4 and 1.6.2.3). The eminent effect of •NO is its direct, high affinity scavenging of other more damaging species, including the hydroxyl ($^{\bullet}OH^{-}$), lipid ($L^{\bullet}$), lipoxide ($LO^{\bullet}$), and lipoperoxide ($LOO^{\bullet-}$) radicals, effectively terminating their cognate chain reactions (O'Donnel & Freeman, 2001; Bulusu *et al*., 2019). Notwithstanding this, in the presence of the superoxide radical (O_2^{-}), •NO acts as a potent pro-oxidant, coupling at a diffusion-limited rate to produce the peroxynitrite anion, $ONOO^{-}$ (Huie & Padmaja, 1992). The $ONOO^{-}$ ion elicits signals via its rich oxidative chemistry, including, but not limited to, modification of protein residues (e.g. Tyr nitration and Cys oxidation; Bartesaghi & Radi, 2018), the formation of nitrogen oxide lipid adducts and initiation of lipid peroxidation (Rubbo *et al.*, 1994; O'Donnel et al., 2001; Wright *et al*., 2006). The oxidative activity of $ONOO^{-}$ is thought to comprise the majority of indirect signals by •NO; free transition metal centres in addition to reactive oxygen species, such as hydrogen peroxide (H_2O_2) can also promote the generation of $ONOO^{-}$ ions (Radi, 2004; Möller et al., 2019).

1.6.1. Endogenous Sources of Nitric Oxide in *Streptomyces* spp.

Whilst it is understandable that nitric oxide signals in pathogenic *Mycobacterium* spp. can be host-derived (i.e. during macrophage infection), how developmentally significant concentrations of •NO arise in free-living actinomycetes such as *Streptomyces* spp. was previously unclear. Recent work has since demonstrated that *Streptomyces* species are capable of generating •NO endogenously, via reductive and oxidative pathways (Sasaki *et al*., 2016).

1.6.1.1 Nitrite Reductase Derived •NO (Reductive Synthesis) and Signalling

In *S. coelicolor* •NO is produced endogenously via the reduction of nitrite at the active site of the dissimilatory nitrate reductase (NarGHI3) molybdoenzyme (Figure 1.12.a – Sasaki *et al*., 2016; Vine & Cole, 2011; Honma *et al*., 2021;). •NO production by *S. coelicolor* NarGHI3 has

been shown to directly control production of the antibiotic actinorhodin (ACT) via the •NO-sensing OsdRK two-component system, a homologue of the DosRS(T) dormancy factors of *Mycobacterium* spp. More specifically, •NO binds to the haem group of OsdK, inhibiting autophosphorylation and phosphotransfer to OsdR, thus inhibiting DNA binding activity. This relieves repression of the ACT pathway specific activator gene, *actII-4*, by OsdR and ultimately increases the production of ACT (Honma *et al*., 2021). The •NO-mediated signalling by OsdRK also modulates *S. coelicolor* entry into sporulation and negatively feeds back on the expression of *narGHI2* to control the levels of endogenous •NO (Urem *et al*., 2016; Fischer *et al.*, 2019; Honma *et al*., 2021). Regulatory agents required for development, such as the anti-anti-sigma factor BldG and the orphan RR, BldM, are also overexpressed in Δ*narGHI3* strains, suggesting a distinct role for nitrite derived nitric oxide signalling in early *Streptomyces* development and secondary metabolism (Honma *et al.*, 2022). Nitrite, which can therefore be viewed as a more stable source of •NO, also functions in inter-cell developmental coordination, exported via dissimilatory NarK pumps (Sasaki *et al*., 2014; Fischer *et al*., 2014; Yukioka *et al*., 2017). In *S. coelicolor*, NarGHI3 is just one of three dissimilatory (respiratory) nitrate reductases encoded within the genome, all of which are controlled developmentally and in response to oxygen availability, possibly indicating similar but specialised roles, compared to NarGHI3 (Fischer *et al*., 2014). The physiological effectors of •NO synthesis by NarGHI3 remain to be discovered.

1.6.1.2. Nitric Oxide Synthase Derived •NO (Oxidative Synthesis)

Intriguingly, *S. venezuelae* does not encode NarGHI enzyme systems; instead, it encodes a putative bacterial nitric oxide synthase (bNOS; *vnz_32420*), an obvious candidate for •NO signalling. The bacterial NOS enzymes are truncated in relation to their eukaryotic NOS counterparts, but catalyse an analogous, haem-dependent synthesis of •NO from the oxidation of L-arginine (Figure 1.12.b – Kers *et al*., 2004; Gusarov *et al*., 2008). The best-studied example in the *Streptomyces* genus is the *S. turgidiscabies* bNOS, TxtD, which generates •NO for the biosynthesis of the phytotoxin, Thaxtomin. The TxtD-derived •NO is ultimately utilised by TxtE Cytochrome P450 (CYP450) for oxidative nitration of L-tryptophan to the L-4-nitrotryptophan intermediate (Kers *et al*., 2004; Barry *et al*., 2012). Intriguingly, however, TxtD is capable of generating a diffusible signal via excess production of •NO (Johnson *et al*., 2008) which is perhaps of particular developmental interest in non-pathogenic species possessing bNOS homologues, such as *S. venezuelae* (vnz_32420). Nevertheless, their role in development has not yet been studied and only a limited number of *Streptomyces* species appear to encode bacterial Nitric Oxide Synthase (bNOS) enzymes.

1.6.1.3 An Expanded View of Reductive •NO production in *Streptomyces* spp.

The reductive generation of •NO in *Streptomyces* spp. closely resembles endogenous •NO synthesis in eukaryotes. Echoing the results that have emerged in eukaryotes, perhaps •NO synthesis could occur much more broadly within the cell at a range of Molybdenum centres (Bender & Schwarz, 2018). Five members of the eukaryotic molybdenum (Mo)-dependent enzyme family (mARC; aldehyde oxidase; nitrate reductase; sulfite oxidase; xanthine oxidoreductase) are known to reduce nitrite to •NO along physiological oxygen and pH gradients, whereby oxygen appears to function as a competitive inhibitor to nitrite reduction (Godber *et al*., 2000; Li *et al*., 2004; Li *et al*., 2009; Sparacino-Watkins *et al*., 2014; Wang *et al.*, 2015). All *Streptomyces* species conserve an assimilatory nitrate reductase (*nasA*; *vnz_11080*, *sco2473*) and two conserved, albeit putative, xanthine dehydrogenase operons (vnz_29425-35 and vnz_13285-75), which could also theoretically contribute to •NO synthesis via their Molybdo-centres, similar to NarGHI3 (Wang & Zhao, 2009; Chandra and Chater, 2014).

1.6.2. •NO Homeostasis and Detoxification

Despite its multi-faceted roles in cell-signalling and radical termination, the majority of signals transduced via •NO are oxidative and thus can become toxic to a cell (collectively known as nitrosative stress), so its tension must be tightly regulated. Due to the reactive nature of •NO, especially with O_2^- and other ROS such as H_2O_2, antioxidant enzymes such as superoxide dismutase and catalase, can also mitigate the cellular damage mediated by nitric oxide by-products. In eukaryotes, superoxide dismutase (SOD) can prolong •NO half-life and signalling via this approach (Radi, 2004). However, the following sections refer to the specific pathways of •NO detoxification and homeostasis.

1.6.2.1. Nitrite Assimilation

It follows that, if •NO is formed from reduction of NO_2^- *in vivo*, alternative pathways which utilise and redirect intracellular NO_2^- can forestall NO generation whilst simultaneously maintaining NO_2^- homeostasis, preventing toxicity. In *S. coelicolor*, the conserved assimilatory nitrite reductase $NirB_1B_2D$ is central to nitrogen metabolism and reduces intracellular NO_2^- to ammonium (NH_4^+). Deletion of *nirB1B2D* yields markedly increased expression of *hmpA1*, which can be seen as a function of •NO concentration (see Section 1.6.2.3), suggesting a significant homeostatic role in *Streptomyces* •NO synthesis (Yukioka *et al*., 2017). Moreover, Δ*nirB1B2D* mutants also exhibited dysregulated Undecylprodigiosin production, reinforcing the link between •NO and secondary metabolism. It seems likely, therefore, that other significant nitrite sinks, such as export by NarK-type pumps, could also have an effect on •NO-homeostasis but

this remains to be determined experimentally (Fischer et al., 2014; Sasaki *et al*., 2016). Similar homeostatic functions for NirBD and NarK have been proposed in *M. tuberculosis*, especially during dormancy (Tan *et al*., 2010).

1.6.2.2. Low Molecular Weight (LMW) Thiols; Mycothiol

Low molecular weight (LMW) thiols refer to small, organic compounds characterized by the presence of a redox active sulfhydryl (-SH) functional group. In cellular systems, LMW thiols often serve as antioxidants, providing a buffer against oxidative damage. However, mycothiol (MSH) is an evolutionarily unique low-molecular-weight thiol found only in Actinobacteria, including *Mycobacterium* and *Streptomyces* spp. However, it conserves many of the characteristics of the widespread glutathione (GSH); scavenging free radicals, serving as a cofactor for antioxidant enzymes and acting as a cysteine reserve which, together, provide comprehensive protection against oxidative and nitrosative stress (Newton *et al*., 1993; Newton *et al*., 1995; Newton *et al*., 2008).

Mycothiol can undergo *S*-nitrosylation by nitric oxide, effectively sequestering the radical and yielding *S*-nitrosomycothiol (MSNO). In *Mycobacterium* spp., MSNO is reduced by the bifunctional MSNO/formaldehyde reductase (MscR). MscR, has a high specific activity towards MSNO, catalysing its reduction to the disulphide mycothione (MSSM), releasing NO_3^- back to the nitrogen oxide cycle, see Figure 1.11 (Vogt *et al*., 2003). The NADPH-dependent disulphide reductase, Mtr, catalyses the subsequent regeneration of MSH from MSSM (Newton et al., 2008). *Streptomyces* spp. possess a clear orthologue of the MscR protein (vnz_06235), indicating that a similar antioxidant pathway exists for MSNO in this organism. Moreover, some Actinobacteria possess the rare capability to synthesise the LMW thiol Ergothioneine, *de novo* (EGT - Newton *et al*., 1993). In *M. smegmatis*, EGT seems to play a specific role in managing nitrosative stress, whereas its protective role appears to be more general in *S. coelicolor* (Vargas *et al*., 2016; Nakajima *et al*., 2015). Nevertheless, specific details are lacking for this rare thiol.

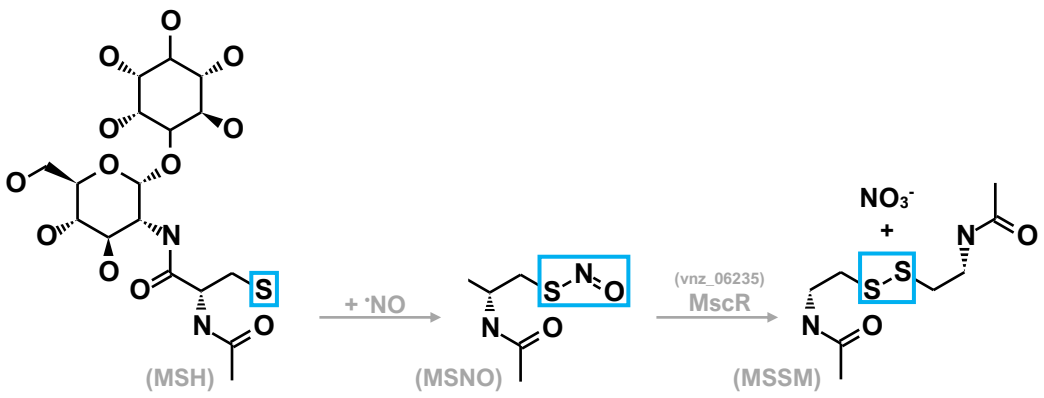

Figure 1.11. Chemical structure of mycothiol (MSH), *S*-nitrosylation by nitric oxide and detoxification of *S*-nitrosomycothiol (MSNO), to mycothione (MSSM) and nitrate. The sulfhydryl group and its derivatives are outlined in blue.

1.6.2.3. Flavohaemoglobins (Nitric Oxide Dioxygenases)

Flavohaemoglobins (Hmp) are the pre-eminent agents of •NO detoxification inside bacterial cells and present a highly conserved tripartite modularity, with tandem NAD-binding, FAD-binding and globin (haem-binding) domains. The globin domain of Hmp preferentially binds nitric oxide (•NO) via oxidative *S*-nitrosylation of the ferrous haem iron (II) centre to Hmp-Fe(III)-NO (Kim *et al*., 1999; Poole, 2020) and reduces this to nitrate in the presence of NADH and molecular oxygen (O_2), completing the nitrogen oxide cycle (Figure 1.12). It has also been reported that Hmp functions anaerobically, whereby •NO can be reduced to N_2O by NADH at the Hmp-haem, albeit at a slower rate (Kim *et al*., 1999; Hausladen *et al*., 2001; Bonamore & Boffi, 2008; Poole, 2020). Intriguingly, there are subtle evolutionary discrepancies in Hmp-mediated nitric oxide detoxification between model *Streptomyces* species; *S. coelicolor* possesses two flavohaemoglobins, which are encoded by *hmpA1* and *hmpA2* (SCO7428 and SCO7094) and repressed by the [4Fe-4S] Rrf2-family regulator NsrR, relieving repression in response to •NO binding the Fe-S cluster (Munnoch *et al*., 2015). On the other hand, *S. venezuelae*, encodes three putative *hmpA*-like genes (vnz_14270; vnz_18160; vnz_35655), which do not seem to be regulated by the evolutionarily divergent NsrR 'homologue' RsrR (Crack *et al*., 2016; Munnoch *et al*., 2016).

1.6.2.4. Nitrobindins: Potential •NO-shuttles

The Nitrobindins (Nbn) are a conserved family of hydrophobic (10-stranded) β-barrel proteins possessing a central solvent-exposed ferric haem iron (III) that selectively binds •NO. Nitrobindins are conserved eukaryotic proteins, however, their distribution amongst bacteria is curiously restricted to the Actinobacteria phylum and all *Streptomyces* species conserve a *nbn*-like gene within their genomes (Chandra & Chater, 2014). *In vitro*, the *M. tuberculosis* and *H. sapiens* Nbn proteins catalyse analogous OH^--mediated (alkaline-dependent) conversion of •NO to HNO_2 concomitant with unique, reductive *S*-nitrosylation of the haem iron (III) by a second •NO molecule, yielding Nbn-Fe(II)-NO (Figure 1.12.a). Evidence of a similar mechanism has been documented for *S*-nitrosylation of the *A. thaliana* (plant) Nbn (Bianchetti *et al*., 2010; De Simone *et al*., 2020a & 2020b). In addition, both *M. tuberculosis* and *H. sapien* Nbn(III) have been shown to be capable of scavenging and detoxifying the superoxide termination product, $ONOO^-$, which protects L-tyrosine against nitration, *in vitro* (De Simone *et al*., 2020). Unfortunately, there is currently a poor understanding of how this relates to the intracellular environment of specific organisms. The closely related 8-stranded β-barrel Nitrophorins (Npn) are equally as elusive but work in the haematophagous insect, *Rhodnius prolixus*, has indicated a role in •NO-trafficking to ultimately promote vasodilation of their blood-prey (Ribeiro et al., 1993; Weichsel et al., 1998). Thus, a similar role has been projected for Nbns. In bacteria, Nbns closely match the distribution

of Wbl proteins, inspiring the hypothesis that they may contribute to Wbl-signalling via •NO-scavenging at the cluster, or from *S*-nitrosothiol groups, with subsequent detoxification and/or trafficking in cooperation with mycothiol (Chandra & Chater, 2014). However, as of yet, these remain hypothetical functions and lack empirical evidence.

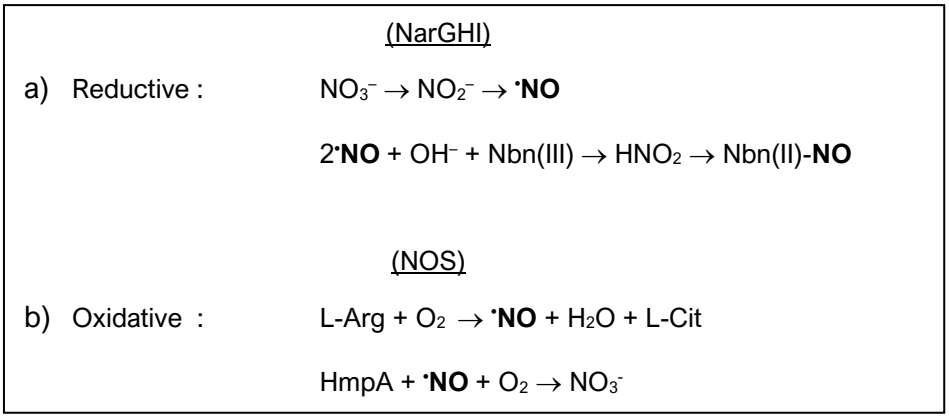

Figure 1.12. Reaction schemes for **(a)** reductive and **(b)** oxidative routes for •NO-synthesis (enzymes shown to right) and detoxification (enzymes incorporated into reaction schemes).

1.7. Summary and Thesis Aims

Streptomyces spp. and similar related organisms undergo a complex, multicellular developmental program reminiscent of fungi but atypical for bacteria; The *Streptomyces* developmental program is underpinned by an array of small molecules, including c-di-GMP, GlcNAc and *S*-adenosylmethionine which act as pivotal developmental signals. The WhiB-like proteins stand out among developmental regulators of *Streptomyces* spp., binding [4Fe-4S] clusters, with mounting evidence for a global, pleiotropic transcriptional function, with *in vitro* evidence for •NO-specific sensing capabilities, especially when in complex with partner proteins. The model species, *S. coelicolor*, has provided evidence for robust pathways for production, detoxification, and potentially trafficking of •NO; the fact that modulating •NO biogenesis can affect both *Streptomyces* development and secondary metabolism begs the question of the depth and complexity to this signal in *Streptomyces* spp.

This thesis explores these themes through the study of the putatively essential *wblE* gene, and its product within *S. venezuelae* strain NRRL B-65442, more specifically:

- To develop a protocol for the heterologous expression and purification of WblE, in order to confirm that it binds a [4Fe-4S] cluster via *in vitro* biochemical analyses.

- Utilise CRISPR-Cas9 technology to probe the essentiality of *wblE* gene and specific components of the gene's product; are the conserved cysteine residues and thus [4Fe-4S] cluster essential for function? Can WblE be tagged with an affinity epitope for whole-cell immunoprecipitation experiments?

- Determine whether WblE binds a global gene regulon via chromatin immunoprecipitation and confirm binding against genes *in vitro*.

- Analyse the WblE interactome using co-immunoprecipitation to attempt to provide a more detailed cellular context to the function of the WblE protein.

Chapter 2

Materials and Methods

2.1. Chemicals and Reagents

Chemicals and reagents used were generally purchased from Sigma Aldrich (UK) or Thermo Fisher Scientific (UK) and are laboratory grade or above (>99%) unless otherwise stated.

2.2. Bacterial Strains and Growth Media

The bacterial species and strains used or generated in this thesis can be found in the appended Table A.3. Working concentrations of antibiotics used for selection are listed in Table 2.1. Growth media are listed in Table 2.2. *E. coli* strains were routinely grown shaking at 220 rpm, in LB broth or on LB agar at 37°C and *S. venezuelae* were grown at 30°C.

Table 2.1. Antibiotics used in this thesis, their solvents, and working concentrations for selection.

Antibiotic Compound	Working conc. (μg.mL^{-1})	Solvent
Apramycin	50.0	dH_2O
(Ampicillin) Carbenicillin	(120.0) 100.0	50% EtOH
Chloramphenicol	25.0	100% EtOH
Hygromycin	50.0	dH_2O
Kanamycin	50.0	dH_2O
Streptomycin	50.0	dH_2O
Nalidixic Acid	25.0	0.3 M NaOH
Thiostrepton	25.0	DMSO

Table 2.2. Growth media used throughout this thesis, and their composition (per L).

Media Name	Composition (per L)		Water	pH
Maltose Yeast Malt (MYM)	4 g	Maltose	Tap & dH_2O 1:1	7.2 - 7.3
	4 g	Yeast Extract (Oxoid)		
	± 20 g	Agar		
Soya Flour Mannitol (SFM)	20 g	Soya Flour	Tap water	-
	20 g	Mannitol		
	20 g	Agar		
Minimal Media (MM)	0.5 g	K_2HPO_4	dH_2O	7.0 - 7.2
	0.2 g	$MgSO_4 \cdot 7H_2O$		
	10 mg	$FeSO_4 \cdot 7H_2O$		
	1.0 g	$(NH_4)_2SO_4$		
	± 15 g	Agar		
Luria-Bertani (LB)	5 g	Yeast Extract	dH_2O	-
	10 g	NaCl		
	10 g	Tryptone		
	± 20 g	Agar		
Luria (L)	5 g	Yeast Extract	dH_2O	-
	0.5 g	NaCl		
	10 g	Tryptone		
	± 20 g	Agar		
2x Yeast Tryptone (2YT)	16 g	Tryptone	dH_2O	7.0
	10 g	Yeast Extract		
	5 g	NaCl		
5x M63 Media (5x M63)	10 g	$(NH_4)_2SO_4$	dH_2O	7.0
	68 g	KH_2PO_4		
	5 mg	$FeSO_4 \cdot 7H_2O$		
	10 mg	Vitamin B1 (Thiamine)		
	1 in 5	Dilution in dH_2O / WA		
Water Agar (WA)	20 g	Agar	dH_2O	-
Tryptone Soya Broth (TSB)	30 g	Oxoid TSB (CM0129)	dH_2O	-

2.3. Measuring Optical Density of Cell Cultures

Optical density measurements were carried out at a wavelength of 600 nm (OD_{600}), using a Genesys 10S UV-Vis (Thermo Scientific™) spectrophotometer. Undiluted culture was used for OD_{600} measurements of *E. coli* and *B. subtilis*. *S. venezuelae* spore stocks were diluted 1 in 20, or 1 in 50 with 20% Glycerol prior to OD_{600} measurements.

2.4. Preparation and Transformation of Electrocompetent *E. coli* strains

A single healthy colony of the required *E. coli* strain was inoculated from LB medium in to 10 mL LB broth (with relevant antibiotics) for overnight growth at 30 or 37°C, 250 rpm. This starter culture was sub-cultured to 200 mL and grown under the same conditions to an OD_{600} of 0.50 - 0.55. Cells were pelleted via centrifugation at 4,000 rpm, 4°C, for 10 minutes and washed twice in 10% (v/v) glycerol. Cells were ultimately resuspended in 2 mL 10% (v/v) glycerol and dispensed as 50 µL aliquots, which were flash frozen in liquid nitrogen and transferred to – 80°C, for storage. Vessels used for *E. coli* (Falcon® and micro-centrifuge tubes) and pipette tips were stored at – 20°C, before and between use. Glycerol solutions were maintained at ≤ 4°C.

To transform *E. coli*, approximately 0.15 - 0.3 µg of DNA was added to 50 µl of electrocompetent cells, in an ice-cold electroporation cuvette, and the mix was electroporated on a BIO-RAD® electroporator (Set to: 200 Ω, 25 µF and 2.5 kV). The electroporated cells were immediately diluted in ice-cold L or LB broth and transferred to a micro-centrifuge tube for non-selective recovery at 37°C and 250 rpm, for 40 to 60 minutes. Recovered cells were plated on appropriately selective L or LB agar and grown overnight at 37°C for transformant selection.

2.5. Preparation and Transformation of Chemically Competent *E. coli* strains

To prepare chemically competent cell-lines, a healthy culture of the required *E. coli* strain was grown and pelleted as previously described. *E. coli* strains were washed twice in 10 mL of $CaCl_2$ (0.1 M) and Glycerol (10% v/v) solution and ultimately resuspended in 2 mL of the $CaCl_2$-glycerol solution. The cells were dispensed as 100 µL aliquots into micro-centrifuge tubes, flash frozen in liquid nitrogen and transferred to – 80°C for storage. Vessels used for *E. coli*, pipette tips and glycerol solutions were also chilled prior to use.

To transform *E. coli*, approximately 0.15 - 0.5 µg of DNA was added to 100 µl of chemically competent cells, mixed, and incubated on ice for 30 minutes. This mixture was then heat-shocked for 35 – 40 seconds at 42°C and immediately placed back onto ice for 5 minutes. Cells were diluted in L or LB broth for non-selective recovery at 37°C and 250 rpm shaking, for 40 to

60 minutes before being plated on appropriately selective media to grow overnight at 37°C for transformant selection.

2.6. Preparation of *Streptomyces* Spore Stocks

S. venezuelae spore stocks were generated from confluent lawns grown on MYM + TE for four days. Spores were gently dispersed into 10 mL dH_2O with a sterile cotton-bud, transferred to a Falcon tube and centrifuged at 4,000 rpm 4°C for 10 minutes. Spore pellets were resuspended in 20% glycerol. A portion of spores were left as a concentrated stock and the rest were normalised to an OD_{600} of 1.0. All stocks were stored at -20°C.

2.7. Preparation of Genomic DNA (gDNA) from *Streptomyces* spp.

S. venezuelae NRRL B-65442, or its derivatives, were inoculated into TSB and grown overnight at 30°C, 250 rpm. This culture was centrifuged at 4,000 rpm for 15 minutes and the mycelia flash-frozen, thawed, and resuspended in 400 µL SET Buffer (75 mM NaCl, 75 mM EDTA, 20 mM Tris-HCl, pH 7.2) in a micro-centrifuge tube. Lysozyme (50 $mg.mL^{-1}$), RNase A (1 $mg.mL^{-1}$) solutions were added to final concentrations of 5 $mg.mL^{-1}$ and 0.1 $mg.mL^{-1}$ respectively, and the mixture incubated at 37°C for 1 hour with occasional agitation. The digested mycelia were placed on ice and SDS was added to a final concentration of 1%. An equal volume of phenol-chloroform was added to the reaction and thoroughly mixed. The mixture was centrifuged at 15,000 rpm and 4°C for 15 minutes, and the aqueous layer separated. This process was repeated until minimal protein precipitate was present at the solvent interface. The upper aqueous layer was added to around three volumes of ice-cold 100% EtOH and inverted by hand until DNA precipitated. The precipitate was pelleted via centrifugation at 15,000 rpm, 4°C, for 20 minutes, washed in 500 µL ice-cold 80% EtOH and allowed to air-dry before being thoroughly resuspended in cold dH_2O and refrigerated overnight. The concentration of purified *S. venezuelae* genomic DNA was normalised to about 100 $ng.\mu L^{-1}$ and aliquots stored at 4°C or -20°C.

2.8. Primer and Oligonucleotide Design

A table of all primers used in this work can be found in the thesis appendix (Table A.1). All primers used in this work were designed on ApE (a plasmid editor) to possess a 16 - 26 bp priming region (not including overhangs) with a T_m generally between 60°C and 63°C. Designed primers were ordered as custom oligonucleotides from Integrated DNA Technologies (IDT®).

Several mutant gene fragments were synthesised by IDT® and can also be found in the appendix, Table A.2.

2.9. Polymerase Chain Reaction (PCR)

For the amplification of DNA, the work reported in this thesis employed two DNA polymerases. The Q5® (NEB) High-Fidelity DNA polymerase was used to amplify DNA fragments which were destined for cloning. Alternatively, the PCRBIO® *Taq* Mix (Red) DNA Polymerase (from PCR Biosystems) was generally used for diagnostic amplifications, such as *S. venezuelae* and *E. coli* colony PCR (see Section 2.10). Reactions were generally conducted using the schemes and mixtures outlined in Table 2.4. The C1000 Touch (BIO-RAD®), DNA Engine PTC 300 (BIO-RAD®) and XT96 (VWR®) thermal cyclers were used interchangeably.

2.10. Colony PCR

2.10.1. *E. coli* Colony PCR

E. coli colony were taken directly from plates or cell pellets, following centrifugation, and used directly as the template for PCRBIO® *Taq* mix PCR reactions using the *Taq* mix reaction scheme (Table 2.3.a)

2.10.2. *S. venezuelae* Colony PCR

An approximately 3 - 5 mm^2 area of confluent mycelia was scraped from the *S. venezuelae* strain of interest, mashed in 200 µL 12% (v/v) DMSO, and incubated at 85^{o}C for 30 minutes. The mixes were vortexed briefly and allowed to cool before a 1 µL aliquot was taken as the 'colony' to provide the template for subsequent PCR amplification with PCRBIO® *Taq* mix or Q5 polymerase (Table 2.3.a & b), using the Q5 Reaction scheme and a 60 or 65 second extension (Table 2.4.a). Samples were frozen for reference.

Table 2.3. PCR reaction mix compositions for (a) NEB Q5® and (b) PCRBIO® *Taq* polymerases

(a) NEB Q5® Mix	
Component	Volume (µL)
5x Q5 Reaction Buffer	5.00
40 mM dNTPs	0.50
10 µM Forward	1.25
10 µM Reverse	1.25
100% DMSO	1.00
template	1.00 - 2.00
Q5 Polymerase	0.25
dH_2O	13.75 - 14.75
Total	25.00

(b) PCRBIO® *Taq* Mix	
Component	Volume (µL)
2x *Taq* Mix (red)	5.00
40 mM dNTPs	0.50
10 µM Forward	2.00
10 µM Reverse	2.00
100% DMSO	1.00
Template	(or colony) 1.00
dH_2O	7.50
Total	25.00 (or 26.00)

Table 2.4. PCR thermocycler reaction schemes for (a) Q5® and (b) PCRBIO® *Taq* reactions

(a) NEB Q5® Reaction Scheme			
Stage	Temperature	Period	
Melting DNA (1)	98°C	2 minutes	
Melting DNA (2)	98°C	15 seconds	32 x
Annealing	55°C or 62°C	15 seconds	
Extension	72°C	45 seconds per kbp	
Final Extension	72°C	5 minutes	
Hold	4°C	Indefinite	

(b) PCRBIO® *Taq* Reaction Scheme			
Stage	Temperature	Period	
Melting DNA (1)	98°C	2 minutes	
Melting DNA (2)	98°C	15 seconds	30 x
Annealing	55°C or 62°C	15 seconds	
Extension	72°C	30 seconds per kbp	
Final Extension	72°C	5 minutes	
Hold	4°C	Indefinite	

2.11. Purification of PCR Products

Amplified PCR products were purified directly from their reaction mixtures using QIAquick columns (QIAGEN®), or Monarch® PCR Clean-up Columns (NEB®), according to the manufacturers' protocols.

2.12. Agarose Gel Electrophoresis

Gels were made by dissolving agarose to a final concentration of 1% (w/v) in TAE Buffer (40 mM Tris, 20 mM ethanoic acid, 1 mM EDTA), with the addition of 1% (10 $mg.mL^{-1}$) stock ethidium bromide to a final concentration of 0.3 $\mu g.mL^{-1}$ and subsequent setting within a gel mould. Samples of DNA were loaded with 6x Tri-Track (Thermo Scientific™) or 6x Purple Loading Dye (NEB®) and run alongside 1kb Plus, 1 kb, or 100 bp DNA Ladders from NEB®. Electrophoresis was carried out at 120 V for 35 minutes or 90 V for 60 minutes in a Sub-cell GT electrophoresis system (Meridian Bioscience®; formerly BIOLINE). The DNA was visualised by transillumination with UV-light, using a Molecular Imager Gel Doc System (BIO-RAD®).

2.13. Purification of Amplified DNA from Agarose Gels

Electrophoresed samples were transilluminated with UV-light, and the desired fluorescent bands excised (with minimal excess gel). No prior UV-imaging was undertaken. The gel slice was dissolved and the DNA extracted with the Monarch® Gel Extraction Kit (NEB®), according to the manufacturer's protocol but with a single wash step and elution with dH_2O. When used for standard cloning (Section 2.17.2) or Gibson assembly (Section 2.18), the purified DNA was processed a second time using a Monarch® PCR Clean-up Columns (NEB®), including both wash steps, and elution in dH_2O.

2.14. Quantification of DNA Concentrations

Isolated DNA was analysed using the Nanodrop 2000 or DeNovix DS-11 UV-Vis spectrophotometers and the Qubit® assay using the Qubit® fluorimeter 2.0. Both the high-sensitivity and the broad-range kits were used depending on the sample concentration estimated by Nanodrop.

2.15. Preparing Vector DNA from *E. coli* (Mini-prep)

Plasmid DNA was routinely extracted from an appropriately selective overnight culture of *E. coli* Top10, DH5α or NEB5α holding the desired plasmid. Purification was carried out using the Wizard® *Plus* SV Miniprep System (Promega®), according to the manufacturer's centrifugation-based protocol. Elution was carried out in 60 - 100 µL dH_2O and prepared vectors were stored at -20°C.

2.16. Generating the pCRISPomyces-2 CRISPR-Cas9 Systems

Deletion of the *S. venezuelae wblE* gene was achieved with the pCRISPomyces-2 CRISPR-Cas9 system, as described by Cobb *et al.* (2015). A protospacer was designed with homology to a unique 20 bp region within, or close to, the *wblE* coding sequence. Iterative BLASTn searches were performed against the *S. venezuelae* NRRL B-65442 genome to ensure that ≥ 50% of the protospacer was unique, including all four possible combinations of the protospacer adjacent motif (PAM, 5'-NGG-3'). The forward and reverse protospacer sequences were ordered as two ssDNA oligonucleotides from IDT® and annealed by heating an equimolar mixture at 95°C for 5 minutes followed by ramping to 4°C at 0.1°C/second. The annealed protospacers were cloned into the BbsI site of the pCRISPomyces-2 vector via Golden Gate assembly (Section 2.17.3), to function as part of the synthetic guide RNA (sgRNA). An

approximate 2 kbp homology repair template was PCR-amplified as fragments from purified *S. venezuelae* NRRL B-65442 genomic DNA. The two flanking arms were Gibson-assembled into an XbaI-digested pCRISPomyces-2 vector (Section 2.17.4). The final, sequenced plasmid was transferred to the desired *S. venezuelae* strain via conjugation with *E. coli* ET12567 pUZ8002 as described in (Section 2.19.2).

2.17. Vector Manipulation and Cloning

2.17.1 Restriction Digests

CutSmart® collection restriction enzymes (NEB®) were used to digest plasmid DNA in 50 µL reactions, in accordance with product guidelines. Digestion of 2 µg of DNA was typically performed at 37°C for 4 hours by adding 2 units of the appropriate restriction enzyme(s). To prevent re-ligation, the linearised vector was dephosphorylated via the addition of 2 µL rapid Shrimp Alkaline Phosphatase (rSAP, NEB®) and incubated at 37°C for a further 20-30 minutes. Enzymes and DNA were separated by gel electrophoresis; the required bands were excised, and gel extracted (Section 2.13) for downstream applications. Linear DNA fragments used for cloning were digested identically, with the exclusion of rSAP treatment.

2.17.2. Standard Cloning; Plasmid-Insert Ligations

Ligation reactions were carried out using the NEB® T4 DNA Ligase, according to the manufacturer's protocol. A molar ratio of 3:1, insert to plasmid, was used routinely for ligation reactions. This was calculated using the (NEB) NEBio Ligation Calculator, which automatically accounts for differences in the molecular weight of the DNA (https://nebiocalculator.neb.com).

2.17.3 Golden Gate Assembly

Golden gate assembly reactions were conducted with 50 – 100 ng purified pCRISPomyces-2 backbone and 0.3 µL of the desired insert in the presence of 2 µL T4 ligase buffer (NEB®) and 1 µL T4 ligase (NEB®) with 1 µL BbsI (NEB®) and dH2O to a total volume 20 µL. This was run in a thermocycler for 10 minutes at 37°C, 10 minutes at 16°C, 5 minutes at 50°C, 20 minutes at 65°C, for a total of 10 cycles. The products were held at 4°C. Assembly of the synthetic protospacers was confirmed by blue/white screening on LB + X-Gal (40 $\mu g.mL^{-1}$) and sequencing by Eurofins™.

2.17.4 Gibson Assembly and Associated Mutagenesis

Genes and multiple DNA fragments possessing 18-30 nucleotide complementary overhangs were assembled directly into digested plasmids using the Gibson Assembly Master Mix (NEB®). A 3:1 ratio of insert to vector was used routinely, reactions were performed at 50°C for 30 minutes. Single nucleotide changes and knockout sequences were reciprocally incorporated within complementary DNA overhangs before assembly, using relevant primers.

2.18. Sequencing of Plasmids and Linear DNA Fragments

Plasmid DNA and linear fragments were confirmed by Sanger sequencing using the Mix2Seq service provided by Eurofins Genomics. Plasmid DNA and the relevant primer, was diluted in dH_2O according to the manufacturer's specifications, with the addition of DMSO to a final concentration of 5%.

2.19. *Streptomyces* Conjugations

Conjugative plasmid transfer into *Streptomyces* spp. was achieved using methods which were adapted from those reported in the 'Practical Streptomyces Genetics' manual (Kieser *et al*., 2000).

2.19.1. Conjugating Integrative Vectors

The non-methylating *E. coli* strain ET12567 pUZ8002, carrying the pIJ10257 or pSS170 plasmids (and their derivatives) were inoculated from a 25% glycerol stock (Section 2.2) into 10 mL L broth containing the relevant antibiotics, and grown overnight at 37°C with 250 rpm shaking. This culture was pelleted at 13,000 rpm and washed three times in 1 mL L broth. The final pellet was resuspended in 200 µL L broth to form a 50x cell concentrate. To promote germination, a 50 µL aliquot of concentrated *S. venezuelae* spores was diluted 1:10 (v:v) in 2YT broth and statically incubated at 30°C for around 30 minutes, prior to conjugation. These pre-germinated *S. venezuelae* spores were pelleted via centrifugation at 4,000 rpm and resuspended in the 50x *E. coli* ET12567/pUZ8002 cell-concentrate. The resulting cell-spore mix was dispensed as 10^0 - 10^{-2} dilutions (in dH_2O), spread evenly across SFM plates containing 10 mM $CaCl_2$, and incubated at 22°C for 18h. Successful ex-conjugants were selected via the application of a 1.1 mL Hygromycin (1.50 $mg.mL^{-1}$) and Nalidixic Acid (0.75 $mg.mL^{-1}$) antibiotic solution and homogenization of the growing bacterial lawn. To recover exconjugants, plates

were incubated at 30°C for 3 - 4 days of growth. Growing exconjugants were streaked on MYM (+ TE 1:500) and selected with Hygromycin.

2.19.2. Conjugating pCRISPomyces-2 CRISPR-Cas9 Vectors

The non-methylating *E. coli* strain ET12567/pUZ8002, carrying the assembled pCRISPomyces-2 plasmid-derivatives, was inoculated from a 25% glycerol stock into appropriately selective LB broth and grown overnight (37°C, 250 rpm). The culture was subsequently inoculated 1:10 in fresh LB (plus relevant antibiotics) and grown to an OD_{600} of 0.80 - 0.85. The culture was pelleted at 4,000 rpm for 10 minutes, washed three times in 1/10 culture volume LB broth (no antibiotics), and ultimately resuspended in 1/100 culture volume LB broth (100x cell-concentrate). All *E. coli* ET12567 wash and centrifugation steps were performed on ice or at 4°C.

A 20% glycerol spore stock of the *S. venezuelae* strain was diluted 1:10 in 2YT broth and incubated statically at 30°C for 45 minutes, to promote germination prior to conjugation. These pre-germinated spores were centrifuged at 4,000 rpm for 10 minutes and resuspended in 200 µL 100x cell-concentrate for every 100 µL of initial spore inoculum. The cell-spore mix was dispensed as undiluted aliquots of 200 µL, spread evenly across SFM plates containing 10 mM $CaCl_2$, and allowed to grow at 22°C for 18 h. Exconjugants were selected via homogenisation of the growing bacterial lawn with 1.1 mL Nalidixic Acid (0.75 $mg.mL^{-1}$, WT only), or Hygromycin (1.50 $mg.mL^{-1}$) and Apramycin (1.50 $mg.mL^{-1}$) solution. Following antibiotic selection, the plates were dried in a laminar flow and transferred to 30°C. For qualitative/test knockouts, a range of spore densities (OD_{600}) were employed. However, for the quantified conjugations of pCi24255KO (Section 2.20), spore stocks of the test strains were normalised to an OD_{600} of 1.0 (Section 2.3).

2.20. Quantifying Frequency of pCi24255KO Exconjugant Survival

2.20.1. Viable Spore Counts (Colony Forming Units)

The OD_{600} 1.0 normalised spore stocks were serially diluted by a factor of $5x10^{-7}$, $5x10^{-8}$ and $5x10^{-9}$, in a final volume of 1 mL. From these dilutions, 200 µL aliquots were plated and the number of colonies were counted after 3 days of growth. The $CFU.\mu L^{-1}$ were determined by inverting the dilution factors respectively. Significant differences between strains were determined via parametric paired *t*-tests in Graphpad Prism 9. Controls had no significant difference and were grouped.

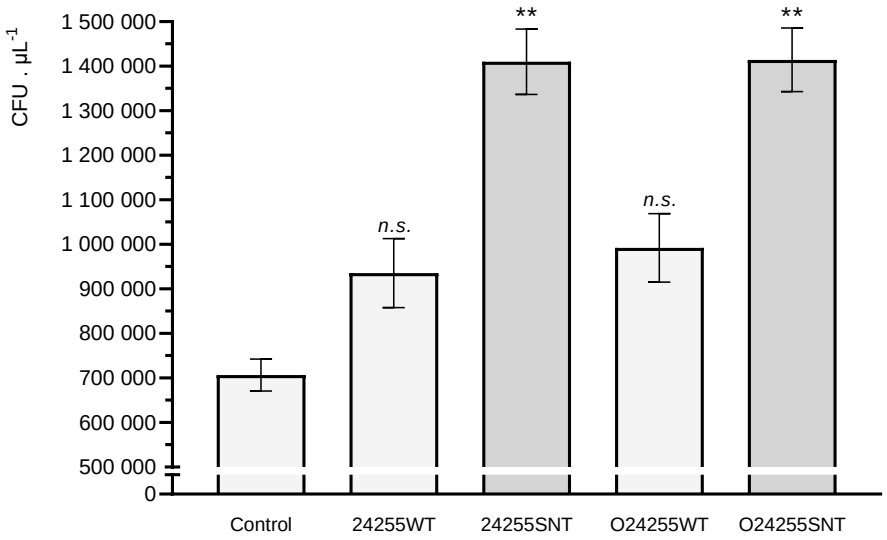

Figure 2.1. Viable spore counts of control strains (WT, pSS170, pIJ10257, *n* = 3 each) and test strains (24255WT / SNT and O24255 WT / SNT, *n* = 9 each). The strains carrying Cas9-protection (SNT) are highlighted in a darker shade. *n.s.* = $p > 0.05$, ** = $p > 0.025$ (Unpaired parametric *t*-tests)

2.20.2. Calculating Conjugation Efficiency and KO frequency

Following conjugation of the pCi24255KO vector into *S. venezuelae* (Section 2.19.2), the exconjugants were grown at 30°C for 6 days. The number of exconjugants which grew were counted for each conjugation plate and divided by the number of spores added to the conjugation reaction, as determined by the CFU/spore counts (Section 2.20.1). As fixed volumes were used for conjugations but significant differences existed between the number of viable counts of some strains, the resulting conjugation frequency was normalised to the control group the lowest $CFU.uL^{-1}$ (WT strain). Means were calculated from the adjusted frequency for each strain. Mann-Whitney U (non-parametric) tests were employed to determine significant differences between strains. A total of up to 50 strains were analysed by PCR amplification of the *wblE* locus (Section 2.20.3) to estimate the KO frequency in each strain; this was calculated separately.

2.20.3. Confirming Knockouts by PCR amplification of the *wblE* locus

To assess whether *wblE* had been deleted at its native locus, the DNA sequence covering the *wblE* gene and the 3' HRT border were amplified by *Streptomyces* colony PCR (Section 2.10.2) with the primer pair LB038R and LB040F (Q5 program) or the optimized pair LB129F and LB040R (*Taq* program). Primer set that was used are stated on gel figures.

2.21. WblE Chromatin-Immunoprecipitation and Sequencing (ChIP-Seq)

The WblE ChIP-seq protocol employed was adapted from those published by Matt Bush *et al.* (2016), and in the PhD thesis of Rebecca Devine (Devine, 2018). The protocol was carried out in technical duplicate between wild-type *S. venezuelae* NRRL-B65442 and three independent strains of *S. venezuelae* Δ*wblE* :: pSS24255CF (see Section 4.7). For each strain, fresh spore stocks were prepared from four-day old confluent lawns and normalised to an OD_{600} of 0.05, with dH_2O. Normalised stocks were plated in aliquots of 250 µL onto solid MYM (+ TE 1:500) overlaid with 325P cellophane discs. Plates were incubated at 30°C for 18 h, 25.5 h or 42 h of growth.

To cross-link proteins and DNA, cellophane discs were liberated from the medium, at the desired time point (18 h, 25.5 h or 42 h), and submerged upside down in 20 mL of a 1% Formaldehyde-PBS solution (pH 7.4) at room temperature, for 20 minutes. Cellophane discs were subsequently transferred to 20 mL of 0.5 M glycine for 5 minutes, to quench the cross-linking reaction. The mycelium was harvested and washed twice with 25 mL ice-cold PBS (pH 7.4) centrifuging at 4,000 rpm, removing the supernatant after each wash. Samples were flash frozen in liquid nitrogen and stored at -80°C until required.

From here on, each time-point was processed individually (groups of 8) and EDTA-free protease inhibitor tablets were added to all buffers, excluding the elution buffers (1 per 10 mL; Roche complete™ mini). To lyse the samples, the harvested mycelia were resuspended in 750 µL lysis buffer (10 mM Tris-HCl pH 8.0, 50 mM NaCl, 10 $mg.mL^{-1}$ lysozyme) and incubated at 37°C for 30 minutes. To complete lysis, and fragment the DNA, 750 µL 1x IP buffer (100 mM Tris-HCl pH 8.0, 250 mM NaCl, 0.5% v/v Triton X-100, 0.1% w/v SDS) was added and mixed with the partially digested samples. Samples were sonicated on ice using a Soniprep 150 (MSE) at 50 Hz (8 µm amplitude), 20s on and 60s off for 20 cycles, per sample. A 25 µL sample of the resulting crude lysates were mixed with 75 µL TE buffer (10 mM Tris-HCl, 1 mM EDTA pH 8.0) and the DNA extracted with 100 µL phenol-chloroform. The aqueous top layer was taken and stored as 'pure extract', of which 25 µL was treated with 2 µL RNase I (1 $mg.mL^{-1}$) for 30 minutes, at 37°C, and run on a 1% agarose gel (see Section 2.12) to visualise DNA fragment sizes. Once fragment size was confirmed to be within the desired range, the remaining crude lysate was centrifuged at 13,000 rpm for 15 minutes to clear the sample of debris.

A 400 µL volume of magnetic, monoclonal M2 antibody beads (Anti-FLAG® - Sigma-Aldrich®) was prepared by two sequential washes in 2 mL 0.5x IP buffer (1x IP diluted 1:1 with dH_2O). For all bead wash steps, a magnetic field was applied to gather the beads and remove the buffer. The magnetic beads were ultimately resuspended in 400 µL 0.5x IP buffer, divided equally

between the 8 samples, and incubated at 4°C overnight on a vertical rotor. The beads were washed a further four times with 500 µL 0.5x IP buffer for 10 minutes at 4°C, on a vertical rotor.

To elute immunoprecipitated DNA-protein complexes, 100 µL bead elution buffer (1% SDS, 10 mM Tris-HCl, 1 mM EDTA, pH 8.0) was added to each sample and incubated at 65°C overnight. The elution buffer was removed and an additional 50 µL was added for an additional 5 minutes, at 65°C. The final 150 µL eluate was incubated at 55°C for 1.5 h with 2 µL proteinase K (10 $mg.mL^{-1}$) and the DNA was extracted with 150 µL phenol-chloroform. The aqueous layer was removed and cleaned on a QIAquick® (Qiagen®) DNA column and eluted in 50 µL Qiagen® elution buffer (10 mM Tris-HCl, pH 8.5). A 2 µL aliquot was used to measure the concentration of DNA, via Qubit, and the remaining volume was snap frozen, and stored at -80°C.

Duplicate samples for all time-points, generated from the WT control and a single test strain (#1) were sent to Novogene for 150 bp paired-end (PE) 20 million read, Illumina sequencing.

2.21.1. Raw ChIP-Seq Data Analysis

The raw Illumina sequencing data was returned as FASTQ format files, which were processed by Dr. Govind Chandra (JIC). A 3000 nt region around the ChIP enrichment peaks was used as the background model to arrive at a local enrichment. Associated *p*-values are based on T-tests between replicates of the samples and the corresponding controls. The reads were aligned against the reference genome for *Streptomyces venezuelae* NRRL B-65442 (NCBI Accessions NZ_CP018074.1 & NZ_CP018075.1; Gomez-Escribano *et al*., 2021) and plotted with quantitative data as '.Bedgraph' files. A cut-off of at least a log2-fold change (2-fold enrichment) with statistical significance ($p < 0.05$*) within at least one of the tested time-points, was applied to the data. Data was visualized using Integrated Genomics Viewer (IGV; Robinson *et al*., 2011) and manually edited with a graphical overlay.

2.21.2. MEME-ChIP Analysis

In order to identify a potential consensus sequence, MEME-Chip was performed using the online meme-suite (https://meme-suite.org/meme/tools/meme-chip). To prepare sequence data, 20 bp regions directly under the apex of each significant peak were extended by 240 bp bidirectionally to generate 500 bp FASTA files (Group_All.txt; 90 sequences). The 'atypical group' peaks were excluded from this analysis (see Chapter 5), but no limit was set for the distance of a peak to the potentially regulated gene(s). Sequences were run against the combined MEME database for Prokaryotic transcription factors binding sites, searching with a

third order background model for three motifs, between 10bp and 15bp, and within a 100 bp central region.

2.21.3. Determining Transcriptional Start Sites (TSS) and WblE Consensus Spacing

Transcriptional start sites (TSSs) for *wblE* genes highlighted in the WblE ChIP-seq were identified using the previously acquired differential (d)RNA-seq timecourse (10, 14, 18, and 24 h) dataset for *S. venezuelae* NRRL B-65442 grown in liquid MYM + TE media. The raw data for this experiment is available on ArrayExpress under accession number E-MTAB-10690 (Buttner *et al*., 2021). The 50 bp region preceding TSSs, were searched for the consensus sites of WblE, as determined by MEME-ChIP (Section 2.21.2), and σ-factor HrdB. The dRNA-seq and ChIP-seq data were visualised in parallel in IGV to determine correlation between the ChIP-seq enrichment peak and putative consensus sites.

2.22. Surface Plasmon Resonance

To test the binding of WblE to promoter DNA *in vitro, s*urface plasmon resonance (SPR) was performed using the ReDCaT method (Stevenson *et al.*, 2013; Stevenson and Lawson, 2021). Experiments were performed in collaboration with Dr Rebecca Devine, who was trained by Clare Stevenson. All buffers used in SPR were filtered through a 0.22 µm filter. The target promoter was fragmented to yield 40 bp segments, overlapping by 15 bp. These sequences were ordered as single-stranded DNA oligos (IDT®) with the reverse-orientation oligos carrying a 20-nucleotide sequence, complementary to the biotinylated ReDCaT linker (5' – CCTACCCTACGTCCTCCTGC – 3'). A full list of oligonucleotides used for SPR can be found in Table A.4. Complementary ssDNA oligonucleotides were diluted to equimolar (100 µM) concentrations, in water, and annealed by heating to 90°C and cooling by 0.1 °C s^{-1} to 4°C, in a thermocycler.

The single-stranded biotinylated ReDCaT DNA-linker (GCAGGAGGACGTAGGGTAGG) was annealed on a Streptavidin Sensor Chip SA (Cytiva™) by Dr Clare Stevenson, and docked in a Biacore 8K+ SPR System (Cytiva™). The WblE-C6xHis protein was diluted to 1000 nM, 100 nM, and 10 nM in standard HBS-EP+ buffer (150 mM NaCl, 3 mM EDTA, 0.05% (v/v) surfactant P20, 10 mM HEPES, pH 7.4). The MtrA-N6xHis protein was diluted to concentrations of 500 nM, 50 nM and 5 nM in high salt HBS-EP+ buffer (300 mM NaCl), Runs used the respective HBS-EP+ buffer, dH_2O, 1 M NaCl and 50 mM NaOH as reagents. The prepared dsDNA promoter fragments were captured on the chip by flowing them over the surface for 60 seconds at 10 µl/min.

The protein of interest was flowed over the chip at 50 µl/min for 60 seconds, allowing protein to bind, followed by another 60 seconds of HBS-EP+ buffer alone to allow the interaction to stabilise. The binding response was recorded at both early and late time-points. A final 'regeneration' step was performed using the 1 M NaCl and 50 mM NaOH reagents (60 seconds at 10 µl.min^{-1}) to removed protein and DNA from the chip before the next cycle. The level of protein binding to the immobilised DNA was measured in arbitrary response units and then expressed as a percentage of the theoretical maximum response, Rmax, where 100% represents the response expected for the mass of the protein or protein complex, which is flowing over the chip and binding to one immobilized dsDNA oligonucleotide.

2.23. Scanning Electron Microscopy

Scanning electron micrographs were acquired primarily by Dr Kim Findlay but also by myself with supervision. *S. venezuelae* colonies (incubated for 3 to 7 days) were mounted on the surface of an aluminum stub with 'optimal cutting temperature compound' (Agar Scientific Ltd.), plunged into liquid nitrogen slush at approximately -210°C to cryopreserve the material, and transferred to the cryo-stage of an Alto 2500 cryotransfer system (Gatan - AMETEK®) attached to a FEI Nova NanoSEM 450 (ThermoFisher Scientific®). Residual frost was sublimated at -95°C for 4 minutes before the sample was sputter coated with platinum at ≤ -110°C for 2 min. The sample was moved onto the main stage of the microscope, maintained at -125°C, and finally viewed with 3 kV primary beam energy.

2.24. Heterologous Expression of *wblE*

The *wblE* gene was codon-optimised for *E. coli* and cloned into a pET28a(+) vector by Genscript™ (Table A.3). The same codon-optimised gene was also cloned into pET29b(+) and pCOLAduet1 plasmids, which were transformed into *E.coli* BL21 λDE3 cells via heat-shock (Section 2.5). Strains carrying the expression constructs were sub cultured inoculated into LB broth (with Kanamycin) and grown to an OD_{600} of 0.6. Cultures were induced with 0.1 – 1 mM IPTG and incubated at 30°C, 200 rpm, for 50 minutes, then grown for 20 hours at 18 - 20°C, 150 rpm. For anaerobic purifications, cultures were supplemented with 200 µM ammonium ferric citrate and 30 µM methionine before growth at 18°C, to support [4Fe-4S] biogenesis (Crack *et al.*, 2014; Kudhair *et al*., 2017). Cells were pelleted via centrifugation at 4,000 rpm for 30 minutes, 4°C; the supernatant was discarded and the cell pellet used immediately for purification or snap-frozen in liquid nitrogen and stored at -80°C.

2.25. Protein Purification

2.25.1 (Anaerobic) Immobilised Nickel Affinity Chromatography

Buffer A (50 mM Tris, 20 mM Imidazole, 0.3 M NaCl, pH 7.5) and Buffer B (50 mM Tris, 0.5 M Imidazole, 0.3 M NaCl, pH 7.5) each were purged of oxygen, with pure Nitrogen gas for 30 minutes and stored in an anaerobic cabinet maintained at ≤10 ppm O_2 overnight, prior to purification. The transgenic *E. coli* cell pellet was thawed and re-suspended in around 20 mL Buffer A for every litre of culture used. To which, 1 mL lysozyme (30 $mg.ml^{-1}$ in Buffer A) was added and the solution pipetted to mix. Cells were kept on fresh ice and further lysed via sonication at 60% power 1 second ON, 2 seconds OFF for 8 m 20 s. A second, identical sonication was performed at 40% power. Cell lysate was ultra-centrifuged for 45 mins at 40,000 rpm, 4°C, and the clarified supernatant was collected in 50 mL Falcon® tubes and loaded onto an ÄKTA prime system, connected to a 5 mL HisTrap™ Column (Cytiva™), and equilibrated in Buffer A. Protein was eluted at a 1 $mL.min^{-1}$ flow rate over a concentration of 0 - 100% Buffer B, programmed at 5%.min^{-1}. Eluent was collected in 2 ml fractions and stored at 0-1 °C, ≤ 10 ppm O_2.

2.25.2 (Anaerobic) Heparin Resin Chromatography

Eluent from anaerobic IMAC purification (see section 2.25.1) was manually injected onto Midi-PD10 Desalting column (GE Healthcare) and eluted with Buffer C (50 mM Tris, 250 mM NaCl, 5% v/v glycerol pH 7.4) at 3 $mL.min^{-1}$. The protein solution was manually injected onto a 5 mL HiTrap™-HP Heparin column attached to an ÄKTA prime system, pre-equilibrated in Buffer C and eluted at 1 $mL.min^{-1}$ over a 0 - 100% gradient (5.0 %.min^{-1}) of Buffer D (50 mM Tris, 850 mM NaCl, 5% glycerol pH 7.4). Eluant was collected in 2 mL fractions and stored at 0 - 1°C, ≤ 10 ppm O_2.

2.25.3 (Aerobic) Immobilised Nickel Affinity Chromatography

Aerobic purifications were carried out in a similar fashion to anaerobic purifications with several key changes. Notably, Buffers were modified to A1 (10% glycerol, 50 mM Tris, 0.3 M NaCl, 20 mM Imidazole, pH 7.55) and B1 (10% Glycerol, 50 mM Tris, 0.3 M NaCl, 0.4 M Imidazole pH 7.55). The buffers were filtered and degassed at ≤ 4 °C prior to purification. Cell debris was separated via centrifugation at 15,000 rpm, 4°C for 45 minutes. The clarified supernatant was loaded onto an ÄKTA pure system, connected to a 1 mL HisTrap™-HP Column (Cytiva™), and sequentially washed with 5 column volumes (c.v) 20% 40% and 60% Buffer B1. Finally, bound protein was eluted with 100% Buffer B1 onto the ÄKTA loop.

2.25.4 (Aerobic) Preparative Gel Filtration

Analytical gel filtration was performed on a Superdex™ 75 Increase 10/300 GL column (Cytiva™), maintained at 4°C, equilibrated and eluted in Buffer A1 or B1 (Section 2.25.3). The mass of eluted proteins was estimated via their elution volume, with reference to a calibration curve generated with Aprotinin, Ribonucelase A, Carbonic Anhydrase, Ovalbumin and Conalbumin (Dr Sibyl Batey, Figure 2.2). The equations used to convert elution volume to approximate molecular weight are shown below; where '*v.v.'* denotes the column's void-volume (9.09 mL), '*c.v.'* is the column's total volume and values for equation (2) are derived from the logarithmic gradient of the standard curve (Figure 2.2) and equation (1); see below. Protein fractions were analysed by SDS-PAGE (Section 2.31).

$$K = \frac{Elution\ Volume - v.vv}{c.v. - v.v.} \qquad (1)$$

$$Mw = e^{\left(\frac{K-2.2406}{-0.198}\right)} \qquad (2)$$

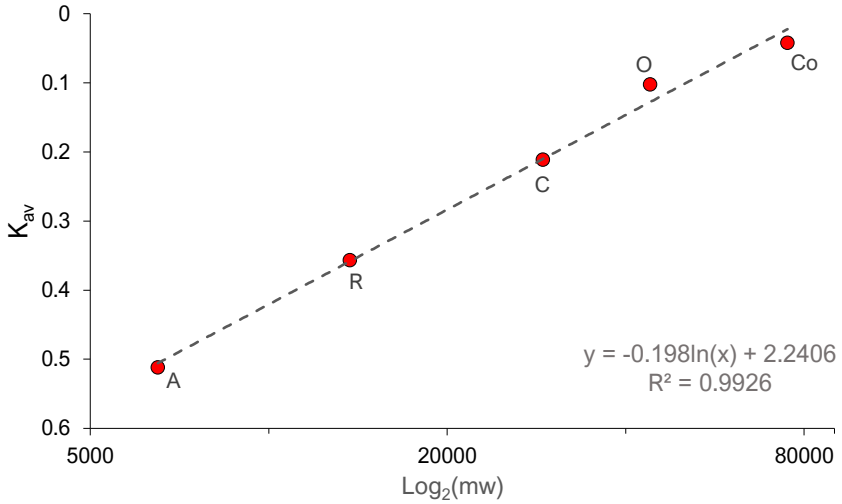

Figure 2.2. Superdex 75 Increase 10/300 GL calibration curve for the K_{av} (elution volume parameter) against their molecular weights: aprotinin (A – 6.5 kDa); Ribonuclease A (13.7 kDa - R); Carbonic Anhydrase (C – 29 kDa); Ovalbumin (O – 44 kDa) and (Co – 75 kDa) Conalbumin. Standard curve gradient and R^2 depicted in bottom right of graph. Note the Log2 scale for molecular weight.

2.26. Spectroscopic Analysis

2.26.1 UV-Vis Spectroscopy

UV-Vis Absorbance spectra for WblE were obtained using a JASCO V500 Spectrophotometer scanning at a rate of 200 $nm.min^{-1}$, with a 2 nm bandwidth and medium response level. Measurements were taken over the range of 260-900 nm, with a sample number of 800 and 1 cycle. Automatic baseline correction was enabled. Samples were measured in an anaerobically sealed, air-tight cuvette.

2.26.2 Circular Dichroism Spectroscopy

Circular Dichroism spectra were obtained using a JASCO J810 Spectropolarimeter, scanning continuously at 200 $nm.min^{-1}$, at a sensitivity of 100 mdeg. Spectra obtained for wavelength ranges of 280-500 nm (2 nm bandwidth) and 450-900 nm (manual bandwidth; slit width set to 120 μm). Five measurements were taken for both ranges and mean results were merged at overlapping wavelengths. Samples were in measured in an anaerobically sealed, air-tight cuvette.

2.27. Determination of Percent [4Fe-4S] Cluster Incorporation

Cluster incorporation was determined, via the ratio of protein to free iron in denatured samples, as calculated by Bradford and Ferene Assays described below. Assays were performed using NHis-WblE protein, anaerobically purified via IMAC and Heparin chromatography (Sections 2.25.1 – 2.25.2).

2.27.1 Bradford Assay for Protein Concentration

Heparin purified WblE was used to provide an accurate estimate of cluster incorporation. Commercial Bradford assays are adapted from Bradford (1976). A solution of 5x Concentrate Bradford dye reagent (BIO-RAD®) was prepared by diluting at a ratio of 1:5 with dH_2O. A 1 $mg.ml^{-1}$ stock of BSA was diluted to generate a range of five standards, ranging from 0.2 – 1.0 $mg.ml^{-1}$. Protein samples were left undiluted. The Bradford reagent was added at a volume of 980 μL to 20 μL of each protein solution. Mixtures were left for 5 minutes and then absorbance was measured at 595 nm in 1 mL cuvettes. Sample concentration was estimated by comparing absorbance to that of the known standards.

2.27.2 Ferene Free-Iron Assay

The Ferene (5,5′(3-(2-pyridyl)-1,2,4-triazine-5,6-diyl)-bis-2-furansulfonate) Free Iron Assay provides an estimate of Fe^{2+} content (Crack *et al.*, 2006). A 20 µL aliquot of the samples/controls were heated at 95°C in 100 µL of 21.7% nitric acid (HNO_3) and cooled on ice. Samples were centrifuged at max speed for 10 seconds, to separate any protein precipitate, before 600 µL 7.5% (w/v) ammonium acetate and 100 µL fresh 12.5% ascorbic acid (w/v) were added and solutions mixed by inversion. Standard iron solutions (SpectrosoL, VWR™) were prepared in the range of 0–200 µM. A 100 µL aliquot of 10 mM Ferene was added and solutions mixed again by inversion. Following 30 minutes incubation at room temperature, absorbance was measured at a wavelength of 593 nm.

2.28. Native, Electrospray-Ionisation Time-of-Flight (ESI-) Mass Spectrometry

ESI-MS Experiments were performed in collaboration with Dr. Melissa Stewart. Heparin-purified Holo-WblE was exchanged into 250 mM ammonium acetate pH 8.0 using a midi-PD10 desalting column (GE Healthcare), under anaerobic conditions. Samples were subsequently loaded directly into the ESI-source of a Bruker micrOTOF-QIII mass spectrometer operating in the positive ion mode, using a gas-tight 500 µL syringe (Hamilton) and a flow rate of 0.3 $mL.hr^{-1}$. The oTOF Control software was used to set the dry gas temperature at the source as 180 °C, with a gas flow rate of 4 $L.min^{-1}$ and nebulizer gas pressure of 0.8 Bar. The source capillary voltage was set at 4500 V, with an offset of -500 V. The Quadrupole was set at an ion energy at 5 eV, a collision cell radio frequency of 650 Vpp, and a collision cell energy of 10 eV. Processing and analysis of MS experimental data was carried out using Compass DataAnalysis version 4.1 (Bruker Daltonik, Bremen, Germany) and *m/z* spectra were deconvoluted for masses ranging between 9,000 - 15,000 Da using the ESI Compass Maximum Entropy deconvolution algorithm (version 1.3). Exact masses (< ±1 Da) are reported from peak centres representing the isotope average neutral mass.

2.29. Denaturing Polyacrylamide Gel Electrophoresis (SDS-PAGE)

Resolving gels were prepared to a concentration of 16-20% (w/v) Acrylamide:Bis-Acrylamide (37.5:1 Fisher Bioreagents), following the recipe in Table 2.5 and cast using a BIO-RAD® Mini-PROTEAN® Tetra gel system with 1 mm glass spacer plates and polymerised at room temperature. A short stacking gel (Table 2.5) was cast atop the resolving gel, and a 1 mm comb used to set the lanes. Gels were submerged in TGS Buffer (25 mM Tris HCl pH 8.3, 192 mM Glycine, 1% SDS v/v) and run at 200 V for 1 hr, then 100 V until finished. Occasionally, commercial 12% Tris-Tricine Gels were used (Abcam®), which were run at 150 V for 1.5 hr. Gels

were incubated at room temperature in Coomassie instant blue stain for 2 hr and left to de-stain in dH_2O overnight.

Table 2.5. SDS-PAGE gel recipe

Component	Resolving Gel (16%)	Stacking Gel (6.5%)
dH_2O	3.4 mL	2.7 mL
1.5 M Tris pH 8.8	2.5 mL	-
1 M Tris pH 6.8	-	0.5 mL
40% acrylamide	4.0 mL	0.6 mL
10% SDS	50.0 µL	20 µL
10% APS	100 µL	40 µL
TEMED	10 µL	4 µL
Total	10.06 mL	3.86 mL

2.29.1 SDS-PAGE M2 Anti-FLAG Western Blots

Colonies of *S. venezuelae* Δ24255CF (see Appended table A.5) were grown on MYM agar (+ 1:500 TE + Hygromycin) for around 40 hours and resuspened in 100 µL 2x NuPAGE LDS loading buffer, without additives, and boiled at 100°C for 15 minutes. Samples were centrifuged at 13,000rpm for 15 minutes and 20 µL aliquots of the denatured samples were run on SDS-PAGE gels as specified in the previous section (see Table 2.5).

Four layers of blotting paper were soaked in transfer buffer (25 mM Tris HCl, 192 mM glycine, 0.1% w/v SDS, 20% v/v methanol, pH 8.0) for 5 minutes and placed on the anode and cathode plates of a Trans-blot® Turbo (BIO-RAD®). A PVDF membrane (BIO-RAD® - 0.2 µm pore size) was soaked in 100% methanol for 1 minute, then transfer buffer for 5 minutes. The membrane was placed atop the blotting paper on the anode plate and the SDS-PAGE gel was sandwich between this and those on the cathode plate. Air bubbles were gently rolled out. The blot was run using the mini-midi standard setting (SD, 25 V, 1A, 30 min).

The membrane was subsequently incubated in Blocking solution (5% w/v fat-free skimmed milk powder in TBST) for 2 hours. The membrane was then incubated in 20 mL M2 Anti-FLAG solution, prepared 1:20,000 in TBST (20 mM Tris HCl, 150 mM NaCl, pH 8.0).

Membrane was washed with TBST thrice for 1 minute. Excess TBST was disposed and Solution A (0.02% H_2O_2 in Tris HCl, pH 8.0) and Solution B (0.1% Luminal v/v, 0.005% v/v coumaric acid in Tris HCl, pH 8.0) were mixed directly on the membrane. After incubation for 2 minutes with gentle agitation, the chemiluminescence was detected using an ImageQuant™ LAS 500 (GE Healthcare UK Limited).

2.30. WblE Co-Immunoprecipitation, Mass Spectrometry (CoIP-MS)

Co-immunoprecipitation of WblE was carried out in technical triplicate between wild-type *S. venezuelae* NRRL-B65442 and three independently generated *S. venezuelae* Δ24255CF (or CFLAG) strains (#1 - #3). The preparation of samples was performed using the same method previously described for WblE chromatin-immunoprecipitation but with only 8 cycles of sonication. At the point of sample elution, 30 µL of 1x modified Laemmli SDS loading dye (62.5 mM Tris-HCl pH 6.8, 0.05% w/v bromophenol blue, 2.5% w/v SDS, 11.25% v/v glycerol, 2.5% v/v β-mercaptoethanol) was added to each sample, which were placed in an oven, pre-heated to 100°C, for 6 minutes. Samples were briefly centrifuged at 1,000 rpm and the solution loaded onto a 10% SDS-PAGE resolving with no stacking layer (Table 2.5).

Samples were electrophoresed at 150V for 6 minutes. The gel-casing and wells were washed thoroughly with tap-water. Each sample well was excised down to the dye front and stored at -20°C overnight prior to washing. To prepare the cross-linked proteins for MS analysis, each were subject to a series of washes. Samples were twice statically incubated at 65°C, in 1 mL fresh 30% ethanol for 30 minutes to bleach gel-slices of bromophenol blue. Bleached slices were subsequently washed with TEAB-ACN (50 mM TEAB in 50% acetonitrile) for 20 minutes on a VXR vortexer (IKA®, max rpm) followed by a static wash in DTT-TEAB (10 mM DTT, 50 mM TEAB), for 30 mins at 55°C. Samples were alkylated via the addition of IAA-TEAB (30 mM iodoacetamide, 50 mM TEAB), and incubated at RT for 30 minutes in the dark, on a vortexer (max rpm). The IAA-TEAB solution was removed and the samples washed in the same way for a further 20 minutes in TEAB solution. This was then repeated with TEAB-ACN for 20 minutes.

The buffer was removed and the slice volume (mm^3) was estimated, before being divided into approximate 1 x 1 mm^3 segments and transferred to a LoBind® microcentrifuge tube. The samples were washed for 20 minutes in TEAB-ACN on a vortex (max rpm), subsequently repeated with 100% ACN instead. A < 1 mm diameter hole was pierced in the lid, and samples dried with a gene-vac, running the 'low boiling point' program for 30 minutes. The final, prepared samples were submitted for mass spectrometric analysis.

2.30.1 SAINT Analysis for Affinity Mass Spec

The co-immunoprecipitation data was processed with the SAINTexpress pipeline (Teo *et al*., 2014) by Dr Carlo Martins and Dr Gerhard Saalbach (John Innes Centre). The fold-change and BFDR outputs were reported to two decimal places.

2.30.2 Building *in silico* Interaction Networks

A cut-off of ≤ 0.1 BFDR and at least a three-fold enrichment was set for *in silico* network building. The current StringDB (2022/23) SVEN_ (peripheral) network was used to provide a 'skeleton' physical interaction network, which was manually expanded in Cytoscape™, using relevant literature searches and comparisons made with the better-annotated 'SCO' (*S. coelicolor* A3(2)) and 'Rv' (*M. tuberculosis* H37Rv) networks.

2.30.3 SignalP6.0 Analysis of Secretion Signal Peptides

To identify known signal peptides SignalP6.0 analysis (Teufel *et al*., 2022) was performed on the DTU Health Tech Webserver (https://services.healthtech.dtu.dk/services/SignalP-6.0/), against a complete list of translated coding sequences from the *Streptomyces venezuelae* NRRL-B65442 genome. This was compared to the WblE CoIP-MS results and the percentage of secreted proteins was calculated.

2.31. Bacterial Two-Hybrid

The bacterial two-hybrid assay was performed by co-transforming *E. coli* strain BTH101 with pUT18/pUT18C (T18 domain fusion) vectors proteins together with pKT25/pKNT25 vectors encoding relevant T25 domain fusion proteins. Transformant strains were grown with LB broth and medium that omitted glucose. The 5x M63 broth was diluted in WA (Table 2.2) and supplemented with the antibiotics ampicillin and kanamycin to select for the two plasmids, and with 40 µg/ml X-gal to allow for visualisation of a positive interaction through the activity β-galactosidase (blue stain). The medium also contained a final concentration of 0.5 mM IPTG to induced expression of the fusion protein from the *lac* promoter. Starter cultures were grown in LB broth (no glucose) to 0.40 OD_{600} and 500 µL was pelleted at 13,000 rpm for 1 min and washed twice in 250 µL 1x M63 (diluted in dH_2O), cells were subsequently plated as 3 µL aliquots of the final mixture. Alternatively, co-transformed BTH101 strains were spread directly from a frozen stock. The plates were imaged at growth after 1, 2 and 3 days at 30°C or at 3 and 5 days at 22°C.

2.32. BLASTp Analysis and Alignments

2.32.1. Standard BLASTp and Pairwise Sequence Alignment

Standard BLASTp searches were performed using the NCBI web-portal (https://blast.ncbi.nlm.nih.gov/). Pairwise alignment of amino acid sequences were carried out with EMBL-EBI's EMBOSS Needle program (https://www.ebi.ac.uk/Tools/psa/).

2.32.2. Reciprocal (and Recursive-Reciprocal) BLASTp Analyses

Reciprocal (r-), and recursive reciprocal (rr-), BLASTp searches were performed by Dr Govind Chandra (JIC), whereby the 14 Wbl proteins of *S. coelicolor* A3(2) were used as input queries against an up-to-date library of 7,941 Actinobacterial genomes. A loose *e*-value cut-off of ≤ 0.1 was applied.

2.32.3. Flanking Genes (FlaGs) Analysis

Synteny describes the co-localisation and co-linearity of genetic loci within an organism's genome. Conserved, or shared, synteny between organisms can be a strong indicator for a functional relationship among genes, especially when observed over long evolutionary periods (Overbeek *et al*., 1999; Gabaldón *et al*., 2004). This can be useful for inferring putative gene functions in the absence of prior knowledge. In order to determine conserved synteny in the *wblE* gene neighbourhood, analysis was performed using the Web-FlaGs (Flanking Genes) tool (https://server.atkinson-lab.com/webflags; Saha *et al*., 2020) which provides a web-based analysis of predicted orthologous neighbourhoods to assess synteny. The WblE (WhiB1) protein sequences from model actinomycetes *C. glutamicum* ATCC 13032 (Kyowa Hakko), *M. tuberculosis* H37Rv, *B. longum* NCC 2705 and *S. venezuelae*, were individually submitted to WebFlaGs, and the BLASTp function was enabled to automatically generate a broader dataset of 30 related homologues for each genus. In an attempt to limit the identification of highly similar WblE paralogues, a strict *E*-value ($E = 1x10^{-20}$) cut-off was used. Otherwise, the WebFlaGs analysis was carried out under the default settings.

2.33. General Graphs and Figures

Generally, graphs were generated with GraphPad Prism v9 (by Dotmatics), or Excel®. Arrangement of photographs and to-scale graphical overlays (ChIP-seq) were achieved in Powerpoint®.

2.34. ReDirect Recombination

ReDirect λ-Red mediated recombination was carried out by Dr Neil Holmes. Primer pairs HNA397 – HNA398 and HNA397 – HNA185 were used to confirm the presence of the native *wblE* locus and *wblE*::*aac(3)IV* locus respectively.

2.35. Macroscopic Imaging of Colonies

Plate images were taken as scans using an 'EPSON® Perfection V600 Photo' (Seiko Epson® Corp, Suwa, Nagano, Japan) scanner at 600 DPI resolution. Macroscopic 4K images taken for *S. venezuelae* NRRL B-65442 and mutant strains were taken at a distance of 15 cm from the plate with a 'DMC-LX15' 4K camera (Panasonic® Corp, Kodama, Osaka, Japan).

Chapter 3.

Purification and Biochemical Characterisation of the WblE Protein

3.1. Introduction

The small WhiB-like proteins ligate iron-sulphur clusters via their conserved arrangement of four cysteine residues (Cys-X_n-Cys-X_2-Cys-X_5-Cys). Several Wbl proteins encoded by *M. tuberculosis* and *S. coelicolor* were originally purified with [2Fe-2S] clusters, however following anaerobic reconstitution could bind [4Fe-4S] clusters (Jakimowicz *et al*., 2005; Singh *et al*., 2007; Alam *et al*., 2007 and 2009; Crack *et al*., 2010). It is thought that holo-Wbl proteins primarily ligate a [4Fe-4S] cluster *in vivo*, which is reinforced by the cryo-EM structures of WhiB(A) and WhiB7, which resolve a [4Fe-4S] cluster in the σ^{HrdB}/σ^{A} transcriptional complex (Lilic *et al*., 2021; 2023). Additional characteristics such as the formation of multimers is common but not universally conserved across the family (Chawla *et al*., 2018; Stewart *et al*., 2020). Nevertheless, no work has tested whether these characteristics are retained by the *Streptomyces* WblE protein. This chapter outlines the purification and *in vitro* characterisation of *S. venezuelae* holo-WblE and its iron-sulphur cluster, in addition to preliminary investigations into apo-WblE and the formation of WblE multimers.

3.2. Heterologous Expression of WblE in *E. coli* BL21 (DE3)

In general, N-terminal tags have worked well for the *in vitro* analysis of Wbl-proteins (Smith *et al*., 2010; Stewart *et al*., 2020). As such, the *S. venezuelae wblE* gene was codon optimised and cloned by Genscript into the multiple cloning site (MCS) of NdeI and HindIII digested pET28a(+) such that the optional N-terminal 6xHis-tag was incorporated, with a thrombin cleavable linker (HHHHHHSSGLVPRGSH-WblE, 101 aa); the theoretical molecular weight of the recombinant WblE-N6xHis peptide was 11,676 Da (g/mol). The pET28a(+)-NWblE plasmid was subsequently transformed into chemically competent *E. coli* BL21 DE3 (strain BL21-NWblE). To test expression an initial 10 mL test culture was induced with 0.4 mM IPTG for 30 minutes at an OD_{600} of 0.60. Whole cell extracts of this culture were loaded onto a denaturing SDS-PAGE gel which resolved a broad band at a position corresponding closely to the predicted weight (~12 kDa), indicating successful expression (Figure 3.1). For large scale purification, the culture volume of BL21-NWblE was increased to 4 L and supplemented with 250 μM ammonium ferric citrate and 50 μM methionine to support long-term extensive iron-sulphur biogenesis. It is

believed that ammonium ferric citrate provides a soluble and non-toxic source of iron ions whereas methionine provides a source of sulphur and supports cysteine biosynthesis by saturating its biosynthetic pathways with precursors whilst avoiding cysteine-toxicity (Crack *et al*., 2014).

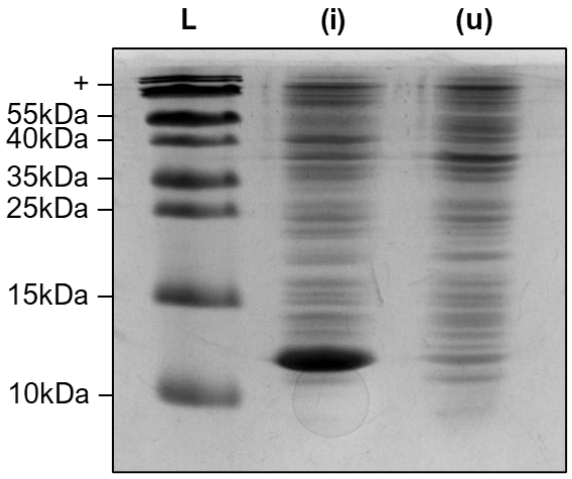

Figure 3.1. 20% SDS-PAGE of whole-cell extracts from 10mL *E.coli* BL21 6xNHis-WblE culture that was (i) induced with 0.4mM IPTG for 1 hour; or (u) uninduced. Run for 1 hour at 200V.

3.3. Anaerobic Purification and Analysis of Holo-WblE

3.3.1. Anaerobic Immobilised Nickel Affinity Chromotography.

The [4Fe-4S] ligating monomers of Wbl proteins are notoriously sensitive to oxygen and many degrade upon contact with air. As such, in order to circumvent oxygen-mediated degradation of the cluster, purification and subsequent storage of WblE was carried out in an anaerobic cabinet maintained at ≤ 10 ppm O_2. Cell pellets were harvested from 4 litres of BL21-NWblE culture and resuspended in 80 mL Buffer A, lysed extensively on ice and the crude lysate was clarified by ultracentrifugation (Section 2.25.1). The supernatant was loaded onto a HisTrap™-HP column connected to an ÄKTA prime and eluted over a linear gradient of Buffer B into 2 mL fractions. The 280 nm absorbance profile of the eluent was tracked during elution (Figure 3.2.a) and three distinct absorbance peaks were clearly observed during this process.

The six fractions which spanned these peaks (F7-12), were collected and an undiluted 6 µL aliquot of each fraction was loaded on to a 20% SDS-PAGE gel in loading dye and run for 200 V for 1 hr and then 100 V for 1 hr. The primary species collected in solution was visually confirmed as a 12 kDa protein, close to the predicted molecular weight for WblE-N6xHis (11,676 Da).

Typically, the first peak eluted represents histidine rich or nickel chelating proteins that bind non-specifically to the column and represent the bulk of non-specifically binding protein contaminants; this corresponded with F6 and F7. The subsequent fractions spanning the second peak eluted with a deep orange-yellow or 'straw' colour which was indicative of a bound [4Fe-4S] cluster (F8 & F9, Figure 3.2). In contrast, later fractions would elute with a pale-pink hue, possibly indicating a mixture of [4Fe-4S] and [2Fe-2S] cluster species (F11 & F12, Figure 1.A). A significant amount of a red-brown species seemed to precipitate on the HisTrap column. It seems likely that this was [2Fe-2S] WblE and would explain the seemingly incomplete elution of a red species into fractions spanning the third peak in the elution profile (F11 and F12). Fractions F8 and F11 best demonstrated these characteristics visually and are shown in Figure 3.2.

3.3.2. Detection of Potential Fe-S Clusters by UV-Vis Spectroscopy

As purified WblE-N6xHis exhibited a straw-yellow colour in solution, consistent with the presence of a [4Fe-4S] cluster. Clusters of this variety tend to exhibit characteristic absorbance peaks at 410 nm, and sometimes 320 nm, when measured by UV-Vis spectroscopy; in contrast, [2Fe-2S] species tend to present a range of broad shoulders at 320 nm, 460 nm and 550 nm wavelengths. Fraction 8 exhibited dominant peaks at 320 nm and 410 nm, where absorbance at 410 nm comprised the dominant peak, indicative of a [4Fe-4S] species in solution. Fraction 11 on the other hand, presented shoulders at 320, 410, 460 and 550 nm, that were indicative of a [2Fe-2S] species in a mixture with a [4Fe-4S] species. At this point, the shared peak at 320 nm between F8 and F11 was considered most likely to originated from [2Fe-2S] WblE that was contaminating the [4Fe-4S] WblE sample.

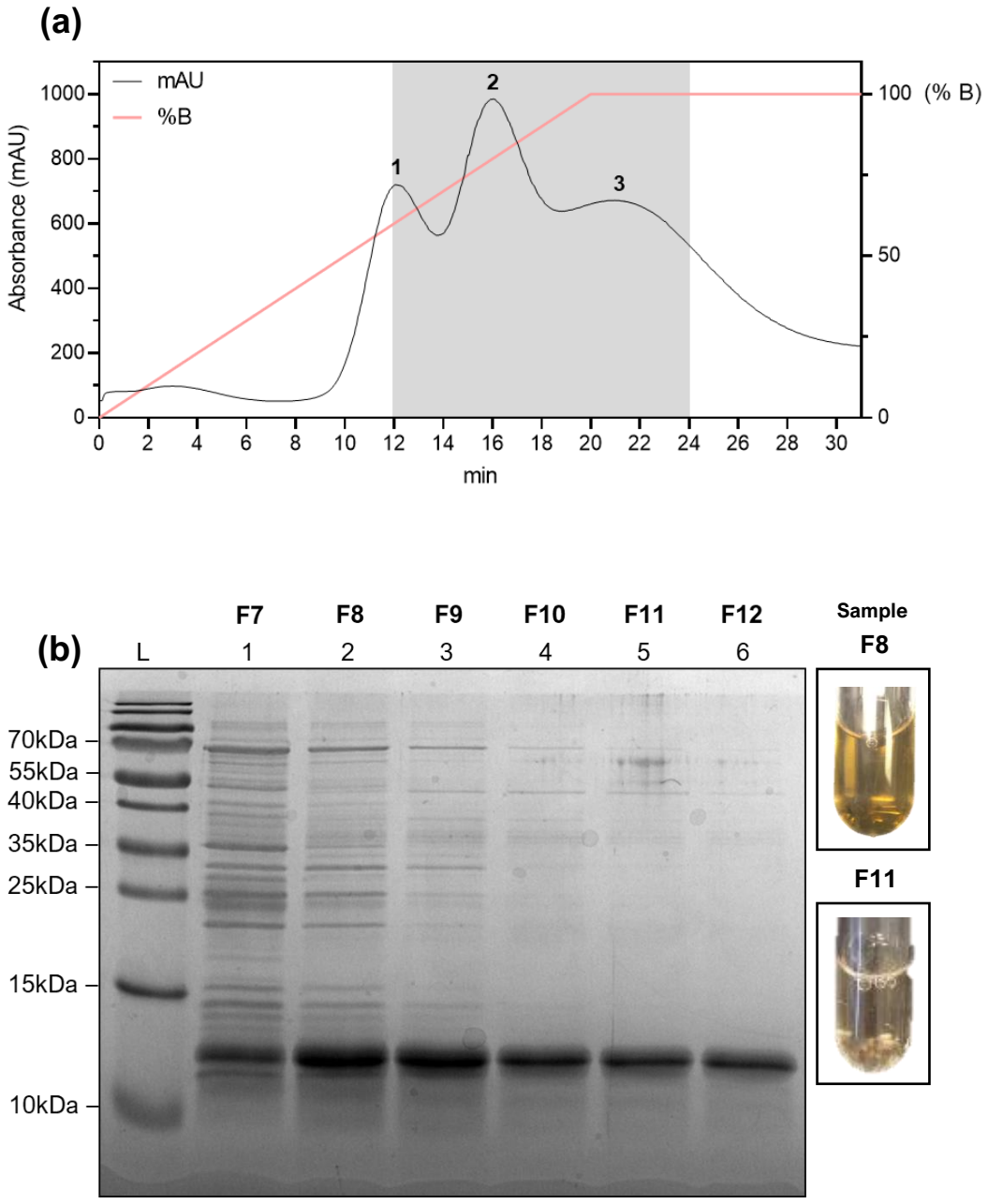

Figure 3.2. (a) AKTA UV (280 nm) absorbance trace for WblE-6xNHis elution. Protein was eluted at a rate of 1 mL. min^{-1}, over a 0 - 100% gradient of Buffer B (red line) into 2 mL fractions – the elution period (min) marked such that it also corresponds to these fractions. Three absorbance peaks were obtained (numbered 1-3 by order of elution). **(b)** 20% SDS-PAGE gel of His-Trap Eluted Fractions (F7-12), suspected to contain WblE-N6xHis SDS-PAGE. Visual appearance of Fraction 8 and 11 before denaturation shown on the right and labelled.

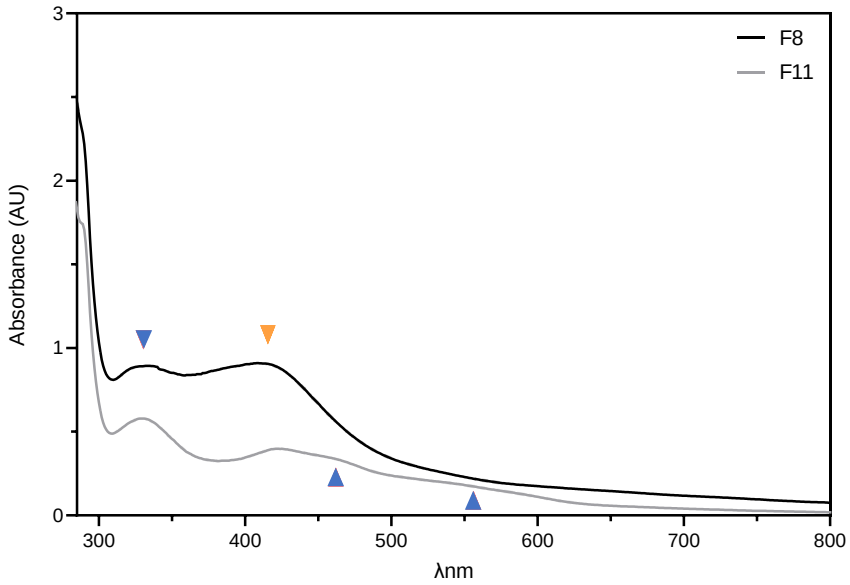

Figure 3.3. UV-Vis Spectroscopic analysis of fraction 8 (black line) and fraction 11 (grey line), acquired by anaerobic His-trap purification of WblE-6xNHis from BL21-NWblE cell lysate. Arrows mark key spectroscopic features of F8 and F11 at ~ 325, 410, 460 and 560 nm that are characteristic of [2Fe-2S] (blue) and [4Fe-4S] (orange) clusters. Arrows marked above represent peaks visible in both spectra, arrows marked below are present only in F11. UV-Vis spectroscopic analysis was carried out in 60% Buffer B.

3.3.3. Heparin (Cation Exchange) Chromatography of WblE

HisTrap™ purified Fractions 8 - 10 were ultimately pooled (6 mL) for heparin chromatography and salt-exchanged into Buffer C (50 mM Tris, 250 mM NaCl, 5% glycerol pH 7.4) and manually injected onto a HiTrap™-HP 1mL Column. Heparin is a highly sulphated glycosaminoglycan that can simulate the polyanionic structure of DNA. As such, in the purification of DNA-binding proteins it is a form of cation exchange chromatography which separates proteins based on positive surface charges which often dominate within DNA binding domains. It was therefore hypothesised that a HiTrap™-HP heparin column (Cytiva™) could help further fractionate Holo-WblE protein from any contaminants by targeting the positive residues in its putative DNA-binding domain.

Adsorption of proteins onto Heparin columns was reversed by an increase in ionic strength of the buffer, eluting over a linear gradient of 0 – 100% Buffer D (50 mM Tris, 850 mM NaCl, 5% v/v glycerol, pH 7.4). Holo-WblE, appeared to elute late within a single 2 mL fraction (F9 - 790 mM NaCl) as assessed by its characteristic straw-yellow fraction colour. Intriguingly, several other species of WblE were eluted at lower concentrations (70 - 80%) of Buffer D (Figure 3.4). Fraction 8 exhibited a seemingly truncated form of WblE (- 1 kDa). Later experiments

demonstrate that this smaller species is in fact an oxidised (disulphide-bonded) form of apo-WblE (Section 3.4.2). Fraction 7 was colourless, and hence seemingly contained only reduced, apo-WblE.

UV-Vis spectroscopy demonstrated that the straw-yellow fraction F9 maintains a dominant peak at 410 nm providing evidence for the retainment of the [4Fe-4S] cluster. Curiously, no evidence of the pink, [2Fe-2S]-associated pigment was visually discernible in any fraction or the flowthrough. Nevertheless, a shoulder at ~ 320 nm suggested that a portion may elute at a similar salt concentration to [4Fe-4S] WblE. However, it cannot be ruled out that buffer exchange caused a loss of the [2Fe-2S] species, which was clearly unstable (Section 3.3.1). In the preparation of some [4Fe-4S] proteins, a second peak can appear at around 310 - 330 nm which better resembles a shoulder and represents a high energy ligand-to-metal (thiolate to iron) charge-transfer which could also account for this feature observed in Buffer C (Jordan *et al*., 2021; Figure 3.5.a).

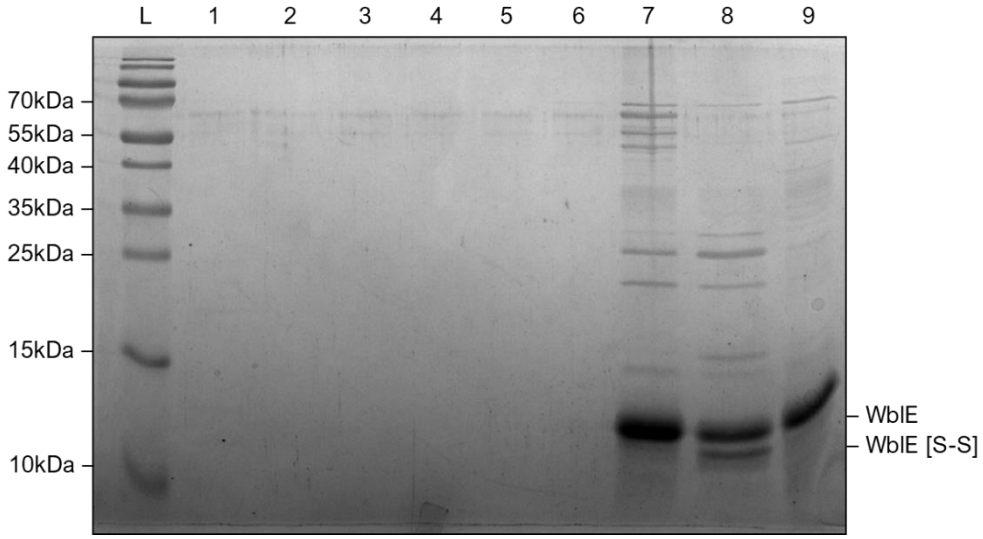

Figure 3.4. 20% SDS-PAGE gel of Hi-Trap Heparin purified WblE-6xNHis Column Eluted Fractions; (L) PageRuler Plus protein weight marker (molecular weights shown in kDa); (1-9) Fractions 1-9 eluted along a linear gradient (0-100%) of Buffer D. Fraction 7

3.3.4. Estimating Cluster Incorporation in Purified Samples

The 2 mL fraction obtained following Heparin purification maintained a straw-yellow colour, and UV-vis spectroscopy indicated that it indeed retains a [4Fe-4S] cluster. To confirm these observations and determine the maximum theoretical incorporation of [4Fe-4S] into the WblE protein, a Ferene free iron assay was carried out in tandem with Bradford assays, as described in Section 2.27, to determine the ratio of iron atoms to WblE monomers. The concentration of apo-WblE monomers in solution was calculated to be 0.66 mg. mL^{-1} or 55.69 µM; and the concentration of free iron was calculated to be at concentration of 87.88 µM. Hence, determining a maximum incorporation of 21.97 µM [4Fe-4S] in the purified sample (39.4%).

3.3.5. Circular Dichroism Spectroscopy of Holo-WblE

Circular Dichroism (CD) is a UV-Vis spectroscopic technique which quantifies the differential absorption of left- and right-handed, circularly polarized light. Optically active chiral molecules will preferentially absorb one direction of the circularly polarized light, this includes the asymmetric arrangement of transition metal centres such as [4Fe-4S] clusters. Wavelengths between 350 and 700 nm are often used for monitoring prosthetic groups within proteins (Kelly *et al*., 2005).

The WblE holoprotein solution was scanned between wavelengths 250 and 850 nm, to further characterise the structure of WblE and the cluster environment (Section 2.26.2); reported here between 300 - 800 nm (Figure 3.5.b). The resulting spectrum exhibited spectral features similar to those of WhiB1 from *M. tuberculosis* (Smith *et al*., 2010) with positive features at 430 nm and 525 nm, a negative sweep between 300 and 400 nm and a subtle but unique feature at 775 nm (Figure 3.5.b). Similar CD spectra have also been obtained for WhiD from *S. coelicolor* and *S. venezuelae* (Crack *et al*., 2009; Stewart *et al*., 2020), highlighting similarities in the local iron-sulphur cluster environment between Wbl proteins.

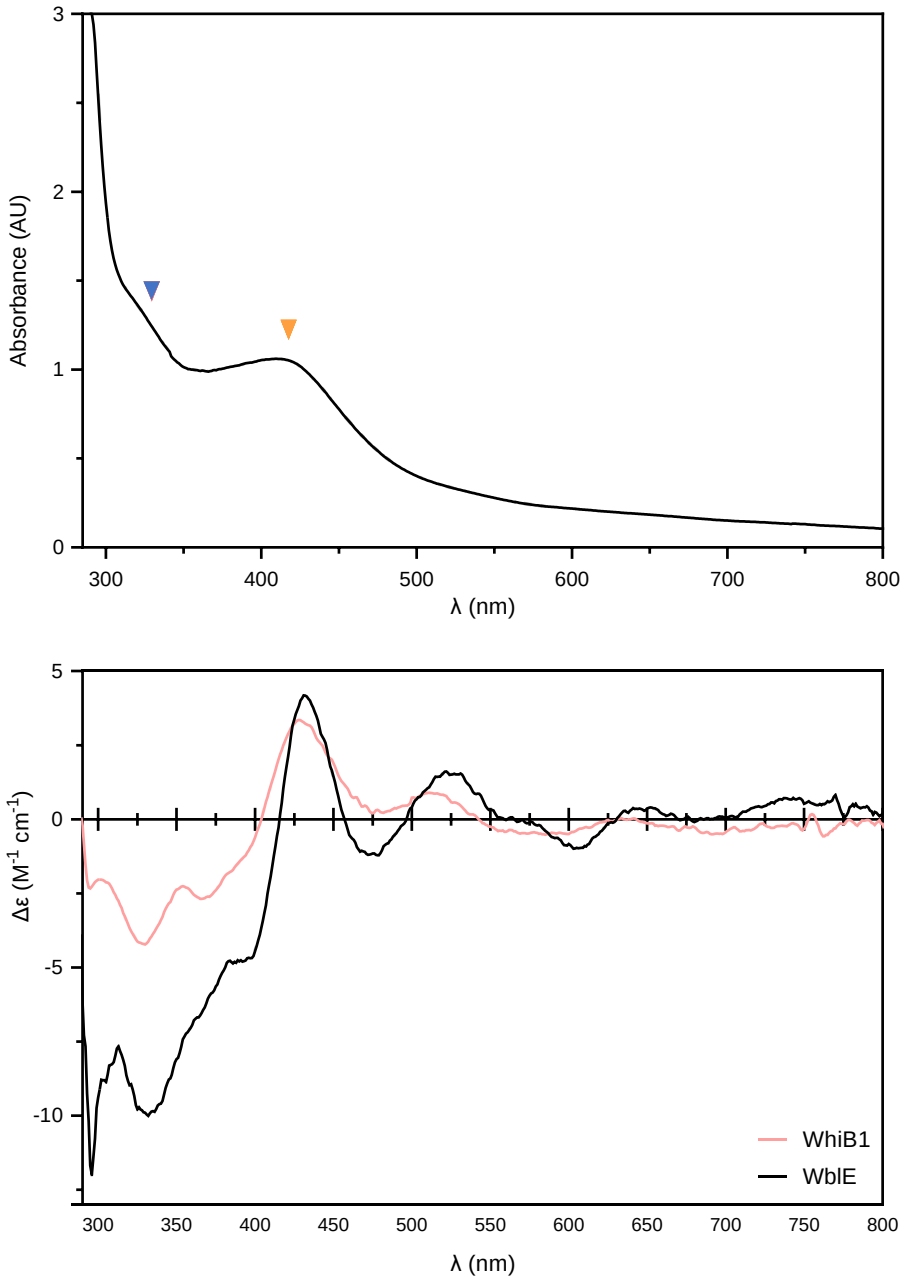

Figure 3.5. (a) Post-Heparin-chromatography, UV-Vis spectroscopic analysis. The orange arrow highlights the characteristic 410 nm [4Fe-4S] absorption peak, the blue arrow highlights retained 310-340nm shoulder. **(b)** Circular Dichroism (CD) Spectroscopic Analysis of 55.7 µM Holo-WblE-6xNHis as purified in this work (39.4%; 21.97 µM [4Fe-4S]), compared against that of 250 µM reconstituted Holo-WhiB1 (78.4%; 196 µM [4Fe-4S] - Smith *et al*., 2010), illustrating similar key spectroscopic features. UV-Vis and CD spectroscopic analyses were carried out in Buffer C.

3.3.6. Non-denaturing ESI – MS: WblE binds a $[4Fe\text{-}4S]^{2+}$ Cluster

Using a salt-exchange column, Holo-WblE was transferred into ammonium acetate pH 8.0, a volatile electrolyte with weak buffering properties that can mimic the solvation properties of proteins under physiological conditions during native ESI-MS (Section 2.28; Konermann, 2017). Non-denaturing electrospray ionisation time-of-flight (ESI-)MS retains noncovalently bound cofactors upon ionization and can measure mass within ±1 Da; as such, it has been shown to be an effective method for studying the nature of the cluster in iron-sulphur proteins (Crack *et al*., 2015 & 2017; Martinez *et al*., 2017; Crack & Le Brun, 2019; Stewart *et al*., 2020).

The theoretical molecular weight for WblE-N6xHis ligating a [4Fe-4S] cluster is 12,027.64 Da, yet deconvolution of the *m/z* spectrum produced by ESI-MS revealed a major peak at 12,025.60 Da; this deviation of -2.04 Da can be attributed to a [4Fe-4S] cluster in its 2+ charge state, where the loss of two protons (H^+) accompanies the loss of two electrons (e^-) and produces the observable difference in mass (Figure 3.6). The second major peak observed at +178 Da from the expected mass of WblE-6xNHis $[4Fe\text{-}4S]^{2+}$ likely arose from α-*N*-6-phosphogluconoylation, a spontaneous post-translational modification that occurs on the polyhistidine-tags of some fusion proteins, expressed in *E. coli*; this modification yields an excess mass of + 258 Da or + 178 Da, the latter of which was observed at 12,204.2 Da, including the weight of the charged holoprotein (Figure 3.6; Geoghegan *et al*., 1999). Several peaks were observed at masses that were 36, 72, and 90 Da in excess of that of $[4Fe\text{-}4S]^{2+}$ WblE. These likely originated from water cluster [M + 18.01057], potentially in mixed clusters with ammonium (NH_4^+) ions [M + 18.03382] that originate from the mobile phase (250 mM ammonium acetate pH 8.0) and can incrementally add weight to the primary analyte (König & Fales, 1998; Keller *et al*., 2008; Figure 3.6).

A small peak observed at 11,672 Da, corresponded to the weight of the tagged apoprotein with all four cysteines participating in disulphide bridges (- $4H^+$; 4 Da). Several peaks of varying intensity at *n*(+32) Da from the apoprotein peak are likely sulphur adducts, present as a result of damaged clusters prior to or during ESI-MS. Another miniscule peak at a weight associated with the apo-protein +178 Da was best associated with α-*N*-6-phosphogluconoylation of Apo-WblE. This is similar, but distinct from, the weight of WblE binding a $[2Fe\text{-}2S]^{2+}$ (+174 Da) or $[2Fe\text{-}2S]^{1+}$ (+175 Da) cluster, for which no peaks could be associated.

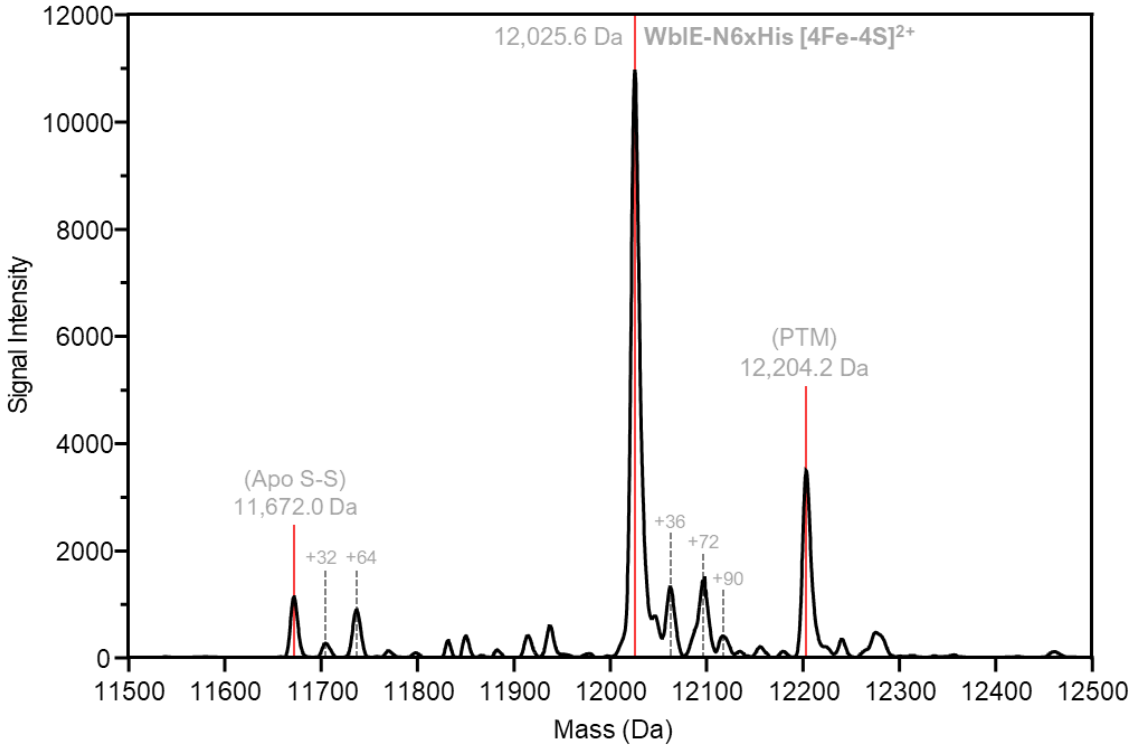

Figure 3.6. Deconvoluted ESI-TOF Mass Spectrum for 55.7 µM Holo-WblE-6xNHis (39.4%; 21.97 µM [4Fe-4S]). Peak centres represent masses within ±1 Da accuracy. The primary species detected by ESI-MS matched the weight of WblE-6xNHis, with a [4Fe-4S] cluster bound in its 2+ charge state (WblE-N6xHis $[4Fe\text{-}4S]^{2+}$). Peaks matching the weight of Apo-WblE (Apo S-S), the +178 Da α-*N*-6-phosphogluconoylation (Geoghegan *et al*., 1989) post-translation modification of Holo-WblE (PTM), and various adducts are also highlighted. WblE-N6xHis was exchanged into 250 mM ammonium acetate for ESI-MS analysis,

3.4. Comparative Aerobic Purification of WblE-C6xHis and WblE-N6xHis

There was curiosity about the effect, if any, of N-terminally tagging Wbl-proteins as C-terminal tags have not been employed, at least within the available literature. The codon optimised sequence for *wblE* (Genscript) was cloned by GeneWiz™ into the NdeI-XhoI site of pET29b(+) such that it incorporated a C-terminal 6xHis-tag with a short custom linker (WblE-KLLPRGSLEHHHHHH), generating the pET29b-CWblE plasmid. The theoretical molecular weight for the product was 11460.94 Da (around 200 Da smaller than the WblE-N6xHis). Purification buffers were modified to have a slightly more alkaline pH (7.55) and increased (10%) glycerol content. Cell pellets from 1 L *E. coli* BL21 DE3 culture, expressing either transgenic protein, were purified in tandem via Ni-IMAC and subsequent preparative gel-filtration (Sections 2.25.3 - 2.25.4). Aerobically purified WblE retained a straw-yellow colour, indicative of a bound [4Fe-4S] cluster, which was lost gradually over 24 hours following exposure to air (not shown).

3.4.1. Apo-WblE Forms Multimeric Species *in vitro*.

Using a calibration curve, it was possible to predict the molecular weights of gel-filtrated proteins based on the elution volume (Section 2.25.4). Peaks one and two were consistent over both tagged forms of WblE and corresponded to the weight of a WblE monomers and dimers (11 kDa and 22 kDa respectively). The two 2 mL fractions directly under each peak were analysed by SDS-PAGE and showed faint bands corresponding to dimeric species. Intriguingly, WblE-N6xHis appeared less capable of forming dimers under these conditions and, moreover, WblE-C6xHis oligomers exhibited additional bands which could not be definitively explained (Figure 3.7.b). The purification was repeated for WblE-C6xHis from 3L of *E. coli* BL21 DE3 but samples were gel-filtrated in a low imidazole buffer (Section 2.25.4). Curiously, when analyzed by SDS-PAGE (Figure 3.7.c), in the absence of any reducing agent, fractions corresponding to monomers appeared to possess multiple additional multimeric species up to tetramers, and dimeric fractions had regenerated monomeric species, illustrating a dynamic characteristic to WblE oligomerisation.

A predicted 70 kDa species was observed for WbE-N6xHis which was attributed to the *E. coli* RNA polymerase primary sigma factor RpoD (σ^{70}) but this was not tested further. This peak only appeared for WblE-C6xHis purified from larger culture volumes (not shown).

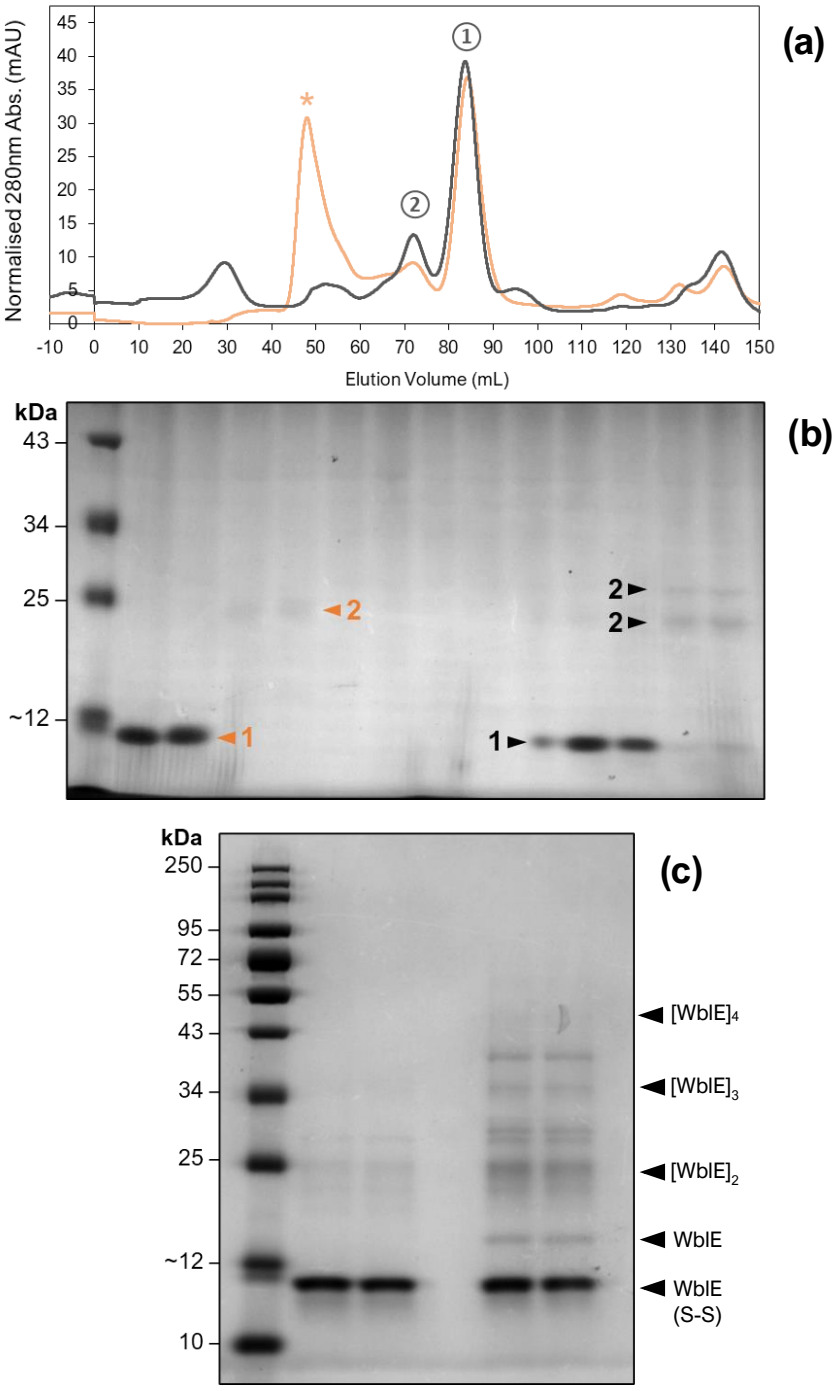

Figure 3.7. (a) Comparative preparative gel-filtration elution profile (280 nm absorbance) for WblE-N6xHis and WblE-C6xHis; WblE-C6xHis and WblE-N6xHis samples are represented by black or orange text/lines/markers, respectively. **(b)** Non-reducing SDS-PAGE gel of gel-filtrated fractions spanning peaks 1 and 2, suspected to contain WblE monomers and dimers. **(c)** Gel-filtrated WblE-C6xHis samples from larger culture volume, eluted in low imidazole Buffer A1. Samples were run against the NEB® Broad Range, Color Prestained Protein Standard (10 - 250 kDa); note that the 17 kDa standard had degraded to a ~12 - 13 kDa species and that the 10 kDa marker ran with the dye front.

3.4.2. WblE Forms Intramolecular Disulphides

The monomeric N- and C-terminally tagged fractions which were isolated during gel-filtration were respectively pooled. Aliquots of the proteins were denatured at 70°C in the presence of 0 mM, 1 mM, 5 mM H_2O_2 or a 1:1 mixture of 5 mM H_2O_2 and DTT (Figure 3.8). In fractions containing H_2O_2 and DTT a visible shift was observed on the gel indicating that under aerobic/oxidative conditions WblE forms intramolecular disulphide bonds and these can be reduced by DTT. Moreover, the addition of DTT seemed to enable increased formation of dimers, in both WblE samples, suggesting that the multimeric forms of WblE are dependent on intermolecular cysteine disulphides. Nevertheless, the N-terminally tagged species seemed less capable of forming multimers, as observed previously.

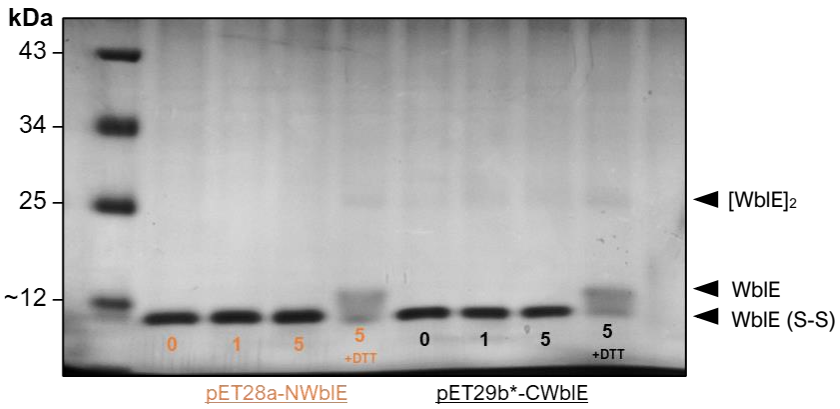

Figure 3.8. Size excluded monomeric WblE-N6xHis and WblE-C6xHis samples exposed to increasing concentrations (0, 1, 5 mM) of H_2O_2 and a final 1:1 mix of 5 mM DTT and H_2O_2, at 70°C for 10 minutes. WblE-C6xHis and WblE-N6xHis samples are represented by black or orange text/lines/markers, respectively. Samples were run against the NEB® Broad Range, Color Prestained Protein Standard (10 - 250 kDa); note that the 17 kDa standard had degraded to a ~12 kDa species and that the 10kDa marker ran with the dye front.

3.5. Discussion

The Wbl family of proteins are typified by their ability to bind [4Fe-4S] clusters via a conserved arrangement of four cysteine residues ($CX_nCX_2CX_5C$). The presence of this motif in WblE suggests that this protein also ligates a [4Fe-4S] cluster, although empirical evidence for this was previously lacking. Consistent with the presence of a [4Fe-4S] cluster, WblE purified with a straw-yellow colour in solution, and UV-Visible absorbance spectra of exhibited a distinct absorbance peak at 410 nm. Furthermore, WblE CD spectra disclosed similar spectral features reported for the orthologous WhiB1 and WhiD proteins ligating a [4Fe-4S] cluster, suggesting that the cofactor is bound by WblE in a similar protein environment (Smith *et al*., 2010). Ultimately, it was established via non-denaturing ESI-MS that a [4Fe-4S] cluster with an overall charge of +2 is bound by a WblE monomer.

With the exception of *S. venezuelae* WhiD, which exists in a unique monomer-dimer equilibrium, other studied [4Fe-4S] holo-Wbl proteins have also presented exclusively as monomers following purification. Notably, WhiD, WhiB3 and the orthologous WhiB1 [4Fe-4S] clusters also purify in their +2 charge states and can undergo a single electron reduction to +1 (Jakimowicz *et al*., 2005; Singh *et al*., 2007; Crack *et al*., 2009; Smith, 2012; Stewart *et al*., 2020). The functional importance of this redox cycle is unclear and was not investigated for WblE in this work but could be explored *in vitro* via electron paramagnetic resonance (EPR) spectroscopy, in the future.

Prior to anaerobic heparin chromatography, UV-visible absorbance spectra presented additional spectral features at 460 and 550 nm which accompanied a pink hue in solution, indicating that WblE may also incorporate a [2Fe-2S] cluster (Figure 3.2.b and Figure 3.3). This is consistent with early observations for aerobically purified WhiB-like proteins of *M. tuberculosis* and *Streptomyces* spp. which were isolated as highly unstable [2Fe-2S] holo-proteins, prone to precipitation (Alam *et al*., 2007 & 2009; Jakimowicz *et al*., 2005; Singh *et al*., 2007). The [2Fe-2S] forms of Wbl proteins are, nonetheless, widely believed to be physiologically inconsequential, instead arising as artifacts of transient oxygen exposure during expression in a host lacking the native cluster chaperone machinery. In the absence of any contrary data, it was considered that a similar situation was true for WblE (Johnson, 1998; Fontecave *et al*., 2005; Jakimowicz *et al*., 2005; Crack *et al*., 2009).

3.5.1. An Emerging Paradigm of Forms Beyond Holo-Wbl proteins

Aerobic overproduction and purification of WblE also initially yielded a straw-yellow solution implying the retention of a [4Fe-4S] cluster. Cluster-loss was gradual but inevitable, although this was not determined via spectroscopic methods. Nevertheless, this suggests an

intrinsic resistance to O_2 mediated oxidation, which is comparable to the mycobacterial homologue WhiB1 and *Streptomyces* WhiD, but not WhiB which appears highly O_2-sensitive (Stewart *et al*., 2020; Stewart, 2022).

Gel filtration analysis of aerobically purified WblE and SDS-PAGE analysis demonstrated that apo-WblE predominantly exists as a monomer capable of forming multimeric complexes with itself via intermolecular disulphide bonds following oxidation. These were visualised up to weights corresponding to WblE tetramers. The formation of intermolecular disulphide-bonded multimeric species has also been observed for the apo-forms of WhiB3, WhiB4, WhiB5 and the phage-derived WhiBTM4 (Alam *et al*., 2007 and 2009; Alam & Agrawal, 2008; Garg *et al*., 2007; Rybniker *et al*., 2010). However, this is the first evidence for an apo-Wbl protein from *Streptomyces* spp. forming multimeric arrangements in solution, that are not associated with inclusion bodies (Jakimowicz *et al*., 2005). Curiously, the formation and diversity of multimers was diminished in WblE-N6xHis, suggesting that the N-terminus may play an important role in WblE multimer formation. With respect to this, it cannot be ruled out that C-terminal tags also inadvertently affected the protein's biochemistry and, to avoid ambiguity, future purifications should ideally employ protease treatments to remove tags, irrespective of their initial placement.

Additional bands resolving slightly above or below the predicted weight of apo-WblE multimers were also observed which were likely due to heterogeneous disulphide arrangements. This is exemplified well by the demonstration that reduced monomeric apo-WblE runs significantly higher than oxidised apo-WblE on SDS-PAGE gels, suggesting compaction of the protein in the disulphide-bonded state. A similar phenomenon is observed for WhiB4 which forms heterogeneous populations of disulphide bonded multimers, but is intrinsically disordered in its reduced monomeric form (Zhai *et al*., 2022). In the case of WhiB4, multimer formation influences DNA-binding, but this could not be concluded for WblE.

Despite resolving under clear peaks, monomer and dimer fractions yielded an array of heavier and lighter apo-WblE species when visualised by SDS-PAGE. This dynamic nature suggests that the apo-WblE protein can undergo disulphide exchange. This is comparable to the disulphide exchange that occurs between apo-WhiB1(S-S) and GlgB in *M. tuberculosis* (Garg *et al*., 2009). This is typical of protein disulphide isomerases. It has previously been shown that apo-WhiB1, WhiB3, WhiB4, WhiB5, WhiB6 and WhiB7 proteins exhibit low-level insulin disulphide reductase activity, *in vitro*, which has been postulated to arise as a product of their central thioredoxin-like (CX_2C) motif (Alam *et al*., 2007; Garg *et al*., 2007; Alam & Agrawal, 2008). However this result has remained controversial (Crack et al., 2009). Protein disulphide isomerases are part of the thioredoxin superfamily (also harbouring the CX_2C motif) but exhibit a more diverse and substrate specific range of activities than specific thioredoxin including the rearrangement of

disulfide bonds through thiol-disulphide exchange reactions. This distinction from thiol-reducing thioredoxins has not been presented thus-far but the distinction could explain the dynamic nature of apo-WblE and the inherent thiol-redox activity of other apo-Wbl proteins.

The work in this chapter aimed to provide an initial biophysical characterisation of the WblE protein, *in vitro*. It reports the successful protocols for the heterologous production and purification of the holo and apo forms via anaerobic and aerobic approaches, respectively. The results depict a scenario whereby WblE can adopt monomeric [4Fe-4S], apo-reduced or apo-disulphide conformations, in addition to multimeric apo-protein complexes which arise under aerobic/oxidative conditions. The data presented adds to the growing paradigm that a complex array of protein conformations exist for certain Wbl proteins, at least *in vitro*, which may contribute to a graduated integration of redox sensing with specific response functions *in vivo*, although this remains to be determined.

Chapter 4

Probing the Function and Essentiality of *wblE* in *S. venezuelae* NRRL B-65442 with CRISPR - Cas9

4.1. Introduction

The *wblE* gene is an orthologue of the essential *whiB1* of *Mycobacterium* spp., that is thought to control virulence and expression of the *groES-EL* chaperonin operon. Multiple independent attempts to delete the *wblE* gene in *Streptomyces* spp. have failed, bearing the hypothesis that the gene product is also essential in this genus. This chapter details the utilisation of the pCRISPomyces-2 plasmid-based CRISPR-Cas9 and ReDirect λ-Red systems to test the hypothesis that the *wblE* gene is essential in *S. venezuelae* NRRL B-65442. Furthermore, CRISPR-Cas9 was used to test the viability of mutant *wblE* alleles with specific amino acid substitutions or truncations and generate strains carrying a genetically incorporated tag. Details for strains generated, utilised and characterised in this section can be found in Appendix A.5.

4.2. Is *wblE* Essential? A CRISPR-Cas9 Approach

Until recently, genome editing in streptomycetes was commonly achieved via low efficiency methods such as ReDirect, that are both time and labour intensive (Kieser *et al*., 2000; Gust *et al*., 2004), especially in comparison to the genetic modification of other microorganisms and if an unmarked mutant is required (Tong *et al*., 2019). More recently, highly efficient tools which utilise CRISPR/Cas9-mediated genome editing have been developed for *Streptomyces* spp. Most notably, the pCRISPomyces-2 plasmid has enabled targeted, unmarked and multiplex mutagenesis in a range of *Streptomyces* species (Cobb *et al*., 2015).

4.2.1. Failed Attempts at Deletion or Modification of *wblE*, *in situ*

The pCRISPomyces-2 vector has fused the crispr (cr)RNA and *trans*-activating (tra)crRNA components of the guide (g)RNA, into a single synthetic guide (sg)RNA; into which a custom protospacer can be assembled via GoldenGate assembly to target an homologous sequence and adjacent ‘NGG’ protospacer adjacent motif/sequence (PAM) within the *S. venezuelae* NRRL B-65442 genome. A separate cloning site is present for the assembly of a mutagenised, homologous repair template (HRT).

Two protospacers were designed and cloned into the pCRISPomyces-2 plasmid sgRNA (Figure 4.1). The first protospacer (5' – CCACCGCCGGAGTGGAAAGA – 3'), targeted the 3' portion of the neighbouring *vnz_24260* gene; derived plasmids were named pCa. The second protospacer (5' – GGGGTCTTCCTCACGACAAA – 3') targeted a sequence within the *wblE* coding sequence and derived plasmids were denoted pCi; This gRNA overcame the possibility that the distance of *wblE* from the cut-site could be affecting homologous recombination.

Two HRTs were assembled in plasmid pCa (Figure A.3), corresponding to a *wblE* knockout (pCa24255KO) and a C40S substitution mutation (pCa24255C40S). Both HRTs carried a silent single nucleotide scar at the cut-site, within *vnz_24260*, that would theoretically inhibit the endonuclease activity in repaired templates and provide evidence of Cas9 activity and successful homologous recombination. Exconjugants were acquired but amplification of the pCa24255KO exconjugant *wblE* locus, revealed no change in the amplicon length compared to the wild type strain; similarly, sequencing of pCa24255C40S exconjugants revealed no evidence of the specified single nucleotide change. Nevertheless, in both cases, amplification and sequencing of the *vnz_24260* locus from genomic DNA revealed regular incorporation of the SNT scar within exconjugants, excluding the possibility of a faulty gRNA (Figure 4.2). The previously mentioned *wblE* knockout HRT was tested in plasmid pCi. Nonetheless, colony PCR of the *wblE* locus from *S. venezuelae* pCi24255KO exconjugants and electrophoresis also yielded wild type sized amplicons (not shown).

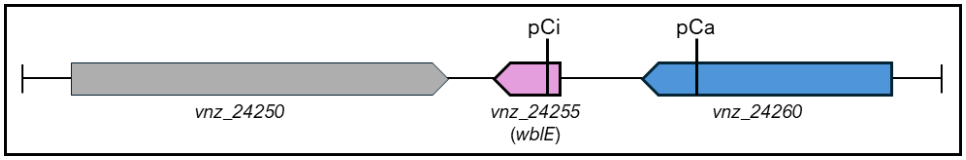

Figure 4.1. The *vnz_24255* (*wblE*) gene neighbourhood, to scale, with pCi and pCa gRNA target locations highlighted within their respective genes

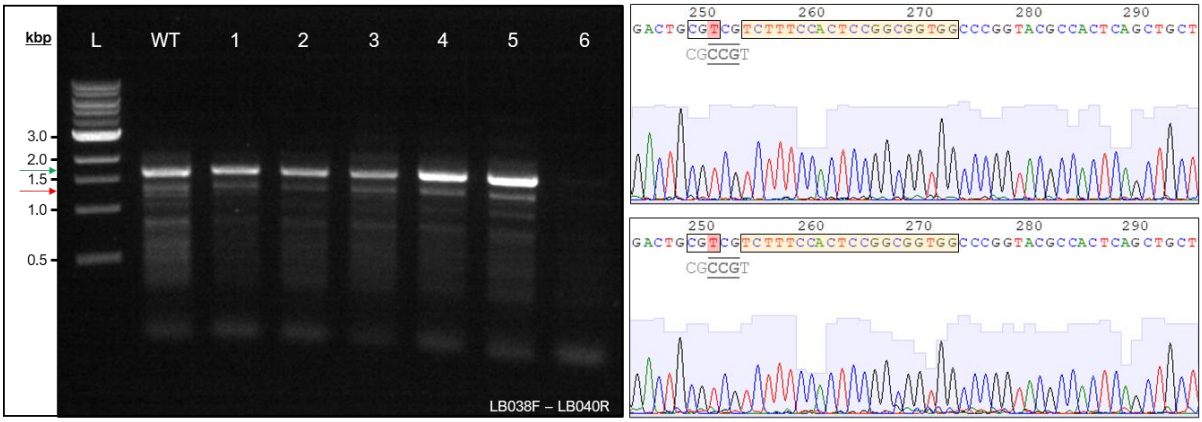

Figure 4.2. (left) Electrophoresis of LB038F – LB040R amplicons from pCa24255KO exconjugants; red and green arrows show expected size for wild type (1682 bp, green arrow) and KO (1371 bp, red arrow) amplicons, respectively**.** Sanger sequencing chromatograms for the *vnz_24260* coding sequence in **(top right)** pCa24255C40S and **(bottom right)** pCa24255KO exconjugant strains. The incorporated silent mutation in the PAM (R249 CGC>CGT) is highlighted red and boxed. Yellow boxes highlight the protospacers. Native sequence is shown below (grey text) with the PAM underlined.

4.2.2. The *wblE* Gene is Essential: pCi24255KO-mediated *wblE* Knockouts

In the published demonstration of their pCRISPomyces-2 CRISPR-Cas9 system, Cobb *et al.* (2015) performed multiplex genome editing (i.e. at multiple genomic sites) by using two unique sgRNAs which cut the DNA at two distinct sites. This was utilised to perform variably sized deletions between 20 bp - 30 kbp or targeted mutagenesis at distinct loci. This suggested that the unique sgRNA within *wblE* could be integrated at a separate genomic locations to provide simultaneous probing of two synonymous copies (Cobb *et al*., 2015). The *Streptomyces* integrative vector, pSS170 targets the ΦBT1 – *attB* integration site within the vnz_22340 coding sequence (start pos. - 4,874,190 bp) around 409 kilobases from, and on the opposite strand to, the native *wblE* locus (start pos. - 5,283,453 bp), thus providing a simple method of introducing an additional allele, *in trans* (Gregory *et al*., 2003). Two different alleles were cloned into pSS170. One, being the native *wblE* sequence with the complete vnz_24260 and vnz_24255 intergenic region as the promoter, yielding strain 24255WT. The second engineered allele was identical but carried a single, silent nucleotide mutation that disrupts the NGG PAM targeted by the pCi24255KO Cas9 system ($_{22}$CGG$_{20}$ to CCG), which was introduced via the complementary overhangs of primers LB050 & LB051, and is denoted by the abbreviation 'SNT'.

The resultant merodiploid *S. venezuelae* strain, carrying a protected *wblE* allele (24255SNT) readily yielded knockout strains (Δ24255SNT) in around 51% of (49 PCR tested) exconjugants after a single generation of growth following selection and significantly improved the overall frequency of exconjugant growth, compared to the WT and 24255WT strains (MW = $p < 0.001$; Figure 4.3). Confirmed Δ24255SNT strains exhibited wild type development, demonstrating complementation (Figure 4.4). It can therefore be ascertained that the reason why pCi24255KO did not yield any Δ*wblE* exconjugants in the wild-type or 24255WT strains was not due to a faulty gRNA, which is comparable to the results obtained with the pCa24255KO and pCa24255C40S CRISPR-Cas9 systems (Section 4.2.1 - Figure 4.2). Intriguingly, strain 24255WT exhibited significantly lower frequency of exconjugant growth than even the controls (MW = $p < 0.05$), following selection for the pCi24255KO plasmid, only one colony grew in this limited controlled trial and it retained a WT *wblE* locus. This suggests that providing two targetable copies actually increased lethality of CRISPR-Cas9 targeting of *wblE*. Together, these results indicate that specifically protecting the *wblE* gene from Cas9 endonuclease activity abrogates lethality and allows deletion in *S. venezuelae*, thus providing evidence that the gene is essential.

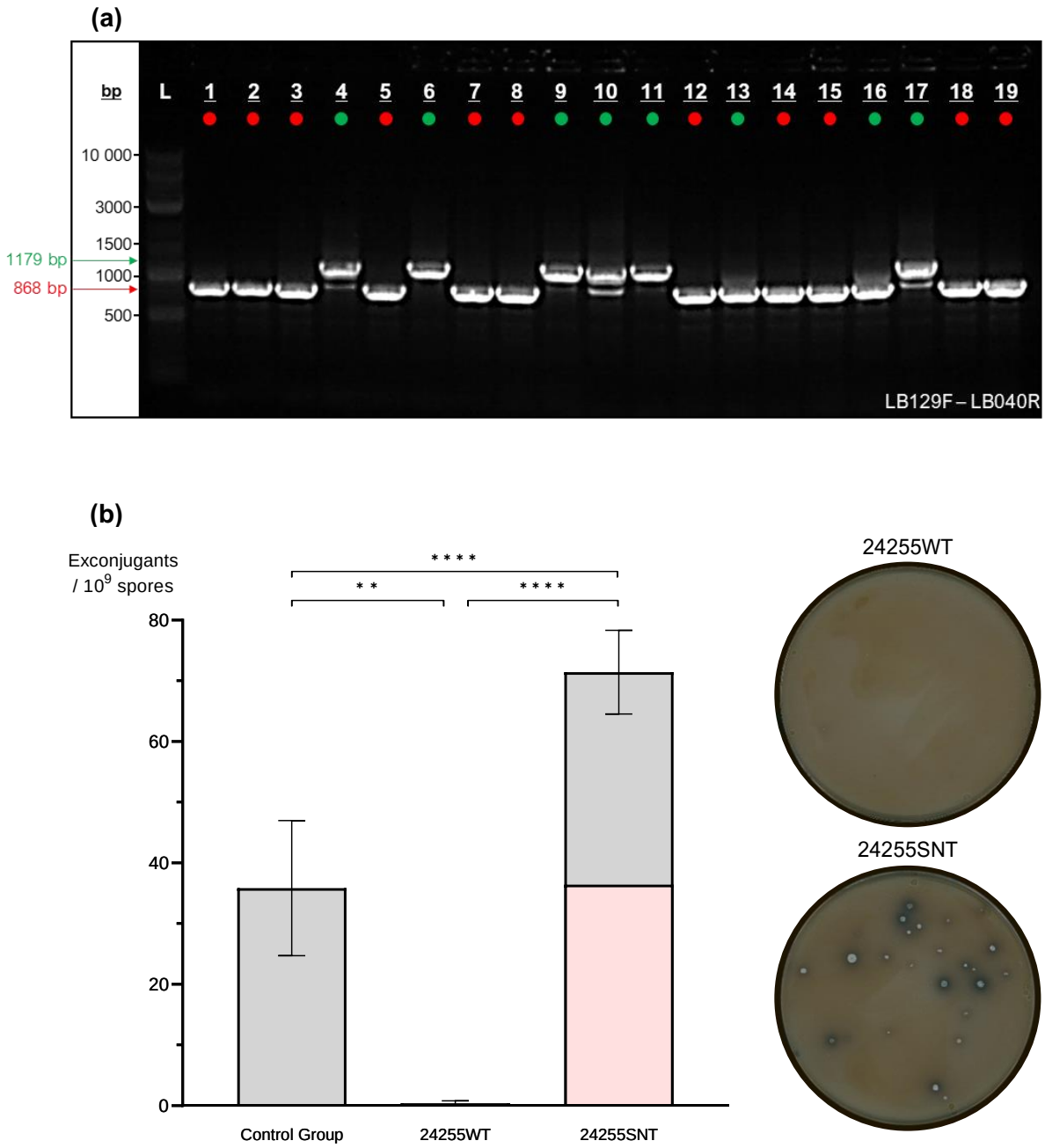

Figure 4.3. (a) Electrophoresis gel of PCR (LB129 – LB130) amplicons from 24255SNT exconjugants. The expected amplicon sizes for *wblE* (green) and Δ*wblE* (red) sequences are shown alongside the 1kb plus NEB DNA ladder. **(b)** Mean exconjugant survivalist counts (± SE) for pCi24255KO conjugation of control strains wild type (*n* = 35), pSS170 (*n* = 18), pIJ10257 (*n* = 20) and test strains 24255WT (*n* = 20), 24255SNT (*n* = 20), normalised by their viable spore counts and represented per billion (x 10^9) viable spores; KO frequency is highlighted in red. **(c)** Example conjugation plates for strains 24255WT and 24255SNT, following selection, are shown to the left of the graph. ** = $p < 0.025$, **** = $p < 0.0001$ (Mann-Whitney U)

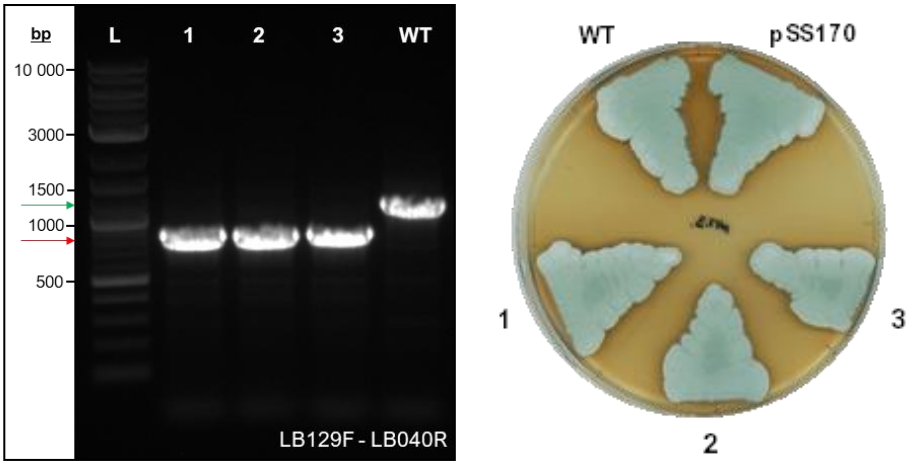

Figure 4.4. PCR Confirmation from gDNA of isolated Δ24255SNT strains and example growth after 4 days on MYM + TE for the WT and empty plasmid strains, compared to isolated isogenic Δ24255SNT strains cured of the pCi24255KO plasmid (1, 2, 3).

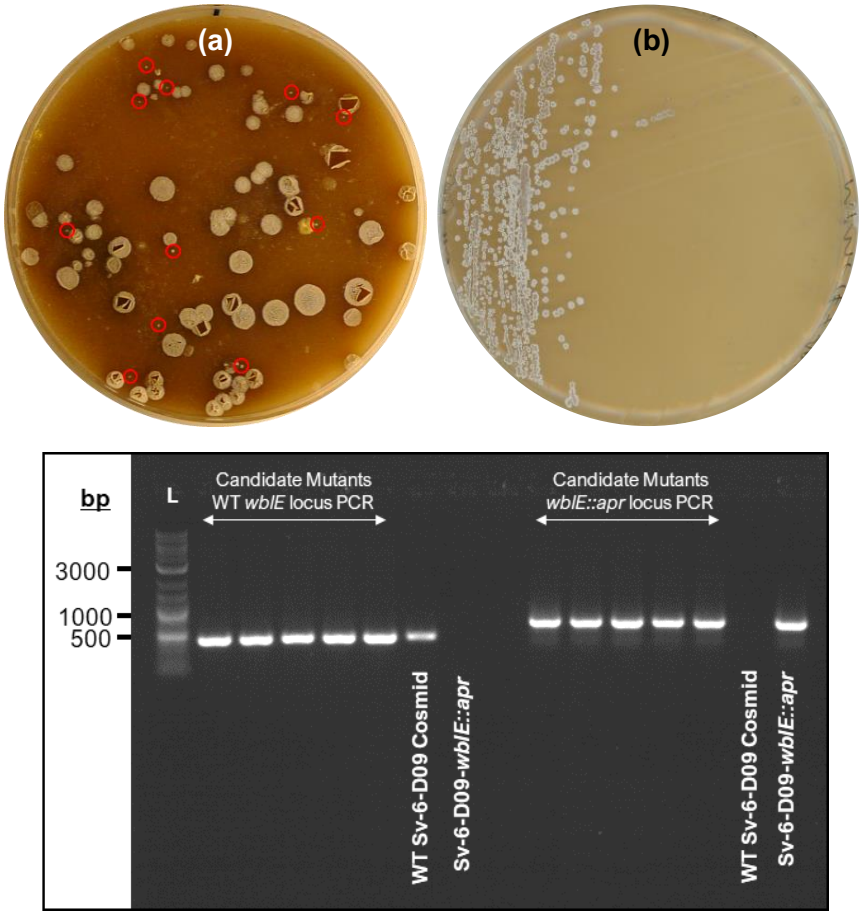

Figure 4.5. (a) Sv-6-D09-*wblE*::*aac(3)IV* (::*apr*) exconjugant plate, with small (*aac(3)IV*$^{+}$, *neo*$^{-}$) colonies circled in red and **(b)** the phenotype of these exconjugants when grown on MYM + TE with the selecting antibiotic, apramycin. Confirmation of the presence of both a native (WT) and disrupted (*wblE::apr*) loci by PCR for 5 possible mutants is shown beneath.

4.2.3. The *wblE* gene is essential: ReDirect (Dr Neil Holmes)

To independently confirm these results, Dr Neil Holmes followed up this work by using ReDirect technology, a PCR targeting mutagenic approach, which utilises λ-Red mediated recombination in a *Streptomyces* cosmid library, in *E. coli* (Gust *et al*., 2004). The *S. venezuelae wblE* gene was replaced with the *aac(3)IV* apramycin resistance cassette, on the kanamycin resistant Sv-6-D09 cosmid (Sv-6-D09-*wblE*::*aac(3)IV*, *neo*^{R}) and conjugated into *S.venezuelae* NRRL B-65442. Remarkably, exconjugants exhibiting small colony phenotypes were isolated with kanamycin sensitivity and apramycin resistance, indicating successful double cross-over events, and potential knockouts. However, PCR amplification soon revealed that exconjugants retained a WT *wblE* locus AND the recombinant *wblE*::*aac(3)IV* sequence (Figure 4.5). When grown without apramycin, exconjugants reverted to WT phenotypes. Thus, it seems *wblE* is kept by any means necessary and is indeed an essential gene.

4.3. A Curious Effect of Cas9 Protection on Viable Spore Counts

As part of the method for quantifying pCi24255KO conjugation efficiency (Section 2.20), viable spore (CFU) counts were performed (Section 2.20.1). Despite exhibiting similar phenotypes and being normalised to an OD_{600} of 0.1, a significant difference in the number of $CFU.\mu L^{-1}$ was observed consistently between the control strains (WT or empty plasmid) and 24255SNT, which carried an extra allele of *wblE* with the Cas9-silencing scar. The O24255SNT strain was also tested which yielded similar results (Chapter 2 - Figure 2.1). It was possible these increases resulted from either increased spore viability *or* increased germination rates but this was not determined experimentally. A slight increase in viable spore counts was also observed for the 24255WT and O24255WT strains, however these were not significant ($p > 0.05$). These differences were normalised in the calculations of conjugation efficiency for 24255WT and 24255SNT (Section 2.22.2).

4.4. Discerning Essential and Non-Essential Residues with Integrated Mutant Alleles

The true power of this approach was a plug and play type approach for gene editing, with an additional protected allele provided *in trans* via the conjugation of an integrative vector. A qualitative approach was used to determine the likely essentiality for a range of residues and domains, encoded by the *wblE* gene. Unfortunately, due to time constraints, these have not been quantified in comparison with the WT and 24255WT 24255SNT strains, although are the result of multiple experiments and nonetheless, still provide important data. Details for viable mutants can be found in Figure 4.6.

4.4.1. The WblE Cysteines are Essential for Function and Survival in *S. venezuelae*

Previous attempts to mutate the conserved WhiB-like cysteine residues to alanine have demonstrated that they are essential for cluster ligation *in vitro* and biological function, *in vivo* (Singh *et al*., 2007; Jakimowicz *et al.*, 2005; Bush *et al*., 2016). Alanine scanning is a typical method for mutagenic screening, however alanine exhibits distinct structural properties to cysteine which could disrupt the protein structure. Serine, on the other hand, is a structural analogue of cysteine which only differs by a single atom in its side chain (-SH / -OH); rarely, serine can even act as an iron-sulphur cluster ligand (Mansy *et al*., 2002). Thus, to specifically investigate the redox and [4Fe-4S]-ligating properties of these residues, *wblE* fragments were generated commercially (Genscript™) carrying SNT Cas9 protection and serine substitutions for each cysteine residue (Table 4.1). The mutated fragments were amplified (LB088 & LB042hf) and fused with a complementary promoter fragment (LB041hf & LB050) in pSS170. No Δ*wblE* strains could be acquired with these mutant alleles integrated in *S. venezuelae*, despite Cas9 protection, indicating that these residues are essential for WblE function. Exconjugant colonies grew on occasion but were highly heterogeneous and retained the native *wblE* locus, according to the size of the PCR amplified locus. It will be important for future work to complement these findings *in vitro* via analysis of cluster incorporation.

Table 4.1 Point mutations and corresponding substitutions (sub.) in integrated *wblE* alleles and associated strains.

Strain	Sub.	Mutation
24255C9S	C9S	$_{25}$TGT$_{27}$ → TCG
24255C37S	C37S	$_{109}$TGT$_{111}$ → TCG
24255C40S	C40S	$_{118}$TGC$_{120}$ → TCG
24255C46S	C46S	$_{136}$TGC$_{138}$ → TCG
24255D13A	D13A	$_{37}$GAC$_{39}$ → GCG
VP5240	N6Q N82Q	$_{16}$AAC$_{18}$ → CGC $_{244}$AAC$_{246}$ → CAG

4.4.2. The DNA-Binding C-Terminus of *S. venezuelae* WblE cannot be Truncated

The *wblE* coding sequence and its native promoter were amplified from plasmid pSS24255$_{SNT}$ (primers LB041hf and LB126) such that the protein possessed a C-terminal truncation of 18 aa (R68 – A85), removing any putative DNA-binding residues and incorporating a new stop codon. No Δ*wblE* exconjugants could be acquired, suggesting that the C-terminal DNA-binding domain is essential for WblE function *in vivo*.

4.4.3. *S. venezuelae* Δ*wblE* :: ΦBT1 pSS24255D13A $_{SNT}$ (Strain Δ24255D13A)

In Wbl proteins, shortly following the first conserved cysteine residue (^{1}Cys), is a near-universally conserved aspartate (Asp; D) which conserves ^{1}Cys + 4 aa spacing. In WblE and WhiB1 this is residue 13. The equivalent residue (D71) is indispensable for *M. smegmatis* WhiB2 (WhiB) function and a D71A substitution is lethal (Raghunand & Bishai, 2009). It was originally hypothesised that D13 is important for ligation of the iron-sulphur cluster, however, the recent Cryo-EM structure of *Streptomyces venezuelae* WhiA-WhiB-σ^{HrdB} transcriptional complex shows that the equivalent residue (D29) is in direct proximity to WhiA-R165 at the WhiA-WhiB interaction interface. This provides an alternative source for its essential role in WhiB(2) function via a critical salt-bridge network by stabilising the interaction with WhiA (Bosshard *et al*., 2004; Lilic *et al*., 2023).

A point mutation was introduced within codon 13 of *wblE* via commercial gene synthesis (GeneWiz™ – Table A.2) which specified a D13A single amino acid change (Table 4.1). Alanine scanning was used in this instance to match the approaches used previously, *in vitro*. The allele fragment was amplified and Gibson assembled into pSS170 and integrated into *S. venezuelae* to generate strain 24255D13A. The *wblE* gene was successfully deleted from *S. venezuelae* 24255D13A, generating strain Δ24255D13A and demonstrating that D13 is dispensable for *wblE* function *in vivo*, in direct contrast to WhiB. Potential reasons for this discrepancy will be discussed.

4.4.4. *S. venezuelae* Δ*wblE* :: ΦBT1 pSSVP5240 (Strain ΔVP5240)

Sequence variation across *Streptomyces* spp. WblE homologues is minimal, however, small variations do exist. The model organisms, *S. venezuelae* and *S. coelicolor* are quite distantly related but share 93.4% nucleotide identity and 97.6% amino acid identity in their *wblE* coding sequence or products. These variations ultimately define two asparagine to glutamine amino acid substitutions in the N-terminal and the C-terminal regions (N6Q and N82Q, respectively). The *S. venezuelae* promoter (LB041hf – LB071) and *S. coelicolor wblE* gene (LBc002 – LBc004) were amplified and fused in pSS170 via Gibson assembly (pSSVP5240).

Despite a high overall nucleotide identity between the two homologues, no SNT-protection was used as significant variations in the protospacer sequence were present in *S. coelicolor wblE* sequence. The lethality of Δ*wblE* was complemented by the *S. coelicolor* homologue (strain ΔVP5240) suggesting equivalent essential functions, *in vivo*. It is possible that the N6Q and N82Q mutations alone are lethal but complement one another; this has not been assessed but these residues are not always conserved together, suggesting that this is unlikely.

4.4.5. *S. venezuelae* Δ*wblE* :: ΦBT1 pIJ24255$_{SNT}$ (Strain ΔO24255SNT)

To rule out the possibility that repression of *wblE* transcription (dictated within the native promoter) was important for function, the *wblE* coding sequence was amplified so that it carried Cas9 protection, with primers LB072 and LB042hf, and assembled into plasmid pIJ10257 under the control of the *ermE** promoter (plasmid pIJ24255$_{SNT}$, strain O24255$_{SNT}$). This strain complemented Δ*wblE* lethality, resulting in strain ΔO24255SNT. Thus, repression at the *wblE* promoter is dispensable for function and cell survival, indicating a constitutive role for WblE.

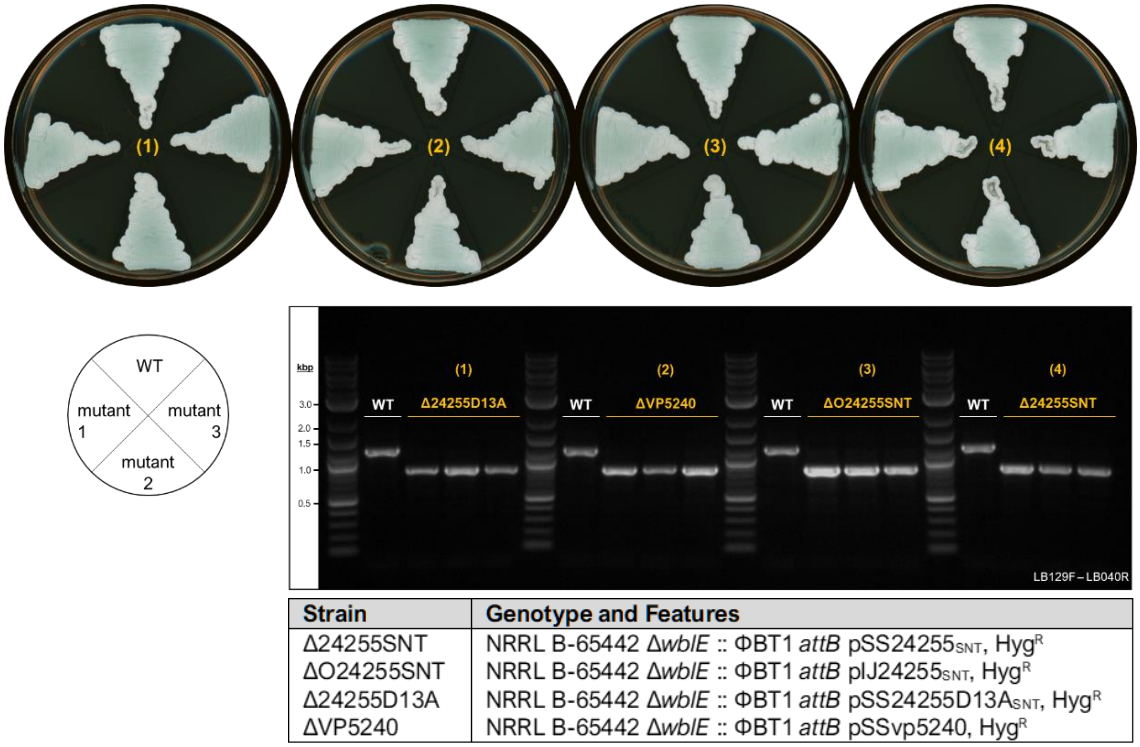

Strain	Genotype and Features
Δ24255SNT	NRRL B-65442 Δ*wblE* :: ΦBT1 *attB* pSS24255$_{SNT}$, Hyg^R
ΔO24255SNT	NRRL B-65442 Δ*wblE* :: ΦBT1 *attB* pIJ24255$_{SNT}$, Hyg^R
Δ24255D13A	NRRL B-65442 Δ*wblE* :: ΦBT1 *attB* pSS24255D13A$_{SNT}$, Hyg^R
ΔVP5240	NRRL B-65442 Δ*wblE* :: ΦBT1 *attB* pSSvp5240, Hyg^R

Figure 4.6. Growth of isolated (1) Δ24255D13A (2) ΔVP5240 (3) ΔO24255SNT and (4) Δ24255SNT mutants grown on MYM + TE for 3 days and *S. venezuelae* colony PCR confirmation of these cultures. Associated mutant genotypes are shown and can also be found in Appendix A.5.

4.5. *N*-Acetylglucosamine Induces Phenotypes in *wblE* Mutants

A somewhat confusing observation made for each of the Δ*wblE* complemented strains reported here was that little to no phenotype was observed, aside from very minor differences in macroscopic morphology and spore pigments (Figure 4.6). Following analysis of the *wblE* genetic neighbourhood with WebFlaGs (Figure A.2), it was noted that genes for *N*-acetylglucosamine metabolism were conserved upstream of the *wblE* locus, including the conditionally essential glucosamine phosphate isomerase *nagB* (*vnz_24235*) and the *N,N'*-diacetylchitobiose ABC transporter operon *dasABCD* (*vnz_24215* - *vnz_24230*). This feature is not conserved in other Actinobacteria. The control and mutant strains developed in this chapter were grown on MYM + TE at 30°C, supplemented with (low) 200 µM and (high) 20 mM GlcNAc, which induced complex developmental and metabolic phenotypes which are broken down here.

4.5.1. *N*-Acetylglucosamine Reveals Polar Effects of *trans*-Integrated Alleles

Polar effects describe mutations which disturb the transcription of a gene (or genes) due to a direct transcriptional relationship; the most common examples of polar mutations occur in polycistronic mRNAs which contain contiguous coding sequences.

Evidence from *S. venezuelae* dRNA-seq (Section 2.21.3), and the ability to complement *wblE in trans* with only the *vnz_24260 – vnz_24255* intergenic sequence as the promoter, make it clear that *wblE* expression is primarily driven from its own promoter under standard liquid and agar growth conditions (MYM + TE, 30°C). Thus, the Δ24255SNT strain should theoretically respond to the amino sugar GlcNAc the same as the wild type and empty plasmid strains, however this was not the case (Figure 4.7 & Figure 4.8). In particular, on MYM + TE supplemented with 20 mM GlcNAc the Δ24255SNT strain developed a striking small-colony phenotype which was shared with the Δ24255D13A strain. Remarkably, overexpressing *wblE* from the *ermE** promoter in a Δ*wblE* background (ΔO24255SNT) almost entirely rescued the small-colony phenotype and presented a colony which was now comparable to the wild type strain, in appearance and bioactivity. These results demonstrate that constitutive expression levels achieved at the native locus are important but not essential for WblE function, and moving *wblE* could have unintentionally affected a previously unappreciated transcriptional element. Intriguingly, the ΔVP5240 strain also partially restored growth, although the reason why is unclear and could be due to variations in the gene sequence or as a result of the substituted residues and hence, function of the gene product.

4.5.2. *N*-Acetylglucosamine Reveals Developmental Functions for WblE

Macroscopic 4K images (Section 2.35) of the 3 day old colonies grown on 20 mM revealed unique topological differences between the strains, which could be due to variations in the development of the underlying vegetative hyphae. It was also notable that unique patterns of emerging aerial hyphae were observed for each of the mutants on 200 µM and 20 mM GlcNAc, potentially demonstrating an early developmental role for WblE (Figure 4.6).

4.5.3. WblE Function is Important for *S. venezuelae* Secondary Metabolism

Several Wbl proteins are known to regulate the secondary metabolism of *Mycobacterium* and *Streptomyces* spp. (Singh *et al.*, 2009; Fowler-Goldsworthy *et al*., 2011). Control strains showed robust bioactivity against the Gram-positive bacterium *B. subtilis* when grown on MYM + TE, supplemented with 200 µM GlcNAc. A loss of bioactivity in the Δ24255SNT strain when compared to the controls and strain O24255SNT was attributed to the polar effects previously described and consistent with this, strain ΔO24255SNT partially rescued this phenotype (Figure 4.7). Strains ΔVP5240 and Δ24255D13A exhibited no region of comparable bioactivity when compared to strain Δ24255SNT. Thus, while it is difficult to separate the direct effects of mutagenesis from the potential polar effects of moving *wblE*, these results clearly show that mutating *wblE*, or disrupting native expression, affects *S. venezuelae* secondary metabolism (Figure 4.7). It was noted that pSS170 seemed to have reduced bioactivity and could be cumulatively affecting these results, although more replicates of this control would be needed to confirm this as variations between replicates are common.

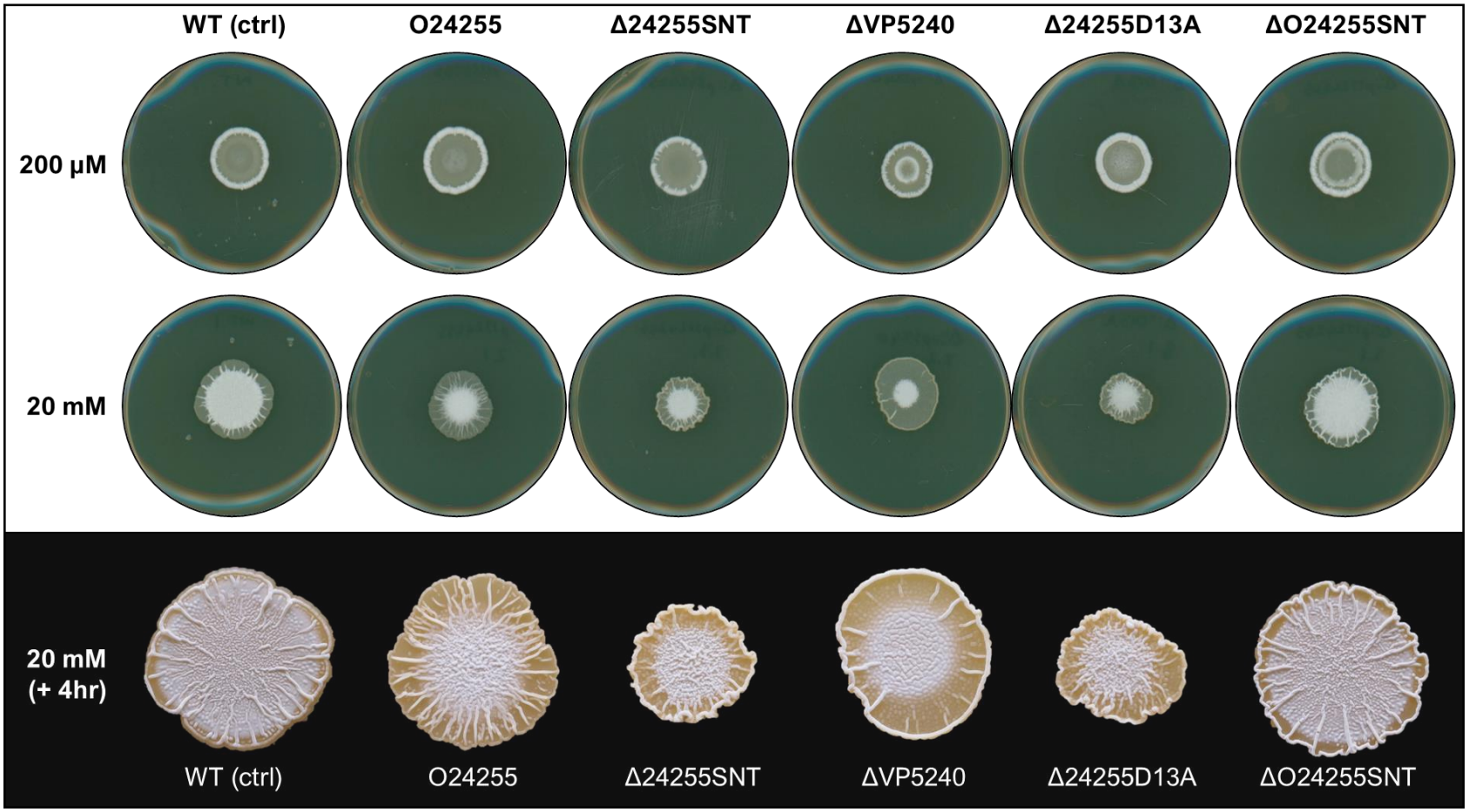

Figure 4.7. Growth phenotypes at 3 days of growth on MYM + TE, supplemented with different concentrations (200 μM and 20 mM) of N-acetylglucosamine. Note that the 4K macroscopic images taken for the growth of strains on 20 mM GlcNAc (bottom black panel) were taken + 4 hrs growth following scanned images.

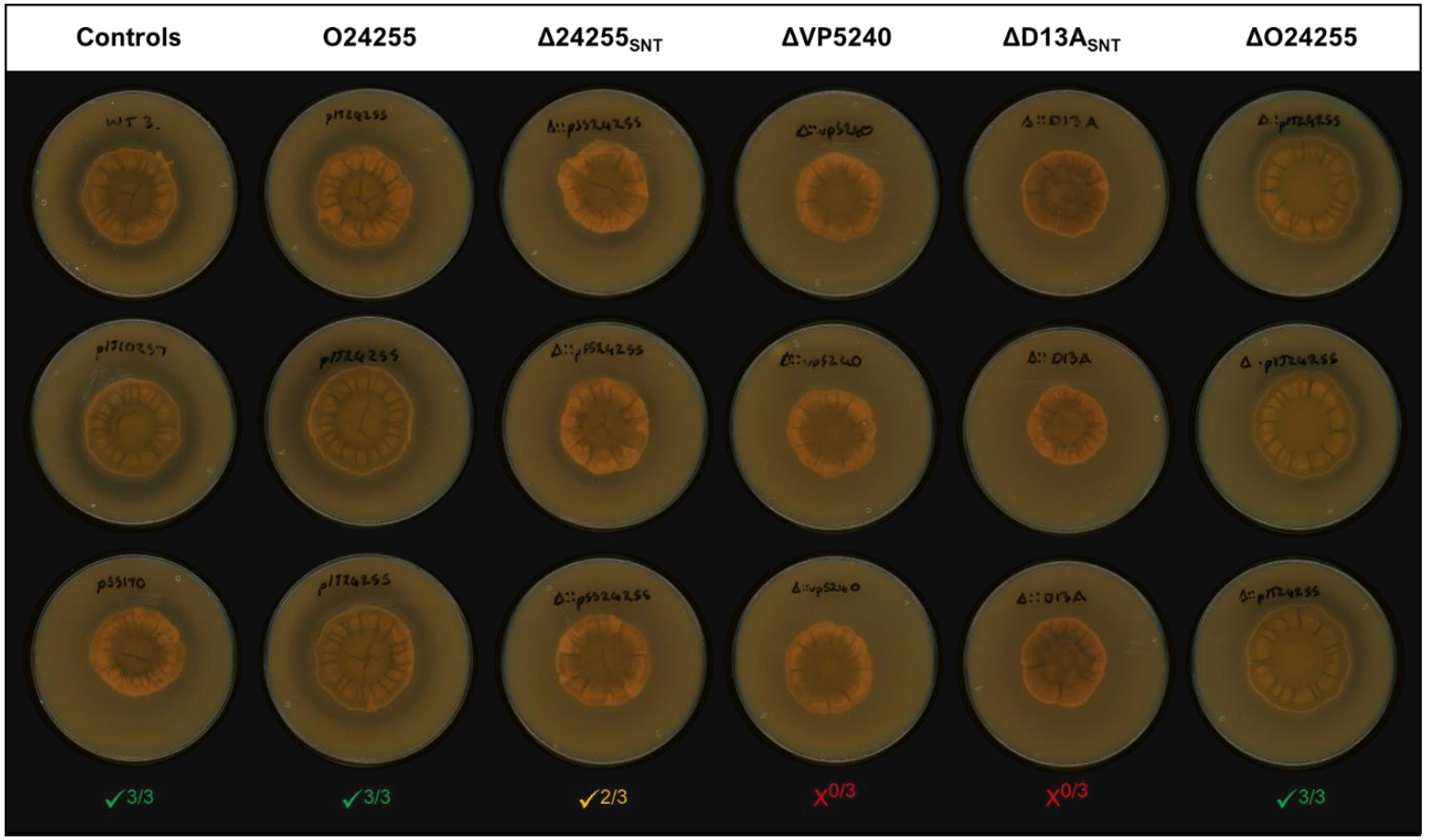

Figure 4.8. *S. venezuelae wblE* mutant bioassays against *B. subtilis* on MYM + TE + 200 µM. Strains are denoted above their respective plate. *S. venezuelae* WT, pSS170, pIJ10257 controls (*n* = 1 each); O24255, Δ24255SNT, ΔO24255, ΔD13A (*n* = 3 each).

4.6. The *vnz_24260* Gene is Recalcitrant to Cas9-mediated Deletion

It was noted that strains arising from pCa24255KO conjugations, carrying a silent mutation in codon 249 (CGC to CGT) exhibited unexpected and significant phenotypes, hence the preferential employment of the pCi plasmid, thereafter. These mutant strains exhibited curling or wrinkled confluent lawns with uncoordinated development (Figure 4.9). A second pCa plasmid was designed which carried a HRT with the majority of *vnz_24260* gene deleted (pCa24260KO), retaining only a small portion of the in-frame sequence which corresponded to an N-terminal 8 aa peptide. Despite evidence that the pCa sgRNA works (Section 4.2.1), *vnz_24260* knockouts could not be acquired. It is possible that the newly formed short peptide is not tolerated by the cell, leading to a pseudo-lethal phenotype; however, the transpositional dead-zone found at the *S. coelicolor wblE* (*sco5240*) locus (Xu *et al*., 2017) also encompasses the full *sco5241* (*vnz_24260*) coding sequence and promoter region, indicating that another essential gene neighbours *wblE*.

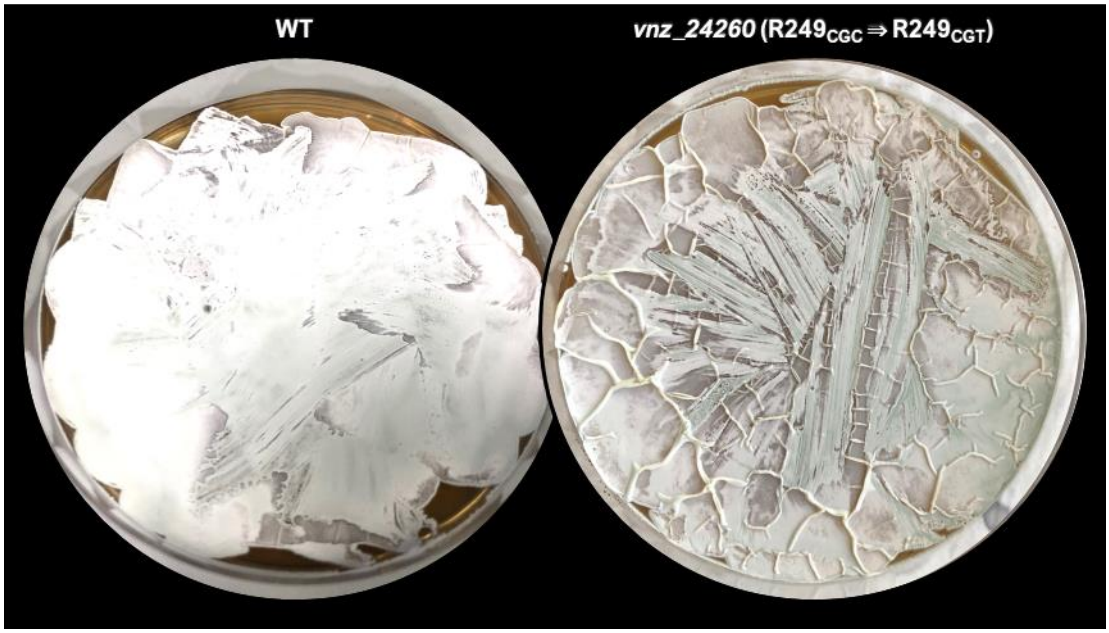

Figure 4.9. Images of confluent growth of wild type *S. venezuelae* NRRL B-65442 (WT) and *S. venezuelae* carrying the silent mutation in codon 249 of *vnz_24260* (CGC⇒CGT). Grown for 3 days from undiluted spore stocks on 90 mm plates.

4.7. Generating a WblE-3xCFLAG Strain for Immunoprecipitation Experiments

The WhiB-like proteins comprise a protein family related by both their protein sequence and structure. As such, there is a risk that polyclonal antibodies raised against WblE could also non-specifically bind epitopes shared by other Wbl proteins and obscure its true regulatory targets. Therefore, this work opted for the incorporation of 3xFLAG tag, and precipitation via monoclonal M2 antibody beads (Anti-FLAG®, Section 2.21). Initially, attempts were made to N-terminally FLAG-tag WblE at its native locus (pCa24255NF) and, subsequently, via pre-complementation with a *trans*-integrated allele (pSS24255NF). However, a stable strain could not be acquired with either approach.

It was thus perceived that the N-terminal tag may be affecting the formation of WblE multimers as was observed for WblE-N6xHis *in vitro* (Section 3.4); alternatively (or additionally), the large size of the FLAG-tag with a linker relative to WblE may have been leading to protein instability or obstruction of function, *in vivo*. As such, pSS170 derivatives were constructed which carried a linker-less, C-terminally 3xFLAG-tagged *wblE* allele, (WblE–DYKDHDGDYKDHDIDYKDDDDK) under the control of its native promoter and with (SNT) Cas9 protection. *S. venezuelae* Δ*wblE*::ΦBT1 pSS24255CF$_{SNT}$ (Δ24255CF1-3) strains were generated via conjugation of the pCi24255KO Δ*wblE* vector, into strain 24255CF which carried the ΦBT1-integrated FLAG-tagged allele. The complemented strain was confirmed via PCR amplification of the *wblE* locus, and size analysis on 1% agarose gel (Figure 4.10). The *S. venezuelae* Δ24255CF1 strain exhibited small phenotypic variations compared to the wild type, but scanning electron micrographs demonstrated wild type microscopic development, very close to that of the wild type (Figure 4.11). This suggests C-terminally FLAG-tagged WblE is functional *in vivo*.

Genetic incorporation and functional retainment of the FLAG-tagged allele was confirmed by an HRP-conjugate M2-antibody western blot against WblE-C3xFLAG, on a PVDF membrane (Figure 4.10). Intriguingly, potential multimeric forms of WblE-CFLAG were faintly visible in the western blot images, similar in nature to those observed for purified WblE-C6xHis (Section 3.4). The WblE-C3xFLAG protein ran around 3 - 4 kDa higher than expected on the polyacrylamide gel (visualized in blot; Figure 4.10). However, sequencing of the additional allele found no evidence for a genetic cause of this extra weight. This was ultimately attributed to the high proportion of negatively charged amino acids in the 3xFLAG-tag, with respect to the small size of WblE. Concentrated stretches of negatively charged (i.e. Asp) residues can lead to a size-shift by disturbing interactions between negatively charged SDS and the protein of interest, ultimately disrupting the repulsive dynamics between SDS and the electric field (Tiwari *et al*., 2019).

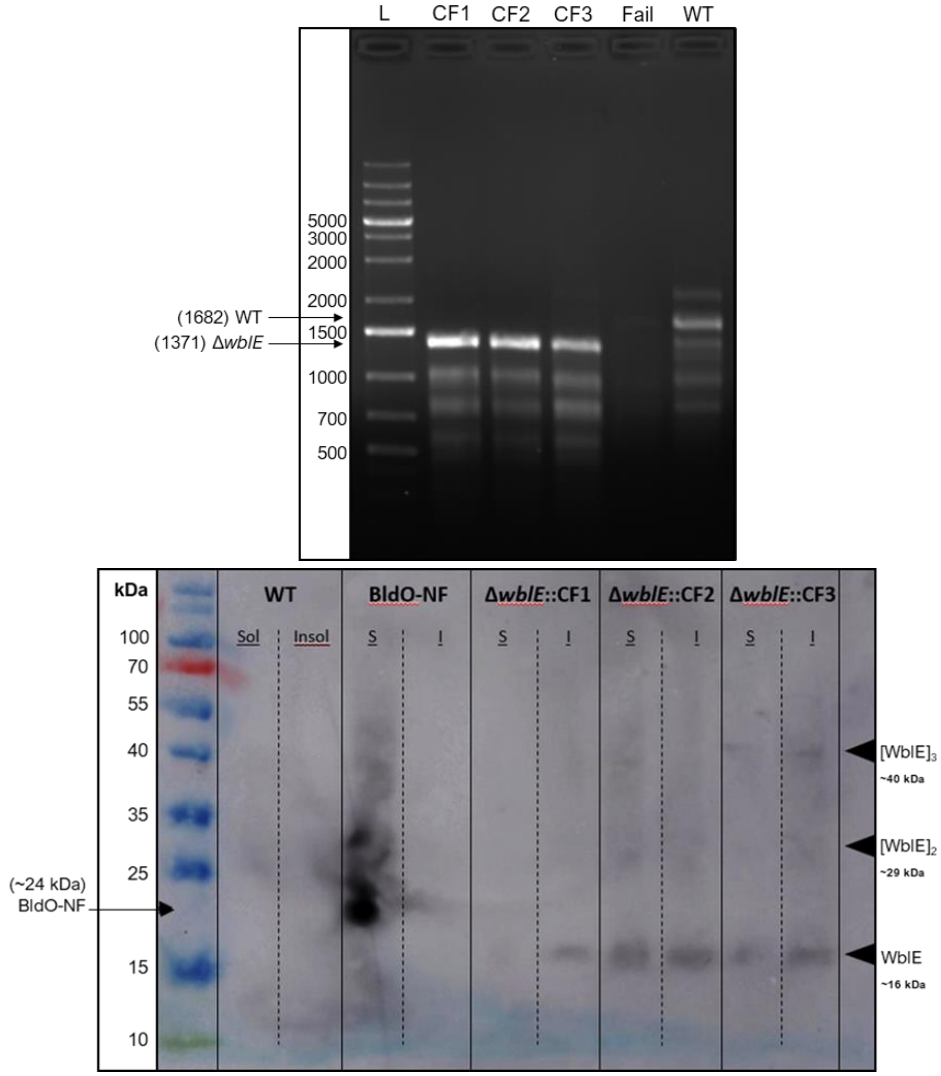

Figure 4.10. (top) The LB038F-LB040R PCR products from the genomic DNA of Δ24255CF1, CF2, CF3 FLAG-tagged strains run against a failed *wblE* knockout and a wild type strain of *S. venezuelae*. **(bottom)** FLAG M2-HRP conjugate antibody western blot of soluble and insoluble fractions from the Δ24255CF1, CF2, CF3 and wild type strains. Inefficient blotting and high apparent molecular weight of WblE can be associated with its strong negatively charge C-terminus as a result of tagging. N-terminally FLAG-tagged BldO (BldO-NF) was used as a positive control.

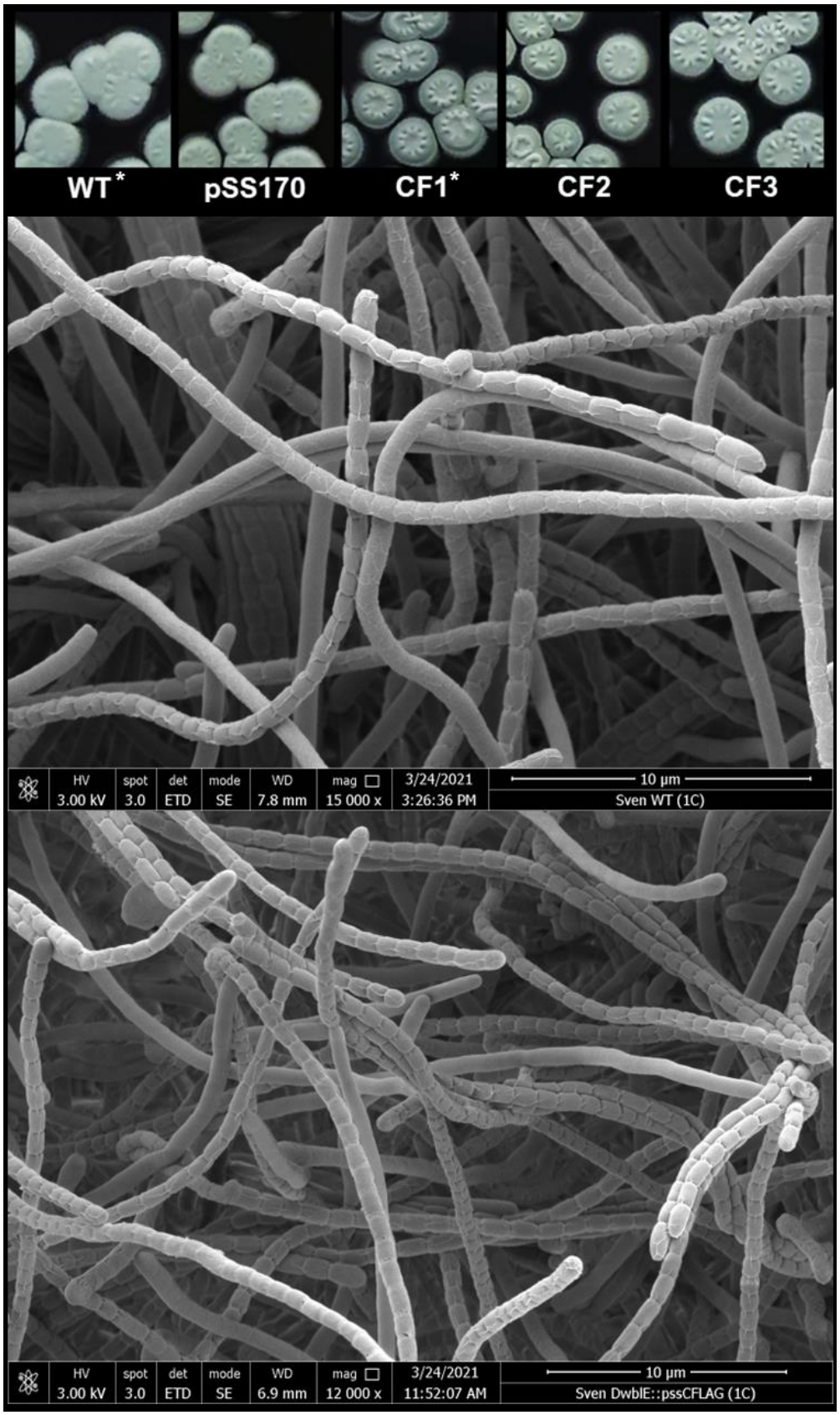

Figure 4.11. *S. venezuelae* NRRL B-65442 wild type strain and the C-terminally FLAG-tagged *wblE* strains (Δ24255CF1 – 3), following 6 days of growth as single colonies on MYM + TE at 30°C **(Top)**. Below this are scanning electron micrographs performed on single colonies grown under the same conditions by Kim Findlay (John Innes Centre) for the wild type strain **(Middle)** and Δ24255CF1 strain **(Bottom)**.

4.8. Discussion.

4.8.1. Addressing the Conflicting Evidence for *wblE* Essentiality

The work in this chapter has demonstrated that the *wblE* gene is essential in *S. venezuelae* NRRL B-65442, and directly corroborates and expands upon previous work which failed to disrupt *wblE* in *S. coelicolor* A3(2) and *S. avermitilis* ATCC 31267 (Fowler-Goldsworthy *et al*., 2011; Liu *et al*., 2017; Xu *et al*., 2017). Specifically, strains carrying an additional, functional CRISPR-Cas9 protected allele, *in trans*, are required to achieve knockouts with the pCRISPomyces-2 system in *S. venezuelae*. Moreover, PCR-targeted, λ-Red-mediated homologous recombination (ReDirect technology) failed to disrupt the native *wblE* gene, despite evidence for successful double-crossover events which would typically yield the desired mutant.

This accumulating evidence for *wblE* essentiality is nonetheless contradicted by two studies. Firstly, early work in *S. coelicolor* reported that *wblE* (*SCO5240*) could be deleted without any obvious phenotypic consequence (Homerová *et al*., 2003). More recently, Cho *et al*. (2017) reported disruption of *wblE* in *S. griseus* strain S4-7, isolated from *F. oxysporum* f.sp. *Fragariae* suppressive soil (Cha *et al*., 2016). In both cases, homologous recombination-based techniques were employed (via pKC1132 and pSIGSC1N, respectively) which are mechanistically equivalent to, albeit less efficient than, ReDirect (Bierman *et al*., 1992; van Wezel & Bibb, 1996). However, as the work (conducted by Dr Neil Holmes) in this thesis has demonstrated, even relevant antibiotic selection and *aac(3)IV* targeted PCR confirmation, together, is insufficient to confirm the generation of true, isogenic Δ*wblE* mutants by recombination-based approaches (Section 4.2.3). Therefore, despite these conflicting results, this work has provided evidence that both studies failed to produce sufficient, substantiative evidence for the generation of an isogenic Δ*wblE* mutant (according to their published methods). Hence, it can be presumed that *wblE* was retained in both species and is in fact an essential gene in this genus. Due to the lack of published research of *wbl* genes in *S. griseus*, the prospect of a unique evolutionary adaptation, which has led to redundancy between *wblE* and the highly similar paralogous gene *wblE2* (77.2% similarity) in this species, cannot be entirely ruled out. Even so, this does not seem to be the case between *wblE* and *wblK* (75.9% similarity) in *S. coelicolor* but will warrant future mutagenic studies in *S. griseus* (Fowler-Goldsworthy *et al*., 2011).

In addition to this, employment of *trans*-integrated mutant alleles with Cas9-protection enabled the generation of a range of viable *wblE* mutants via CRISPR-Cas9. However, it did not permit substitution of any of the four cysteine residues (C9, C37, C40, C46) with the structural analogue serine, nor truncation of the putative DNA-binding domain (Section 4.4). This reinforces the notion that the *wblE* gene and its DNA-binding product are essential and, moreover, that the cysteine residues are each indispensable for WblE function, *in vivo*. These findings are commensurate with published data regarding *Streptomyces* spp. WhiB and WhiD, whereby

cysteine to alanine mutations yield phenotypes that are equivalent to their respective null mutants (Jakimowicz *et al*., 2005; Bush *et al*., 2016). To date, no cysteine substituted mutants studied *in vitro* can stably ligate a [4Fe-4S] cluster, suggesting that this inorganic cofactor underlies the essentiality of the cysteine residues.

There are, however, exceptions to this paradigm, *in vivo*; the *M. smegmatis* and *M. tuberculosis* WhiB2 N-terminal Cys1 (C27 and C67 respectively) mutants are curiously functional, *in vivo*. It was originally proposed that this resulted from alternative cluster ligation by a conserved aspartate residue proximal to Cys1 with + 4 amino acid spacing (D31 and D71, respectively), which could theoretically contribute to Fe-S ligation and, in contrast, is essential for WhiB2 function (Raghunand & Bishai, 2006). In this chapter however, CRISPR-Cas9 mediated *wblE* knockouts were readily achieved with a *trans*-integrated allele carrying a D13A substitution, in direct contrast to the four conserved cysteine residues (Section 4.4.1), suggesting that D13A plays a negligible role in Fe-S ligation at least in *S. venezuelae* WblE. This result corroborates data acquired *in vitro* for purified *M. tuberculosis* WhiB1-D13A which stably ligates an iron-sulphur cluster with identical biophysical characteristics and sensitivity to O_2 / $^{\bullet}NO$ as wild type WhiB1 (Smith *et al*., 2012).

Recent work in *S. venezuelae* has demonstrated that the analogous WhiB aspartate residue (D29) forms a crucial part of the WhiA-WhiB interface via a salt bridge with WhiA-R165, providing an alternative basis for its necessity for WhiB function, *in vivo* (Lilic et al., 2023). Therefore, if this function is conserved and WblE contributes to a similar multipartite assembly, which coordinates a regulator at the transcription complex, either the interaction is not essential for WblE function or D13 is not essential but only contributes to such an interaction. With respect to this latter point, D13 is nestled amongst a stretch of other negatively charged glutamate residues, a characteristic that is unique to this Wbl archetype ($_{11}$EE<u>D</u>PE$_{15}$). Nonetheless, it will first be important to identify if there are indeed candidate co-regulators because to date, none have been proposed for WblE.

4.8.2. Potential Disruption of a *wblE* 5' UTR *cis*-Regulatory Mechanism

An intriguing feature of the *trans*-complemented Δ*wblE* strains was the polar effect which deleteriously affected growth, development and secondary metabolism, when grown on media supplemented with the preferred *Streptomyces* spp. carbon source, GlcNAc. Overexpression of *wblE* from the constitutive *ermE** promoter in a Δ*wblE* genetic background largely complemented these phenotypes, indicating that constitutive expression levels achieved at the native *wblE* locus are important (but not essential) for the gene's function and these were lost in *trans*-integrated alleles. Integrated alleles employed the entire *vnz_24260 – vnz_24255* (*wblE*)

intergenic sequence as the promoter, suggesting that transcription of *wblE* in *Streptomyces* spp. may originate from a promoter element further upstream, embedded within the *vnz_24260* coding sequence, or from the *vnz_24260* promoter itself, although this did not explain the importance of GlcNAc in transcription.

In *S. clavuligerus* ATCC 27064, *S. lividans* TK24 and *S. venezuelae* NRRL B-65442 the *wblE* gene is transcribed with a long 5' UTR (170 bp) and premature transcription termination has been reported for *S. clavuligerus wblE CRV15_08000* (Hwang *et al*., 2021; Droste *et al*., 2021; dRNA-seq Section 2.21.3). The *M. tuberculosis* H37Rv *whiB1* (*rv3219*) mRNA conserves this 5'UTR and the promoter is highly enriched with the NusA transcription termination factor (Uplekar *et al*., 2013). These data provide the hallmarks of a conserved *cis*-regulatory element, controlling *wblE/whiB1* transcription in *Mycobacterium* and *Streptomyces* spp., such as transcription attenuation or a riboswitch. It was therefore believed that the polar effects induced by *trans*-complemented Δ*wblE* strains were a result of disrupting transcription over this *cis*-regulatory element which is conditionally induced (directly or indirectly) by the essential metabolite GlcNAc, in *S. venezuelae*. If this is the case, it would also imply a level of transcriptional coordination between *wblE* and *vnz_24260*, although the basis for this remains unclear.

Overcoming this polar effect and pinpointing important features of this intergenic regulatory mechanism could be achieved *in vivo*, by the *trans*-complementation of Δ*wblE* mutants with the entire *vnz_24260* gene or various fragments of the coding sequence, with comparative phenotypic analysis on GlcNAc-supplemented media. This will undoubtedly be important for more accurate analysis of *wblE* mutant phenotypes in future studies.

Chapter 5.

Deciphering the WblE Regulon in *S. venezuelae* NRRL B-65442

5.1. Introduction

At present, no regulatory targets have been identified or proposed for WblE in *Streptomyces* spp., and none have been determined experimentally. Moreover, only a few have been deduced on a case-by-case basis (*in vitro*) in *M. tuberculosis* including the molecular chaperone *groEL2,* the TVIISS components *espACD* necessary for the virulence program, and *whiB1* itself (Stapleton *et al*., 2012**;** Kudhair *et al*., 2017). Meanwhile, expansive, pleiotropic regulons have been identified *in vivo* for both WhiB(A) (Bush *et al*., 2015) and WblC (Lee *et al*., 2020) in *Streptomyces* spp. The work in this chapter applied Chromatin Immunoprecipitation with downstream sequencing (ChIP-Seq) to identify putative WblE targets *in vivo*, predict a WblE consensus binding sites and test this *in vitro* via surface plasmon resonance (SPR).

ChIP-Seq is a widely employed technique used to identify putative target sites for DNA-binding proteins, across an organism's entire genome. Specifically, the compound formaldehyde is used to covalently crosslink organic macromolecules (such as proteins and DNA) throughout the growing biomass. The cells are then lysed, and DNA sheared into small fragments which are 'immunoprecipitated' using an antibody with specific affinity for the regulator of interest, or a genetically incorporated affinity tag attached to the regulator. The isolated DNA is sequenced, and the sequencing reads aligned back to the genome, to identify regions of enrichment which represent putative binding sites for the regulator of interest. This technique is particularly effective for the analysis of WhiB-like proteins, as the sensitivity of the [4Fe-4S] cluster is circumvented once the protein has been cross-linked to DNA *in vivo* (Bush *et al*., 2015; Lee *et al.*, 2021).

5.2. WblE Chromatin Immunoprecipitation and Sequencing

Developmental work in *S. venezuelae* is typically performed in liquid media, however, in most *Streptomyces* species, aerial mycelium formation and sporulation are blocked in liquid culture (Manteca *et al.*, 2010). Only a small portion of *Streptomyces* spp. studied appear to have the ability to undergo complete differentiation in submerged cultures, however, all species conserve *wblE*. Thus, as a first investigation into WblE function, this work opted for growth on solid agar medium to be most applicable to a wider range of *Streptomyces* spp. Sample

acquisition was carried out at three time-points which coincided with three major developmental stages: tp1 (18 h), established vegetative growth; tp2 (25.5 h), onset of 'white' aerial growth; and tp3 (42 h), onset of sporulation pigmentation (42 h) (Figure 5.1).

As a conservative first-pass approach, isolated DNA from a single full technical replicate of the wild type and Δ24255CF1 *S. venezuelae* strains, was sent to Novogene™ for Illumina sequencing. Variation between two biological replicates is generally low in ChIP-seq data (Ho *et al*., 2011), thus ensuring a degree of confidence in any significant results obtained. Nonetheless, a full triplicate study was pre-emptively undertaken but additional samples were maintained at -80°C for any further analysis. A relatively low DNA yield was acquired for timepoint 1 however this did not seem to affect the experiment. The raw sequencing data were analysed by Dr Govind Chandra (John Innes Centre) and the results are presented here.

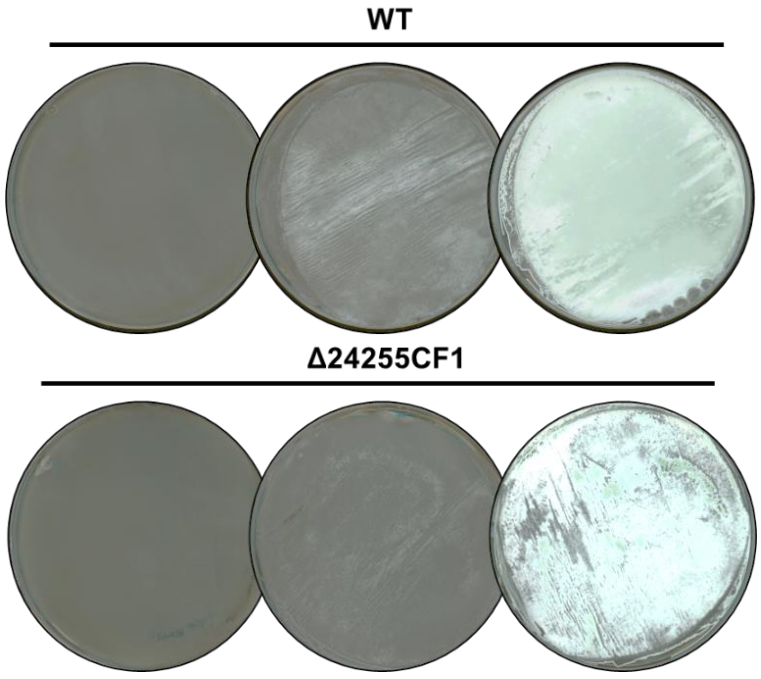

Figure 5.1. Growth of confluent lawns for WT *S. venezuelae* NRRL B-65442 and the Δ24255CF1 strain at 18h (tp1), 25.5h (tp2) and 42h (tp3), from left to right.

5.3. WblE is a Global DNA-Binding Protein in *S. venezuelae*

Over the experimental time-course, a total of 97 peaks were identified which exhibited a greater than log2-fold enrichment and were significant across at least one time-point, compared to the wild type control ($p \leq 0.05$). Regions of local enrichment were globally distributed across the *S. venezuelae* genome and around 25% of the ChIP-seq peaks sat at divergent promoters, potentially putting the transcription of 124 transcriptional units under the control of WblE. A genome-wide overview of these data is shown in Figure 5.1 and a detailed summary of hits are provided in Table 5.1.

ChIP-seq on its own does not provide accurate quantification of DNA binding, nevertheless, each experimental time-point was carried out under the same conditions and an overall reduction in enrichment was observed for most promoters between each timepoint (Figure 5.2). Intriguingly, a distinct set of promoters were specifically enriched during tp2 and are distinguished as 'Group 2' genes. A third set of enriched sequences were differentiated as an 'Atypical Group' as they represented regions of DNA which seemed inconducive to transcription (e.g. between convergent genes).

Two additional promoters, for *bldA (vnz_14210)* and *ssgR (vnz_18200),* exceeded the enrichment cut-off but fell just short of statistical significance ($p = 0.051$ and 0.063 respectively). These peaks have been tentatively included due to their relationship to other enriched targets, their convincing peaks, and the assumption that their significance would be rectified with data from the additional replicates. Nevertheless, these two genes are distinguished in Table 5.1.

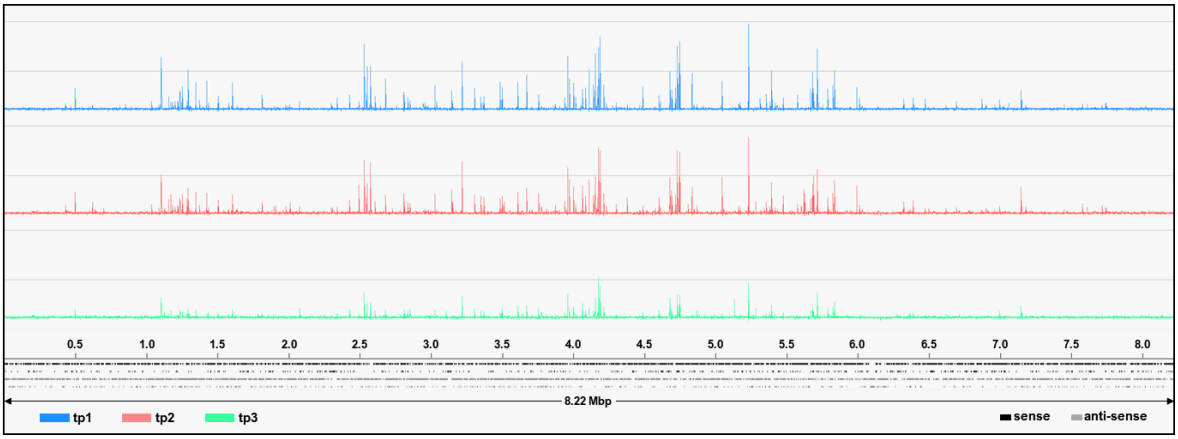

Figure 5.2. Temporo-spatial enrichment of the *S. venezuelae* NRRL B-65442 genomic sequence, following WblE-3xCFLAG ChIP-seq. The genome is depicted along the bottom of the image, and keys for interpreting this figure are shown below. Visualised in Integrated Genomic Viewer.

Table 5.1. Summary of WblE ChIP-seq peaks that were significantly enriched compared to the wild type control. (Group 1) Enriched during tp1 (Group 2) specifically enriched during tp2; and (Group 3) atypical peaks (e.g. between convergent genes/without clear regulatory target).

Group 1 Promoters					tp1 (18 hr)		tp2 (25.5 hr)		tp3 (42 hr)	
n	locus	type	strand	gene product (gene name)	lfc1	*p*-val1	lfc2	*p*-val2	lfc3	*p*-val3
1	vnz_24025	tRNA	1	tRNA-Met (*cat*)	3.125	0.014	2.978	0.004	2.049	0.022
2	vnz_19045	tRNA	1	tRNA-Met (*cat*)	2.931	0.009	2.741	0.018	1.955	0.039
3	vnz_21805	CDS	1	50S ribosomal protein L13 (*rplM*)	2.840	0.001	2.722	0.010	1.610	0.044
4	vnz_11450	CDS	-1	elongation factor 4 (*lepA*)	2.795	0.009	2.554	0.014	1.712	0.055
	vnz_11455	CDS	1	30S ribosomal protein S20 (*rpsT*)						
5	vnz_21635	CDS	1	30S ribosomal protein S10 (*rpsJ*)	2.756	< 0.001	2.743	0.011	1.626	0.028
6	vnz_19005	CDS	1	RNA helicase	2.720	< 0.001	2.801	< 0.001	2.237	< 0.001
7	vnz_26165	CDS	1	50S ribosomal protein L19 (*rplS*)	2.700	0.011	2.325	0.021	1.715	0.095
8	vnz_18870	tRNA	-1	tRNA-Gly (*tcc*)	2.602	0.024	2.121	0.037	1.484	0.051
9	vnz_17940	tRNA	-1	tRNA-Ile (*gat*)	2.544	< 0.001	2.372	0.022	1.639	0.093
10	vnz_04715	rRNA	-1	16S ribosomal RNA	2.520	0.030	2.184	0.009	1.489	0.066
	vnz_04720	CDS	1	phosphoenolpyruvate--carbohydrate phosphotransferase (*crr-ptsI* operon)						
11	vnz_14500	CDS	1	50S ribosomal protein L25/general stress protein (*ctc*)	2.429	0.004	2.528	0.019	1.587	0.029
12	vnz_21760	CDS	1	translation initiation factor IF-1 (*infA*)	2.376	0.005	2.135	0.029	1.169	0.043
13	vnz_11645	CDS	-1	50S ribosomal protein L21 (*rplU*)	2.308	0.002	2.491	0.011	1.253	0.075
14	vnz_11540	tRNA	-1	tRNA-Ala (*ggc*)	2.287	< 0.001	1.900	0.030	1.186	0.059
15	vnz_18630	tRNA	-1	tRNA-Ser (*cga*)	2.227	0.014	2.013	0.012	-	-
16	vnz_05575	CDS	-1	putative 4-amino-4-deoxychorismate synthase operon (*pabBA*)	2.214	0.015	1.733	0.028	-	-
	vnz_05580	tRNA	1	tRNA-Gly (*gcc*)						
17	vnz_26685	rRNA	1	16S ribosomal RNA	2.177	0.028	1.998	0.027	1.292	0.033
18	vnz_24770	CDS	1	50S ribosomal protein L31 (*rpmE*)	2.174	0.026	1.925	0.044	1.102	0.068
19	vnz_21365	CDS	-1	hydrolase	2.152	0.002	2.098	0.030	1.507	0.089

	vnz_21370	tRNA	1	tRNA-Thr (*ggt*)						
20	vnz_26030	CDS	1	hypothetical protein	2.129	0.004	1.884	0.043	-	-
21	vnz_22160	CDS	1	succinate-CoA ligase operon (*sucCD*)	2.076	0.001	1.766	0.021	-	-
22	vnz_16520	tRNA	1	tRNA-Pro (*cgg*)	2.056	0.008	1.712	0.028	-	-
23	vnz_17980	CDS	-1	chromosomal replication initiation protein (*dnaA*)	1.918	0.041	2.038	0.019	1.016	0.072
24	vnz_12065	CDS	-1	energy-dependent translational throttle protein (*ettA*)	1.904	0.025	1.425	0.026	-	-
25	vnz_23210	CDS	1	transglycosylase domain-containing protein	1.837	0.080	2.120	0.007	-	-
26	vnz_06150	CDS	-1	cysteine--1-D-myo-inosityl 2-amino-2-deoxy-alpha-D-glucopyranoside ligase (*mshC*)	1.830	0.003	1.519	0.047	-	-
27	vnz_15670	CDS	-1	NAD(P)-dependent epimerase	1.793	0.003	1.227	0.026	-	-
28	vnz_16260	tRNA	-1	tRNA-Thr (*cgt*)	1.774	0.001	1.536	0.038	-	-
29	vnz_05845	CDS	-1	translation initiation factor IF-3 (*infC*)	1.771	0.002	1.569	0.034	-	-
	vnz_05850	CDS	1	DUF1844 domain-containing protein						
30	vnz_18100	CDS	-1	Hypothetical protein	1.769	0.010	1.763	0.037	1.006	0.049
	vnz_18105	CDS	1	30S ribosomal protein S6 (*rpsF*)						
31	vnz_21710	CDS	1	30S ribosomal protein S8 (*rpsH*)	1.726	0.035	1.271	0.046	-	-
32	vnz_18805	tRNA	-1	tRNA-Ser (*gga*)	1.689	0.045	1.398	0.050	-	-
33	vnz_26635	CDS	1	30S ribosomal protein S15 (*rpsO*)	1.657	0.014	1.520	0.055	-	-
34	vnz_18955	tRNA	-1	tRNA-Asp (*gtc*)	1.634	0.015	1.291	0.030	-	-
35	vnz_05370	CDS	-1	30S ribosomal protein S4 (*rpsD*)	1.608	0.044	1.455	0.090	-	-
36	vnz_20490	CDS	-1	hypothetical protein	1.596	0.091	-	-	-	-
	vnz_20495	CDS	1	MarR family transcriptional regulator						
37	vnz_27285	CDS	1	peptidase	1.591	0.029	1.796	0.016	-	-
38	vnz_15740	CDS	1	tryptophan--tRNA ligase	1.578	0.008	1.357	0.030	-	-
39	vnz_21600	CDS	1	30S ribosomal protein S12 (*rpsL*)	1.570	0.006	1.420	0.010	-	-
40	vnz_18500	CDS	-1	hypothetical protein (SSI-like)	1.558	0.035	1.164	0.027	-	-
	vnz_18505	tRNA	1	tRNA-Ser (*gct*)						
41	vnz_14860	tRNA	-1	tRNA-Ala (*cgc*)	1.546	0.032	1.431	0.053	-	-

42	vnz_02185	CDS	1	cold shock domain protein (*cspD*)	1.533	0.022	1.571	0.050	-	-
43	vnz_26515	CDS	1	translation initiation factor IF-2 (*infB*)	1.518	0.011	1.323	0.002	-	-
44	vnz_25905	tRNA	1	tRNA-Gln (*ctg*)	1.514	0.002	1.215	0.027	-	-
45	vnz_18400	CDS	-1	RsbU-like phosphatase	1.485	0.078	1.777	0.033	-	-
	vnz_18405	CDS	1	DNA primase						
46	vnz_21460	CDS	1	50S ribosomal protein L10 (*rplJ*)	1.469	0.010	1.314	0.050	-	-
47	vnz_32255	CDS	-1	GNAT family N-acetyltransferase	1.441	< 0.001	1.755	0.044	-	-
48	vnz_18840	tRNA	-1	tRNA-Gly (*gcc*)	1.437	0.039	-	-	-	-
49	vnz_14210	tRNA	-1	tRNA-Leu (*bldA*)	1.434	0.051	1.646	0.051	-	-
	vnz_14215	CDS	1	ABC transport ATPase						
50	vnz_05280	CDS	-1	bifunctional *pyr* operon transcriptional regulator/uracil phosphoribosyl transferase (*pyrR*)	1.431	0.045	1.251	0.062	-	-
	vnz_05285	CDS	1	transcriptional regulator (*bldD*)						
51	vnz_12630	CDS	1	AraC family transcriptional regulator (*adpA*)	1.376	0.020	1.483	0.033	-	-
52	vnz_05295	CDS	-1	elongation factor P (*efp*)	1.373	0.021	1.053	0.035	-	-
53	vnz_26000	CDS	-1	50S ribosomal protein L28 (*rpmB*)	1.346	0.040	1.309	0.041	-	-
	vnz_26005	CDS	1	dihydroxyacetone kinase						
54	vnz_26070	CDS	1	hypothetical protein	1.282	0.079	2.137	0.027	-	-
55	vnz_11515	tRNA	-1	tRNA-Ala (*ggc*)	1.263	< 0.001	1.302	0.026	-	-
	vnz_11520	CDS	1	hypothetical protein						
56	vnz_26145	CDS	1	30S ribosomal protein S16 (*rpsB*)	1.258	0.019	-	-	-	-
57	vnz_24620	CDS	-1	hypothetical protein	1.240	0.002	1.057	0.035	-	-
	vnz_24625	CDS	1	histidine kinase (*cvnA5*)						
58	vnz_16930	CDS	-1	dCTP deaminase	1.230	0.030	1.523	0.049	-	-
	vnz_16935	tRNA	1	tRNA-Gly (*ccc*)						
59	vnz_12640	tRNA	1	tRNA-His (gtg)	1.211	0.053	1.075	0.028	-	-
60	vnz_07970	CDS	-1	30S ribosomal protein S1 (*rpsA*)	1.210	0.041	1.016	0.045	-	-
	vnz_07975	CDS	1	SAM-dependent methyltransferase						
61	vnz_11015	tRNA	-1	tRNA-Asn (*gtt*)	1.200	0.016	1.167	0.053	-	-

	vnz_11020	CDS	1	hypothetical protein						
62	vnz_25525	CDS	1	GGDEF-domain containing protein (*rmdB*)	1.193	0.002	-	-	-	-
63	vnz_21010	CDS	-1	cold-shock protein (*scoF2*)	1.181	0.040	1.326	0.047	-	-
	vnz_21015	CDS	1	menaquinone biosynthesis protein (*mqnD*-like)						
64	vnz_21470	CDS	1	DNA-directed RNA polymerase subunit beta	1.155	0.026	1.019	0.054	-	-
65	vnz_18510	tRNA	1	tRNA-Arg (*acg*)	1.153	0.021	1.365	0.022	-	-
66	vnz_06560	CDS	-1	lipase	1.151	0.028	1.166	0.031	-	-
	vnz_06565	CDS	1	glycosyl transferase						
67	vnz_11775	tRNA	-1	tRNA-Pro (*tgg*)	1.129	0.004	1.077	0.070	-	-
	vnz_11780	tRNA	1	tRNA-Gly (*tcc*)						
68	vnz_04915	CDS	1	hypothetical protein (*rbpA*)	1.108	< 0.001	1.204	0.038	-	-
69	vnz_15145	CDS	1	DUF397 domain-containing protein	1.100	0.014	1.327	0.050	-	-
70	vnz_12750	tRNA	1	tRNA-Lys (*ctt*)	1.092	0.027	1.042	0.036	-	-
71	vnz_15035	CDS	-1	RNA polymerase subunit sigma (*hrdD*)	1.083	0.003	1.368	0.044	-	-
	vnz_15040	CDS	1	hypothetical protein						
72	vnz_18200	CDS	1	lclR transcriptional regulator (*ssgR*)	1.079	0.063	-	-	-	-
73	vnz_21445	CDS	1	50S ribosomal protein L11 (*rplK*)	1.054	0.007	-	-	-	-
74	vnz_17835	tRNA	-1	tRNA-Leu (*cag*)	1.050	0.006	1.108	0.035	-	-
	vnz_17840	CDS	1	phospho-peptide binding protein						
75	vnz_25170	CDS	1	superfamily 1 helicase	1.023	0.034	1.404	0.038	-	-
76	vnz_10615	tRNA	-1	tRNA-Val (tac)	1.019	0.021	-	-	-	-
	vnz_10620	CDS	1	hypothetical protein						
77	vnz_18990	tRNA	-1	tRNA-Glu (*ttc*)	1.014	0.011	-	-	-	-
	vnz_18995	CDS	1	minimal metalloprotease domain protein						
78	vnz_24420	CDS	-1	DNA-binding protein	1.003	0.025	-	-	-	-
	vnz_24425	CDS	1	transcriptional regulator						
Group 2 Promoters										
79	vnz_11300	CDS	-1	2-isopropylmalate synthase (*leuA*)	-	-	1.861	0.038	-	-

	vnz_11305	CDS	1	peptidase M4 family protein						
80	vnz_25720	CDS	1	3-isopropylmalate dehydrogenase (*leuB*)	-	-	1.681	0.022	-	-
81	vnz_21445	CDS	1	50S ribosomal protein L11	-	-	1.638	0.037	-	-
82	vnz_25750	CDS	1	citramalate synthase (*cimA*)	-	-	1.500	0.042	-	-
83	vnz_05000	CDS	1	TVIISS AAA ATPase (*eccA*)	-	-	1.447	0.026	-	-
84	vnz_19975	CDS	-1	glucosyl-3-phosphoglycerate synthase	-	-	1.273	0.026	-	-
85	vnz_19980	CDS	1	threonine synthase						
86	vnz_05520	tRNA	-1	tRNA-Val (*cac*)	-	-	1.224	0.027	-	-
87	vnz_15785	CDS	-1	dihydroxy-acid dehydratase	-	-	1.088	0.050	-	-
88	vnz_24255	CDS	-1	WhiB family transcriptional regulator (*wblE*)	-	-	1.067	0.009	-	-
89	vnz_28740	CDS	-1	extradiol dioxygenase	-	-	1.041	0.077	-	-
90	vnz_28745	CDS	1	aconitate hydratase 1						
91	vnz_14230	CDS	-1	NADH dehydrogenase	-	-	1.012	0.081	-	-
92	vnz_02595	CDS	-1	LuxR family transcriptional regulator	-	-	1.003	0.017	-	-
Atypical Group Promoters										
93	vnz_07000	rRNA	-1	16S ribosomal RNA	1.788	0.008	1.443	0.021	-	-
	vnz_07005	CDS	1	hypothetical protein						
	vnz_07010	CDS	-1	3-methyladenine DNA glycosylase						
94	vnz_19125	CDS	1	MarR family transcriptional regulator	1.692	0.011	1.506	0.032	-	-
	vnz_19130	CDS	-1	hypothetical protein						
	vnz_19135	rRNA	1	16S ribosomal RNA						
95	vnz_13570	rRNA	-1	16S ribosomal RNA	1.686	0.030	1.476	0.029	-	-
	vnz_13575	CDS	1	hypothetical protein						
	vnz_13580	CDS	-1	hypothetical protein						
96	vnz_18410	CDS	1	hypothetical protein	1.035	0.033	1.814	0.034	-	-
	vnz_18415	CDS	-1	topoisomerase II						
97	vnz_28985	CDS	1	hypothetical protein	1.003	0.026	1.149	0.021	-	-
	vnz_28990	CDS	-1	(Secreted) polysaccharide deacetylase						

5.3.1. WblE is a Predominantly 'Bald' Developmental Regulator

To date, all studied WhiB-like proteins have been key regulators of reproductive 'white' developmental decisions, with the exception of the non-developmental WblC which does, however, bind the *wblE* promoter (Lee *et al*., 2020). On the contrary, ChIP-seq revealed that WblE predominantly binds 'bald' developmental genes (Figure 5.3). Most notably, WblE was enriched at the divergent *bldD* (*vnz_05285*) promoter, encoding the master developmental repressor which senses c-di-GMP to globally repress genes involved in reproductive growth, amidst its broad regulon (Tschowri *et al*., 2014). Moreover, WblE binds to the promoter of the highly conserved (GGDEF/EAL) c-di-GMP phosphodiesterase (PDE) *rmdB* gene during tp1, which catabolises c-di-GMP to ultimately promote development via BldD (Tschowri *et al*., 2014; Al-Bassam *et al*., 2018).

Intriguingly, WblE does not bind to c-di-GMP anabolic enzymes such as *cdgB,* thus, presenting an intriguing case of a regulator that may coordinate production of both the sensor and catabolism of its ligand. The other developmental promoters bound by WblE comprise two key targets of BldD; the rare tRNA *bldA* (Leu:UAA) and the contingent, TTA-containing gene *adpA* (also known as *bldH*), which are essential for the onset of the extracellular proteolytic cascade, aerial development and antibiotic production (Takano *et al*., 2003; Hirano *et al*., 2006; Płachetka *et al.*, 2021). In *S. lividans* AdpA represses the expression of *wblE*, implying that this cascade involves a feedback loop (Guyet *et al*., 2014).

In possible contradiction to this 'bald' developmental paradigm, the promoter of *ssgR* was also enriched in the WblE ChIP-seq dataset (Table 5.1: no.72); the gene product appears to play an intermediary function between early and late reproductive cell-division. In *S. coelicolor*, *ssgR* is transcribed independently of any typical Whi-regulators but is crucial for activation of the cell-division gene *ssgA*, and mutants consequentially yield white colonies defective in sporulation (Traag *et al*., 2004). There are functional discrepancies with the *S. griseus* homologue *ssfR,* which does not regulate *ssgA* but yields a similar phenotype (Jiang & Kendrick, 2000). Comparatively little is known about *ssgR* in *S. venezuelae*, but its transcription is dependent on the early developmental regulator BldM (Al-Bassam *et al*., 2014); this characteristic will become important later in this thesis.

5.3.2. WblE is Enriched at the *dnaA* Promoter

Chromosomal replication and partitioning between daughter cells are central to cell-division and predominantly controlled at the initiating step. In bacteria, the conserved *dnaA* gene encodes the initiating protein for DNA replication and often sits at the heart of developmental programs. DnaA binds 'DnaA-box' sequences at the origin of replication (*oriC*), oligomerising in

an ATP-dependent manner to form the nucleoprotein 'pre-replication complex', which promotes the subsequent recruitment of the DNA replication machinery (e.g. DNA Polymerase III), concomitant with melting of the *oriC* DNA duplex, forming the replication fork (Atlung & Hansen, 1993; Miller *et al*., 2009; Katakayama & Sekimizu, 1999).

The *dnaA* promoter was enriched throughout the WblE ChIP-seq experiment (Figure 5.2.b) indicating a significant and constitutive role for WblE in regulating *dnaA* expression and, consequentially, cell-cycle progression. The developmental activator AdpA binds and sequesters the 5' region of *oriC* to suppress DnaA binding and oligomerisation (Wolański *et al*., 2012). It is intriguing, therefore, that AdpA also negatively regulates *wblE S. lividans* (Guyet *et al.*, 2014) and that the *adpA* promoter is itself bound by WblE in *S. venezuelae.*

DNA primase-polymerases (PrimPols) are emerging enzymes which synergise with the replicative DNA Polymerase III to simultaneously promote replication and continuous replication fork progression in eukaryotes and archaea (Díaz-Talavera *et al*., 2022). Functional homologues exist in bacteria but are poorly studied *in vivo* (García-Quintans *et al*., 2020). One such conserved PrimPol gene in *Streptomyces spp.*, vnz_18405 was also bound by *S. venezuelae* WblE (divergently encoded from an RsbU-like protein - Section 5.3.5) and may be involved in its replicative function.

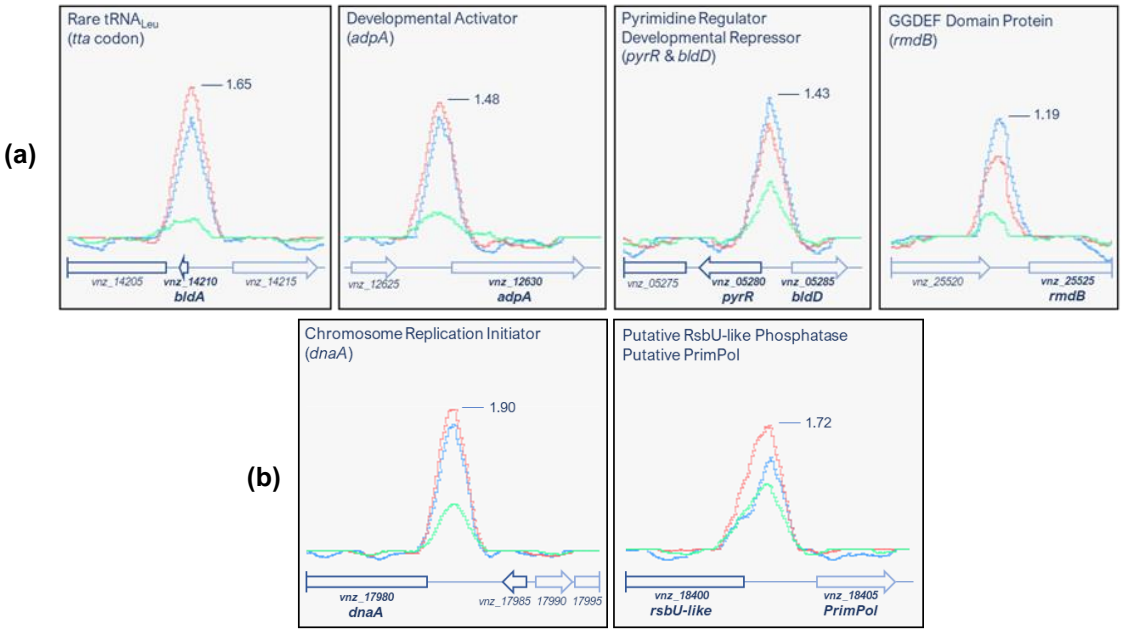

Figure 5.3. WblE ChIP-seq enrichment peaks associated with (a) development, and (b) the cell cycle replication initiator *dnaA*, and putatively associated locus encoding a PrimPol-like product. Maximum log2 fold change is labelled at peak apex. Blue (tp1); red (tp2); green (tp3).

5.3.3. WblE Shares Ancestral Functions with its Orthologue, WhiB1

M. tuberculosis WhiB1 has been shown to bind its own promoter *in vitro* and a similar situation seems apparent for its *Streptomyces* counterpart, suggesting autoregulation is common for WblE homologues (Smith *et al*., 2010). The 'blocky' nature of the *wblE* peak was intriguing but hard to explain, possibly indicating unique binding configurations at its own promoter (Figure 5.4). In addition to its own promoter, WhiB1 binds and regulates the *espA-espC-espD* operon of *M. tuberculosis*, *in vivo* (Kudhair *et al*., 2017; Garces *et al*., 2010). The cluster encodes components indispensable for ESX-1 (Type VII secretion) mediated virulence (Garces *et al*., 2010; Chen *et al*., 2012) and is specifically associated with pathogenic mycobacteria and is absent from non-parasitic species, including *Streptomyces* spp. Even so, WblE was found to bind a homologue of the cytosolic CbxX-family ATPase *eccA* (*vnz_05000*), which is also essential for ESX-1 mediated virulence in *M. tuberculosis.*

Intriguingly, the *eccA* gene is distally encoded from the rest of the *Streptomyces* TVIISS components, akin to *M. tuberculosis espACD*. Investigation has, so-far, eluded *eccA* but the functions for most components of *Streptomyces* TVIISS machinery remain enigmatic as mutants lack clear phenotypes (Fyans *et al*., 2013). In contrast, the known TVIISS substrates, EsxA and EsxB, play roles in reproductive growth and chromosomal organisation, seemingly independent of secretion (San Roman *et al*., 2010; Fyans *et al*., 2013). The presence of targets similar to those identified for *M. tuberculosis* WhiB1 was intriguing and both enriched genes were among the group two genes, suggesting a specific importance for their (positive or negative) regulation during the onset of aerial growth (tp2, 25.5hr).

The essential chaperone *groEL*, is also direct target of *M. tuberculosis* WhiB1 but the homologous gene promoter in *S. venezuelae* was absent from the ChIP-seq data (Stapleton *et al*., 2012).

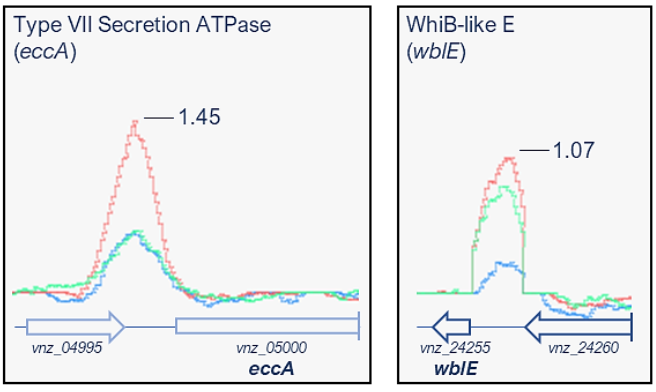

Figure 5.4. WblE ChIP-seq enrichment peaks for the *wblE* and *eccA* promoters. Maximum log2 fold change is labelled at peak apex. (tp1) blue; (tp2) red; (tp3) green.

5.3.4. A Translational Gene-set Dominated the WblE ChIP-seq Data

Translation is central to the function of cells and many of the core and adaptive components are conserved, highly expressed and essential for cell growth and survival (Bubunenko *et al*., 2007). Of the nearly 100 unique sites of enrichment identified by WblE ChIP-seq, a staggering proportion were associated with genes relating to translation and the ribosome, including ribosomal (r)RNA, transfer (t)RNAs and ribosomal proteins (RPs).

A total of 24 ribosomal proteins and 31 of the 68 tRNA genes in *S. venezuelae* were significantly enriched in the WblE ChIP-seq. Several tRNAs formed possible operons with additional tRNA genes, pushing the proportion much higher. In addition, five rRNA genes also had nearby peaks; three rRNA loci exhibited remarkably similar gene arrangements which were associated with an atypical WblE enrichment peak (Table 5.1: no. 93 - 95), situated within a neighbouring hypothetical gene. In addition, the promoter regions of two predicted RNA helicase genes (*vnz_19005*; *vnz_25170*) which could process or maintain transcribed rRNA and tRNA were also enriched in the data (Figure 5.5).

There has been concern expressed that highly expressed genes such as rRNAs, tRNAs and RPs, may occur as 'false-positives' in Wbl ChIP-seq experiments due to the happenstance cross-linking of Wbl proteins competing for HrdB which is already occupying these promoters (Mark Buttner, personal communication). Nevertheless, tRNAs, ribosomal proteins and RNA processing enzymes have appeared in all Wbl ChIP-seq experiments to date; in addition, deletion of *whiB* dysregulates RNA processing enzymes, while deletion of *wblC* affects ribosomal composition (Bush *et al*., 2015; Lee *et al*., 2022). Other transcription factors which stably interact with the principal sigma factor, including RbpA (and CarD in *M. tuberculosis*) are also known to broadly influence binding and regulation of tRNA, RP and rRNA genes (Stallings *et al*., 2009; Tabib-Salazar *et al*., 2013; Šmídová *et al*., 2021).

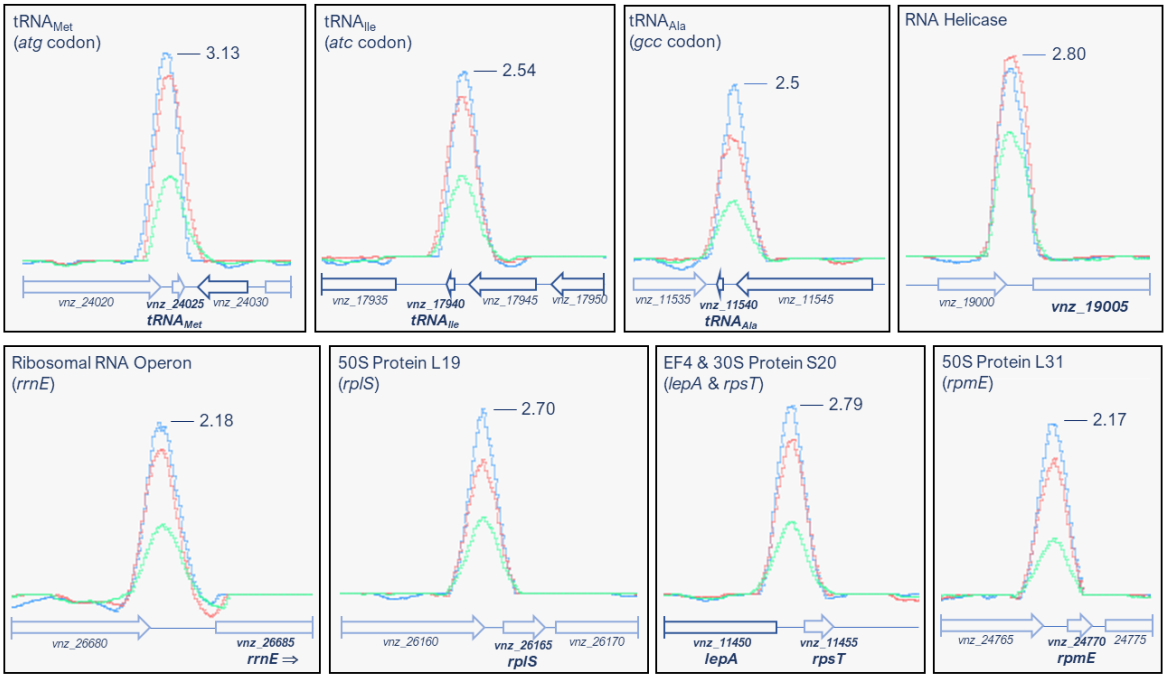

Figure 5.5. A range of WblE ChIP-seq enrichment peaks associated with translational processes, including promoters associated with ribosomal proteins stable tRNA and rRNA genes (EF = Elongation Factor). Maximum log2 fold change is labelled at peak apex. (tp1) blue; (tp2) red; (tp3) green.

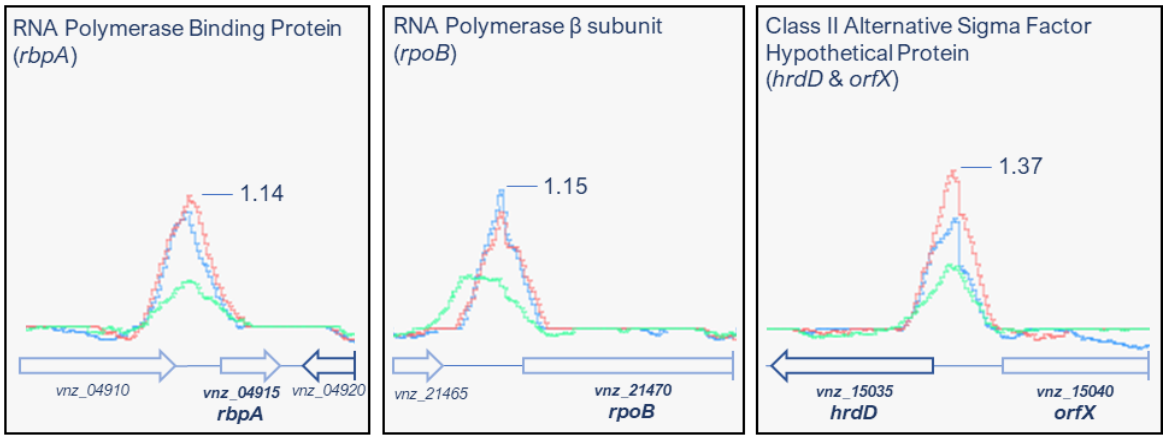

Figure 5.6. A range of WblE ChIP-seq enrichment peaks associated with the function of the RNA Polymerase and Transcription. Maximum log2 fold change is labelled at peak apex. (tp1) blue; (tp2) red; (tp3) green.

5.3.5. WblE Enriched Upstream of Genes Encoding RNA Polymerase Components

The ChIP-seq results indicated that WblE also bound to the promoters of the RNA polymerase β-subunit (*vnz_21470*; *rpoB*) and the σ-binding transcription factor gene *rbpA* (*vnz_04915*). Notably, WblE also bound to the divergent *hrdD* / *orfX* (*vnz_15035* / *vnz_15040*) promoter; it has previously been predicted that the transcription of these two genes is linked as a consequence of the overlapping nature of their TSSs (Buttner *et al*., 1990). The *hrdD* gene encodes a Class II σ-factor with sequence specificity similar to that of housekeeping σ^{HrdB} but it lacks key residues in region 4.2 necessary for interaction with WblE.

In addition to the physical RNA polymerase components, the promoter of a gene encoding a putative RsbU homologue, divergently encoded from a putative DNA PrimPol (Section 5.3.3.1), was also enriched in the ChIP-seq dataset. RsbU-like phosphatases are typically regulators of multi-component (RsbUVW) anti-sigma-factor phosphorylation cascades, which ultimately influence RNA polymerase composition and promote expression of stress-response pathways via alternative sigma factors (more detail in Section 6.3.6).

These results suggest a broad role for WblE in regulating RNA Polymerase composition both directly (*rpoB, rbpA*, *hrdD*) and indirectly (*vnz_18400*), thereby also influencing its own ability to participate in transcription.

5.3.6. WblE Enriched at the Promoters of Primary Metabolic Genes

5.3.6.1. Specific Aspects of Amino Acid Metabolism

A portion of the genes enriched in the ChIP-seq dataset related to primary metabolism. In particular, two L-leucine biosynthetic genes, isopropylmalate synthase (*leuA – vnz_11300*) and dehydrogenase (*leuB – vnz_25720*), were among the group 2 genes specifically enriched during tp2 (Table 5.1: no.79 - 80). Intriguingly, temporal control over the flux of the branched amino acid leucine has an underlying importance in development and secondary metabolism and BldD binds upstream of *leuA* to repress this biosynthetic pathway during vegetative growth. This may be related to the developmental function of the rare leucine tRNA (*bldA*), which is also bound by both WblE and BldD (Section 5.3.1; den Hengst *et al*., 2010).

5.3.6.2. Central Carbon Metabolism

The citric acid cycle sits at the centre of carbon metabolism, within which the succinate-CoA ligase (SCL) catalyses the reversible conversion between succinyl-CoA and succinate and is a vital component for cellular metabolism and energy generation. The enzyme functions as a heterodimer or tetramer assembled from α- (SucD) and β- (SucC) subunits, typically favouring the generation of succinate. The standalone importance of SCL is exemplified by the fact that it

is the only enzyme in the citric acid cycle that catalyses substrate-level phosphorylation of GDP and ADP to form the high-energy triphosphates, GTP and ATP respectively (Murakami *et al*., 1972; Schürmann *et al*., 2011). The α- and β-subunits are generally encoded within the same operon and the corresponding *sucC-sucD* operon in *S. venezuelae* (*vnz_22160 – vnz_22165*) was significantly enriched within the WblE ChIP-seq data (Table 5.1: no. 21). Succinyl-CoA serves as a primary entry point into the citric acid cycle for the branched chain amino acids, valine, isoleucine and methionine. In addition, succinyl-CoA also supplies fatty acid anabolism and synthesis of the haem precursor, δ-aminolaevulinic acid (Stojanovski *et al*., 2009; Russell & Taegtmeyer 2013). Therefore, via regulation of SCL, WblE could exert potent metabolic and respiratory control by managing the flux of succinyl-CoA. This group of genes also includes the *crr-ptsI* (*vnz_04720 – vnz_04725*) sugar phosphotransferase operon.

5.3.6.3. Putative Glycerophospholipid Biosynthesis Targets

WblE bound the promoters of two promoter regions associated with the metabolism of membrane phospholipids and their glycosylation. The *vnz_15670 – vnz_15665* operon stood out as it is conserved in *Streptomyces* spp., encoding an enzyme with strong homology to the lysophosphatidic acid (*sn*-1-acylglycerol-phosphate) acyltransferases (LPAATs or AGPATs); crucial enzymes that function between the 'Kennedy' and 'Lands' cycles, which are necessary for the *de novo* biosynthesis of glycerophospholipids and the dynamic remodelling of their fatty acid composition, respectively. The gene preceding this in the operon is an enzyme with close homology to NDP-sugar epimerases, which are often closely linked with cell envelope and cell wall glycosylation. For example, GalE catalyses the interconversion of UDP-4-Galactose and UDP-4-Glucose which is necessary for the synthesis of complex glycosphingolipids and cell-wall glycans.

The other promoter bound by WblE was divergently positioned between a conserved lipid esterase (*vnz_06560*) shown to have true lipase activity (TAG + H_2O → DAG + fatty acyl) in *S. coelicolor* A3(2), and the less-well conserved *vnz_06565 – vnz_06570* operon which encodes a pair of unstudied family-2 glycosyl transferases (Bielen *et al*., 2009). The latter gene encodes an undefined member of this glycosylase family, but the former encodes a DPM1-like enzyme, which function in the synthesis of polyprenol-phosphate mannose donors for extracellular glycosylation reactions (See also Section 6.3.9).

5.3.6.4. Major Respiratory Enzyme Targets

Prior to this doctoral research, WblE was found to be a direct target of the (NADH:NAD^+)-sensor/regulator Rex, which controls the expression of important aerobic respiratory enzymes in *S. avermitilis* (Liu *et al*., 2017). Concurrent with this, amongst genes relating to primary and intermediary metabolism were those relating to aerobic respiration in *Streptomyces* spp. Notably, the ChIP-seq dataset indicated significant binding to the divergent promoter of the *mqnD* gene, encoding an enzyme which catalyses the conversion of cyclic dehypoxanthine futalosine to 5,8-dihydroxy-2-naphthoic acid, an important step in the futalosine menaquinone (MK) biosynthesis pathway (described in more detail in Section 6.3.4.1 – Hiratsuka *et al*., 2008; Manion-Sommerhalter *et al*., 2021). A discernible but sub-significant level of enrichment was also manually observed at the MK-dependent NADH-quinone oxidoreductase operon *nuoACDEFGHILKMN* (*vnz_21055 – 21120*) cluster, encoding essential components of respiration and aerobic growth that are also under the control of Rex (Liu *et al*., 2017).

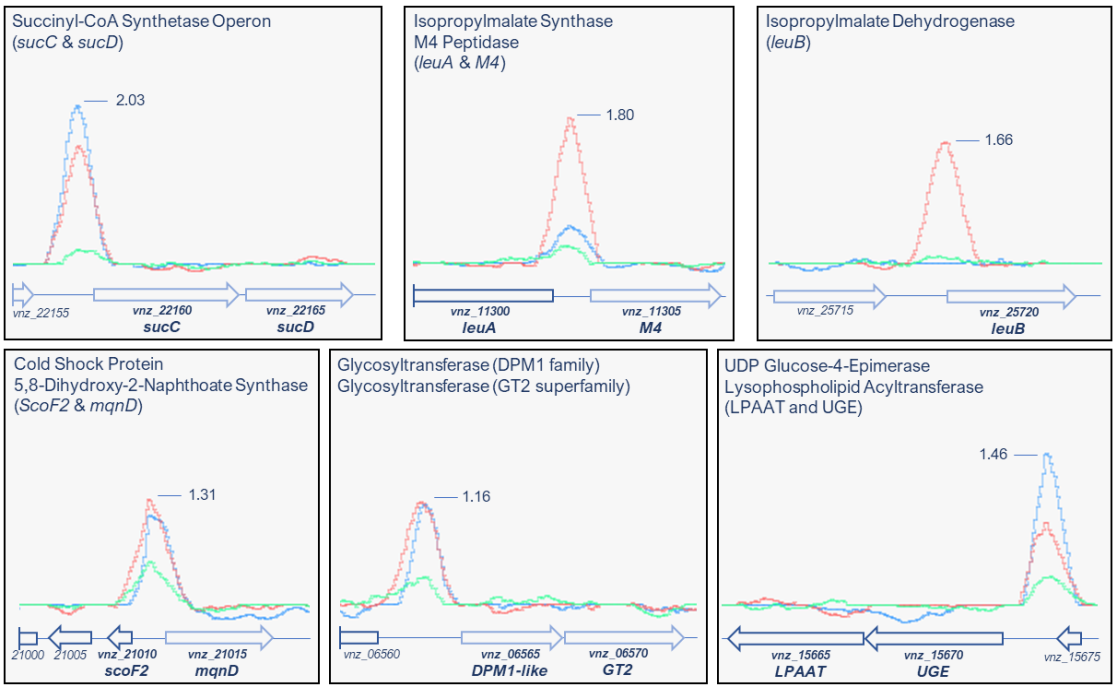

Figure 5.7. WblE ChIP-seq peaks associated with *S. venezuelae* NRRL B-65442 primary metabolism. Maximum log2 fold change is labelled at peak apex. (tp1) blue; (tp2) red; (tp3) green.

5.3.7. WblE is Enriched at Promoters for Molecular Antioxidants and Osmolyte Synthesis

Mycothiol (MSH), is the evolutionarily unique LMW thiol found only in Actinobacteria and is an effective antioxidant of nitric oxide (see Section 1.6.2.2). The biosynthetic pathway consists of five enzymatic steps involving a glycosyltransferase (MshA), a phosphatase (MshA2), a deacetylase (MshB), a cysteine ligase (MshC) and finally the mycothiol synthase (MshD). The ChIP-seq data indicates that WblE binds to the *mshC* (*vnz_06150*) promoter and hence may directly regulate MSH biosynthesis; deletion of the homologous gene (Δ*sco1633*) in *S. coelicolor* abolishes MSH biosynthesis (Park and Roe 2008; Nakajima et al., 2015). Intriguingly, deletion of *wblC*/*whiB7* dampens mycothiol synthesis, presumably via loss of induction of *sigR* (Burian *et al*., 2012; Yoo *et al*., 2016), encoding the thiol-oxidative response sigma factor (σ^R). However, this is the first evidence suggesting that a Wbl protein may directly regulate MSH biosynthesis (Figure 5.8).

WblE also bound the divergent promoter of a putative glucosyl- (*gpgS*) or mannosyl-3-phosphoglycerate synthase (*mpgS*) gene; enzymes that synthesise the precursors to the compatible solutes Glucosylglycerate (GG) or Mannosylglycerate (MG), respectively (Figure 5.8). These compounds are widespread throughout bacteria and accumulate under osmotic stress and nitrogen starvation, but their true functions and mechanisms are elusive (Empadinhas & da Costa, 2010). *Streptomyces* spp. are only known to produce GG and thus further reference to the *vnz_19975* will refer to it as *gpgS*; In *Streptomyces* spp. specifically, the role of GG as an osmolyte is supported by reports from *S. caelestis*, whereby intracellular concentrations are induced during growth with elevated salt concentrations (Pospíšil et al., 2007). The *gpgS* gene forms an operon with *vnz_19970* (hypothetical).

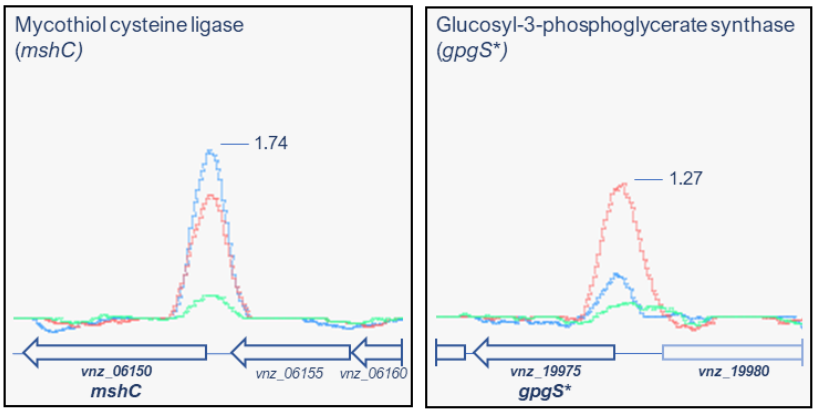

Figure 5.8. WblE ChIP-seq peaks associated with synthesis of MSH and the osmolyte GG (or MG) in *S. venezuelae* NRRL B-65442. Maximum log2 fold change is labelled at peak apex. (tp1) blue; (tp2) red; (tp3) green.

5.3.8. Potential Regulation of Secondary Metabolite Synthesis by WblE

Amongst the set of enriched promoters, one preceding a gene encoding a 'Large ATP-binding LuxR' (LAL) type regulator, was of particular interest as it was situated within a cryptic secondary metabolite BGC, resembling a typical Lantibiotic gene cluster (BGC#5; Chapter 1, Table 1.1). In addition, enrichment was observed for *scr2* (*vnz_15145*), encoding a homologue of BldB which cooperates with Scr1 (vnz_15140) to positively regulate secondary metabolism in a range of *Streptomyces* spp. (Santamaría *et al*., 2018).

These findings prompted additional searches for enrichment peaks in known *S. venezuelae* secondary metabolite BGCs. Remarkably, convincing peaks were found in several BGCs, just below the statistical cut off. These included a peak between the divergently encoded chloramphenicol transporter genes *cmlF* and *cmlN* (*vnz_04410, 04415*), the Foroxymithine siderophore biosynthetic genes, *cchA* and *cchB* (*vnz_34770*, *34775*), and a distantly encoded ferric siderophore reductase (vnz_05960; Figure 5.9). Curiously, the *S. venezuelae* aminodeoxychorismate synthase operon (*vnz_05575* – *vnz_05570*; *pabB* – *pabA*) sits at a divergent promoter with several tRNAs, that were also common ChIP-seq hits (Table 5.1: no.16). The encoded heterodimeric enzyme diverts chorismate away from aromatic amino acid synthesis, to complete the first shared step in the biosynthetic pathways of folate (an essential metabolite) and the secondary metabolite, chloramphenicol (Chang *et al.*, 2001).

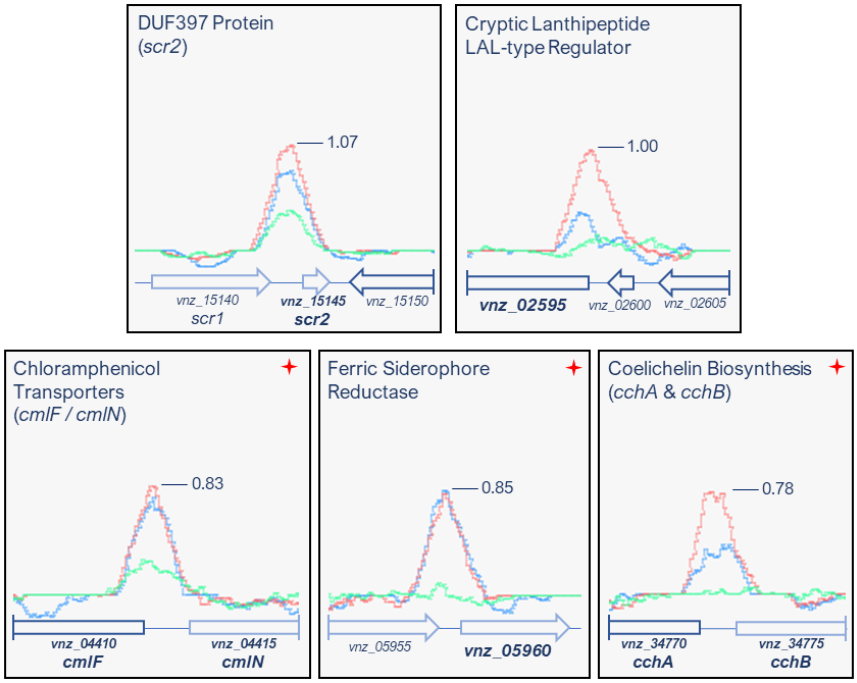

Figure 5.9. WblE ChIP-seq peaks associated with *S. venezuelae* NRRL B-65442 secondary metabolite biosynthesis. Red stars indicate visually discernible but sub-significant peaks, identified by manual inspection of the data. Maximum log2 fold change is labelled at peak apex. (tp1) blue; (tp2) red; (tp3) green.

5.4. Identifying a Putative Consensus DNA-binding Motif for WblE

5.4.1. MEME-ChIP

In order to identify a potential consensus sequence, MEME-ChIP was performed (https://meme-suite.org/meme/tools/meme-chip), which provides comprehensive discovery and analysis of potential transcription factor binding sites in larger data sets. The atypical group peaks were not included in this analysis as they were most likely to represent spurious hits. No limit was set for the distance of a peak to the potentially regulated gene(s), to be included in the analysis. Sequences were searched for three motifs between 10bp and 15 bp (~1.0 – 1.5 turns). Typically, a 50 bp central region is used, however this was extended to 100bp as the resolution was expected to be lower due to extended regions of cross-linking resulting from the RNA polymerase in complex (Bailey *et al*., 2015). Nevertheless, multiple searches were run under second and third order background models with varying central regions (50 – 200 bp) and these predominantly returned the same albeit less well-defined motifs, arbitrarily named MEME-1 (M1) to MEME-3 (M3) (Figure 5.10.a). Centrimo identified several degenerate (centrally recurring) M1 motifs which may contribute to binding, each conserving a contiguous A/T-rich sequence (e.g. TTT/ATT and their complements; Figure 5.9.a). WhiB and WblC were shown to bind similar AT-rich regions preceding the -35 site (Lilic *et al*., 2021; 2023).

5.4.1.1 RNA Polymerase Architecture Reflected in MEME Results

Spaced Motif Analysis Tool (SpaMo) runs alongside MEME-ChIP and infers interactions between transcription factors based on conserved spacing between predicted binding sites in different promoters. SpaMo identified conserved 20-22 bp spacing (end to end) between M1 and M2, in multiple promoters, resembling the spacing between the -10 bp and -35 bp promoter elements (Figure 5.10.b). In accordance with this, the M2 consensus closely resembles the -10 bp site for σ^{HrdB} in *S. coelicolor* and *S. lividans* (Jeong *et al*., 2016; Šmídová *et al*., 2018; Lee *et al*., 2019). In the probabilistic visualization of all three MEME motifs, the position of M3 sites tends to exhibit a bimodal distribution which clusters either side of M1 sites (Figure 5.10.c). It is possible that this alludes to the existence of a co-regulator acting with WblE**,** although observable similarities in MEME-3 and MEME-2 sequence and distances from M1, suggest this is simply a variant -10 bp site (Figure 5.10.a). By process of elimination, M1 was deemed most likely to represent the *wblE* consensus binding motif.

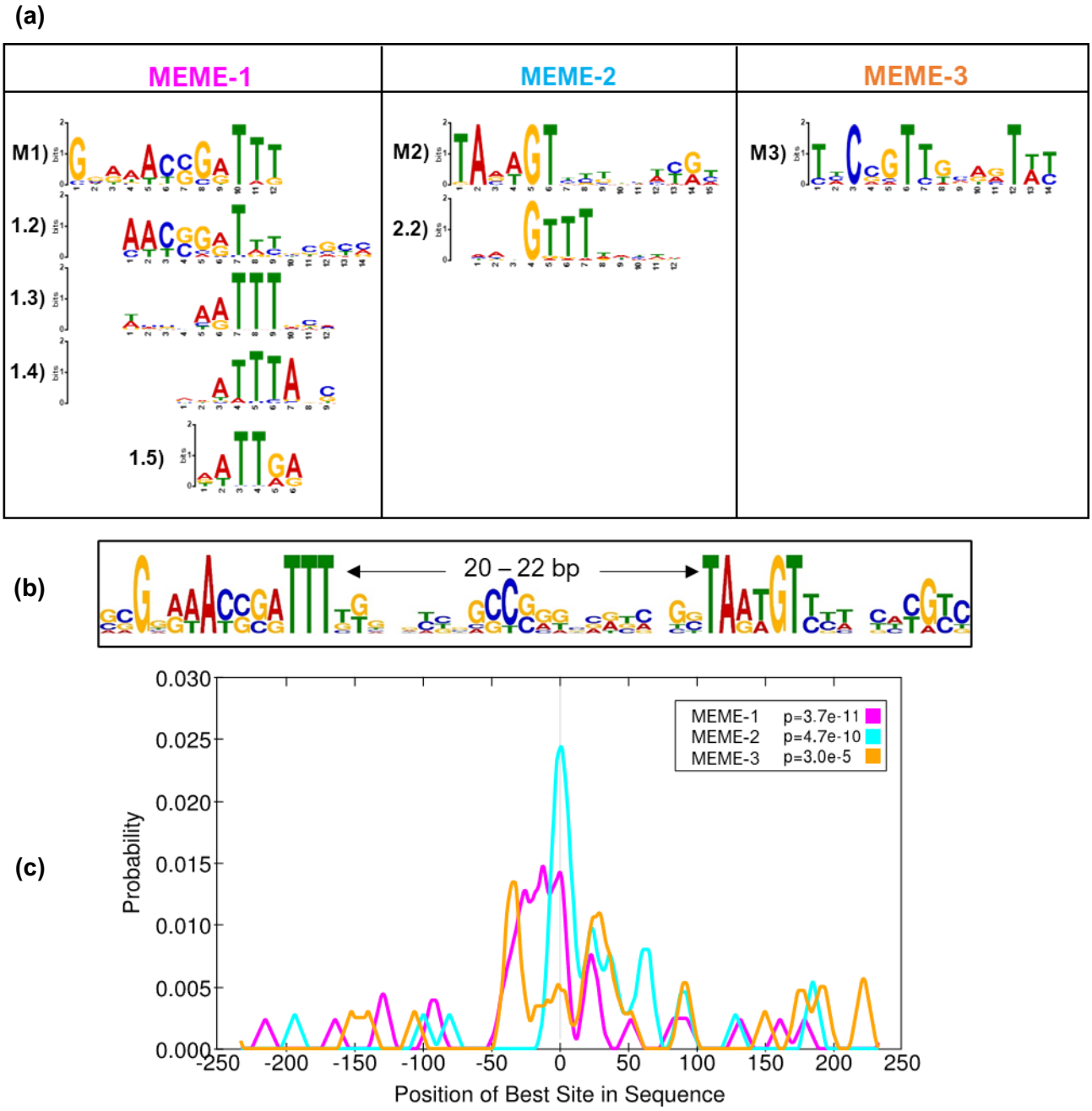

Figure 5.10. (a) The MEME-1 to MEME-3 consensus motifs, predicted by MEME-ChIP, with degenerative motifs identified by CentriMo listed beneath. Note that for M1.5, alignment was carried out manually; **(b)** Spacing between M1 (3' end) and M2 (5' end) resemble spacing between the -10 and -35 elements recognised by HrdB. **(c)** Probabilistic occurrence of motifs M1, M2 and M3 in WblE enriched promoters was calculated by SpaMo. The graph is arbitrarily centred on M2 (-10) which was the most consistently positioned motif among WblE-bound promoters.

5.4.2. Comparing Architecture of WhiB-like Associated -35 sites

An established paradigm in Wbl biochemistry is the interaction with σ^{HrdB} – protecting the [4Fe-4S] cluster from oxygen-based degradation. Recently, structures of WhiB(A) and WhiB7 have been solved in open promoter complexes with the RNAPol (αββ'ω) and RbpA, at their respective *sepX* and *whiB7* promoters, via Cryo-EM; both proteins predominantly target the minor groove and make non-specific contacts with an A/T-rich stretch, upstream of the -35 element (Lilic *et al*., 2021, 2023). It was hypothesised that a similar positioning will occur for WblE in complex with HrdB (Confirmed in Sections 6.3.1 and 6.4.1). As such, a second, more targeted approach was utilised, which compared the architecture of the -35 adjacent motif in WblE-bound promoters.

Differential (d)RNA-seq facilitates the identification of transcriptional start sites (TSSs) by distinguishing between terminal 5' triphosphates and 5' monophosphate groups found on primary and processed transcripts, respectively. The previously existing time course dRNA-seq data for *S. venezuelae* (see Section 2.21.3) were used to predict the -35 sites for putative WblE target genes, with reference to available data on the σ^{HrdB} -35 consensus as guidance (Jeong *et al*., 2016; Šmídová *et al*., 2019; Lee *et al*., 2019). Predicted -35 hexamers for WblE targets, and an additional 10 bp preceding them, were aligned with the M1 consensus motif. In addition, comparisons were made to the analogous sequences from the *sepX* and *whiB7* promoters.

The results show that WblE, WhiB7 and WhiB bound promoters all display similar AT-rich stretches preceding the -35 bp element (Figure 5.11). However, WblE target promoters seem to strongly conserve a unique '(A/G)T' dinucleotide sequence directly preceding the -35 element. The longer '(A/G)TTT' sequence predicted in MEME-1 was likely the result of the simultaneous identification the -35 bp element, which often contain one or two 5'-T bases in *Streptomyces* spp. (Jeong *et al*., 2016; Šmídová *et al*., 2019; Lee *et al*., 2019 – Figure 5.12). It cannot be ruled out that these bases can influence binding; in the modified RNAPol-WhiB-*sepX* promoter structure, WhiB binds to the newly introduced T-bases of the engineered *sepX* -35 element, implying a significance for these positions in Wbl-recognition (Lilic *et al*., 2023). Additional A/T positions occurred frequently throughout -35 adjacent motifs of WblE-bound promoters; in particular, positions -6 to -9 (from the -35 site) were well-conserved and thus may also have a significant role in binding. Nevertheless, the potential importance of other less well conserved A/T positions for WblE-binding at individual promoters should not be disregarded.

-7 -6 -5 -4 ___••••___ (-35)	**(1) WhiB & WhiB7**	
C**A**G**AAAT**CGG(TTGTGG)	WblC-*wblC*	
GCC**AATT**GGC(CGATGC)	WhiB-*sepX*	(native)
GCC**AATT**GGC(TTGACA)	WhiB-*sepX**	(modified)
GGGC**ATA**CGC(TCGATG)	WhiB-*filP*	(predicted)
GG**A**CCG**A**GGG(GGCCGA)	WhiB-*26280*	(predicted)
CGGCG**A**GGCG(GTCCTT)	WhiB-*whiG*	(predicted)
-8 -7 -6 -2 -1 __•••___•• (-35)	**(2) WblE targets**	
nn**AAA**CCG**RT**(TTSnnn)	M1 consensus	
G**TAAA**CCG**AT**(TTCGTG)	$tRNA_{Met}$	(*vnz_19045*)
C**TTAA**CGG**AT**(TTGCGC)	$tRNA_{Met}$	(*vnz_24025*)
GG**A**CCCGG**AT**(TTCACT)	$tRNA_{Ala}$	(*vnz_11540*)
AAAACCGG**AT**(TTCGTC)	$tRNA_{Pro}$	(*vnz_16520*)
GG**T**G**AT**CG**AT**(TGGGTG)	*ctc*	(*vnz_14500*)
ACC**A**G**T**G**AAT**(TTCAAC)	*rpsF*	(*vnz_18105*)
G**A**G**AT**CG**AAT**(TTGCGA)	asRNA*	(*vnz_18410*)
GG**A**G**T**CCG**AT**(TTGCCA)	RNA Helicase	(*vnz_19005*)
GG**T**CC**T**CG**GT**(TAGCGA)	*pyrR*	(*vnz_05280*)
ACC**ATT**CG**G**C(TTGACG)	*bldD*	(*vnz_05285*)
G**A**G**AA**C**TTGT**(CACGCC)	*adpA*	(*vnz_12630*)
ATAAG**A**C**AA**C(ATCGGG)	*bldA*	(*vnz_14210*)
TC**AA**C**T**CC**G**C(TTGACC)	*eccA*	(*vnz_05000*)
GG**A**C**AA**C**AA**C(TTGAAC)	*dnaA*	(*vnz_17980*)
TGCCGG**AAAA**(TTGTCC)	PrimPol	(vnz_18405)
TG**AA**CGCG**GT**(CCCGCC)	*scr2*	(*vnz_15145*)
CCCCGCCG**AT**(GCCCAC)	*mqnD*	(*vnz_21015*)
GG**A**G**A**GCGC**T**(GCCCGT)	*rmdB*	(*vnz_25525*)
CGG**AT**CCG**GT**(TCGTAT)	*mshC*	(*vnz_06150*)
G**AT**C**T**GCG**AT**(TTAGGG)	*sucC-sucD*	(*vnz_22160-65*)
CCGG**T**CGC**GT**(TCGTTC)	SEST Lipase	(*vnz_06560*)
GG**AAAA**GC**G**G(GCCACA)	PPM1-GT operon	(*vnz_06565-70*)
TCCC**T**CGG**AT**(TACAAG)	UGE-LPAAT operon	(*vnz_15665-70*)

Figure 5.11. WhiB-like -35 consensus alignments. The -35 hexanucleotide sequence is enclosed by brackets. The ~4 bp Wbl A/T-recognition sequence, upstream of the -35 is highlighted in bold. Highly conserved A/T base positions are highlighted by dots at the top of columns. Conserved positions are numbered respective to the -35 element.

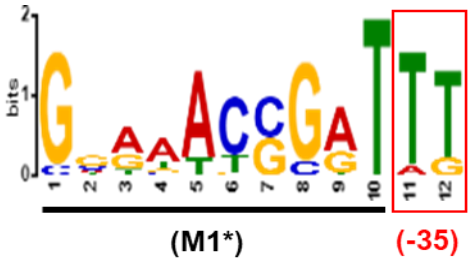

Figure 5.12. Distinction of WblE (M1*) and -35 derived sequences identified within the M1 consensus.

5.4.3 *In silico* Predictions for an Expanded WblE Regulon

The 20 million read, 150 bp, paired-end Illumina sequencing defined a total nucleotide budget of 6×10^9 bp (20,000,000 × 150 × 2), providing 715-times coverage of *S. venezuelae* NRRL B-65442's chromosome and plasmid (8.22 Mbp + 158 kbp), which was sufficient for detecting binding sites. However, all Wbls proteins tested so-far have bound over 100 transcriptional units and, in this case, a greater nucleotide budget would likely be required to resolve the majority of peaks from the background and legitimate binding sites could have fallen below significance (personal communications, Dr. Govind Chandra, JIC; Bush *et al*., 2015; Lee *et al.*, 2021). Therefore, it is very likely that additional binding sites for WblE exist.

Using FIMO (MEME-suite), the complete M1 motif was exported from MEME-ChIP to FIMO and searched against the entire *S. venezuelae* NRLL B-65442 genome, including its mega-plasmid 'pvnz' in the hope of identifying additional WblE targets. A total of 313 additional potential binding sites were identified under strict constraints (p = 1 x 10^{-4}). Intriguingly, a large portion of high significance consensus sites sat directly in the centre of certain genes and, in some cases, seemed transcriptionally inert with no nearby TSSs (not shown). A selection of the most significant results from this analysis are shown in Table 5.2. Upon manual inspection of the ChIP-seq data, a few of the promoters identified *in silico* possessed a consensus site with -35 spacing and sub-significant but discernible levels of enrichment, suggesting that the M1 consensus identified in this chapter was likely a legitimate WblE binding site (Figure 5.13).

Table 5.2. High confidence MEME-1 FIMO hits against the *Streptomyces venezuelae* NRRL B-65442 genome. (+) denotes that the matched sequence is not the same or overlap with the putative -35 consensus, i.e. there is multiple consensus sites throughout the promoter and/or no -35 consensus. The peak column denotes (Y) visible but non-significant levels of enrichment at these promoters or (N) no visible enrichment. Several reiterated ChIP-seq peaks were identified and are highlighted at the base of the table for comparison.

p-value	Matched Seq.	Locus tag	Gene	••• •• (-35)	Peak
1.36 x10^{-6}	GCGAACCGATTT	vnz_18960	ATP-dependent RNA helicase (*hrpA*)	G**TAAAT**CG**GT**(TCGCCG)	Y
2.29 x10^{-6}	GGGAACCGATTG	vnz_05365	ATP dependent Regulator	GGG**AA**CCG**AT**(TGTACG)	Y
3.49 x10^{-6}	GCGAACCGGTTT+	vnz_24730	CheY-like protein / tRNA-Arg	G**TAAAA**CCCG(GACGCA)	Y
5.32 x10^{-6}	GGGAACGGGTTG	vnz_05520	tRNA-Val	**TTT**G**AA**CG**AA(**GGGCGC)	Y
3.14 x10^{-5}	GGAATCCCGTTT	vnz_02815	Hypothetical	GG**AAT**CCC**GT**(TTGTCC)	Y
1.37 x10^{-7}	GGAAACGGATTT	vnz_20065	Chloramphenicol phosphotransferase	**T**G**AAAT**CC**GT**(TTCCGC)	N
6.60 x10^{-6}	GGATACGGATTT	vnz_23455	Hypothetical	G**TAAAT**CC**GT**(ATCCGC)	N
3.99 x10^{-6}	GCGAACGGGTTT	vnz_31025	Sirtuin SIRT7-like	G**TAAA**CCC**GT**(TCGCGG)	N
2.68 x10^{-5}	CCGAACCGATTT	vnz_11230	Glycine-tRNA ligase	CCG**AA**CCG**AT**(TTGATA)	N
3.96 x10^{-5}	GGAAAACCGTTC	vnz_20360	Phosphotransferase	GG**AAAA**CC**GT**(TCGCCG)	N
4.03 x10^{-5}	GATATCCGATTT+	vnz_12710	Hypothetical	GCC**AAA**C**T**C**A**(GCGTAG)	N
7.24 x10^{-5}	GTGTACGCATTT	vnz_03985	Putative alpha beta hydrolase (TAP Domain)	G**T**G**TA**CGC**AT**(TTCGTC)	N
7.24 x10^{-5}	GTGTACGCATTT+	vnz_04045	Putative NlpC P60 lipoprotein	CG**TTT**C**A**GC**T**(CGGATT)	N
7.85 x10^{-5}	GAAAACCCGTTG	vnz_33870	TIGR02452 family	GG**AAAA**CCCG(TTGTCC)	N
9.31 x10^{-5}	CGAAAACCGTTT*	vnz_01680	Hypothetical	CG**AAAA**CC**GT**(TTGACG)	N
6.07 x10^{-6}	GGAAACGCGTTT	vnz_03980	LPAAT / sugar epimerase operon	/	N
1.36 x10^{-5}	GGGAACGGTTTT	vnz_33085	50S ribosomal protein L31	/	N
1.50 x10^{-5}	GGTCACGGATTT	vnz_23695	Methyltransferase	/	N
1.63 x10^{-6}	GTAAACCGATTT	vnz_19045	tRNA_Met	G**TAAA**CCG**AT**(TTCGTG)	ChIP
6.07 x10^{-6}	GCAAACGGATTG+	vnz_06565	Glycosyl transferase	GG**AAAA**GCGG(GCCACA)	ChIP
1.53 x10^{-5}	GGAGTCCGATTT	vnz_19005	RNA Helicase	GG**A**G**T**CCG**AT**(TTGCCA)	ChIP
1.36 x10^{-5}	GCGTACGGGTTT+	vnz_02605	Cryptic lantibiotic cluster	/	ChIP
4.13 x10^{-5}	GCACATGGATTT+	vnz_15035/40	*hrdD* / *orfX*	/	ChIP

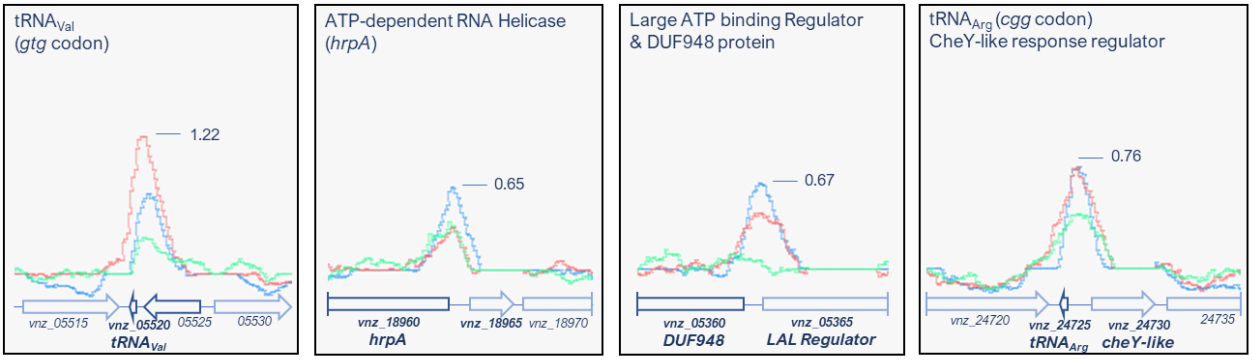

Figure 5.13. Non-significant peaks in the ChIP-seq also identified by a FIMO search against the *S. venezuelae* NRRL B-65442 genome with the M1 motif.

5.5. ReDCaT Surface Plasmon Resonance (SPR)

Surface plasmon resonance refers to the excitation of electrons by light, in a thin metal sheet, at a particular angle of incidence. The excited electrons travel in parallel to the metal sheet as an electromagnetic surface wave that is highly sensitive to any change in the environment, including the adsorption of analytes or biomolecular interactions at the interface with the conducting metal surface. Reusable DNA Capture Technology (ReDCaT) is an SPR technique which tests the interaction between designed biotinylated DNA probes and a purified DNA-binding protein, *in vitro* (Stevenson *et al*., 2013; Stevenson & Lawson, 2021). The following sections outline the employment of ReDCaT-SPR to test binding of WblE to the *wblE* and *dnaA* promoters that were enriched in the ChIP-seq data (Section 5.3.2 - 5.3.3), as well as binding of the response regulator MtrA to the *wblE* promoter (Section 1.4.6). Promoter fragments are numbered incrementally towards the start of the gene, thus '_p1' represents the furthest promoter fragment from the start codon. It is notable that oxidation was not controlled under the experimental parameters used here.

5.5.1. WblE binds its own promoter, *in vitro*

Many transcriptional regulators bind their own promoters and autoregulate their expression, and there is evidence for this in some WhiB-like proteins; WblE appears to be no different with a significant peak observed in the ChIP-Seq data at time-point 2. To confirm this *in vitro*, oligonucleotides were designed to make double stranded DNA probes spanning the entire *wblE* promoter to use in ReDCaT SPR experiments. Each probe was annealed to the SPR chip in turn, and three concentrations of purified 6xHis-WblE (apo- / holo- mixture) were washed over the surface to check for binding of the protein to the DNA. Binding of WblE to the DNA probes gave very high responses. When these responses were normalized to the molecular weight of a WblE-C6xHis trimer, the %Rmax values were still above 300% at the highest protein

concentration. This suggests WblE may binds strongly to its own promoter DNA, with potentially several multimers binding single oligos at a time.

There was little evidence of sequence specific binding, as the %Rmax values were similar across all the DNA probes that were tested (Figure 5.14). Attempted optimisation of the methods, for example by lowering protein concentrations and/or increasing salt concentrations to reduce non-specific binding, did not bring the %RMax values down. Whilst this makes identifying a consensus binding site within the wblE promoter challenging, it can be noted that the lowest binding response was observed for fragment p16, which is predominantly in the coding region of wblE, suggesting there is some sequence-specificity for the promoter over coding regions of DNA. Similar multi-site binding was observed during DNase I footprinting of (*M. tuberculosis*) apo-WhiB1 over just a small stretch of *whiB1* promoter DNA (Smith *et al*., 2010). Notably, A/T-rich stretches which could function as binding sites are abundant throughout the *wblE* promoter, which has an uncharacteristic 56% GC ratio. The extent of binding across the *wblE* promoter could explain the 'blocky' nature of the WblE ChIP-seq peak (Section 5.3.3). Nevertheless, these data confirms that WblE likely regulates its own expression by binding its own promoter.

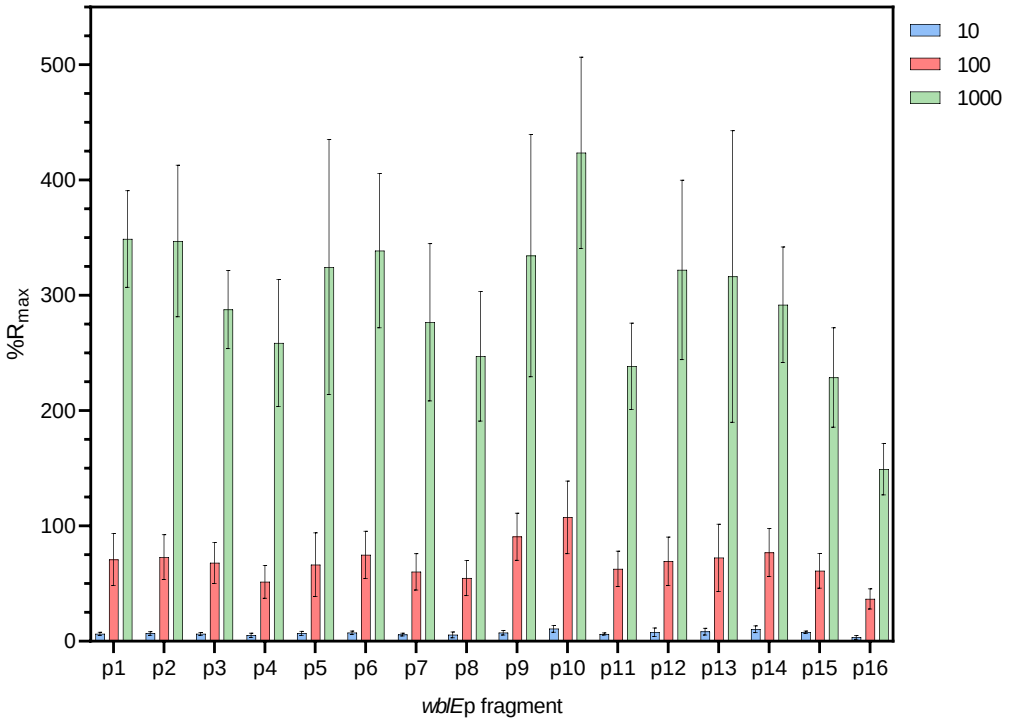

Figure 5.14. DNA oligos were designed to cover the entire *wblE* promoter, and binding by WblE was tested by ReDCaT SPR. Binding was high across all DNA sequences tested, suggesting WblE binds very strongly to its own promoter, potentially at multiple sites.

5.5.2. WblE binds the *dnaA* promoter, *in vitro*.

Among the most consistently and highly enriched genes in the ChIP-seq was the chromosomal replication initiator gene, *dnaA*, which is essential for cell-cycle progression. Binding of WblE to the *dnaA* promoter was tested via SPR; WblE solutions (apo- / holo- mixture) were diluted to 5nm, 50nm and 500nm. Binding of WblE to the *dnaA* probes gave high responses across all tested probes but normalization to the predicted maximum molecular weight of the WblE-C6xHis trimer, the Rmax values resolved to values between 40% and 120% (at the highest protein concentration). Three broad peaks (Figure 5.15) were bound at an Rmax ≥ 100% and exhibited remarkable equidistant spacing along the *dnaA* promoter. These peaks comprised "*dnaA*_p3, p4, p5", "*dnaA*_p11, p12, p13", and "*dnaA*_p19, p20, p21". An additional single probe 40bp upstream of the gene's start codon, *dnaA*_p26, was also bound at similar levels (Rmax 115%).

As the most strongly bound probes, it was expected that these 10 sequences would possess multiple or strong matches to the WblE M1* consensus and were scanned for matches to the M1* motif (Figure 5.11), and aligned with the positional matrix described in Figure 5.11. An abundance of AT-rich segments matching the M1* sequence and format were discovered in all 10 probes (Figure 5.15). Implying that purified WblE specifically targets A/T rich stretches which match the format of the M1* sequence preceding -35 elements. The apex of the ChIP-seq peak for *dnaA* (Section 5.3.2) falls in a region most conducive with WblE binding to *dnaA*_p19, *dnaA*_p20 or *dnaA*_p21, which encompass two key *dnaA* -35 elements (dRNA-seq, Section 2.21.3), providing a strong indication that a role of WblE *in vivo* is activation of *dnaA*, at least under the standard lab conditions used here.

Intriguingly, these results also suggest that WblE is capable of binding DNA fragments at multiple sites, or in different multimeric conformations, *in vitro*, whereby 33.3%, 66.6% and 100% Rmax values would represent the monomeric, dimeric and trimeric WblE species, respectively. With respect to this, *dnaA*_p11 contained a mirrored repeat, centred on the '(A/G)T' dinucleotide sequence and *dnaA*_p5 possessed a tandem repeat which could represent WblE-multimer binding sites. Nevertheless, these data does not account for potential background noise (which could nonetheless be low); repeats with mutated or shuffled sequences could function as useful controls to rule this possibility out.

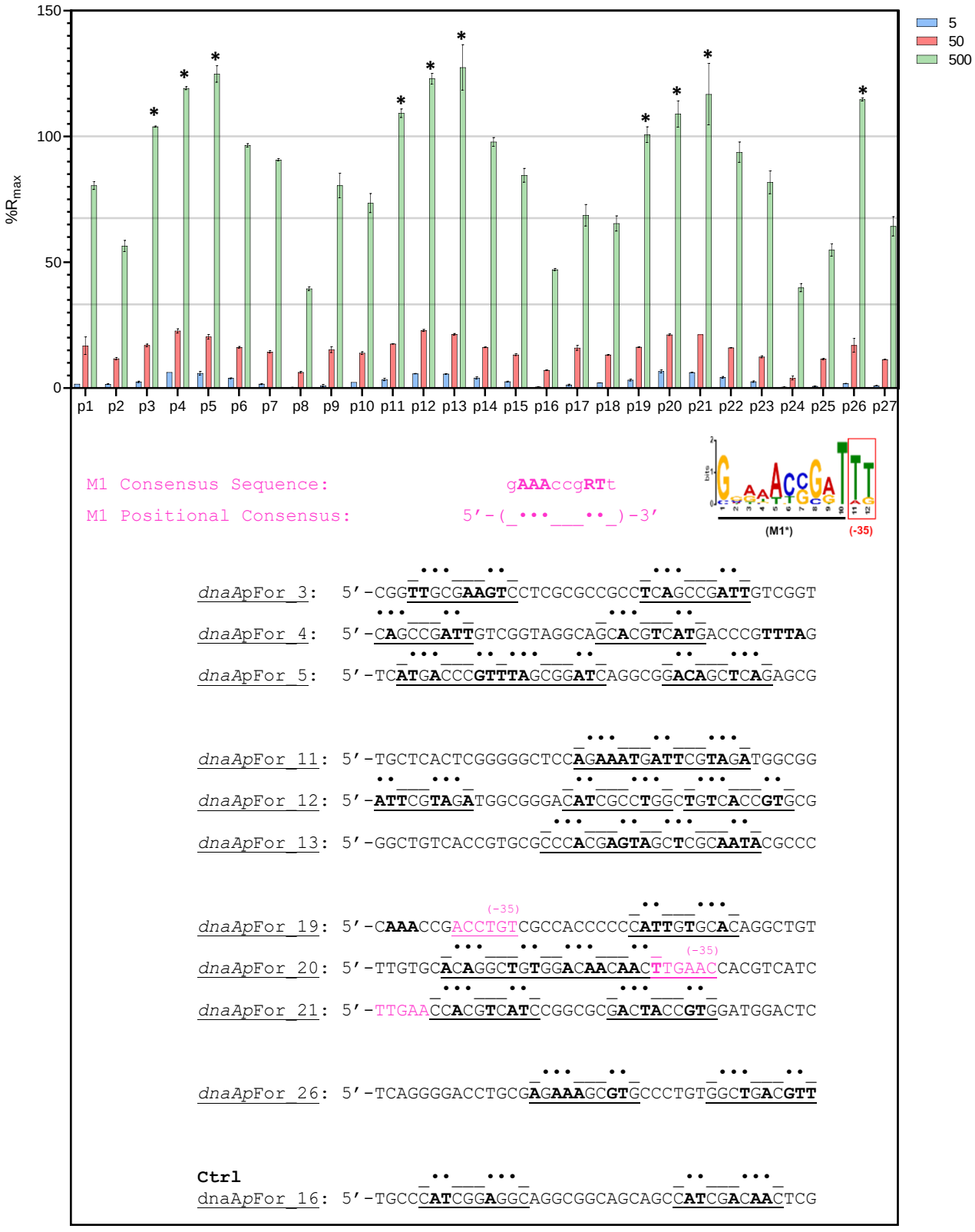

Figure 5.15. DNA oligos were designed to cover the entire *dnaA* promoter, and binding by WblE was tested by ReDCaT SPR. Binding was high across all DNA sequences tested, but there were four regions of apparent sequence specificity with >100% RMax from each broad peak were searched for M1

5.5.3. MtrA Binds with High Specificity to the *wblE* Promoter

The OmpR-like response regulator MtrA, part of the conserved actinobacterial MtrAB(-LpqB) two component system, is an important global regulator broadly coordinating development and metabolism in *Streptomyces spp.* More specifically, MtrA appears to function as a developmental regulator by binding the *dnaA* promoter and the promoters of the morphogenetic protein encoding genes *adpA*, *chpC-H*, *bldM*, *whiI*, and *bldG*. In agreement with this, *mtrA* mutants exhibit defects in cell-morphology and conditionally bald phenotypes, accompanied by dysregulated antibiotic synthesis (Som et al., 2017a; 2017b; Zhang et al., 2017). More recently, it has been demonstrated that MtrA also antagonizes GlnR-mediated activation of nitrogen metabolism, by competing for GlnR-boxes (GTnAC-n_6-GTnAC), thus, establishing the gene product as a key coordinator of early developmental decisions and primary and secondary metabolism (Zhu *et al.*, 2019; Zhu *et al.*, 2022). Importantly, a common target of MtrA in both *S. venezuelae* and *S. coelicolor* is *wblE* (Som et al., 2017a, 2017b).

To confirm that MtrA binds to the *wblE* promoter, binding of N6xHis-tagged MtrA (purified by Dr. Rebecca Devine) was tested *in vitro* against the *wblE*p fragment library. Although some background binding was observed for all DNA fragments, a significant and concentration-dependent signal was detected for the *wblE*p_4 fragment (105% R_{Max} at 50 uM), with slightly lower affinity observed for *wblE*p_6 and *wblE*p_13 (~70% R_{Max}), when compared to the rest of the promoter region which was generally below 50% R_{Max}. FIMO was used to search for the palindromic (GTnAC-n_6-GTnAC) GlnR-box repeat, proposed to bind MtrA in *S. coelicolor* (Zhu *et al*., 2019). A strong match was found within *wblE*_p4 and a weaker match was determined in *wblE*p_13 (Figure 5.16).

Additional work conducted by Dr. Rebecca Devine identified a refined MtrA consensus motif by testing MtrA-binding against multiple promoters *in vitro*, including *mtrA*, *ssgB*, *whiI*, and the divergent promoters between the chloramphenicol transport genes, *cmlFN* (unpublished). The revised consensus (TswCmwr), the MtrA-box, was also found to be present in both *wblE*_p4 and *wblE*_p13 fragments; in both cases, overlapping to varying extents with the predicted GlnR-box (Figure 5.16). Therefore, these results strongly imply that *wblE* is bound by MtrA, in a sequence specific manner at two distinct sites, with precedent for competition with GlnR.

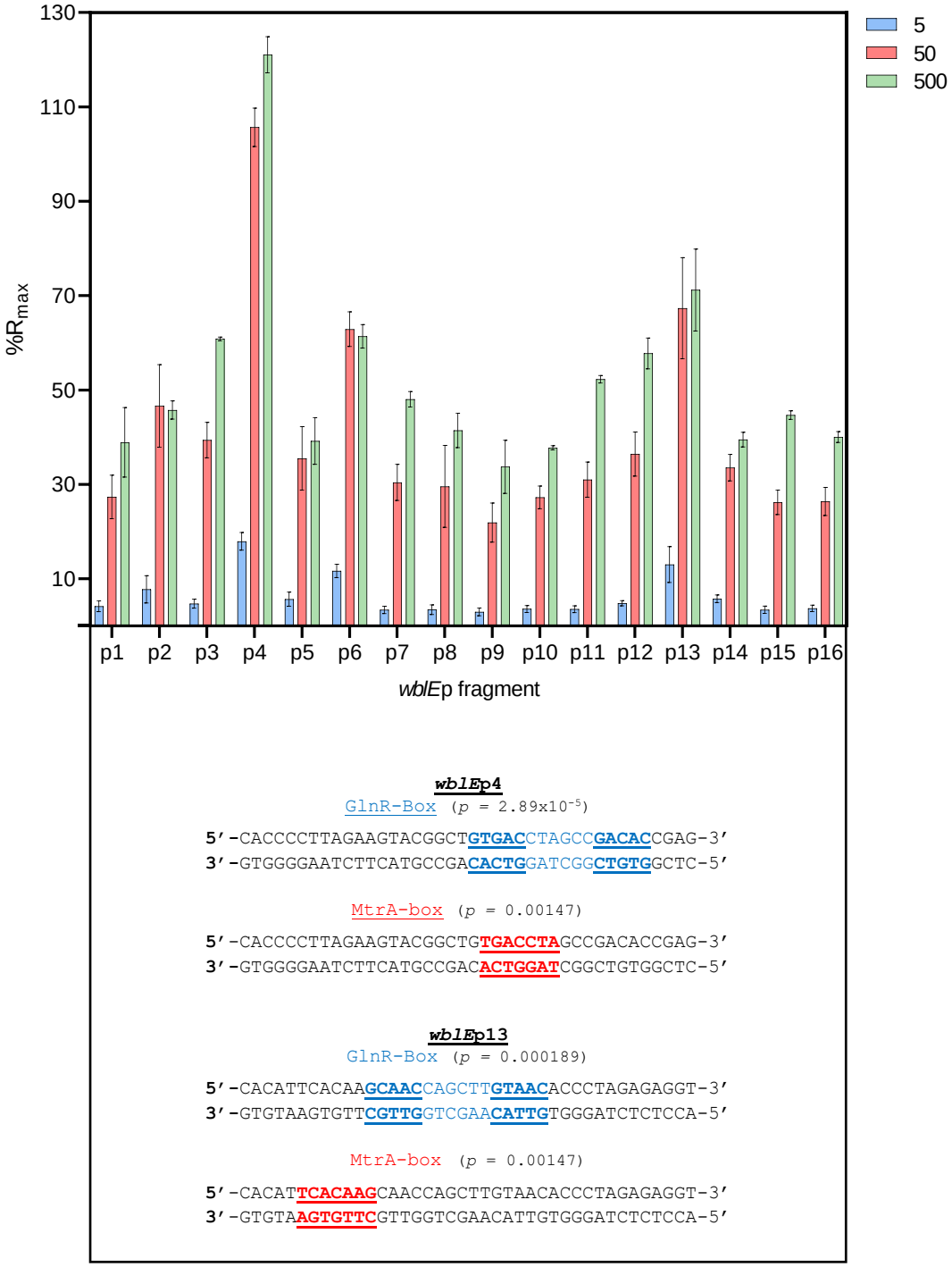

Figure 5.16. DNA oligos were designed to cover the entire WblE promoter, and binding by MtrA was tested by ReDCaT SPR. Strong, sequence-specific binding was observed for *wblE*p fragments 4 and 13. Both DNA fragments were found to contain overlapping sequence motifs for MtrA (red) and the GlnR-box (blue), suggesting MtrA directly regulates the expression of *wblE*, possibly in competition with GlnR.

5.6. Expression analysis of *wblE* in developmental mutants

To further explore the early developmental role illustrated in this chapter, the expression patterns of *wblE* in existing time course microarray data for wildtype *S. venezuelae* (grown at 30°C in liquid MYM + TE) was compared to that of the Δ*bldN*, Δ*bldM*, Δ*whiA,* Δ*whiB*, Δ*whiD* (unpublished), Δ*whiG*, Δ*whiH* and Δ*whiI* developmental mutants, acquired under identical conditions throughout development (Bibb *et al*., 2012; Bush *et al*., 2013; Al-Bassam *et al*., 2014; Bush *et al*., 2016; Gallagher *et al*., 2020). It should be noted that the liquid conditions used for microarray experiments differ from the solid growth used in the WblE ChIP-seq. The full collated dataset was acquired from Dr Govind Chandra (John Innes Centre).

In the wild type *wblE* expression was constitutively high throughout development but dysregulation was observed broadly across all developmental mutants (Appended Figure A.1). Specifically, 'White' developmental mutants overwhelmingly accompanied upregulation of *wblE* but only *S. venezuelae* Δ*bldN* exhibited a noticeable and consistent drop in *wblE* expression, supporting a constitutive role for WblE that is particularly important during early development (Figure 5.17). Intriguingly, the variations in *wblE* expression in the Δ*bldN* and Δ*whiB* mutants correlated well with the peaks of the respective gene's wild-type expression profiles (Figure 5.17), potentially indicating more intimate, or even direct, control of *wblE* expression by their products. This relationship was not clearly observed with *bldM*, *whiA, whiD*, *whiG*, *whiH* or *whiI* mutants (Appended Figure A.1).

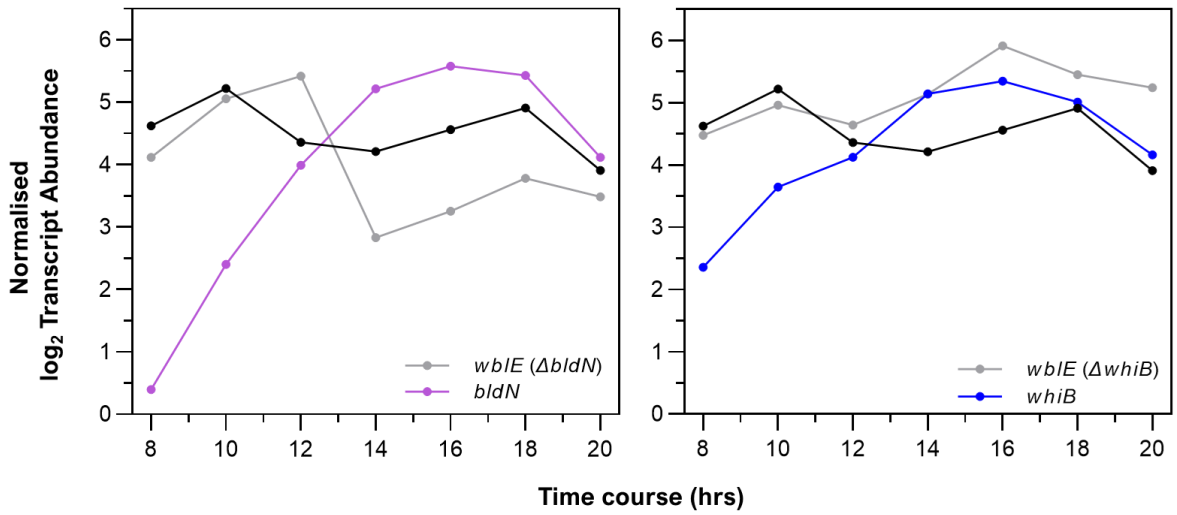

Figure 5.17. The *wblE* transcript expression profile in wild-type *S. venezuelae* (black), plotted against Δ*bldN* and Δ*whiB* mutant *wblE* expression profiles (grey), showing the negative and positive shifts respectively. Wild type expression profiles for the *bldN* (purple) and *whiB* (blue) genes are plotted with their respective mutants. Keys are provided for each graph. Log_2 transcript abundances were normalized to the median of the data.

5.7. Discussion

The work in this chapter has demonstrated that, much like other Wbl proteins studied to-date, WblE functions as a global regulator binding to a range of promoters throughout the genome; among which are genes relating to multiple conserved aspects of the multicellular developmental program of *Streptomyces* spp., primary metabolism, translation (tRNA, rRNA, ribosomal proteins), respiration, and stress responses. Furthermore, there was significant binding to genes involved in *S. venezuelae* secondary metabolism and the regulation thereof. Nevertheless, ChIP-seq should be considered an initial screening experiment and future experiments via such as SPR or *in vitro* transcription assays will be needed to demonstrate biological significance of enrichment at specific promoters

It is well understood that holo-Wbl proteins share a [4Fe-4S] dependent interaction with the initiating transcription factor σ^{HrdB} (specifically addressed for WblE in Chapter 6) and this thesis has demonstrated that WblE and its [4Fe-4S] cluster are essential (Chapter 4). Consistent with this, MEME analysis of the WblE ChIP-seq data identified an AT-rich consensus (Section 5.4) with derivatives directly adjacent to the possible σ-factor -35 sites in the majority of promoters enriched in the 3xFLAG-WblE ChIP-seq dataset. This discussion therefore follows the presumption that holo-WblE primarily functions in concert with the primary RNA polymerase sigma factor σ^{HrdB} as an activating transcription factor (See also Section 6.3) although other mechanisms of regulation are possible.

5.7.1. A Putative Essential Function for WblE as a Major Cell-Cycle Activator

In *Streptomyces* spp., DNA replication is distinct from other prokaryotes, as it occurs continuously from the earliest stages of spore germination (Wolánski *et al*., 2011), thus, there is a clear constitutive element driving replication events in this genus. Yet, remarkably, no transcriptional activators have been identified for *dnaA*, other than evidence that it may occur as a house-keeping function of the primary σ^{HrdB} factor (Šmídová *et al*., 2019). Through a combination of ChIP-seq and ReDCaT SPR, this chapter has shown strong evidence for WblE binding to the *dnaA* promoter raising the hypothesis that the essentiality of WblE and its Fe-S (Chapter 4) may, at least in part, originate from a principal role in *dnaA* activation, via a [4Fe-4S]-dependent interaction with σ^{HrdB}. In addition, WblE appears to bind the *vnz_18405* promoter, encoding a putative PrimPol homologue; a protein family known to be potent facilitators of replication fork progression in archaea and eukaryotes. The Fe-S clusters of WhiB-like proteins are protected from O_2 but not nitric oxide ($^{\bullet}NO$) via interaction with the primary σ-factor in *Mycobacterium* and *Streptomyces* spp. (Wan *et al*., 2020; Stewart *et al*., 2021). It has thus been proposed (but not proven *in vivo*) that WhiB-like proteins sense $^{\bullet}NO$ via their Fe-S cofactors and this is consistent with evidence that $^{\bullet}NO$ can act as a signaling molecule to control development

(Honma *et al*., 2022). If this is correct then •NO might act via WblE to inhibit the cell-cycle and DNA replication. WblE also appears to globally bind promoters of rRNAs, tRNAs and RPs which could also lead to lethality following widescale abrogation of their transcription, via *wblE* deletion. This would also explain the apparent necessity of its DNA-binding C-terminus (Section 4.4.2).

Reinforcing a predominantly positive role for WblE in the initiation, *wblE* expression seems to be coordinately repressed with DNA replication by the limited set of known and predicted cell-cycle regulators in *Streptomyces*. As demonstrated by ReDCaT SPR, MtrA binds the *wblE* promoter in a sequence specific manner, *in vitro* (Chapter 5.5.3). There is evidence that MtrA binds to the DnaA protein and to *oriC* and the *dnaA* promoter as a cell-cycle repressor in *Mycobacterium* spp., with limited reports of a similar function for the *S. venezuelae* orthologue (Fol *et al*., 2006; Purushotham *et al*., 2015; Som, 2016). How exactly MtrA influences DNA replication in *Streptomyces* spp. remains undetermined; nevertheless, by analogy to its function in *Mycobacterium* spp., it can be assumed that MtrA is a repressor of DNA replication. Moreover, in *Streptomyces* spp., MtrA functions to antagonise GlnR-mediated activation to globally repress nitrogen metabolism and a strong GlnR-box motif is present in the *wblE* promoter fragment bound by MtrA. It therefore seems likely that a similar competition occurs in the *wblE* promoter, whereby MtrA represses *wblE*. MtrA also binds to three sites upstream of the three WblE binding sites at the *dnaA* promoter (unpublished data), it is possible that simultaneous MtrA and (apo-)WblE binding results in winding of the DNA and repression of *dnaA* expression. In *S. lividans*, a species closely related to *S. coelicolor*, Δ*adpA* mutants overexpress *wblE*, implying a mechanism of (direct or indirect) *wblE* repression (Guyet et al., 2014); *adpA* encodes a *bona fide* repressor of DNA replication (in *S. coelicolor*) which competitively binds to 5' region of *oriC* and inhibits DnaA-mediated cell-cycle initiation (Wolański *et al*., 2012). Nonetheless, the situation is likely to be even more complex given that both WblE and MtrA bind to the promoter of *adpA*, implying a level of cross-talk.

5.7.2. A Potential Role for WblE in Priming the '*bld*' Developmental Cascade

Among the developmental genes identified in the ChIP-seq, WblE bound almost exclusively to an interconnected subset of the *bld* cascade that, together, are necessary for controlling the onset of multicellular differentiation and secondary metabolism. These include the major developmental repressor *bldD* and the BldD (c-di-GMP) regulon distinctly overlaps with that revealed for WblE in this chapter, and includes the *bldA*, *adpA*, *leuA* and *leuB* genes (Den Hengst *et al*., 2010). Therefore, it is proposed that holo-WblE plays a premiere role in priming the developmental cascade by activating *bldD*, the product of which subsequently gates further WblE-mediated developmental progression, via repression of the *bldA* and *adpA* (Chapter 1.3.3), until the appropriate drop in local c-di-GMP levels is perceived (Figure 5.18).

Intracellular concentrations of c-di-GMP are held in balance by the opposed activity of anabolic diguanylate cyclases (DGCs) and catabolic phosphodiesterases (PDEs); ChIP-seq revealed that WblE also binds the *rmdB* PDE and a putative WblE consensus can be found upstream of the *rmdA* operon predicted -35 site, albeit on the antisense strand (Figure 5.18). Intriguingly, all studied DGCs are direct targets of BldD repression, likely as a means to prevent c-di-GMP saturation and insurmountable developmental repression. However, the PDE genes *rmdB* and *rmdA* retain independence from BldD repression, across species, indicating that they are part of overlapping but distinct signaling modules, during early development (Hull *et al*., 2012; Makitrynskyy et al., 2020).

It is possible that *rmdB* and *rmdA* PDE repression is specifically governed by •NO and nitrosylation of the WblE [4Fe-4S] cluster; this coincides with reports that deletion of the *S. coelicolor* (•NO-producing) nitrate reductase *narG1*, *narG2*, and *narG3* subunits leads to reduced c-di-GMP concentrations and precocious development, which has hitherto been poorly understood (Honma *et al*., 2022). It is believed that this connection between •NO, c-di-GMP and WblE also provides context to the elusive PAS9 haem-binding domain in RmdA and potentially multiple DGCs (Hull *et al*., 2012) as stand-alone •NO-sensing modules which can tailor their catalytic activity.

The interdependent *bldA* and *adpA* gene products are ultimately responsible for the activation of the *ramBASC* operon and production of the morphogenic surfactant lanthipeptide, SapB (Willey *et al*., 1993; Kodani *et al*., 2004). According to mutant expression analysis (Section 5.6), the *wblE* gene also seems to be an important target of σ^{BldN}-mediated activation. The σ^{BldN} protein and its cognate anti-sigma factor RsbN control expression of the cooperative chaplin and rodlin families of hydrophobic peptides in response to an unclear stimulus. In this way, there seems to be a pattern linking WblE to regulatory cascades that ultimately control the production of these morphogenic peptides. Understanding the signals that control RsbN anti-sigma factor activity may elucidate this connection.

5.7.3. A Basis for Coordination Between *wblE* and *vnz_24260* Transcripts

The paralogous WhiB3 and WhcD were shown to influence lipid, cell-wall and cell-envelope biosynthesis in *Mycobacterium* and *Corynebacterium*, although similar functions have not been demonstrated for *Streptomyces* spp. homologues. Nonetheless, WblE ChIP-seq demonstrated enrichment at the promoters of a probable lysophosphatidic acid acyltransferase (LPAAT) operon (Section 5.3.6.30. The LPAAT family members are acyltransferases which can simultaneously contribute to *de novo* glycerophospholipid synthesis (Kennedy Pathway) and remodeling (Lands' Cycle).

A range of evidence was previously described which hints at a putative *cis*-acting regulatory mechanism in the 5'UTR of *wblE* (Section 4.8.2). It was suggested that this may 5'UTR regulate transcription originating either from the *vnz_24260* promoter or within the *vnz_24260* coding sequence, implying transcriptional coordination between the two genes. The *vnz_24260* gene preceding *wblE* encodes a protein with strong homology to the soluble diacylglycerol kinase (i.e. DgkB), a conserved and essential protein in Gram-positive bacteria, which performs the ATP-dependent phosphorylation of diacylglycerol (DAG) to phosphatidic acid (PA), the simplest phospholipid (Koch et al., 1984; Taron et al., 1983; Jerga et al., 2007; Xu *et al*., 2017). A role in lipid and cell-envelope metabolism provides a functional basis for this genomic organization and potential coordination of *vnz_24260* (*dgkB*) and *wblE* transcripts.

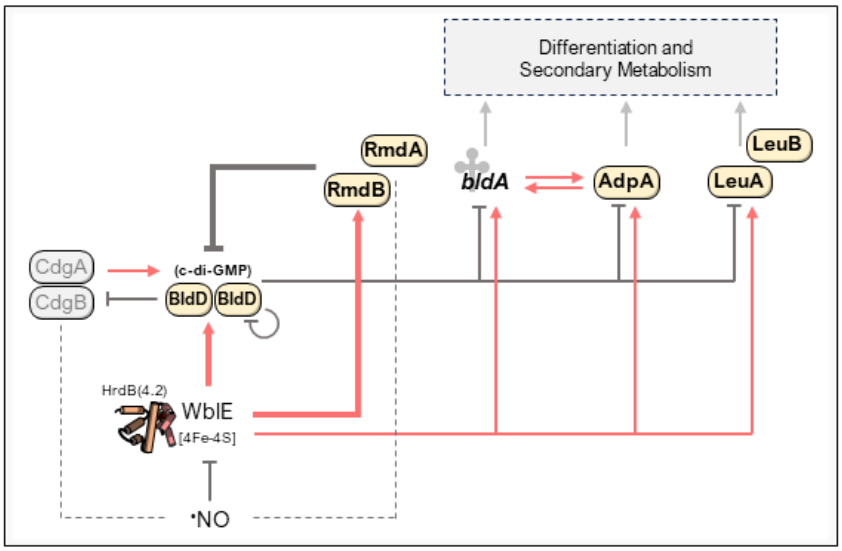

-8 -7 -6 -2 -1 __•••___•• (-35)	Target Gene
nn**AAA**CCG**RT** (TTSnnn)	
GG**A**G**A**GCGC**T** (GCCCGT)	*rmdB* (vnz_25525)
AGGC**AAA**G**AT** (GAGCGA)	*rmdA* (-) (vnz_33675)

Figure 5.19. Putative antagonistic activity of WblE and BldD in the activation of the Bld cascade. Activating signals are shown as red arrows. Repressive signals are shown as grey flat arrows. Bold lines represent signals affecting the cascade that are independent of BldD repression and putative •NO-targets are connected via dashed lines. Table shows comparison of the -35 WblE consensus for *rmdB*, compared with the manually identified *rmdA* -35 site.

Chapter 6.

Identification of the *S. venezuelae* NRRL B-65442 WblE Interactome and Novel Interactions

6.1. Introduction

Protein-protein interactions are a defining feature of WhiB-like functions. The conserved cluster-dependent interaction with the primary Sigma factor is a significant contributor to WhiB-like regulation and, in the case of *Streptomyces*' WhiB, forms a scaffold for the tripartite interaction between WhiA, WhiB and HrdB, which is essential for WhiB-mediated regulation of sporulation-septation (Bush *et al*., 2016; Lilic *et al*., 2023). Intriguingly, stable interactions have also been reported for Apo-Wbl proteins, but these seem to be differentially conserved across genera. In *Streptomyces* and *Corynebacterium* spp., WblA (WhcA) interacts with the dioxygenase SpiA to tailor the antioxidant response. Similarly, the *C. glutamicum* WblE homologue (WhcE) interacts with the transporter 'SpiE' but an identifiable homologue is absent from both *Streptomyces* and *Mycobacterium* spp., where *wblE* (*whiB1*) is essential (This work; Smith *et al*., 2010). Intriguingly, whole-cell work in *Mycobacterium* spp. once suggested that WhiB7 (WblC) and WhiB3 (WhiD) are in fact among the most highly interconnected proteins within the tubercule cell and co-purify with a broad range of partners *in vitro* (Wang *et al*., 2010). Irrespective of this, it is also presumed that WblE must acquire its [4Fe-4S] cluster from dedicated cluster biogenesis machinery, *in vivo* (see Section 1.5.1).

Following the successful generation of an isogenic FLAG-tagged WblE mutant (Δ24255CF), it became possible to perform targeted WblE co-immunoprecipitation with downstream mass spectroscopic analysis (CoIP-MS) to identify novel interactions which may occur *in vivo*, and possibly provide context to other poorly understood WhiB-like functions. CoIP-MS follows a similar premise to ChIP-seq, although targeted towards the capture of *in vivo* protein-protein interactions via covalent cross-linking and analysis by MS. This chapter describes identification of putative WblE partners via CoIP-MS, Network building, and subsequent confirmation of a subset of partners via pairwise bacterial two-hybrid assays.

6.2. Co-Immunoprecipitation and Mass Spectroscopy (CoIP-MS)

To produce comparable results, growth and sample acquisition for CoIP-MS was performed under identical conditions to the ChIP-seq experiments (Section 2.30 and 2.21 respectively). Only time point 1 (tp1) and time point 2 (tp2) were tested via CoIP-MS as part of this thesis. The study was performed in biological and technical triplicate with the *S. venezuelae* NRRL B-65442 control (WT) and Δ24255CF (1-3) strains. Subsequent spectral acquisition was performed by Dr Carlo Martins and Dr Gerhard Saalbach (John Innes Centre, Proteomics Facility) and spectral counts were processed with SAINT*express*. The Significance Analysis of Interactomes (SAINT)*express* pipeline has been streamlined for datasets with robust control samples (such as the one used here), attempts to reduce noise in CoIP-MS data and produce a probabilistic measure for each putative interaction which is summarised in the 'SAINT-score' (S_0; 0.00 – 1.00) and an abundance-derived fold-change (*f.c*). The pipeline also enables the calculation of the Bayesian false discovery rate (*BFDR*), providing a defined statistical evaluation of error for each putative partner, something lacking in similar interactome pipelines (Nesvizhskii *et al*., 2007; Teo *et al*., 2014).

Over both experimental time-points, a staggering 142 and 107 total unique peptides were determined to be significantly enriched for tp1 and tp2, respectively (excluding WblE), within the quantitative and statistical boundaries set ($S_0 \geq 0.65$, *f.c* > 3.00, *BFDR* ≤ 0.1). Reinforcing the results obtained with ChIP-seq, the CoIP-MS data suggest that WblE predominantly associates with proteins involved in 'Bald' developmental decisions. To provide a broad overview hits were sorted into COG classes (Clusters of Orthologous Groups) by Dr. Govind Chandra, demonstrating enrichment of proteins in classes relating to transcription, proteostatic processes (e.g. chaperones, proteases), and the metabolism of fatty acid and terpene lipids, over both time-points (Figure 6.1 & 6.2). A dramatic shift in several groups of enzymes were seen between tp1 and tp2, largely relating to biosynthesis or catabolism of the cell-wall and phospholipids (Figure 6.1 & 6.2) and a shift from 0.7% (1/142) secreted peptides to 37.4% (40/107), as determined by SignalP6.0 and manual identification for the TVIISS target EsxA. Over 30 individual proteins with poorly defined functions or hypothetical classification (Table 6.1) were significantly enriched over the course of the experiment, with a large number of these being enriched specifically during tp2.

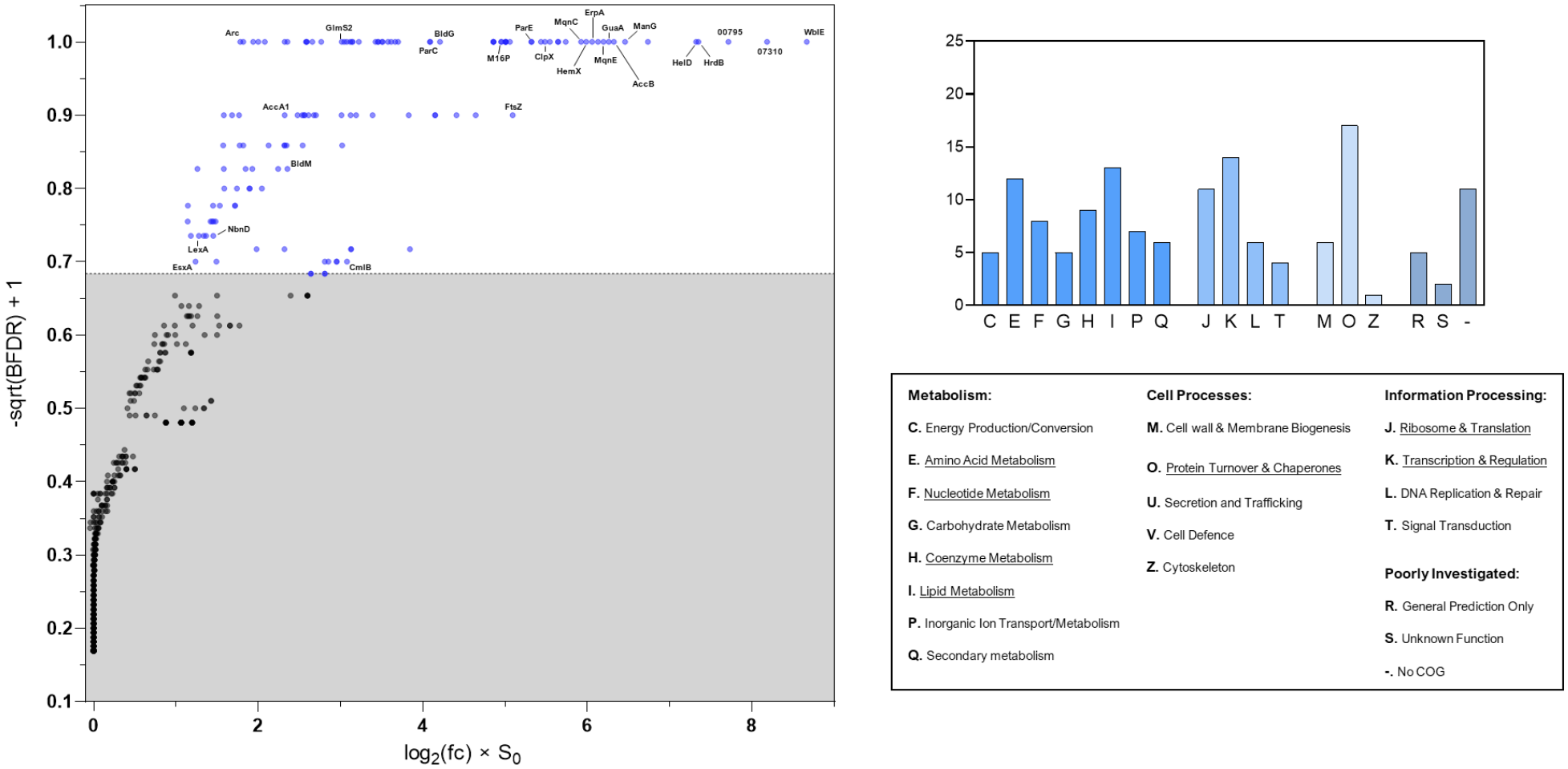

Figure 6.1. Significance and log2-fold abundance change for timepoint 1 CoIP-MS WblE hits. Non-significant hits are shaded out. The BFDR (0.00 - 0.10) is transformed by the negative square root +1, such that significance values range between 0.10 - 1.00, and the $\log_2(f.c)$ x-values have been multiplied by the SAINT score to emphasise the most significant datapoints. A Bar-graph showing COG-category counts for each significant hit in the tp1 WblE CoIP-MS data, categories for each letter are shown below with the dominant classes underlined.

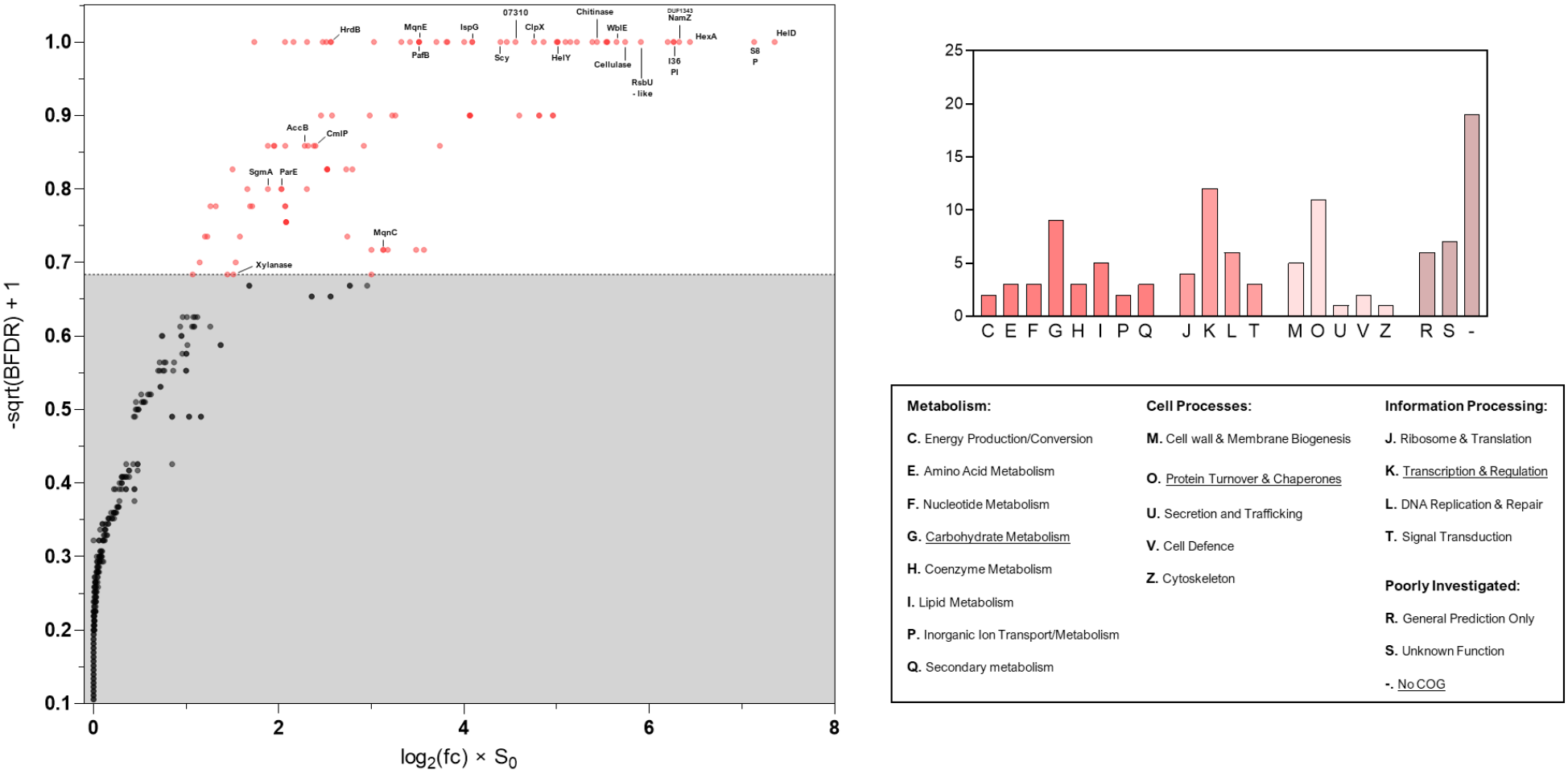

Figure 6.2. Significance and log2-fold abundance change for timepoint 2 CoIP-MS WblE hits. Non-significant hits are shaded out. The BFDR (0.00 - 0.10) is transformed by the negative square root +1, such that significance values range between 0.10 - 1.00, and the $\log_2(f.c)$ x-values have been multiplied by the SAINT score. for comparison. A Bar-graph showing COG-category counts for each significant hit in the tp2 WblE CoIP-MS data, categories for each letter are shown below with the dominant classes underlined.

6.3. CoIP-MS Networking

In contrast to ChIP-seq where results can largely be reduced to a binary description (either binding or not binding) based on the designated statistical cut-off. This does not work well for CoIP-MS, where highly significant hits can be enriched as non-specific peripheral cross-links with true partners, in heteromeric complexes or transient localisation. As such, it is important to try and extract these interdependent networks. Initially, StringDB was used to apply a basic skeleton to nodes, which was expanded with extensive manual literature searches for each hit. Several distinct, global cellular biochemical networks were seemingly well-resolved, and predominantly centre around one or two key/core nodes of interest; defined as nodes enriched over both time points and exhibiting 20-fold change or greater enrichment over control, in at least one time-point. Those networks are summarised here.

6.3.1 WblE CoIP-MS Resolves the *S. venezuelae* Transcriptional Apparatus

WhiB-like regulators are well-documented to interact with region 4.2 of the primary sigma factor, in a range of Actinobacteria. Reassuringly, WblE consistently co-precipitated with its canonical partner σ^{HrdB} over the course of the experiment, and it was one of the most highly enriched proteins during tp1 (*fc*: 160.00/5.91, S_0: 1.00, *BFDR*: 0.00). The small, general transcription factor, RbpA (vnz_04915), was also present across both time points (*fc*: 106.67/33.33, S_0: 1.00/0.99, *BFDR*: 0.00). Specific to the actinomycetes, RbpA plays a salient role in housekeeping transcription, promoting core RNAP stability via an interaction with Group I (e.g. HrdB) and II (HrdA/C/D) σ-factors, as well as the β' subunit. *In vitro,* RbpA binds to region 2 concomitant with WhiB7 or WhiB(A) binding region 4 of σ^{A} (σ^{HrdB})*,* respectively, but they do not interact directly (Lilic *et al.*, 2021; 2023). It seems likely, therefore, that a similar functional conformation is adopted *in vivo*, with WblE. The so-far unstudied RbpA paralogue, RbpB (vnz_07720) was also present, indicating a similar but specialised function with the sigma-factor (*fc*: 30.00/20.00, S_0: 0.99/0.94, BFDR: 0.00/0.01).

Sigma factors make a broad range of physical contacts with the core subunits of the RNA polymerase (RNAP), in order to stabilise the complex on promoter DNA (Paget, 2015). Reflecting this, the core subunits RpoA (α), RpoB (β), RpoC (β'), and RpoZ (ω), were also modestly but significantly enriched as peripheral pull-downs, likely cross-linked with σ^{HrdB} (tp1 only – Figure 6.3). Group I Sigma factors were traditionally considered dedicated initiation factors which obligately dissociate from the RNAP complex following initiation; σ^{70} factors are in fact retained in complex for significant distances throughout elongation (Raffaelle *et al*., 2005). Thus, the presence of NusG, NusA, Rho and the poorly characterised Tex (vnz_31710) was most likely a result of peripheral cross-links in σ-retaining elongation complexes (Figure 6.3). Nonetheless,

these results strongly support a role for WblE as an initiating transcription factor via its interaction with σ^{HrdB}.

6.3.1.1. Helicase D

In the context of the other RNAP components, including HrdB, the consistently high enrichment of HelD over tp1 and tp2 (*fc*: 160.00/163.33, S_0: 1.00, *BFDR*: 0.00) was surprising. In Gram-positive organisms, HelD, is an NTP-dependent transcription complex recycling factor, distantly related to the superfamily 1 (SF1) Helicases. The SF1 helicases' activity is typically modulated through interactions with other proteins and this is conserved in HelD, whereby the accessory RNAP subunit δ (*rpoE*) is known to synergistically enhance RNAP turnover in multiple species (Raney *et al*., 2012; Wiedermannova *et al*., 2014; Pei *et al*., 2020). However, the δ-subunit, is notably absent from *Streptomyces* spp. in direct contrast to the closely related *Mycobacterium* species.

6.3.2. WblE Coprecipitates with Putative co-Regulators

Transcription initiation is governed by activators and repressors, which bind promoter DNA to influence RNAP and σ-factor binding. Co-regulators can be defined as proteins that regularly bind DNA proximal to the WblE-RNAP complex, and/or directly interact to promote transcription (as in the WhiAB-RNAP complex; cite). A total of 4 bona-fide and 3 putative DNA-binding proteins, which could function as co-regulators, were identified via WblE CoIP-MS. These regulators are highlighted in Figure 6.3. One of these was a putative MocR-type regulator (vnz_28560) expected to sense pyridoxal-5-phosphate and/or amino compounds, but is of unknown function (Tramonti *et al.*, 2018).

6.3.2.1. The Developmental Regulator BldM

The atypical, orphan response regulator BldM (vnz_22005) is a crucial regulator of *Streptomyces* development and was somewhat enriched during tp1 (*fc*: 6.50, S_0: 0.83, *BFDR*: 0.03). The heterodimeric partner, WhiI, which specifies BldM DNA-binding to later-stage developmental genes, was not present in the data, suggesting that this pull-down was specific to BldM and/or its homodimer which would also explain its temporal enrichment during vegetative growth (tp1 - 18hr). Coincidentally, this thesis has also demonstrated that WblE binds two of the same promoters as BldM, binding within the *ssgR* (*vnz_18200* – Section 5.3.1) and *scr2* (*vnz_15145* – Section 5.3.8) promoter regions which are important for development and secondary metabolism, respectively. Thus, in addition to co-purifying with one another, BldM and WblE appear to share at least two DNA-binding targets.

6.3.2.2. The DNA Damage Response (DDR) Regulators

In most bacterial phyla, the LexA-RecA system is the only known pathway providing general regulation of the DNA damage response (DDR). The winged (w)HTH regulator, LexA, binds and represses a global regulon of DDR genes; DNA-damage induces RecA-mediated auto-proteolytic cleavage of LexA and DDR gene expression (Stratton et al., 2020). Unlike most bacteria, *Mycobacterium* and *Streptomyces* species retain DDR expression in a Δ*recA* background, via an independent DDR pathway (Rand *et al.*, 2003; Huang & Chen, 2006). The *pafB* and *pafC* genes encode two winged-HTH regulators which heterodimerise around ssDNA with their N-terminal WYL (Trp-Tyr-Leu) domains and likely control the Actinomycete-specific, RecA-independent branch of the DDR (Müller *et al*., 2018; Müller *et al*., 2019; Adefisayo *et al*., 2021). Remarkably, despite not being grown under DNA-damaging conditions, WblE co-precipitated with LexA during tp1 (vnz_27115: *fc* = 3.75, S_0 = 0.67; *BFDR* = 0.01), accompanied by non-significant enrichment of RecA. In addition, PafB and PafC were both present in the tp2 data (fc:12.00/9.00, S_0:0.98/0.86, BFDR: 0.00/0.03, respectively). Importantly, a partial Cryo-EM structure of *M. tuberculosis* PafBC-σ^A transcription complex illustrates intercalation of the PafBC-wHTH domains between σ^A region 4.2 and the DNA, such that cooperation between WhiB1 and PafBC is conceivable in this genus (Müller *et al*., 2021a). No work has yet directly investigated these proteins in *Streptomyces* spp. but the potential for this interaction and its physiological importance will be discussed.

6.3.2.3. DeoR-Type Metabolic Regulators

Named after the *E. coli* deoxyribose (*deo*) operon regulator, DeoR-type regulators are typically repressors of carbohydrate catabolic genes and are induced by the associated phosphorylated carbohydrate of their cognate pathways. Many examples possess complex oligomeric DNA-binding patterns, and broad global regulons (Elgrably-Weiss *et al*., 2006; Gaigalat *et al*., 2007; Engels & Wendisch, 2007).

The vnz_05140 DeoR-type protein was the only identified regulator which maintained significant enrichment between tp1 and tp2 (*fc*: 20.0/9.0, S_0: 0.65/0.94, *BFDR*: 0.09/0.01). The *vnz_05140* gene is highly conserved in the *Streptomyces* genus and possesses homology to the AI-2 Quorum-sensing repressor LsrR (Wu *et al*., 2013). Deletion of the homologue in *S. coelicolor* (Δ*sco1463*) yields pleiotropic defects in the initiation of aerial growth, secondary metabolism, and an accumulation of succinyl- and propionyl-CoA; no direct genetic targets are yet known for this regulator (Jeon *et al*., 2019). A second, conserved DeoR-type regulator, vnz_15020 (SCO3198), was also somewhat enriched during tp2 (*fc*: 3.33, S_0: 0.66, *BFDR*: 0.09). The protein shares homology and genetic synteny with the global carbon catabolite regulator, FruR. The *C.*

glutamicum orthologue (cg2115, SugR) globally represses various sugar PTS components and broad aspects of carbon metabolism (Gaigalat *et al*., 2007; Engels & Wendisch, 2007). Proteomic assessment of the *S. coelicolor* nucleoid has previously indicated a global role for the protein (Bradshaw *et al*., 2013). In light of these results, it is intriguing that promoters of a succinate-CoA ligase and the sugar phosphotransferase *crr-ptsI* operon, were both enriched in the WblE ChIP-seq data (Section 5.1 – no.10), potentially indicating concomitant binding at these promoters as the source of these results, respectively, although this would require further specific testing to confirm.

6.3.2.4 The Hopene Biosynthetic Gene Cluster Regulator, HpnR

A xenobiotic responsive element (XRE) HTH regulator (vnz_31840) was also significantly enriched during tp2. The gene is conserved immediately downstream of the *Streptomyces* Hopene biosynthetic operon and is predicted to be the regulatory unit, HpnR (Sandoval-Calderón et al., 2017). Hopanoids are pentacyclic triterpene secondary metabolites which function as sterol analogues and important determinants of membrane fluidity/permeability in eubacteria (Rohmer *et al*., 1979; Sáenz *et al*., 2012). In *Streptomyces* spp., hopanoids are dispensable, but their synthesis is tightly regulated with the onset of aerial development (matching HpnR's temporal enrichment in the CoIP-MS; Figure 6.3) and is missing from most *bld* mutants (Seipke & Loria, 2009; Poralla *et al*., 2000). This was just one of many aspects of global terpenoid and lipid metabolism present in the CoIP-MS data (Section 6.3.4.1 and 6.3.5).

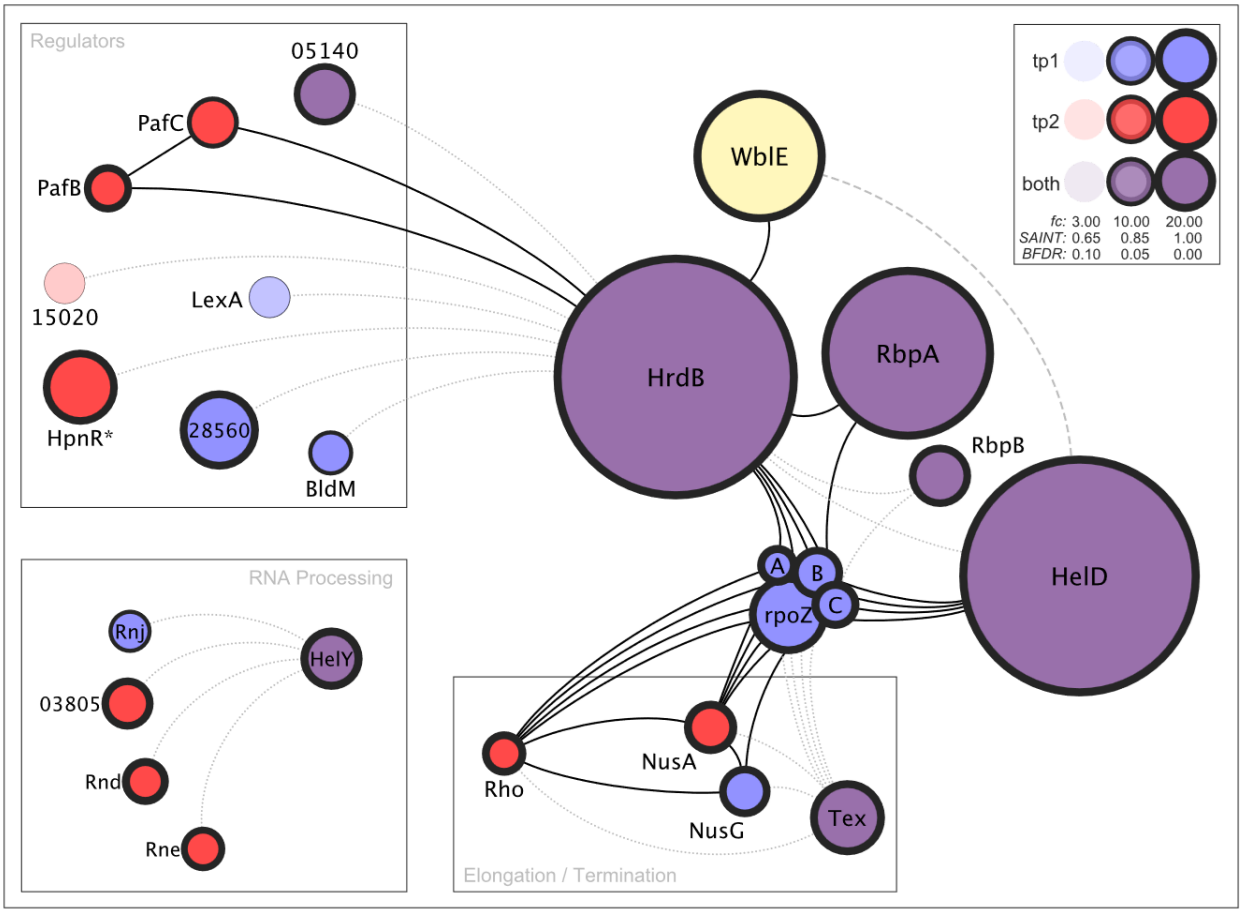

Figure 6.3. WblE RNA Polymerase and Regulator Network. Tp1 hits are shown in red, tp2 in blue and shared hits in purple. Key for interpreting SAINT scores (S_0) and *BFDR* is in the top right (*n* = 25 excl. WblE).

All Networks: Grey diamonds represent connected nodes that were not present in the CoIP-MS data. Short dash arrows represent multiple biochemical steps between proteins. Connected nodes that are present but not-significantly enriched in the data are arbitrarily shown as circular grey nodes. Grey edges are those which connect to non-significant hits or are hypothetical in nature. Tp1 hits are shown in blue, tp2 in red and shared hits in purple. The SAINT score (S_0) and BFDR for hits are represented by border thickness node transparency (0% = 0.00 BFDR / 95% = 0.10 BFDR), respectively. The non-transformed spectral count fold-change is shown by node circumference. For reference, nodes in the key are arbitrarily represented by a 2.00 f.c and WblE is differentiated in maroon with 75 *f.c.*

6.3.3. WblE co-Precipitates with a Diverse Proteostatic Network

Proteostasis refers to the dynamic, competing and integrated pathways within cells that coordinate the biogenesis (translation), folding, maintenance (chaperones) and turnover and proteases) of intra- and extracellular proteins (Rebeaud *et al*., 2021). This thesis has already presented evidence for the widespread binding of WblE to the promoters of tRNA, rRNA and ribosomal protein genes, which represent foundational roles in protein translation. In addition, a single in vitro study once demonstrated ATP-independent chaperone-like (i.e. holdase) activity for Mycobacterium spp WhiB2 (Konar *et al*., 2012). To this end, it was particularly intriguing to see a comprehensive network of chaperones, co-chaperones, ribosome-associated proteins and a range of poorly studied proteases enriched in the CoIP-MS data.

6.3.3.1. Enrichment of Hsp100 Chaperones and Diverse Co-Chaperones

Chaperones, or heat shock proteins (Hsp), are evolutionarily conserved proteins across all domains of life and are fundamental post-ribosomal elements in protein synthesis and regulating appropriate turnover. The Hsp100 family of chaperones describes ring-like AAA+ family proteins (ATPases Associated with diverse Activities), such as ClpX (vnz_11755) which formed one of the core-nodes of this network, being both highly and consistently enriched over both timepoints (*fc*: 44.75 / 27.00, S_0: 1.00, *BFDR*: 0.00). The homohexameric AAA+ family protein functions alone as an energy-dependent chaperone, unfolding individual proteins and dismantling protein aggregates (Wawrzynow *et al.*, 1995; Levchenko *et al*., 1995; Weber-Ban *et al*., 1999). ClpX also forms an important aspect of a major proteolytic complex within bacterial cells, ClpXP; a system that is essential in *Streptomyces* and *Mycobacterium* spp. (d'Andrea *et al*., 2022; Reinhardt *et al*., 2022). However, the associated proteolytic elements, ClpP1 (vnz_11760), ClpP2 (vnz_11765) were present but far below significance (). Similarly, the 'Arc' (vnz_06060) ring-like AAA+ of the functionally similar eubacterial proteasome was enriched during tp1 (*fc*: 3.44, S_0: 1.00, *BFDR*: 0.00), while its proteolytic alpha (PrcA – vnz_06040) and beta subunits (PrcB – vnz_06045) were present only at sub-significant levels (S_0: 0.04 – 0.46, *BFDR*: 0.45 – 0.73). Both AAA+ proteolytic complexes have functions that are especially important for development (De Crécy-Lagard *et al*., 2002; Boubakri *et al*., 2015). In particular, the enriched cytoskeletal element FtsZ is a direct target of ClpX activity that was co-enriched during tp1 and hence was connected to this node (Sugimoto *et al*., 2010). Also enriched were the aggregation-prone Rhodanese (CysA - vnz_19375) and Luciferase-like enzyme (vnz_18275) which are common chaperone substrates.

While the chaperone network distinctly revolved around the AAA+ chaperone ClpX, the data also presented the significant enrichment of the co-chaperone, DnaJ2 (vnz_11415 – *fc*:

26.67/6.67, S_0: 0.83/0.74, *BFDR*: 0.03/0.06). *Streptomyces* spp. carry two conserved DnaJ (Hsp40) proteins but these remain largely unstudied and are presumed to function similarly to known homologues in substrate targeting, ATPase stimulation for the cognate chaperone, DnaK. However, while the cognate nucleotide exchange factor GrpE (*fc*: 5.00, S_0: 0.75, *BFDR*: 0.04) and possible co-chaperone FkpB (vnz_06015) were significantly enriched, DnaK (Hsp70) enrichment was sub-significant. The co-chaperone GroES (Hsp10) was also modestly enriched in the data, however GroEL enrichment was sub-significant.

CnoX (originally YbbN) is a more recently appreciated bacterial co-chaperone with independent functions as a holdase and thioredoxin (i.e. a chaperedoxin), which can cooperate directly with both the DnaJ–K–GrpE and GroES–EL chaperone systems, in order to direct a specific set of redox-sensitive proteins for refolding or degradation (Kthiri *et al*., 2008; Dupuy *et al*., 2023; Goemans *et al*., 2018a & 2018b). A highly similar and conserved *Streptomyces* protein, annotated as TrxA4 in *S. coelicolor* (SCO5419), and tentatively named here as CnoX (vnz_25065), was significantly enriched and fitted well within this network (*fc*: 4.67, S_0: 0.83, *BFDR*: 0.03).

6.3.3.2. Enrichment of an Extensive Protease Repertoire (and an Inhibitor)

A total of 14 individual known and putative proteases were significantly enriched during the CoIP-MS experiment and the majority were associated with strong S_0 ($\geq$ 0.80) and *BFDR* ($\leq$ 0.05) scores. Nevertheless, no hits were consistently enriched over both timepoints, suggesting a dynamic (direct or indirect) association with this group of proteins (Figure 6.4).

The vegetative dataset (tp1) presented only intracellular metalloproteases, albeit of various families. However, these proteins remain unstudied in the context of *Streptomyces* biology. The M20-family peptidase vnz_06215 genomically precedes the conserved chaplin, *chpH*, and may therefore be important for development. Two co-translated and conserved M16 proteases (vnz_27275 and vnz_27280) were also significantly enriched indicating a cooperative nature to the proteins which is typical of the M16A/B heterodimeric subtypes (Johnson *et al*., 2006b; Aleshin *et al*., 2009).In stark contrast to tp1, the tp2 dataset was dominated by serine proteases; the putative vnz_32055 extracellular S8 protease and was the highest ranked protein during the onset of aerial development (*fc*: 140.00, S_0: 1.00, *BFDR*: 0.00). Two other related S8 proteases were also significantly enriched, vnz_29370 and vnz_11880 (Suzuki *et al*., 1997). The proteins apparently share little similarity other than their proteolytic domains, N-terminal SEC (type I) signal peptides and a transmembrane-anchoring helix. A secreted S15 (vnz_31670) and intracellular S9 (vnz_31190) protease were also enriched but remain unstudied. Nevertheless, in contrast to this tp2 paradigm, the developmental M4 peptidase SgmA was also enriched.

The vnz_14415 protein is one of several similar, hypothetical, extracellular proteins that were enriched in the tp2 data possessing a C-terminal, VCBS-repeat β-propellor domain (vnz_19015, vnz_14535, pvnz_37465; Table 6.1). However, vnz_14415 appears unique as it also possesses an 'I36' protease-inhibitor domain, suggesting an extracellular proteostatic function. The I36 family are specific to *Streptomyces* spp. and the only studied example functions as a general M4 peptidase inhibitor, with notable activity towards SgmA (Oda *et al*., 1979; Seeram et al., 1997; Hiraga et al., 1999), therefore potentially explaining the concurrent enrichment of this developmental protease in the tp2 data.

6.3.3.3. The Top Hit – A Putative Novel Proteostatic Protein 'vnz_07310'

A 448aa, 47.2 kDa protein (vnz_07310) that is well conserved in *Streptomyces* spp., but with no detectable sequence homology to any known proteins, was the most highly and significantly enriched protein in the tp1 data (*fc*: 291.00, S_0: 1.00, *BFDR*: 0.00). This enrichment diminished but was equally significant during tp2 (*fc*: 23.50) and insinuated the exciting possibility of a novel WblE interaction partner; this is explored further in Section 6.4.2.

A predicted structure was generated by C-I-TASSER (Contact-guided Iterative Threading ASSEmbly Refinement), an extension of I-TASSER which generates significantly more accurate models for sequences that do not possess homologous templates in the PDB, such as vnz_07310. As such it also performed better than other homology-based models (e.g. AlphaFold 2) under such constraints (Zheng *et al*., 2021).

The results predicted an α-toroidal 3D structure to the protein, from which COFACTOR identified clear structural homology with the multifaceted RPN1 ubiquitin receptor and scaffold for the eukaryotic 26S proteasomal-cap (0.871 coverage – *Spinacia oleracia*), despite very limited sequence identity or similarity. The *S. griseus* homologue SGR_5650 exhibits the greatest difference in its amino acid sequence among *Streptomyces* spp. homologues, and was modelled for comparison; remarkably, a similar structure with increasingly explicit structural similarity to the *S. cerevisiae* RPN1 protein (0.961 coverage) was identified, including its intrinsically disordered C-terminus (Figure 6.5 – Shi *et al*., 2016; Kandolf *et al*., 2022). Other C-I-TASSER models for the vnz_07310, SGR_5650, SCO1842 homologues resembled similar α-solenoid structures, with the α-toroid in varying states of extension/flexion. The RPN1 protein is a major scaffold for the proteasome-activating PAN/ARC/Rpt AAA+ ATPases and could allude to a specific origin for the enrichment of ClpX and Arc, in the CoIP-MS data. Additionally, a range of enriched proteins are putative targets for modification by the prokaryotic ubiquitin-like protein. As such, the protein was tentatively connected to this network (Figure 6.4).

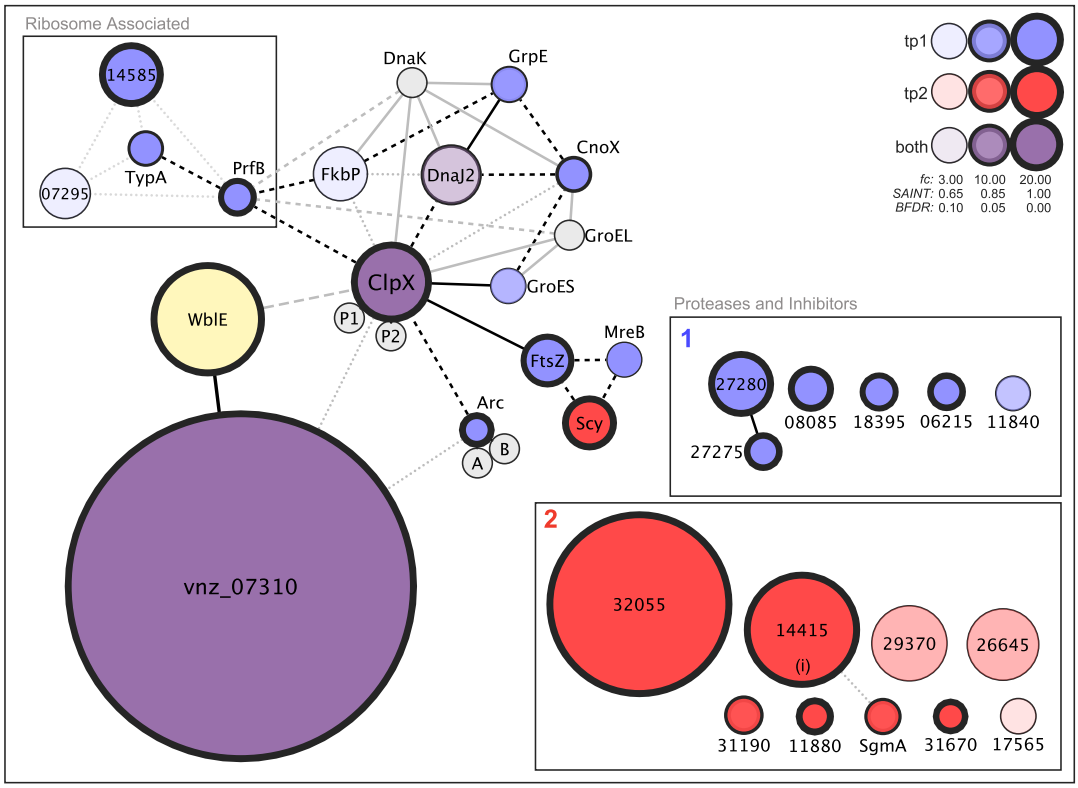

Figure 6.4. WblE CoIP-MS Proteostatic network. Chaperone network and targets presented centrally, temporally enriched proteases and protease inhibitors are shown on the right (boxed). Ribosome associated proteins shown left (boxed). numbered and colour-coded by their timepoint (1 or 2); protease inhibitor vnz_14415 is marked with '(i)' for distinction. *n* = 30 excl. WblE

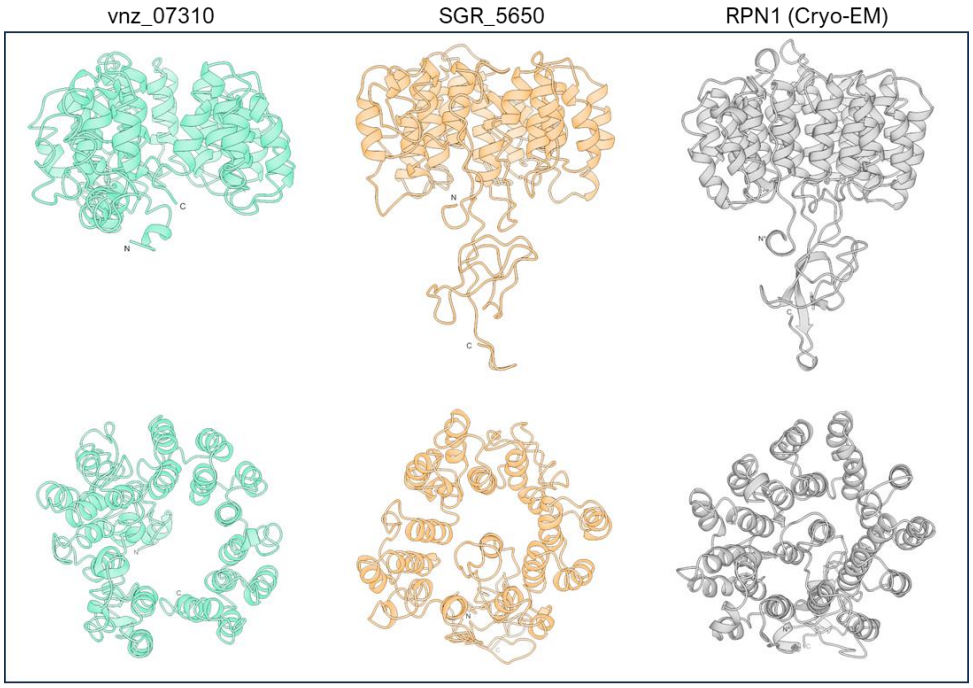

Figure 6.5. The C-I-TASSER predicted 3D models for full length vnz_07310 and SGR_5650 peptides, compared with the Cryo-EM structure of *Saccharomyces cerevisiae* RPN1 toroidal receptor domain (aa 314 – 813;), which shares 0.961 coverage with SGR_5650. The highest structural similarity to the CIT model of vnz_07310 is *S. oleracea* RPN1 (0.871 coverage – not shown).

6.3.4. The Metallo-Cofactor, Respiration and Isoprenoid and Network

6.3.4.1. Factors Potentially Maintaining the WblE [4Fe-4S] cluster

The CoIP-MS data indicated enrichment of components of the *Streptomyces* spp. Fe-S chaperone machinery (Section 1.5.1); the A-Type [4Fe-4S] carrier (ErpA) was highly enriched during tp1 (*fc*: 66.67, S_0: 1.00, *BFDR*: 0.00), more so than the SufBC$_2$D cluster chaperone complex, of which only SufD registered significantly (Figure 6.7).

Together with the enrichment of the Fe-S chaperone machinery, the CoIP-MS data provided an intriguing snapshot of the potential electrochemical maintenance taking place at the WblE cluster, *in vivo*. The vnz_11275 protein was strongly enriched during tp1 (*fc* = 66.67, S_0 = 1.00, *BFDR* = 0.00) and possessed notable similarity to Ferredoxin-NADPH Reductases; in particular, to the essential FprA (Rv3106) of *Mycobacterium tuberculosis* H37Rv and Adrenodoxin Reductase (AdR) of eukaryotes. FprA catalyses the NADPH-derived 1e$^-$ reduction of the [4Fe-4S] ferredoxin (Rv0763c), for subsequent transfer to CYP450 haems, driving their monooxygenation reactions (Fischer *et al*., 2002; McLean *et al*., 2005; Ugalde *et al*., 2018). Excitingly, in the absence of any potential cognate ferredoxin in the complete dataset, this result could imply an unorthodox ferredoxin-like role for WblE in an electron transport chain, or perhaps a general importance in maintaining the charge on the WblE cluster.

The phylogenetic distribution of Nitrobindin (Nbn) in bacteria closely matches that of Wbl proteins, hence it was proposed that Nbn scavenges •NO from the Wbl cluster environment to circumvent cluster-collapse and modulate Wbl-signaling (Section 1.6.2.4). *Streptomyces venezuelae* Nbn (vnz_19410), was modestly enriched during tp1 (*fc* = 4.50, S_0 = 0.67, *BFDR* = 0.07) and provides the best experimental evidence for this transient interplay, hypothesised a decade ago (Chandra and Chater, 2014). By extension, it is thought that Nbn-Fe-NO could be detoxified by mycothiol and subsequently by the putative nitroso-mycothiol reductase (MSNOR; vnz_06235), which was also identified within an extended cut-off (S_0: 0.60, *BFDR*: 0.16 – not shown).

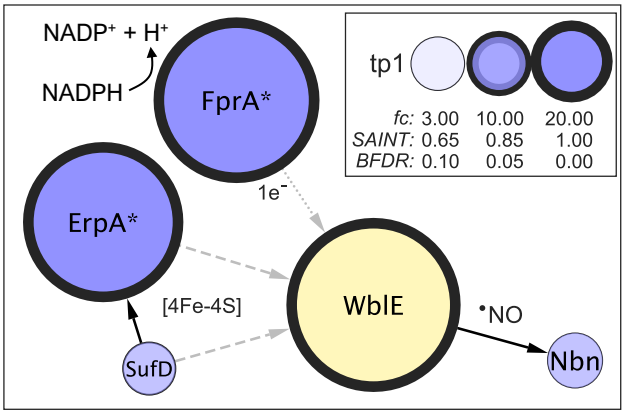

Figure 6.7. Putative WblE [4Fe-4S] Cluster and Redox Maintenance Network resolved via CoIP-MS. Substrates are highlighted.

6.3.4.2. Enrichment of Enzymes for Isoprene and Menaquinone Biosynthesis

The isoprenoid (terpenoid) lipids are among the most diverse and abundant natural products on earth, with important cellular functions in respiration and coping with various stressors. *In vivo,* terpenoids (including Hopene) are predominantly assembled from two isomeric five-carbon starter units, isopentenyl diphosphate (IPP) and dimethylallyl diphosphate (DMAPP) which are synthesized via the Mevalonate (MVN), or 2-C-methyl-D-erythritol 4-phosphate (MEP) pathways. Most *Streptomyces* species, including *S. venezuelae*, are only equipped with the MEP pathway, for which the 1-Deoxy-D-xylulose-5P reductoisomerase, Dxr, performs the first committed step, forming the branched polyol 'MEP' after which the pathway is named. Dxr was moderately enriched (*f.c*: 6.00, S_0: 0.79, *BFDR*: 0.04, tp1) in the WblE Co-IP experiments in addition to the [4Fe-4S] protein IspG during tp2, which catalyses the final step in IPP synthesis (*f.c*: 17.00, S_0: 1.00, *BFDR*: 0.00).

Arguably, the most important isoprenoid derivatives in bacteria are the Menaquinones (MK), which play an essential membrane-bound role in electron transport and respiration. Their synthesis diverges between one of two evolutionarily ancient pathways in bacteria. The 'Futalosine' (MQN) machinery constitutes the less abundant but more broadly distributed and ancient biosynthetic pathway, utilised across all forms of respiration (Zhi *et al*., 2014). Fittingly, the Futalosine pathway *mqnA-E* genes were first recognised in *Streptomyces coelicolor* and function as the primary MK biosynthetic pathway in this genus. The hallmarks of the Futalosine pathway are the [4Fe-4S]-binding Radical *S*-Adenosyl Methionine (rSAM) enzymes; Aminodeoxyfutalosine synthase (MqnE – vnz_15365) and Dehypoxanthine futalosine cyclase (MqnC – vnz_21020), which form the core nodes of the network as two of the most significantly enriched hits within the CoIP-MS data, present over both time points and with an associated ChIP-seq target (*mqnD – vnz_21015*, Section 5.3.6.4). The MQN and MEP pathways are dense in [4Fe-4S] biochemistry, with the MqnE, MqnC, IspG and IspH enzymes all possessing [4Fe-4S] clusters necessary for their function, isoprenoid synthesis and respiration.

6.3.4.3. The Uroporphyrinogen III Synthase and Methyltransferase: HemD

HemD (vnz_15625, SCO3317) in *Streptomyces* spp. is a bifunctional haem-biosynthesis protein comprised of two domains. The C-terminal domain is an active Uroporphyrinogen III synthase (HemD), catalysing cyclisation of the linear tetrapyrrole (hydroxymethylbilane) to produce the first critical macrocyclic haem intermediate, uroporphyrinogen III, that is common to all haem-synthesis pathways (Rondon *et al*., 1997; Amin *et al*., 2012). The N-terminal sirohaem synthase (CysG) domain, by homology, catalyses the sequential SAM-dependent methylation of uroporphyrinogen III to sirohaem, via the adenosylcobalamin (Vitamin B_{12}) precursors, precorrin-2 and sirohydrochlorin (Rondon *et al*., 1997). Similar fusions between HemD and CysG (or the

related protein CobA) are observed broadly in Gram-positive bacteria (Johansson & Hederstedt, 1999). Coincidentally, like *wblE*, *hemD* is also regulated by the NAD(H)-sensor Rex, in *S. avermitilis*, with which it shares an operon (Liu *et al.*, 2017).

Haem *b* (protoporphyrin IX) functions in the respiratory Succinate:Quinone (Complex II), Quinol:Cytochrome *c* (Complex III), and Quinol:Nitrate (NarGHI) oxidoreductase enzymes; the latter of which is involved in reductive •NO synthesis in *S. coelicolor* (Figure 6.6). With respect to this, haem is also present in all NOS enzymes (more relevant to *S. venezuelae*). Haem *b* is also a necessary co-factor for •NO scavenging and detoxification by Nitrobindins, •NO-dioxygenases, as well as other antioxidant enzymes (den Hengst & Buttner, 2008; De Simone *et al*., 2020a & 2020b). Sirohaem on the other hand, is specifically employed for the reduction of Nitrite anions by the assimilatory nitrite reductase ($NirB_1B_2D$), which plays a role in *Streptomyces* •NO homeostasis (Campbell and Kinghorn, 1990; Fischer *et al*., 2012; Yukioka *et al*., 2017).

Intrguingly, Haem often functions cooperatively with menaquinone and menaquinone biosynthesis featured significantly in both the ChIP and CoIP experiments (Sections 5.3.6.4 & 6.3.4.1). A post-translational interplay between WblE and HemD has broad implications for a role in regulating respiration, •NO-signalling and •NO-detoxification via haem availability.

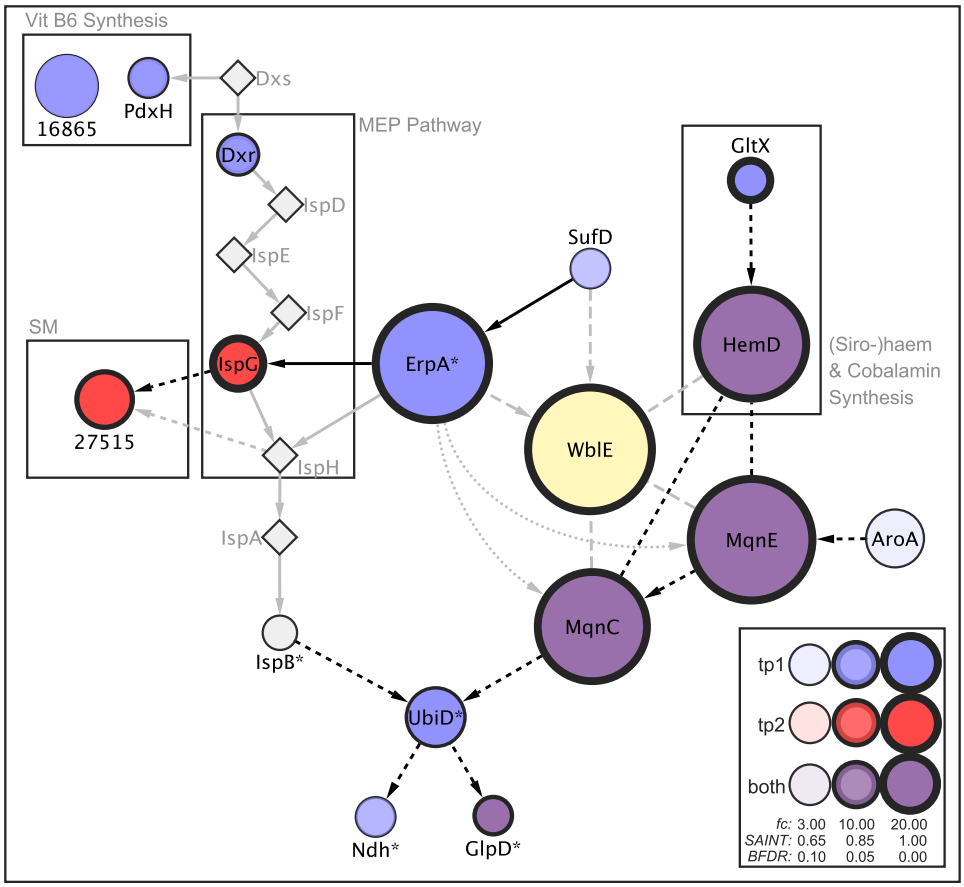

Figure 6.6. The Menaquinone and Isoprenoid (MEP) Network. Specific pathways are boxed and annotated as SM (Secondary Metabolism); Vit B6 (Pyridoxal-5-phosphate) synthesis.

6.3.5. WblE co-Precipitates with a Fatty Acid Metabolic Network

A broad range of proteins known or predicted to contribute to fatty acid biosynthesis or β-oxidation, were over-represented amongst the CoIP-MS data obtained during tp1 and were generally associated with strong SAINT (> 0.80) and BFDR (< 0.05) scores. Considering the broad historic connection between Wbl-proteins and fatty acid metabolism, these hits were particularly intriguing.

6.3.5.1. The Acyl-CoA Carboxylase and Type II Biosynthesis Machinery

The first committed step in long-chain fatty acid biosynthesis is the irreversible carboxylation of acetyl-CoA to malonyl-CoA, universally catalysed by biotin-dependent acyl-CoA carboxylases (ACCs), a structurally heterogeneous class of proteins (Cronan & Thomas, 2009; Cronan *et al*., 2021). Actinomycetes, including *Streptomyces* and *Mycobacterium* species express multiple copies of a distinct group of ACCs which employ two catalytic subunits (α and β). In *Streptomyces*, specifically, two copies of the α and β subunits are well-conserved: AccA1 and AccA2 represent structurally redundant α-subunits, that form mutually exclusive 1:1 hexameric complexes with either AccB (ACC-A), or PccB (ACC-P) β-subunits which confer substrate specificity (Rodŕiguez & Gramajo, 1999; Diacovich *et al*., 2002; Diacovich *et al*., 2004; Gago *et al*., 2006). Notably, the AccB protein is essential in *Streptomyces* as it is the only subunit capable of utilising acetyl-CoA, whereas PccB is dispensable and can utilise only propionyl- or butyryl-CoA (Rodŕiguez *et al*., 2001). All catalytic components for both the ACC-A and ACC-P complexes were enriched in the CoIP-MS data, whereby AccB (*fc*: 80.00/5.67, S_0: 1.00/0.91, *BFDR*: 0.00/0.02) represented the key node of the network (Figure 6.8); the other components, AccA1/A2 and PccB, were also significantly enriched but only during tp1.

Downstream of acetyl-CoA carboxylation, highly conserved type II (dissociate) fatty acid biosynthetic machinery catalyses the sequential condensation, reduction, dehydration and second reduction that elongates growing acyl-chains. The β-ketoacyl-ACP synthase III (FabH) conducts the first condensation reaction between acetyl-CoA and malonyl-ACP (acyl-carrier protein) to form 3-ketoacyl-ACP and was highly enriched during tp1 (*fc*: 53.33, S_0: 1.00, *BFDR*: 0.00). In addition, the FabG 3-ketoacyl-ACP-reductase (vnz_07115) and FabI/InhA enoyl-ACP-reductase (vnz_07110), which catalyse the first and last reductive steps of acyl-chain elongation respectively, to produce an elongated acyl-CoA molecule (Revill *et al*., 2001; Singh & Reynolds, 2015). Thus, WblE strongly associated with key enzymes that are necessary for entry of acetyl-CoA into fatty acid biosynthesis, via malonyl-CoA (ACC), in addition to multiple components of the type II fatty acid synthetic machinery.

It is also pertinent to note the enrichment of homologues of the actinomycete pyruvate dehydrogenase complex (AceE and DlaT; vnz_10680 – vnz_09035) and its lipoamide synthesis and redox maintenance system (LipA and AhpC – AhpD; vnz_09110 and vnz_23230 – 23225) in the dataset. Pyruvate dehydrogenase completes the anaplerotic conversion of pyruvate to acetyl-CoA and feeds fatty acid synthesis. These unique complexes have only been characterised in *Mycobacterium* spp., thus far, but these data suggests a homologous system also functions in *Streptomyces* spp. (Bryk *et al*., 2002; Tian *et al*., 2005; Rhee *et al*., 2011).

6.3.5.2. Fatty Acid β-Oxidation Machinery

The catabolic β-oxidative machinery, also had a range of representative enzymes enriched within the CoIP-MS data, albeit at lower levels. Most notable was the enrichment of the conserved catabolic FadAB complexes, FadA1-B1 (vnz_28805 - 10) and FadA2-B2 (vnz_31630 - 35) during tp1, with enrichment of FadA2 in the tp2 data (Menendez-Bravo *et al*., 2017). Two FadE2-family proteins were enriched during tp2 which could catalyse first oxidative (dehydrogenation) reactions to form a *trans*-enoyl-CoA species. One of the FadE2-like proteins, vnz_00800, was encoded at the genomic periphery, along with two predicted acyl-CoA metabolising enzymes (vnz_00790 & vnz_00795); vnz_00795 was among the most highly ranked proteins in the tp1 dataset (*fc*: 210.00, S_0: 1.00, *BFDR*: 0.00). The gene-set's location and sporadic conservation indicate a specialised role in *S. venezuelae*. The primary fatty acid oxidation machinery likely works in close proximity to the synthetic machinery (see previous section) as they share substrates, suggesting that these could be peripheral pull-downs.

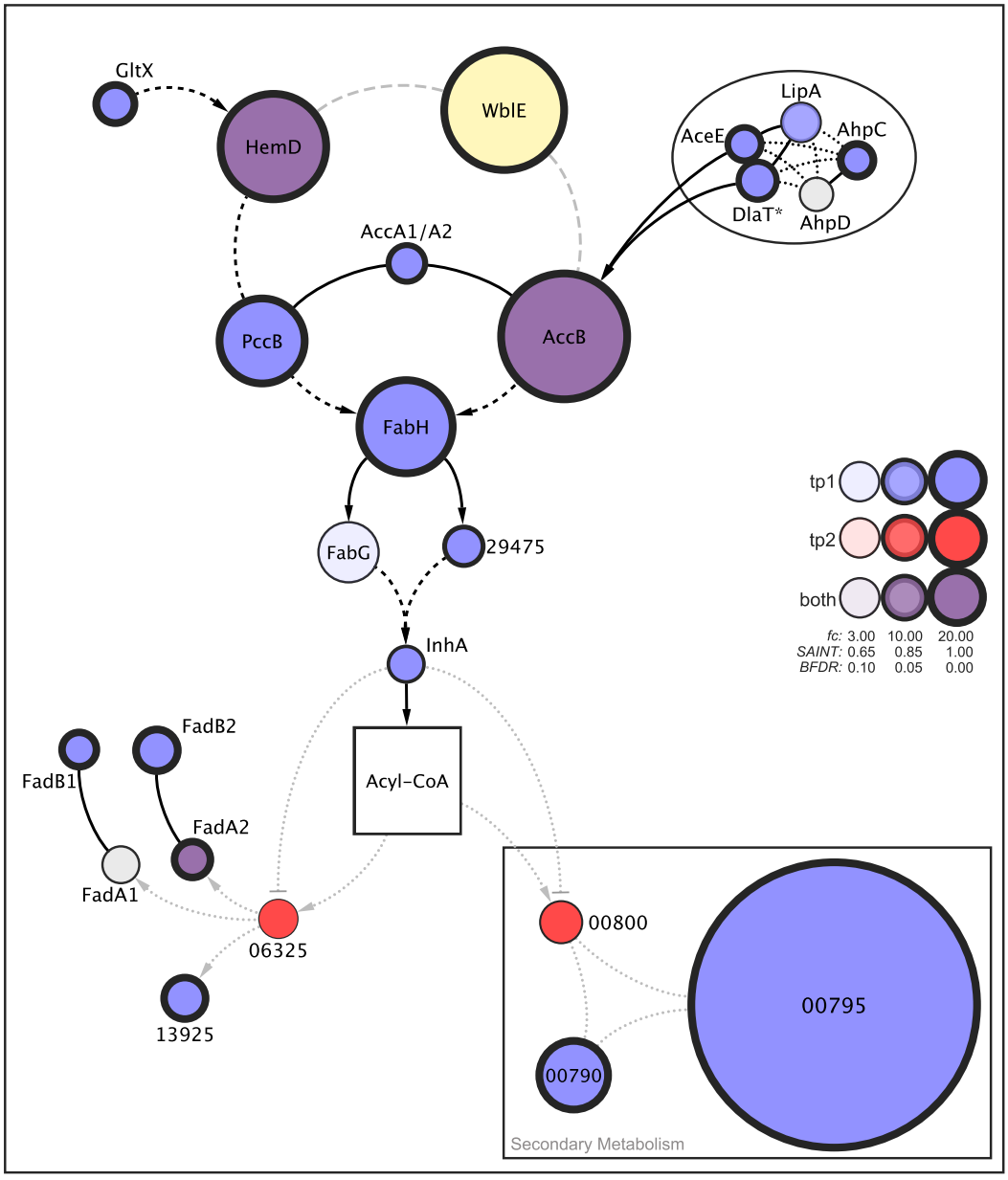

Figure 6.8. The acyl-CoA carboxylase, fatty acid synthesis (before acyl-CoA node) and β-oxidation WblE CoIP-MS Network (after acyl-CoA Node). Key is shown centre right. The putative secondary metabolite BGC machinery is boxed and labelled. The actinomycete pyruvate dehydrogenase complex is circled.

6.3.6. WblE co-Precipitates with an Developmental RsbUVW Network

In the archetypal RsbU-RsbV-RsbW-σ^B cascade, of *Bacillus subtilis*, the ASA RsbV governs expression of the stress-response factor, SigB (σ^B) via ATP-dependent phosphorylation of its anti-sigma factor RsbW and subsequent release of σ^B, redirecting the RNA Polymerase to a global regulon of stress-related genes (Benson *et al*., 1993). third component, RsbU, dephosphorylates RsbV to drive the cascade under inducing conditions, such as osmotic stress (Voelker *et al*., 1995). *Streptomyces* species usually possess eight or more closely related group 3 alternative σ-factors (σ^B homologues) which is often reflected by their high number of *rsbU, rsbV, rsbW* copies, indicating a complex network underlying the stress response. In particular, the conserved σ^B and σ^H proteins both function in the general stress response, with overlapping regulons, yet σ^H possesses additional developmental functions (Mittenhuber *et al*., 2002; Takano *et al*., 2003; Sevcikova *et al*., 2021).

The *Streptomyces* BldG protein is a highly conserved, morphogenic RsbV-like anti-sigma antagonist (ASA) which was significantly enriched during tp1 of the CoIP-MS experiment (*fc* = 18.5, S_0 = 1.00, *BFDR* = 0.00). BldG appears to sequester multiple anti-sigma factors, including the conserved neighbouring gene's product, ApgA (to which no σ-factor has presently been associated) and the anti-σ^H factor, UshX (which is important for both development and osmotic stress responses in *Streptomyces* species). Moreover, BldG is not phosphorylated by either ApgA or UshX (Parashar *et al*., 2009; Sevcikova *et al*., 2010 and 2020; Takano *et al*., 2011); in *S. coelicolor*, this occurs independently as a result of at least six other RsbW (HATPase_c) anti-sigma factors. Of those conserved in *S. venezuelae* only UshX was present in the full data-set, and it was not significantly enriched – but these are quite distal interactions.

By analogy to the *B. subtilis* model (Figure 6.9), at least one RsbU-like phosphatase may also control BldG dephosphorylation and may be an important driver of activity. However, there is a gap in the literature regarding the potential contribution of an RsbU-like phosphatase to the function of BldG and no candidates have been proposed from the many similar proteins in *Streptomyces* spp. Coincidentally, an RsbU phosphatase (vnz_05805) was conspicuously enriched over both CoIP-MS time-points (*fc*: 20.00/60.00, S_0: 1.00, BFDR: 0.00) and connected well with this network. Two other RsbU phosphatases carrying additional domains were enriched during tp2; vnz_23260 (fc: 23.33 S_0: 0.66 BFDR: 0.10) and the conserved vnz_23470 (*fc*: 5.00 S_0: 0.78, *BFDR*: 0.07). In light of these results, it is intriguing that *wblE*, *whiB1* and *whcE* all conserve genomic synteny with *sigH* and *ushX* (*rshA*) in *Streptomyces, Mycobacterium and Corynebacterium* spp. genomes, respectively (WebFLaGs - Appended Figure A.2, see also Section 2.54). These data strongly indicate a connection between WblE and at least one RsbU-like phosphatase in *Streptomyces* spp. which may, in turn, control BldG activity.

A range of other putative phosphate metabolising and signalling enzymes were detected in the WblE CoIP-MS. This includes the vnz_01270 protein, a conserved Phosphotransferase (APH)-like protein that was enriched in the tp1 and tp2 data (*fc*: 19.00/15.00, S_0: 0.98/1.00 *BFDR*: 0.01/0.00).

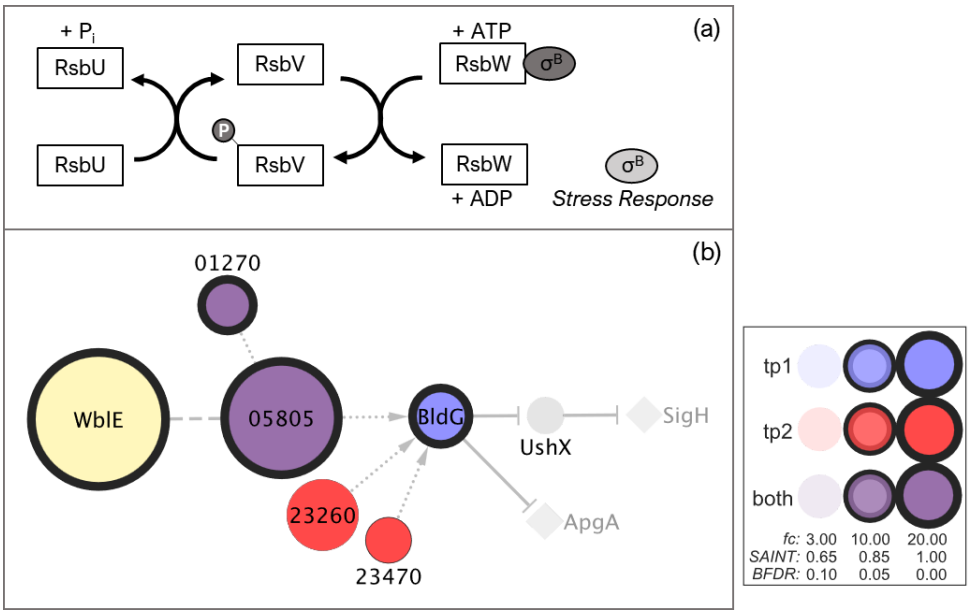

Figure 6.9. (a) The RsbU-RsbV-RsbW phosphotransferase cascade model for induction of group 3 alternative σ-factors. **(b)** The putative RsbU-RsbV(BldG)-RsbW(UshX) network enriched within the CoIP-MS Data. Conserved phosphatase vnz_01270 has been putatively linked to this network. Pointed arrows indicate activating signals, flat-ended arrows indicate repressive signals.

6.3.7. The return of the cell cycle: DNA replication, repair, and topology.

A range of proteins relating to DNA replication and topology were enriched in the CoIP-MS data (Figure 6.10). It is most likely that a significant portion of these proteins precipitated peripherally with WblE due to co-localisation on segments of DNA (Section 6.3).

Machinery associated with chromosomal replication and segregation were significantly enriched, and could potentially be attributed to WblE binding the *dnaA* promoter, which is close to the origin of replication (Chapter 5). This included the DNA polymerase DnaN (vnz_17975; *fc*: 9.33, S_0: 1.00, *BFDR*: 0.00), a ParA paralogue (*fc*: 7.00, S_0: 0.74, *BFDR*: 0.06) and TopA (vnz_16300, fc: 6.00, S0: 1.00, BFDR: 0.00), which are known to participate in chromosome replication and segregation.

The core node of this network was the topoisomerase IV subunit ParE (*fc*: *50.00*, S_0: 1.00, *BFDR*: 0.00) which consistently co-precipitated with its cognate subunit, ParC (*fc*: *17.00*, S_0: 1.00, *BFDR*: 0.00) comprise the. Topoisomerase IV is canonically required for the essential process of separating concatenate chromosomes, following the replication of circular DNA molecules. In *Streptomyces*, however, *parC* and *parE* are non-essential, presumably as the chromosome is linear (Huang *et al*., 2013). Nonetheless, *Streptomyces* spp. transiently circularise their chromosomes and ParCE appears to be necessary for decatenation of these molecules during replication, and it is presumed that ParCE is still redundantly important for the resolution of DNA knots and positive supercoiling (Tsai *et al*., 2011).

Several proteins relating to the nucleotide excision repair pathway of the DDR, including UvrA, UvrB (non-significant), Ung, a putative Rad25-like polymerase and RecQ-helicase were enriched and tentatively linked with this network.

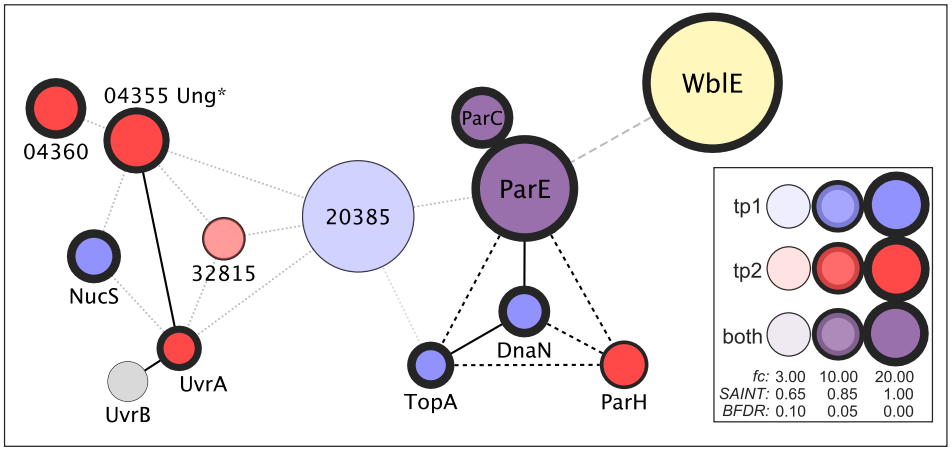

Figure 6.10. WblE CoIP-MS DNA replication, repair and topology network. A key is shown bottom right.

Table 6.1. Significantly enriched Co-IP hits across tp1 and tp2, according to the SAINTexpress pipeline, exceeding a ≥ 3-fold change, ≥ 0.65 SAINTscore and ≥ 0.1 BFDR cutoff. Significant hits are listed in descending order according to their fold change and BFDR. tp1 and tp2 values are separated, but hits which appeared significantly over both time-points are highlighted in blue and are displayed with their tp1 values. The highest associated SAINT score for each hit is depicted in the S_{MAX} column. SignalP6.0 protein secretion predictions are summarised in the 'Exp' column (/ = not secreted).

Prey Locus	Product / Name	fc(tp1)	BFDR(tp1)	fc(tp2)	BFDR(tp2)	S_{Max}	Exp.
WblE							
vnz_24255CF	WblE (-3xCFLAG)	406.67	< 0.005	50.00	0.00	1.00	/
Transcription and Regulation							
vnz_27210	Housekeeping Vegetative Sigma (HrdB)	163.00	< 0.005	5.91	< 0.005	1.00	/
vnz_13335	Superfamily I Helicase (HelD)	160.00	< 0.005	163.00	< 0.005	1.00	/
vnz_04915	RNA Polymerase Binding Protein (RbpA)	106.67	< 0.005	33.33	< 0.005	1.00	/
vnz_07720	RNA Polymerase Binding Protein (RbpB)	36.67	0.01	20.00	0.01	0.98	/
vnz_05230	DNA-directed RNA polymerase subunit omega (RpoZ)	33.33	< 0.005	-	-	0.99	/
vnz_28560	Putative MocR-like transcriptional regulator	33.33	< 0.005	-	-	0.99	/
vnz_31710	Putative RNA-binding Transcriptional Accessory Protein (Tex)	30.00	< 0.005	6.67	0.01	0.99	/
vnz_05140	DeoR-type Transcriptional regulator	20.00	0.09	9.00	0.01	0.65	/
vnz_21470	DNA-directed RNA polymerase subunit beta (RpoB)	11.93	0.00	-	-	1.00	/
vnz_21440	Transcription termination/antitermination factor (NusG)	11.50	0.00	-	-	0.98	/
vnz_21475	DNA-directed RNA polymerase subunit beta' (RpoC)	8.86	0.00	-	-	1.00	/
vnz_22005	DNA-binding response regulator (BldM)	6.50	0.03	-	-	0.83	/
vnz_27115	SOS regulatory protein (LexA)	3.75	0.07	-	-	0.67	/
vnz_21780	DNA-directed RNA polymerase alpha chain (RpoA)	3.13	0.01	-	-	0.96	/
vnz_31840	XRE family transcriptional regulator (HpnR)	-	-	30.00	0.01	0.98	/
vnz_26510	Transcription termination/antitermination protein (NusA)	-	-	13.00	< 0.005	1.00	/
vnz_06010	WYL domain transcription factor (PafB)	-	-	12.00	< 0.005	0.98	/
vnz_06005	WYL domain transcription factor (PafC)	-	-	9.00	0.03	0.86	/
vnz_24760	Transcription termination factor (Rho)	-	-	6.00	0.00	0.99	/
vnz_15020	Putative DeoR-Type Fructose Operon Repressor (FruR)	-	-	3.33	0.09	0.66	/

DNA Replication, Recombination and Repair							
vnz_20385	Rad25-like Superfamily II Helicase	53.33	0.08	-	-	0.67	/
vnz_27225	Topoisomerase IV subunit B (ParE)	50.00	< 0.005	5.33	0.04	1.00	/
vnz_27270	Topoisomerase IV subunit A (ParC)	17.00	< 0.005	4.00	0.04	1.00	/
vnz_24910	Endonuclease	11.00	< 0.005	-	-	1.00	/
vnz_17975	DNA Polymerase III Beta chain (DnaN)	9.33	< 0.005	-	-	1.00	/
vnz_16300	DNA topoisomerase I (TopA)	6.00	< 0.005	-	-	1.00	/
vnz_04355	uracil-DNA glycosylase (Ung)	-	-	20.00	0.01	0.94	/
vnz_06885	Chromosome partitioning ATPase (Soj-like)	-	-	7.00	0.06	0.74	/
vnz_07795	ABC excision nuclease subunit A (UvrA)	-	-	4.00	0.02	0.94	/
vnz_32185	ATP-dependent DNA helicase (RecQ-like)	-	-	3.29	0.07	0.70	/
Cell Wall / Membrane / Envelope Biogenesis							
vnz_04695	Putative Bifunctional Mannose-1-Phosphate Gaunyltransferase / Phosphomannomutase (ManC3)	88.00	< 0.005	-	-	1.00	/
vnz_13620	Phosphomannomutase (ManB)	26.67	0.08	-	-	0.66	/
vnz_13725	UDP-glucose 6-dehydrogenase (Ugd)	20.00	0.10	-	-	0.65	/
vnz_11605	Putative bactoprenol glucosyl transferase	5.50	0.04	-	-	0.77	/
vnz_31470	Sugar Phosphate Isomerase/Epimerase (IolE-like)	-	-	26.67	0.08	0.66	Tat
vnz_12370	2-keto-myo-inositol dehydratase	-	-	20.00	0.01	0.94	/
vnz_25590	Phospholipase C, phosphocholine-specific	-	-	4.19	< 0.005	1.00	Tat
Chaperones, Posttranslational modification, Protein turnover							
vnz_08915	Putative Iron-sulfur cluster insertion protein (ErpA)	66.67	< 0.005	-	-	1.00	/
vnz_11755	Hsp100 AAA+ ATPase Chaperone (ClpX)	44.75	< 0.005	27.00	< 0.005	1.00	/
vnz_27280	Peptidase M16	31.00	< 0.005	-	-	1.00	/
vnz_11415	Molecular chaperone (DnaJ2)	26.67	0.08	7.00	0.06	0.74	/
vnz_06015	Peptidyl-prolyl cis-trans isomerase (FkpB)	20.00	0.10	-	-	0.65	/
vnz_08085	Aminopeptidase N	13.00	< 0.005	-	-	1.00	/
vnz_18395	Xaa-Pro aminopeptidase (PepPI)	6.50	0.01	-	-	0.95	/

vnz_27275	Peptidase M16	6.25	< 0.005	-	-	0.98	/
vnz_06215	Peptidase M20 (Chaplin-neighbouring)	6.20	< 0.005	-	-	0.98	/
vnz_16895	Nucleotide exchange factor (GrpE)	5.00	0.04	-	-	0.75	/
vnz_25065	Trx-domain chaperone (YbbN/CnoX)	4.67	0.03	-	-	0.83	/
vnz_21940	10 kDa co-chaperonin (GroES)	4.33	0.06	-	-	0.70	/
vnz_23230	Alkyl hydroperoxide reductase (AhpC)	4.00	< 0.005	-	-	1.00	/
vnz_11840	Aminopeptidase N	3.86	0.07	-	-	0.70	/
vnz_07630	Fe-S cluster assembly protein (SufD)	3.33	0.07	-	-	0.68	/
vnz_06060	Proteasome AAA ATPase (Arc)	3.44	< 0.005	-	-	1.00	/
vnz_32055	Peptidase S8 (ucf1)	-	-	140.0	< 0.005	1.00	Sec
vnz_14415	Putative peptidase Inhibitor I36 (VCBS repeat domain)	-	-	76.67	< 0.005	1.00	Sec
vnz_29370	Peptidase S8 (ucf6)	-	-	40.00	0.08	0.67	Sec
vnz_26645	Peptidase M16 (associated with pnp)	-	-	36.67	0.08	0.67	/
vnz_32255	GNAT family *N*-Acetyltransferase	-	-	33.33	< 0.005	0.99	/
vnz_31190	acyl-peptide hydrolase S9	-	-	7.00	0.04	0.82	/
vnz_11880	Peptidase S8	-	-	5.70	< 0.005	1.00	Sec
vnz_25255	Peptidase M4 (SgmA)	-	-	5.00	0.04	0.81	Sec
vnz_31670	Xaa-Pro dipeptidyl-peptidase S15	-	-	3.41	< 0.005	0.98	Sec
vnz_17565	Aminopeptidase M18	-	-	3.13	0.10	0.65	/
Translation and RNA Maintenance/Turnover							
vnz_08490	Isoleucyl-tRNA synthetase	40.00	< 0.005	-	-	1.00	/
vnz_14585	Putative ABC-F Family ATPase	30.00	< 0.005	-	-	0.99	/
vnz_16055	tRNA-Ile-lysidine(34) synthetase (TilS)	26.67	0.01	-	-	0.98	/
vnz_05980	HelY-like Superfamily II RNA Helicase	20.00	0.10	32.00	< 0.005	1.00	/
vnz_07295	Putative ABC-F Family ATPase	16.67	0.10	-	-	0.65	/
vnz_25535	Aspartyl/glutamyl-tRNA amidotransferase subunit A (GatA)	11.00	0.01	-	-	0.98	/
vnz_25895	Glutamyl-tRNA synthetase (GltX)	8.43	< 0.005	-	-	1.00	/
vnz_13395	Peptide chain release factor 2 (PrfB)	6.33	0.01	-	-	0.96	/

vnz_17490	Methionyl tRNA synthetase (MetG)	6.00	0.01	-	-	0.98	/
vnz_26680	RNase J family beta-CASP ribonuclease	5.00	0.03	-	-	0.83	/
vnz_11745	Valyl-tRNA synthetase (ValS)	5.00	< 0.005	-	-	1.00	/
vnz_23520	GTP-binding protein (TypA-like)	4.29	< 0.005	-	-	0.99	/
vnz_25545	Aspartyl/glutamyl-tRNA amidotransferase subunit B (GatB)	4.20	0.05			0.74	/
vnz_03805	DEAD/DEAH box helicase	-	-	12.00	< 0.005	0.98	/
vnz_28815	Rnd-like Ribonuclease	-	-	8.00	0.03	0.84	/
vnz_11650	Rne/Rng family ribonuclease	-	-	6.00	0.01	0.95	/
Cytoskeleton							
vnz_08520	Cell division cytoskeletal protein (FtsZ)	20.00	0.01	-	-	0.96	/
vnz_11695	Cytoskeletal, rod-shape determining factor (MreB)	4.00	0.06	-	-	0.72	/
vnz_24955	*Streptomyces* cytoskeletal element (Scy)	-	-	21.00	< 0.005	1.00	/
Fatty Acid Lipid Metabolism							
vnz_25805	Acetyl-coenzyme A carboxyltransferase alpha chain (AccB)	80.00	< 0.005	5.67	0.02	1.00	/
vnz_10795	3-oxoacyl-ACP synthase (FabH)	53.33	< 0.005	-	-	1.00	/
vnz_22720	Propionyl-CoA carboxylase complex B subunit (PccB)	46.67	< 0.005	-	-	1.00	/
vnz_08020	PaaI-like thioesterase	33.33	< 0.005	-	-	0.99	/
vnz_07115	3-oxoacyl-[acyl-carrier-protein] reductase (FabG)	20.00	0.10	-	-	0.65	/
vnz_31635	3-hydroxyacyl-CoA dehydrogenase (FadB2)	11.33	< 0.005	-	-	1.00	/
vnz_13925	Acetyl-CoA C-acyltransferase (FadA1)	11.00	< 0.005	-	-	0.99	/
vnz_31630	Acetyl-CoA C-acyltransferase (FadA2)	6.43	< 0.005	4.40	0.02	0.99	/
vnz_29475	3-oxoacyl-[acyl-carrier-protein] reductase (FabG-like)	6.33	0.02	-	-	0.87	/
vnz_22690	Acyl-CoA carboxylase complex A subunit (AccA1 or AccA2)	5.75	0.01	-	-	0.92	/
vnz_28805	3-hydroxyacyl-CoA dehydrogenase (FadJ-like)	5.20	< 0.005	-	-	0.99	/
vnz_17970	6-phosphogluconate dehydrogenase (decarboxylating)	3.00	0.06	-	-	0.72	/
vnz_07110	Enoyl-(acyl-carrier-protein) reductase (InhA)	2.94	0.03	-	-	0.81	/
vnz_26465	1-hydroxy-2-methyl-2-(E)-butenyl 4-diphosphate synthase (GcpE/IspG)	-	-	17.00	< 0.005	1.00	/
vnz_06325	Acyl-CoA dehydrogenase (FadE2-like)	-	-	3.43	0.07	0.69	/

Phosphate Metabolism and Signalling							
vnz_05805	SpoIIE-like Phosphatase	20.00	0.01	60.00	< 0.005	1.00	/
vnz_10660	TerD-like chemical-damage resistance protein	23.33	0.01	-	-	0.97	/
vnz_16350	Anti-sigma B factor antagonist (BldG)	18.50	< 0.005	-	-	1.00	/
vnz_01270	Phosphotransferase (Proximal to GeoA)	15.00	0.01	10.67	< 0.005	1.00	/
vnz_07530	TerZ-like chemical-damage resistance protein	8.00	0.08	-	-	0.66	/
vnz_23205	PhoH-like ATPase with RNA Helicase/RNase domain	4.79	0.09	-	-	0.66	/
vnz_12260	Putative Phytase	-	-	33.33	0.01	0.98	Sec
vnz_09625	PhoD-like alkaline phosphatase	-	-	29.0	< 0.005	1.00	Tat
vnz_11670	CHAD and phosphatase domain protein	-	-	26.67	0.01	0.97	/
vnz_23260	SpoIIE-domain protein	-	-	23.33	0.10	0.66	/
vnz_23470	PAS & SpoIIE Domain Protein	-	-	5.00	0.07	0.78	/
vnz_08450	PhoD-like alkaline phosphatase	-	-	3.07	0.05	0.78	Tat
Vitamin and Coenzyme Metabolism							
vnz_15365	Aminofutalosine synthase (MqnE)	73.33	< 0.005	12.00	< 0.005	1.00	/
vnz_21020	Putative dehypoxanthine futalosine cyclase (MqnC)	63.33	< 0.005	26.67	< 0.005	0.99	/
vnz_15625	Putative bifunctional uroporphyrinogen-III C-methyltransferase/uroporphyrinogen-III synthase	63.33	< 0.005	9.00	0.02	1.00	/
vnz_15385	Putative menaquinone biosynthesis decarboxylase (MenA-like)	20.00	0.10	-	-	0.65	/
vnz_16865	Putative Pyridoxamine 5'-phosphate oxidase	20.00	0.10	-	-	0.65	/
vnz_26295	Aminotransferase (BioA-like)	13.00	< 0.005	-	-	0.99	/
vnz_19375	Rhodanese / Thiosulfate sulphur transferase (CysA)	6.75	0.01	-	-	0.98	/
vnz_26455	1-deoxy-D-xylulose 5-phosphate reductoisomerase (Dxr)	6.00	0.04	-	-	0.79	/
vnz_09110	Lipoic acid synthetase (LipA)	5.00	0.05	-	-	0.74	/
vnz_20760	Pyridoxamine 5'-phosphate oxidase (PdxH)	4.33	0.04	-	-	0.75	/
vnz_22215	bifunctional methylenetetrahydrofolate dehydrogenase/methenyltetrahydrofolate cyclohydrolase (FolD)	3.83	0.07	-	-	0.69	/
Carbohydrate Metabolism							
vnz_11190	Pyruvate, phosphate dikinase (Ppdk)	40.00	< 0.005	-	-	1.00	/

vnz_07710	Glucose-6-phosphate isomerase (Pgi)	9.00	0.01	-	-	0.95	/
vnz_13330	NAD-Dependent Malic Enzyme	8.25	< 0.005	-	-	1.00	/
vnz_12610	Glucosamine-fructose-6-phosphate aminotransferase, isomerizing (GlmS2)	8.25	< 0.005	-	-	0.99	/
vnz_09035	Pyruvate dehydrogenase E2 component: Dihydrolipoamide acetyltransferase (DlaT)	7.00	0.01	-	-	0.93	/
vnz_10680	Pyruvate dehydrogenase E1 component (AceE)	3.63	0.01	-	-	0.95	/
vnz_12600	Beta-N-acetylhexosaminidase (HexA)	-	-	86.67	< 0.005	1.00	Sec
vnz_06340	DUF1343 (NamZ)	-	-	80.00	< 0.005	1.00	Tat
vnz_33110	Cellulase (GH Family 6)	-	-	53.33	< 0.005	1.00	Sec
vnz_23445	Chitinase (GH Family 18)	-	-	46.67	< 0.005	0.98	Sec
vnz_33225	Putative O-Glycosyl Hydrolyase (Superfamily 30)	-	-	17.00	0.07	0.67	Tat
vnz_08710	N-acetylmuramoyl-L-alanine amidase	-	-	14.00	< 0.005	1.00	Sec
vnz_12475	Putative secreted *N*-acetylglucosaminidase (Hex)	-	-	6.33	0.02	0.87	Tat
vnz_03785	Peptide-N4-asparagine amidase A	-	-	5.10	< 0.005	0.98	Sec
vnz_33230	Endo-1,4-beta-xylanase	-	-	5.00	0.10	0.65	Sec
Nucleotide Metabolism							
vnz_22065	GMP Synthase (GuaA)	76.67	< 0.005	-	-	1.00	/
vnz_18890	Phosphoribosyl formylglycinamidine synthase II (PurL)	9.00	< 0.005	8.00	0.03	0.99	/
vnz_06905	CTP Synthase (PyrG)	8.67	< 0.005	-	-	1.00	/
vnz_26240	Uridylate Kinase (PyrH)	8.33	0.02	-	-	0.83	/
vnz_28145	NUDIX Hydrolase	7.67	0.01	3.30	0.02	0.91	/
vnz_05270	Dihydroorotase (PyrC)	5.50	0.04	-	-	0.77	/
vnz_24115	Ribonucleoside-diphosphate reductase subunit alpha (NrdL)	3.83	< 0.005	-	-	1.00	/
vnz_22190	bifunctional phosphoribosylaminoimidazolecarboxamide formyltransferase/IMP cyclohydrolase (PurH)	3.50	0.02	-	-	0.87	/
vnz_12835	Putative ecto-nucleotide pyrophosphatase	-	-	50.00	< 0.005	0.98	Tat
vnz_34895	Cytosine deaminase	-	-	76.67	< 0.005	1.00	/
Amino Acid Metabolism							
vnz_16610	Putative aspartokinase (Ask)	31.00	< 0.005	-	-	1.00	/

vnz_11585	Gamma-glutamyl phosphate reductase (ProA)	23.33	0.09	-	-	0.65	/
vnz_08845	Phosphoribosylanthranilate transferase (TrpD)	23.33	0.09	-	-	0.65	/
vnz_27060	Diaminopimelate epimerase (DapF)	20.00	0.09	-	-	0.66	/
vnz_08310	Indoleglycerol phosphate synthase (TrpC)	20.00	0.10	-	-	0.65	/
vnz_26450	3-phosphoshikimate 1-carboxyvinyltransferase (AroA)	16.67	0.10	-	-	0.65	/
vnz_24745	Homoserine dehydrogenase (ThrA)	7.50	0.03	30.00	0.01	0.81	/
vnz_24740	Diaminopimelate decarboxylase (LysA)	6.50	0.02	-	-	0.86	/
vnz_15785	Dihydroxy-acid dehydratase	4.12	0.02	-	-	0.89	/
vnz_20550	Phosphoserine aminotransferase	4.00	0.06	-	-	0.71	/
vnz_12505	Putative Agmatinase (SpeB-like)	3.89	0.05	-	-	0.74	/
vnz_24750	Threonine synthase (ThrC)	3.57	< 0.005	-	-	0.99	/
vnz_09440	Glutamine Synthetase (GlnA2)	-	-	33.33	0.01	0.98	/
ABC Transport Machinery							
vnz_34815	Putative Foroxymithine (Fxm) ABC Transporter ATP-binding subunit	50.00	< 0.005	-	-	1.00	/
vnz_30760	SalX-like AMP ABC transporter ATPase component	11.00	0.08	-	-	0.67	/
vnz_07045	Fe/Mn ABC-transport ATPase subunit	6.60	0.01	-	-	0.91	/
vnz_09775	Fe(III)-Siderophore ABC-transport substrate-binding protein	5.33	0.02	-	-	0.88	/
vnz_19250	Phosphate ABC transport system ATP-binding protein (PstB)	4.18	0.02	-	-	0.86	/
vnz_36245	ABC transporter substrate binding protein (UgpB-like)	-	-	36.67	< 0.005	0.99	Sec
vnz_04360	Putative Peptide ABC Transporter (DppA-like)	-	-	16.00	< 0.005	1.00	Sec
Energy Production and Conversion							
vnz_11275	Probable ferredoxin reductase (FprA)	70.00	< 0.005	-	-	1.00	/
vnz_24835	F0:F1 ATP synthase subunit gamma (AtpG)	17.00	< 0.005	-	-	1.00	/
vnz_18275	Luciferase-like F420 Monooxygenase	16.67	0.1	-	-	0.65	/
vnz_22635	Aldehyde dehydrogenase	6.80	< 0.005	-	-	1.00	/
vnz_06130	Aerobic glycerol-3-phosphate dehydrogenase (GlpD-like)	4.00	0.03	8.00	0.03	0.84	/
vnz_14230	FAD-dependent NADH dehydrogenase	4.14	0.06	-	-	0.71	/
vnz_24920	Luciferase-like F420 Monooxygenase	-	-	20.00	0.01	0.94	/

Intracellular Trafficking and Secretion							
vnz_19410	FABP Nitrobindin-like protein	4.50	0.07	-	-	0.67	/
vnz_26610	WXG100 Family Type VII secretion target (EsxA)	3.67	0.09	-	-	0.66	T7S
Secondary Metabolism							
vnz_00795	Putative CoA-transferase	210.00	< 0.005	-	-	1.00	/
vnz_00790	Putative 2,3-dihydroxybenzoate-AMP ligase	33.33	< 0.005	-	-	1.00	/
vnz_04435	Aminodeoxychorismate synthase, component I (Cml Cluster)	26.67	0.09	-	-	0.65	/
vnz_04470	Adenylate synthase (Cml Cluster)	12.25	< 0.005	-	-	1.00	/
vnz_34820	Putative amidohydrolase (Fxm cluster)	12.00	< 0.005	-	-	0.98	/
vnz_04480	Aldo/keto reductase (Cml Cluster)	6.20	0.02	-	-	0.89	/
vnz_27515	Putative Isoprene Cyclase Class II protein	-	-	19.00	0.02	0.88	/
vnz_00800	Putative FadE2-like Acyl-CoA dehydrogenase	-	-	7.00	0.06	0.74	/
vnz_27095	Putative lucA-like Siderophore synthetase (BGC 20)	-	-	7.00	0.06	0.74	/
vnz_04445	Chloramphenicol non-ribosomal peptide synthetase (CmlP)	-	-	6.08	0.02	0.92	/
General Prediction, Unknown Function, Hypothetical Proteins							
vnz_07310	Hypothetical	291.00	< 0.005	23.50	23.50	1.00	/
vnz_13250	Hypothetical	43.33	< 0.005	-	-	1.00	/
vnz_05365	Hypothetical (DUF3903: possible ATPase)	33.33	< 0.005	-	-	0.99	/
vnz_02720	Hypothetical (DUF4097)	30.00	< 0.005	6.50	0.02	0.99	/
vnz_27400	Hypothetical	20.00	0.10	-	-	0.65	/
vnz_28415	Hypothetical	16.67	0.10	4.67	0.05	0.65	/
vnz_15555	Short-chain oxidoreductase	10.50	0.02	-	-	0.89	/
vnz_28410	Hypothetical	10.00	0.01	-	-	0.94	/
vnz_32045	Hypothetical	10.00	0.01	-	-	0.96	/
vnz_01845	Carbonic anhydrase	3.60	0.01	-	-	0.91	/
vnz_05400	Hypothetical	2.92	0.05	-	-	0.74	/
vnz_09020	Hypothetical	-	-	73.33	< 0.005	1.00	Sec
vnz_35985	Putative alpha/beta hydrolase	-	-	46.67	< 0.005	1.00	Sec

vnz_21145	Hypothetical	-	-	46.67	< 0.005	1.00	Sec
vnz_25245	Hypothetical (RHS repeat protein)	-	-	43.33	< 0.005	0.99	Sec
vnz_03525	Hypothetical (LVIVD domain; choice-of-anchor B domain)	-	-	40.00	< 0.005	0.98	Sec
vnz_14310	Putative AmpC-like beta-lactamase hydrolase	-	-	36.67	< 0.005	0.98	Sec
vnz_17810	Hypothetical (DUF2252)	-	-	26.67	0.08	0.67	/
vnz_06345	Putative erythromycin esterase	-	-	23.33	0.08	0.66	Sec
vnz_00220	Hypothetical	-	-	22.00	< 0.005	1.00	Sec
vnz_35330	Hypothetical	-	-	17.00	< 0.005	1.00	Sec
vnz_09100	Hypothetical	-	-	14.50	< 0.005	0.99	/
vnz_28340	Hypothetical (COG1479; DUF1524; DNA transferase)	-	-	10.50	< 0.005	0.96	/
vnz_01435	Putative Hydrolase	-	-	10.50	0.01	0.95	Tat
vnz_19015	Hypothetical (VCBS repeat domain)	-	-	10.00	< 0.005	1.00	Sec
vnz_14535	Hypothetical (VCBS repeat domain)	-	-	9.50	0.03	0.86	Sec
pvnz_37465	Hypothetical (VCBS repeat domain)	-	-	8.50	< 0.005	0.98	Sec
vnz_17590	Hypothetical (LURP-1 like; COG4894)	-	-	8.00	0.03	0.84	/
vnz_35450	Hypothetical (Heparinase-like domain)	-	-	6.00	0.05	0.80	/
vnz_36080	Putative alpha/beta hydrolase (MhpC-like)	-	-	6.00	0.05	0.80	/
vnz_02915	Hypothetical (MAEBL-like domain)	-	-	5.55	< 0.005	1.00	Sec
vnz_32465	Hypothetical	-	-	5.33	0.04	0.84	/
vnz_10320	Hypothetical (DUF891)	-	-	5.00	0.09	0.66	/
vnz_08065	Hypothetical (SIMPL domain)	-	-	4.50	0.02	0.90	/
vnz_32075	Hypothetical (RHS repeat protein)	-	-	4.67	0.10	0.65	/
vnz_03780	Oxidoreductase (Gfo/Idh/MocA Family)	-	-	4.46	< 0.005	1.00	Tat
vnz_29175	Hypothetical	-	-	4.40	0.05	0.79	Sec
vnz_28935	Hypothetical	-	-	4.00	0.02	0.94	/
vnz_01385	Putative penicillin amidase	-	-	3.33	0.05	0.76	Sec

6.4. Confirming WblE Interactions via Bacterial Two-Hybrid Analysis

In this chapter, Co-IP identified a strikingly large (albeit putative) WblE-interactome of over 200 proteins, within *S. venezuelae* NRRL B-65542, many of which are entirely novel to WhiB-like biochemistry. Of these, 28 were pulled down in both experimental timepoints. Henceforth, it became a necessity to try and confirm if these proteins were true physical interactions. To test this, pairwise interactions between WblE and several putative partners and related controls from the dataset were probed with an adenylate cyclase based bacterial two-hybrid (B2H) assay.

Adenylate cyclase enzymes catalyse the synthesis of cAMP, a potent nucleotide secondary messenger with roles in diverse signal transduction pathways. The human pathogen, *Bordetella pertussis*, employs an Adenylate Cyclase (CyaA) toxin to hijack intracellular signalling (Cerny *et al.*, 2015). The CyaA toxin constitutes two domains, denoted T18 and T25, which function cooperatively to rapidly synthesise cAMP from ATP, however, physically separated subunits cannot self-assemble and are unable to synthesise cAMP. However, interacting proteins fused to either subunit can spatially complement the enzyme's activity (Karimova *et al.*, 1998, 2000). The Euromedex™ BAC2H system exploits this bipartite and modular architecture, within an adenylate cyclase deficient (*cya*$^{-}$) *E. coli* host e.g. strain BTH101 (see Appendix A.5).

In *E. coli*, cAMP allosterically regulates the Catabolite Activator Protein (CAP/CRP) which functions as a transcriptional activator of the *lac* (lactose) and *mal* (maltose) catabolic genes. Assuming an interaction between the 'Bait' (T18) and 'Prey' (T25) fusions, reconstituted CyaA activity and subsequent CAP-mediated activation of the *lacZ* gene (β-galactosidase) can be qualified by various β-galactosidase assays. The work in this thesis used M63 Minimal Medium, supplemented with 0.3% w/v Maltose (≥ 99.9%) and the lactose-analogue indole dye, X-Gal (5-bromo-4-chloro-3-indolyl-β-D-galactopyranoside). On this medium, growth and X-Gal staining are dependent on the reconstitution of cAMP synthesis and can provide less ambiguous results compared to growth permitting media such as LB + X-Gal.

The BAC2H system delivers the T18 & T25 subunits on two sets of replication compatible vectors, carrying either a 5' (N-terminal) or 3'- (C-terminal) multiple cloning site, allowing the generation of in-frame fusions within each subunit's coding sequence, and subsequent co-transformation to generate up to four possible plasmid (and fusion protein) combinations (See Figure 6.13). Nevertheless, testing all putative targets identified by Co-IP, in all combinations, was not feasible. Instead several of the most significant and highly enriched proteins were selected for further analysis, including WblE itself, the canonical partner HrdB, as well as the hypothetical protein vnz_07310, ClpX, MqnC, Scy. In addition, MtrA – an important metabolic and developmental regulator which directly binds the *wblE* promoter (Section 5.5.3, Som *et al.*,

2017a & 2017b), was present in the Co-IP data but fell below the BFDR significance cut-off (BFDR = 0.27); this protein was also tested as control.

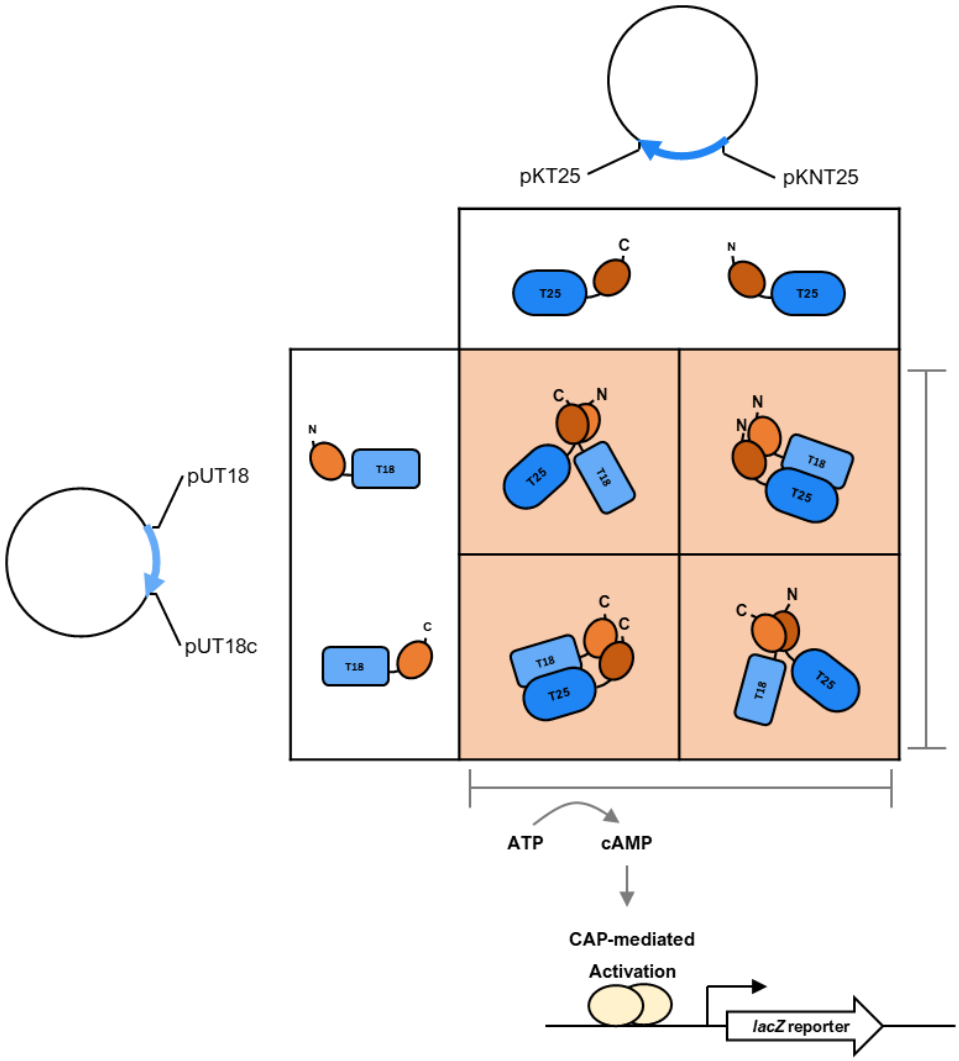

Figure 6.13. A basic scheme for the position of multiple cloning sites in the *cyaA* genes of pK(N)T25 (top) and pUT18(c) (left) and cartoon representations of their theoretical fusion products (prey and bait in orange). Four potential combinations arise from the two plasmid pairs which can reconstitute cAMP synthesis, if prey and bait physically interact, and induce CAP-dependent activation of the *lacZ* reporter gene.

6.4.1. WblE interacts with itself and HrdB in optimised bacterial two hybrid assays

The *hrdB* (region 4.2), *wblE*, *scy*, *mtrA* genes were codon optimized, cloned into the full BAC2H vector set and co-transformed into *E. coli* BTH101 in all possible combinations (Figure 6.13). This 'optimised' set of strains were run together with each inoculum normalised to an OD_{600} of 0.1 and washed in M63 to remove residual LB medium which may permit growth. Strains BTHLB4, BTHLB10, BTHLB16 and BTHLB22 (WblE:HrdB) and strains BTHLB2, BTHLB7 (WblE:WblE) demonstrated robust growth and blue staining comparable to that of the positive control. However, no growth or staining was observed for fusions of MtrA or Scy (not shown). A single false-positive result was obtained for *E. coli* strain BTHF11 between HrdB and T18, however this demonstrably had no effect on any of the positive results (Figure 6.14.a).

6.4.2. WblE interacts with vnz_07310 in 'crude' bacterial two hybrid assays

In contrast to the 'optimized' group, *mqnC,* and *clpX* were cloned as their full-length, native sequences from the *S. venezuelae* genome and co-transformed with codon optimised *wblE* plasmids. The *vnz_07310* locus presented an incredibly difficult gene to clone, likely owing to its near 80% GC ratio. As such, the gene was split into two separate N- and C-terminal sequences. Due to time constraints, these genes were only tested within a limited set of vector combinations (Figure 6.14.b). Moreover, these runs were performed at 22^{o}C to promote the stability of fusion-proteins. The strains from the first assay were run to control for temperature-based effects on growth/mutagenesis. The results show a clear indication of interaction between WblE and the N-terminus of vnz_07310, with a weaker responses from the C-terminal portion, highlighting this protein as a novel partner for WblE. Processing of the raw (binary) data with SAINT*express* was a necessity for the identification of vnz_07310, but not σ^{HrdB}, demonstrating that significant noise can obscure legitimate results in *Streptomyces* spp. CoIP-MS experiments. A similarly weak result was regularly observed against full length MqnC, compared to the negative control and associated false-positive controls. Intriguingly, no growth or staining was observed for ClpX (not shown) despite ClpP1 being identified as a necessary protein for degrading WhiB1 in *Mycobacterium* spp. (Raju *et al*., 2014; d'Andrea *et al*., 2022). Occasionally ClpX requires adaptors to interact with lower affinity substrate proteins and it cannot be ruled out that an adaptor is required for the interaction between ClpX and WblE. Alternatively, endogenous *E. coli* ClpP complexes could have degraded WblE, weakening the BTH response.

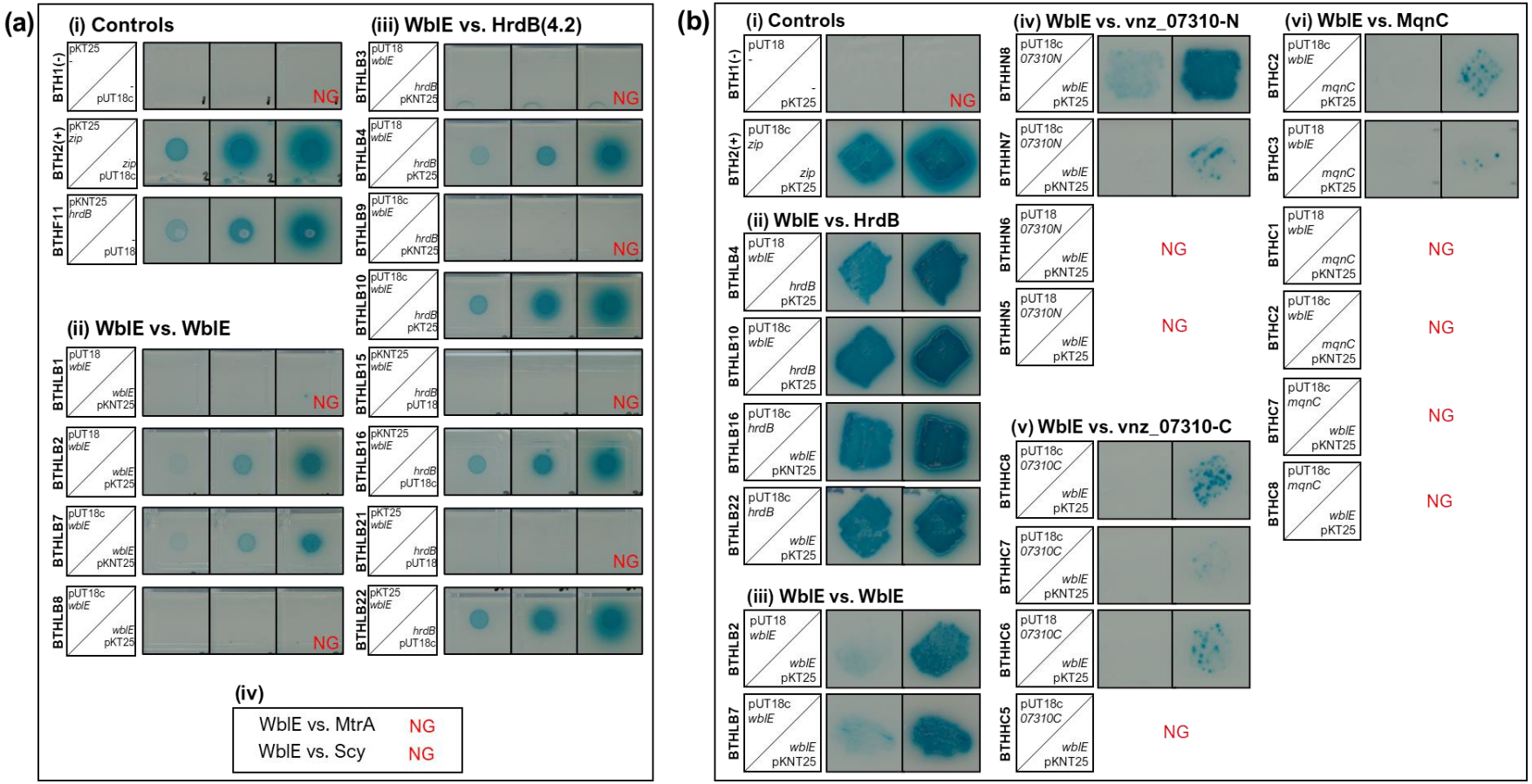

Figure 6.14. **(a)** Optimised Blue-White BAC2H growth assays on M63 medium at 30°C. **(i)** control strains and HrdB false positive BTHF11 **(ii)** WblE:WblE and **(iii)** WblE:HrdB region 4.2. **(iv)** WblE:MtrA and WblE:Scy assays. Growth visualised over 3 days. **(b)** Non-optimised Blue-White BAC2H assays on M63 media at 22°C showing **(i)** Controls; **(ii)** positive WblE:HrdB strains; **(iii)** positive WblE:WblE strains; **(iv & v)** test strains for WblE vs vnz_07310 N-terminal and C-terminal portions, respectively; **(vi)** test strains for WblE vs MqnC. Growth visualised at 3 days and 5 days. Growth comparable to negative controls or associated false positives controls has been marked as 'NG'. Each row shows strain names and respective plasmid combinations in the box (See also Table A.5).

6.5. Discussion

Protein-protein interactions underpin the functions of the WhiB-like protein family; this chapter explored the possibility that WblE may contribute to similar, and possibly diverse, interactions in the cell via 3xFLAG-tagged WblE CoIP-MS (CoIP-MS) and analysis of the data with SAINT*express*. The three most highly ranked proteins identified by CoIP-MS were the WblE-3xFLAG bait, (vnz_24255 – rank 1), the conserved hypothetical protein vnz_07310 (rank 2), and the sigma factor HrdB (vnz_27210 – rank 3), which were each subsequently confirmed as *bona fide* interactors by positive results in bacterial two hybrid assays. A vast potential WblE interactome was identified with high significance and individual hits were subsequently sorted into functional groups and, where possible, developed into networks based on interdependent function and known/expected interactions. Among these were networks relating to transcription, proteostasis (translation, chaperones, proteases), metallocofactor synthesis (Fe-S, Haem), terpene and fatty acid lipid metabolism. Gene products associated with 'bald' developmental decisions and signals dominated in terms of number of hits and their respective significance.

It is important to note that CoIP-MS experiments are prone to generating obtuse results due to highly interconnected interaction networks and complexes which form in the cell; for example, the interacting components of the RNA Polymerase complex are likely to co-exist in datasets, hence putative interactions which lack further characterisation by alternative methods, such as B2H, remain speculative and further work is vital to determine their legitimacy.

6.5.1. Insights into WblE-containing transcription complexes and ˙NO-sensing *in vivo*

The [4Fe-4S] dependent interaction between Wbl proteins and the primary sigma factor σ^{HrdB} (σ^{A}) is well established across multiple actinobacteria genera and is central to their function as DNA-binding transcription factors. With respect to this, WblE CoIP-MS revealed a snapshot of a complete transcription complex ($\alpha_2\beta\beta'\omega$) that is likely associated with the WblE:σ^{hrdB} subcomplex, including significant enrichment of the auxiliary transcription factors RbpA, which binds the σ-factor simultaneously with Wbl proteins, and (the previously unreported) RbpB. Multiple known (BldM, HpnR, PafBC, FruR, vnz_05140) or putative (vnz_28560) regulators were significantly enriched in the WblE CoIP-MS. In the case of WhiB, the co-occuring [4Fe-4S]-dependent interaction with WhiA is requisite for WhiB DNA-binding and co-regulation of their shared regulon (Bush *et al*., 2016; Lilic *et al*., 2023). Most notably, WblE ChIP-seq demonstrated that three *bona fide* BldM target promoters are shared with WblE. It seems likely, therefore, that these regulators interact with WblE to direct binding and transcription of a subset of genes, analogous to WhiA and WhiB. These data will undoubtedly prove useful for future structural and functional studies of WblE.

Previous work has demonstrated that the interaction with the primary σ-factor protects the WhiB, WhiD, WhiB1 and WhiB3 Fe-S clusters from oxygen-based degradation, *in vitro*, alluding to a potential role as specific •NO sensor-regulators via their iron-sulphur cluster (Wan *et al*., 2020; Stewart *et al*., 2021; Lilic *et al*., 2023). Consistent with a similar role for WblE as an •NO sensor, *in vivo*, WblE co-precipitated with Nitrobindin, a specific •NO scavenging, trafficking and detoxifying haemoprotein (Nbn – Section 6.3.4.2). The role for Nbn in remains largely speculative *Streptomyces* spp. but is derived from work on *M. tuberculosis* and *H. sapiens* homologues which, despite their domain-spanning divergence, exhibit analogous activity *in vitro* (De Simone *et al*., 2020a & 2020b). By contrast, other antioxidant proteins present in the data were far below significance in all replicates (not shown). The prospect of a specialised role for Nbn in modulating nitrosylation of Wbl proteins is supported by their co-evolution in Actinobacteria (Chandra & Chater, 2014).

6.5.2. The Potential for Novel WhiB-like [4Fe-4S] Electrochemistry

In the available literature, the WhiB-like [4Fe-4S] clusters are generally considered sensory and structural cofactors, with little to no evidence for roles in electron transport. For this reason, the strong and significant enrichment of a probable NADPH:ferredoxin oxidoreductase (vnz_11275), homologous to the novel (adrenodoxin reductase-like) FprA of *Mycobacterium* spp., was surprising. The FprA flavoenzyme catalyses the $1e^-$ reduction of cognate ferredoxins for transfer to cognate cytochrome P450 systems in this organism but remains unstudied in *Streptomyces* spp. However, as previously mentioned, no potential cognate ferredoxin, ferredoxin-like or flavodoxin-like proteins encoded by *S. venezuelae* were present in the CoIP-MS datasets which suggests that WblE [4Fe-4S] may contribute to a non-canonical electron transport pathway, *in vivo*.

Two of the core proteins of the CoIP-MS dataset were the radical SAM (rSAM) [4Fe-4S] enzymes MqnC (vnz_21020) and MqnE (vnz_15365) which function in the synthesis of the membrane-bound respiratory electron shuttle menaquinone (MQN) and a weak interaction between WblE and MqnC was indicated by B2H, suggesting that these proteins may comprise a cognate electron transport pathway for this proposed novel function (Cooper *et al*., 2013; Mahanta *et al*., 2013). The catalytic cycle of all rSAM enzymes requires the reduction of the iron-sulphur cluster from the catalytically inactive $[4Fe\text{-}4S]^{2+}$ to the active $[4Fe\text{-}4S]^{1+}$ state, which is necessary for the reductive cleavage of SAM to the 5'-deoxyadenosyl radical (5'-dAdo•). It has been postulated that specialised rSAM electron transfer systems are likely widespread in order to accommodate the diverse functions, surface topologies and evolutionary divergence of these enzymes and this is reflected in the emerging literature (Knappe *et al*., 1969; Bruender *et al*., 2015; Eastman *et al*.,

2023; Brimberry *et al*., 2023). The *T. maritima* tRNA-modifying rSAM enzyme MiaB, for example, is activated *in vitro* by endogenous [4Fe-4S] ferredoxins, with the reducing electron ultimately derived from the cognate TM1639-TM1640 NADPH:ferredoxin-oxidoreductase (Arcinas *et al*., 2019). Previous work with reconstituted holo-WhiD, holo-WhiB3 and holo-WhiB1 has demonstrated that the clusters can undergo 2+ to 1+ chemical reduction, however, native (as-purified) holo-WhiD is resistant to chemical reduction, indicating a highly reductive redox potential (– 460mV or less) that would suit a ferredoxin like role (Jakimowicz *et al*., 2005; Singh *et al*., 2007; Crack *et al*., 2009; Smith, 2012). Nonetheless, investigations into the electrochemistry and redox potential of Wbl [4Fe-4S] clusters, especially WblE, are lacking and the interpretation of these results remains highly speculative. The identification of potential redox partners in this CoIP-MS experiment will allow a more direct analysis of these characteristics with WblE *in vitro*, which, if legitimate, could ultimately shift the paradigm of WhiB-like function.

So far, all work on holo-Wbl proteins has relied upon reconstitution of the cluster via non-physiological approaches which, as discussed above, have been shown to measurably effect cluster electrochemistry, and their reactions with both $^{\bullet}NO$ and O_2 (Crack *et al*., 2009). Otherwise, strenuous anaerobic purification methods and storage are required to capture native conformations and dynamics (Stewart *et al*., 2020). The possibility that the A-type carrier, ErpA, can facilitate WblE cluster biogenesis may offer a potential surrogate for reconstitution and subsequent transfer to Wbl proteins via a more biologically relevant route, that implores further investigation.

6.5.3. Is WblE Phosphorylated *in vivo*?

Phosphorylation is a common and reversible PTM employed to control the protein function and activity, including transcriptional regulators; the best documented examples of this in prokaryotes is the PTM of response-regulators by cognate sensor kinases in two-component systems (e.g. MtrA or AbrC3). Evidence already exists for phosphorylation of WhiB2, the mycobacterial WhiB homologue; the effect of phosphorylation on WhiB2 DNA-binding has not been explored but this modification may be vital for its proposed chaperone-like activity (Konar *et al*., 2012). Thus, the prospect for WhiB-like phosphorylation exists, although its importance is poorly studied, and potential *in vivo* phosphorylation mechanisms have not been proposed.

In this this work, WblE consistently co-precipitated with an aminoglycoside phosphotransferase (APH)-like protein (vnz_01270) which could potentially phosphorylate WblE to modulate aspects of its function. While APHs are considered antibiotic phosphotransferases, the three-dimensional structures of APHs are strikingly similar to those of eukaryotic protein Ser/Thr kinases (EPKs) and are sensitive to EPK inhibitors, ultimately indicating a similar enzymatic mechanism (Daigle

et al., 1998). Indeed, APH enzymes are capable of phosphorylating EPK substrates, *in vitro*, albeit exclusively on serine residues (Daigle *et al*., 1998). It is possible, therefore, that vnz_01270 represents a protein kinase which phosphorylates WblE on one or multiple of its serine residues, which are positioned by the C-terminal domain and GVWGG motifs, to modulate function.

Chapter 7.

A Broadening Horizon for Wbl Research: General Discussion, Conclusions and Future Work

7.1. Summary

The overarching aim of this doctoral work was to characterise the WhiB-like *wblE* gene and the function of its product, in the model organism *S. venezuelae* NRRL B-65442. In general, the WhiB-like family have emerged as unique [4Fe-4S]-binding transcription factors which control vital cellular processes in Actinobacteria, via a conserved interaction with the primary σ-factor. However, prior to the inception of this project, no work had directly characterised *wblE* in *Streptomyces* spp. hence these characteristics remained speculative.

Consistent with the WhiB-like paradigm, this work has demonstrated that WblE binds a [4Fe-4S]$^{2+}$ cluster, *in vitro*. An engineered pCRISPomyces-2 CRISPR-Cas9 platform was utilised to confirm the hypothesis that the *wblE* (*vnz_24255*) gene and its product, including all four cluster-ligating cysteines, are essential in *S. venezuelae* NRRL B-65442. Nevertheless, several residues were also shown to be dispensable for function.

WblE-3xCFLAG ChIP-seq experiments confirmed that WblE likely functions as a global DNA-binding transcription factor that binds with an 8 bp motif (AAACGGAT) that is often adjacent to -35 bp sites, consistent with an interaction with σ^{HrdB}. The promoters of a range of stable RNA and asRNA genes dominated the data. Intriguingly, WblE also bound the promoter of the cell-cycle initiator *dnaA* and its own promoter, *in vivo* and *in vitro*. Putative developmental targets indicate that WblE controls primarily '*bld'* developmental decisions.

Subsequent WblE-3xCFLAG CoIP-MS experiments provided the first snapshot of the protein environment associated with a Wbl protein, *in vivo*. Guided by the CoIP-MS data, bacterial two-hybrid assays confirmed interactions between WblE and σ^{HrdB} (as anticipated), itself, and the novel protein vnz_07310. Proteins that were previously only presumed to cooperate with WblE were also identified, such as iron-sulphur biogenesis machinery and nitrobindin, providing vital cellular context to WblE and insights into dynamics of the [4Fe-4S] cluster.

7.2. Towards an Understanding of *wblE* Essentiality in *Streptomyces* spp.

A key question remains, regarding *wblE* and its homologues in *Streptomyces* spp: What is responsible for the product's essentiality?

As previously discussed in Chapter 5, the essentiality of *wblE* may stem from its ability to bind and activate expression of the essential gene, *dnaA*, the initiator of chromosomal DNA replication. Nonetheless, WblE also globally associated with the promoters of stable RNAs, ribosomal proteins, core subunits of the RNA polymerase, respiration and central carbon metabolism; widescale dysregulation of the transcription of these genes, via the deletion of *wblE*, could also potentially elicit a lethal phenotype. Nevertheless, WblE also regularly co-precipitated with multiple, presumably essential, proteins involved in respiration (HemD, MqnC, MqnE, FprA) and lipid metabolism (AccB), and may play vital post-translational roles in the quality control or function of these proteins. Indeed, interactions beyond the RNA polymerase have been reported previously but are poorly understood.

Future work should generate conditional *wblE* knockdowns using an inducible promoter or dCas9-mediated gene-silencing, to overcome the lethality associated with the Δ*wblE* phenotype, and enable subsequent transcriptomic and proteomic analyses to quantify global cellular changes associated with the abrogation of *wblE* expression. Significant changes can then be compared with the ChIP-seq and CoIP-MS data to pinpoint overlapping, putatively essential functions for more specific analyses.

7.3. Exploring Complex Potential Functions for WblE in Transcriptional Complexes

A range of potential co-regulators were identified in the CoIP-MS, which may interact with WblE in transcription complexes (Chapter 6). To date, such an interaction has only been demonstrated for WhiB and WhiA but this may imply broader conservation of this characteristic.

As stated by Prof. Mark Buttner (personal communications) this behaviour is reminiscent of the general transcription factors (GTFs) of eukaryotes which orchestrate the formation of multipartite pre-transcriptional complexes to contact distal genetic (enhancer) elements that are not limited to promoter regions and tightly regulate transcriptional initiation (Panigrahi & O'Malley, 2021). Studying these interactions could unveil a similar paradigm for actinobacterial transcription complexes which may contribute to the cryptic nature of certain BGCs.

Attempts at generating Cryo-EM structures of the RNA polymerase in complex with BldM and WblE at their shared promoters could help clarify this. However, with the exception of BldM (Al-Bassam *et al*., 2014), no putative regulatory targets have been identified for regulators identified in the CoIP-MS. Additional ChIP-seq experiments could be performed to ascertain a broader

range of promoters which potentially rely upon this unique mechanism of prokaryotic transcription initiation. *In vitro* transcription assays could help clarify how RNA polymerase in complex with WblE affects the transcription of specific genes at target genes in the presence or absence of these putative co-regulators.

7.4. The WhiB-like [4Fe-4S] Cluster Conundrum

It has been 20 years since Wbl proteins were shown to bind Fe-S clusters. However, our understanding of the dynamics of Wbl clusters is lacking. It has become widely accepted that Wbl Fe-S clusters are likely to act primarily as sensory/structural cofactors. However, the enrichment of FprA challenged this paradigm (Chapter 6.3.4.1), suggesting that Wbl clusters can be reduced akin to ferredoxins. It is of utmost importance to experimentally determine this fact as it could vastly expand the function of this protein family. A property of $[4Fe\text{-}4S]^{2+}$ clusters is that they are diamagnetic (S = 0) and yield silent electron paramagnetic resonance (EPR) spectra. Conversely, reduced $[4Fe\text{-}4S]^{1+}$ clusters are paramagnetic (S = ½) and yield distinct EPR spectra. Hence, the hypothesis that holo-WblE is reduced by the activity of FprA could be tested *in vitro* by incubating the purified proteins in the presence of NADPH and assessing EPR spectra compared to a control sample without FprA and NADPH. It may also be possible to demonstrate an interaction between WblE and FprA in the B2H assays, such as those used in this thesis.

In the same way that nitric oxide mediated [4Fe-4S]-nitrosylation is an important regulatory signal for WhiB-like function, cluster incorporation is hypothesised to be foundational for these signalling pathways *in vivo*. However it has still not been ascertained how Wbl proteins receive their cluster. This work demonstrates that Wbl proteins may not receive their cluster directly from the Suf apparatus (SufD), as would be presumed. The possibility that the A-type carrier, ErpA, can facilitate WblE cluster biogenesis offers a potential surrogate for reconstitution and subsequent transfer to Wbl proteins via a more biologically relevant route *in vitro*. So far, all work on holo-Wbl proteins has relied upon reconstitution of the cluster via non-physiological approaches which, as discussed above, have been shown to measurably effect cluster electrochemistry, and their reactions with both $^{\bullet}NO$ and O_2 (Crack *et al*., 2009). Otherwise, strenuous anaerobic purification methods and storage are required to capture native conformations and dynamics (Stewart *et al*., 2020). Assessments of interactions between these proteins in bacterial two hybrid and *in vitro* assessment of transfer between holo-ErpA and apo-WblE should form the foundation of this branch of Wbl research.

7.5. Exploring a Function for WblE and vnz_07310 within *Streptomyces* PPS

The vnz_07310 protein is novel to WhiB-like biochemistry and has only appeared transiently in a single PhD thesis and scientific publication to date (Xu *et al*., 2017; Al-Tarawni, 2019). C-I-TASSER predicted unprecedented structural homology between vnz_07310 (and SGR5650) to the RPN1 ubiquitin receptor, an essential component of the eukaryotic ubiquitin proteasome system (UPS). Although largely absent from eubacteria, Actinobacteria carry an evolutionarily distinct but analogous system, the prokaryotic ubiquitin-like protein (Pup) proteasome system (PPS). The PPS is vital for overcoming Nitrosative-stress in *Mycobacterium* spp. and in the analogous Eukaryotic systems, hence, it is an attractive proposition that an •NO-sensing [4Fe-4S] protein interacts with a putative Pup-receptor and contributes to the PPS.

From the work performed in thesis, it was not possible to ascertain whether WblE interacts with vnz_07310 in its apo- or holo-form which provides direction for future research into this interaction. This could be achieved through *in vitro* purification and biochemical analysis of the complex as well as mutagenesis of WblE Cys residues to assess the effect on the interaction. Work by Konar *et al*., (2012) previously proposed *in vitro* chaperone-like activity for apo-WhiB2, suggesting that WhiB2 acts as a novel small heat shock protein (smHSP). A similar function for WblE may be linked to a role in the PPS, and the broad range enrichment of proteins in the CoIP-MS data beyond transcription, including the aggregation-prone luciferase and rhodanese-like proteins. Notably, WhiB regulates the *pafA2* Pup-ligase with WhiA and provides precedent for such a function in *S. venezuelae*.

Investigations into the *Streptomyces* spp. PPS systems are still in their infancy and no work has yet investigated pupylation targets in *S. venezuelae*. However, comparison of Pup-targets assigned in *S. coelicolor* and *Mycobacterium* spp. (Compton *et al*., 2015; Boubakri *et al*., 2015) with the CoIP-MS data revealed a surprising number of homologues in *S. venezuelae* that are distributed broadly throughout the significant hits. These circumstantial observations indicate a role for vnz_07310 as a Pup-binding protein, analogous to RPN1, but more direct analysis of vnz_07310 via knockouts, CoIP-MS and bacterial two hybrid analysis between vnz_07310 and Pup (vnz_06025), could help determine whether it truly functions within the PPS and generate a more definitive description of its role.

7.6. Closing Statement

In closing, this work has offered the first insight into the functions of the essential WhiB-like regulator, WblE, in *Streptomyces*. The gene fits the WhiB-like paradigm whereby it binds a [4Fe-4S] cluster and functions as a global regulator, at least in part via a [4Fe-4S]-dependent complex with the primary sigma factor. Nevertheless, WblE has additional cellular partners which indicates roles beyond transcription and our current understanding. It is hoped that the findings and speculations of this thesis will inspire future research and discoveries, especially for homologues present in key pathogens such as Rv3219 (WhiB1) of *Mycobacterium tuberculosis*.

Chapter 8.

References

Adefisayo O.O., Dupuy P., Nautiyal A., Bean J.M., Glickman M.S., (2021) Division of labor between SOS and PafBC in mycobacterial DNA repair and mutagenesis. *Nucleic Acids Research*. Vol.49(22):12805-12819 https://doi.org/10.1093/nar/gkab1169

Aínsa J.A., Parry H.D., Chater K.F., (1999). A response regulator-like protein that functions at an intermediate stage of sporulation in *Streptomyces coelicolor* A3(2). *Molecular Microbiology*. Vol.34(3):607-619 https://doi.org/10.1046/j.1365-2958.1999.01630.x

Aínsa J.A., Ryding N.J., Hartley N., Findlay K.C., Bruton C.J., Chater K.F., (2000) WhiA, a protein of unknown function conserved among Gram-positive bacteria, is essential for sporulation in *Streptomyces coelicolor* A3(2). J Bacteriol 182: 5470–5478. https://doi.org/10.1128/JB.182.19.5470-5478.2000

Akanuma G., Hara H., Ohnishi Y., Horinouchi S., (2009). Dynamic changes in the extracellular proteome caused by absence of a pleiotropic regulator AdpA in *Streptomyces griseus*. *Molecular microbiology*. Vol.73(5):898-912 https://doi.org/10.1111/j.1365-2958.2009.06814.x

Alam S., Agrawal P., (2008). Matrix-assisted refolding and redox properties of WhiB3/Rv3416 of *Mycobacterium tuberculosis* H37Rv. *Protein Expression and Purification.* Vol.61(1):83-91 https://doi.org/10.1016/j.pep.2008.04.010

Alam S., Garg S.K., Agrawal P., (2007). Molecular function of WhiB4/Rv3681c of *Mycobacterium tuberculosis* H37Rv: a [4Fe−4S] cluster co-ordinating protein disulphide reductase. *Molecular Microbiology*. Vol.63(5):1414-1431 https://doi.org/10.1111/j.1365-2958.2007.05589.x

Alam S., Garg S.K., Agrawal P., (2009). Studies on structural and functional divergence among seven WhiB proteins of *Mycobacterium tuberculosis* H37Rv. *The FEBS Journal*. Vol.276(1):7693 https://doi.org/10.1111/j.1742-4658.2008.06755.x

Al-Bassam M.M., Bibb M.J., Bush M.J., Chandra G., Buttner M.J., (2014) Response regulator heterodimer formation controls a key stage in *Streptomyces* development. *PLOS Genetics*. Vol.10(8):e1004554 https://doi.org/10.1371/journal.pgen.1004554

Al-Bassam M.M., Haist J., Neumann S.A., Lindenberg S., Tschowri N., (2018). Expression Patterns, Genomic Conservation and Input Into Developmental Regulation of the GGDEF/EAL/HD-GYP Domain Proteins in *Streptomyces*. *Frontiers in Microbiology*. Vol.9:2524 https://doi.org/10.3389/fmicb.2018.02524

Aleshin A.E., Gramatikova S., Hura G.L., Bobkov A., Strongin A.Y., Stec B., Tainer J.A., Liddington R.C., Smith J.W., (2009). Crystal and solution structures of a prokaryotic M16B peptidase: An open and shut case. *Structure*. Vol.17(11):1465-1475 https://doi.org/10.1016%2Fj.str.2009.09.009

Alhadlaq M.A., Green J., Kudhair B.K., (2021). Analysis of *Kytococcus sedentarius* strain isolated from a dehumidifier operating in a university lecture theatre: systems for aerobic respiration, resisting osmotic stress, and sensing nitric oxide. *Microbial Physiology*. Vol.31(2):135-145 https://doi.org/10.1159/000512751

Amin R., Reuther J., Mitulski A., Wohlleben W., (2012) Novel GlnR-target gene nnaR is involved in nitrate/nitrite assimilation in *Streptomyces coelicolor*. *Microbiology*. Vol.158(pt.5):1172-1182 https://doi.org/10.1099/mic.0.054817-0

Angelini S., Gerez C., Ollagnier-de-Choudens S., Sanakis Y., Fontecave M., Barras F., Py B., (2008). NfuA, a new factor required for maturing Fe/S proteins in *Escherichia coli* under oxidative stress and iron starvation conditions. *Journal of Biological Chemistry*. Vol.283(20):14084-14091 https://doi.org/10.1074/jbc.M709405200

Aravind L., Landsman D., (1998). AT-hook motifs identified in a wide variety of DNA-binding proteins. *Nucleic Acids Research*. Vol. 26(19):4413-4421 https://doi.org/10.1093/nar/26.19.4413

Atlung T., Hansen F.G., (1993). Three distinct chromosome replication states are induced by increasing concentrations of dnaA protein in *Escherichia coli*. *Journal of Bacteriology*. Vol.175(20):6537-45 https://doi.org/10.1128/jb.175.20.6537-6545.1993

Ausmees N., Wahlstedt H., Bagchi S., Elliot M., Buttner M.J., Flärdh K., (2007). SmeA, a small membrane protein with multiple functions in *Streptomyces* sporulation including targeting of a SpoIIIE/FtsK-like protein to cell division septa. *Molecular Microbiology*. Vol.65(6):1458-73 https://doi.org/10.1111/j.1365-2958.2007.05877.x

Averina O.V., Zakharevich N.V., Danilenko V.N., (2012). Identification and characterization of whiB-like family proteins of the *Bifidobacterium* genus. *Anaerobe.* Vol.18(4):421-429 https://doi.org/10.1016/j.anaerobe.2012.04.011

Bailey T.L., Johnson J., Grant C.E., Noble W.S., (2015). The MEME Suite. *Nucleic Acids Research*. Vol.43(1):39-49 https://doi.org/10.1093/nar/gkv416

Bartesaghi S., Radi R., (2018). Fundamentals on the biochemistry of peroxynitrite and protein tyrosine nitration. *Redox Biology*. Vol.14:618-625 https://doi.org/10.1016%2Fj.redox.2017.09.009

Battistuzzi FU Feijao A & Hedges SB (2004) A genomic timescale of prokaryote evolution: insights into the origin of methanogenesis, phototrophy, and the colonization of land. *BMC Evolutionary Biology*. Vol.4:44 https://doi.org/10.1186/1471-2148-4-44

Beinert H., Holm R.H., Münck E., (1997). Iron-sulfur clusters: nature's modular, multipurpose structures. *Science*. Vol.277(5326):653-659 https://doi.org/10.1126/science.277.5326.653

Beites T., Oliveira P., Rioseras B., Pires S.D.S., Oliveira R., Tamagnini P., Moradas Ferreira P., Manteca A., Mendes M.V., (2015). *Streptomyces natalensis* programmed cell death and morphological differentiation are dependent on oxidative stress. *Nature Scientific Reports*. Vol.5:12887 https://doi.org/10.1038/srep12887

Bender D., Schwarz G., (2018). Nitrite-dependent nitric oxide synthesis by molybdenum enzymes. FEBS Lett, Vol.12(592):2126-2139. https://doi.org/10.1002/1873-3468.13089

Benson A. K., Haldenwang W.G., (1993). *Bacillus subtilis* σ^B is regulated by a binding protein (RsbW) that blocks its association with core RNA polymerase. *PNAS USA* Vol.90:2330-2334 https://doi.org/10.1073%2Fpnas.90.6.2330

Bentley S.D., Chater K.F., Cerdeño-Tárraga A-M., Challis G.L., Thomson N.R., James K.D, Harris D.E., Quail M.A., Kieser H., Harper D., Bateman A., Brown S., Chandra G., Chen C.W., Collins M., Cronin A., Fraser A., Goble A., Hidalgo J., Hornsby T., Howarth S., Huang C-H., Kieser T., Larke L., Murphy L., Oliver K., O'Neil S., Rabbinowitsch E., Rajandream M-A., Rutherford K., Rutter S., Seeger K., Saunders D., Sharp S., Squares R., Squares S., Taylor K., Warren T., Wietzorrek A., Woodward J., Barrell B.G., Parkhill J., Hopwood D.A., (2002). Complete genome sequence of the model actinomycete *Streptomyces coelicolor* A3(2). *Nature*. Vol.417(6885):141-147 https://doi.org/10.1038/417141a

Bernier S.P., Surette M.G., (2013). Concentration-dependent activity of antibiotics in natural environments. *Frontiers in Microbiology*. Vol.4:20 https://doi.org/10.3389/fmicb.2013.00020

Bianchetti C.M., Blouin G.C., Bitto E., Olson J.S., Phillips G.N., (2010). The structure and NO binding properties of the nitrophorin-like heme-binding protein from *Arabidopsis thaliana* gene locus At1g79260.1. *Proteins*. Vol.78(4):917-931 https://doi.org/10.1002/prot.22617

Bibb M.J., Buttner M.J., (2003). The *Streptomyces coelicolor* developmental transcription factor sigmaBldN is synthesized as a proprotein. *Journal of Bacteriology*. Vol.185(7):2338-2345 https://doi.org/10.1128/jb.185.7.2338-2345.2003

Bibb M.J., Domonkos Á., Chandra G., Buttner M.J., (2012). Expression of the chaplin and rodlin hydrophobic sheath proteins in *Streptomyces venezuelae* is controlled by σBldN and a cognate anti-sigma factor, RsbN. *Molecular Microbiology*. Vol.84(6):1033-1049 https://doi.org/10.1111/j.1365-2958.2012.08070.x

Bibb M.J., Molle V., Buttner M.J., (2000). Sigma(BldN), an extracytoplasmic function RNA polymerase sigma factor required for aerial mycelium formation in *Streptomyces coelicolor* A3(2). *Journal of Bacteriology*. Vol.182(16):4606-4616 https://doi.org/10.1128/jb.182.16.4606-4616.2000

Bielen A., Cetković H., Long P.F., Schwab H., Abramić M., Vujaklija D., (2009). The SGNH-hydrolase of *Streptomyces coelicolor* has (aryl)esterase and a true lipase activity. *Biochimie*. Vol.91(3):390-400 https://doi.org/10.1016/j.biochi.2008.10.018

Bierman M., Logan R., O'Brien K., Seno E. T., Rao R.N., Schoner B.E., (1992). Plasmid cloning vectors for the conjugal transfer of DNA from *Escherichia coli* to *Streptomyces* spp. *Gene*. Vol.116(1):43-49 https://doi.org/10.1016/0378-1119(92)90627-2

Bignell D.R.D., Colvin K.R., Leskiw B.K., (2003). The putative anti-anti-sigma factor BldG is post-translationally modified by phosphorylation in *Streptomyces coelicolor*. *FEMS Microbiology Letters*. Vol.255(1):93-99 https://doi.org/10.1016/s0378-1097(03)00504-4

Bignell D.R.D., Warawa J.L., Strap J.L., Chater K.F., Leskiw B.K., (2000). Study of the *bldG* locus suggests that an anti-anti-sigma factor and an anti-sigma factor may be involved in *Streptomyces coelicolor* antibiotic production and sporulation. *Microbiology*. Vol.146(9):2161-2173 https://doi.org/10.1099/00221287-146-9-2161

Blanco G., Pereda A., Brian P., Méndez C., Chater K.F., Salas J.A., (1993). A hydroxylase-like gene product contributes to synthesis of a polyketide spore pigment in *Streptomyces halstedii*. *Journal of Bacteriology*. Vol.175(24):8043–8048. https://doi.org/10.1128%2Fjb.175.24.8043-8048.1993

Blin K., Shaw S., Augustijn H.E., Reitz Z.L., Biermann F., Alanjary M., Fetter A., Terlouw B.R., Metcalf W.W., Helfrich E.J.N., van Wezel G.P., Medema M.H., Weber T., (2023) antiSMASH 7.0: new and improved predictions for detection, regulation, chemical structures and visualisation. *Nucleic Acids Research*. Vol.51(W1):W46-W50 https://doi.org/10.1093/nar/gkad344

Bobek J., Halada P., Angelis J., Vohradsky J., Mikulik K., (2004). Activation and expression of proteins during synchronous germination of aerial spores of *Streptomyces granaticolor*. *Proteomics*. Vol.4(12):3864–3880 https://doi.org/10.1002/pmic.200400818

Bobek J., Šmídová K., Čihák M., (2017). A waking review: old and novel insights into the spore germination in Streptomyces. *Frontiers in Microbiology*. Vol.8:2205 https://doi.org/10.3389%2Ffmicb.2017.02205

Bonamore A., Boffi A., (2008). Flavohemoglobin: Structure and reactivity. *IUBMB Life*. Vol.60(1):19-28. https://doi.org/10.1002/iub.9

Bonfio C., Valer L., Scintilla S., Shah S., Evans D.J., Jin L., Szostak J.W., Sasselov D.D., Sutherland J.D., Mansy S.S., (2017). UV-light-driven prebiotic synthesis of iron–sulfur clusters. *Nature Chemistry*. Vol.9:1229–1234. https://doi.org/10.1038/nchem.2817

Boubakri H., Seghezzi N., Duchateau M., Gominet M., Olga Kofroňová, Oldřich Benada, Philippe Mazodier, Pernodet J-L., (2015). The absence of pupylation (prokaryotic ubiquitin-like protein modification) affects morphological and physiological differentiation in *Streptomyces coelicolor*. *Journal of Bacteriology*. Vol.197(21):3388-3399 https://doi.org/10.1128/jb.00591-15

Bradshaw E., Saalbach G., McArthur M., (2013). Proteomic survey of the *Streptomyces coelicolor* nucleoid. *Journal of Proteomics*. Vol.(83):37-46 https://doi.org/10.1016/j.jprot.2013.02.033

Brekasis D., Paget M.S.B., (2003). A novel sensor of NADH/NAD^+ redox poise in *Streptomyces*. *EMBO Journal*. Vol.22(18):4856-4865 https://doi.org/10.1093%2Femboj%2Fcdg453

Brimberry M., Corrigan P., Silakov A., Lanzilotta W.N., (2023) Evidence for porphyrin-mediated electron transfer in the radical SAM enzyme HutW. *Biochemistry*. Vol.62(6):1191-1196 https://doi.org/10.1021/acs.biochem.2c00474

Bruender N.A., Young A.P., Bandarian V., (2015). Chemical and biological reduction of the radical SAM enzyme 7-carboxy-7-deazaguanine synthase. *Biochemistry*. Vol.55(12):1939 https://doi.org/10.1021/acs.biochem.6b00147

Bryk R., Lima C.D., Erdjument-Bromage H., Tempst P., Nathan C., (2002). Metabolic enzymes of mycobacteria linked to antioxidant defense by a thioredoxin-like protein. *Science*. Vol.295(5557):1073-1077 https://doi.org/10.1126/science.1067798

Bubunenko M., Baker T., Court D.L., (2007) Essentiality of ribosomal and transcription antitermination proteins analyzed by systematic gene replacement in *Escherichia coli*. *Journal of Bacteriology*. Vol.189(7):2844-2853 https://doi.org/10.1128/jb.01713-06

Bulusu R.K.M., Wandell R.J., Gallan R.O., Locke B.R., (2019). Nitric oxide scavenging of hydroxyl radicals in a nanosecond pulsed plasma discharge gas-liquid reactor. *Journal of Physics D: Applied Physics*. Vol.52(50):504002 http://dx.doi.org/10.1088/1361-6463/ab431a

Burian J, Ramon-Garcia S, Sweet G, Gomez-Velasco A, Av-Gay Y, Thompson CJ. (2012). The mycobacterial transcriptional regulator whiB7 gene links redox homeostasis and intrinsic antibiotic resistance. *Journal of Biological Chemistry.* Vol.287(1):299–310. https://doi.org/10.1074/jbc.M111.302588

Bush M., (2018). The actinobacterial whiB-like (wbl) family of transcription factors. *Molecular Microbiology*. Vol.110(5):663-676 https://doi.org/10.1111/mmi.14117

Bush M., Chandra G., Bibb M.J., Findlay K.C., Buttner M.J., (2016). Genome-wide chromatin immunoprecipitation sequencing analysis shows that whiB is a transcription factor that cocontrols its regulon with WhiA to initiate developmental cell division in *Streptomyces*. *mBio* Vol.7(2):e00523. https://doi.org/10.1128/mbio.00523-16.

Bush M.J., Bibb M.J., Chandra G., Findlay K.C., Buttner M.J., (2013). Genes required for aerial growth, cell division, and chromosome segregation are targets of WhiA before sporulation in *Streptomyces venezuelae*. *mBIO*. Vol.4(5):10.1128/mbio.00684-13 https://doi.org/10.1128%2FmBio.00684-13

Bush M.J., Chandra G., Findlay K.C., Buttner M.J., (2017). Multi-layered inhibition of *Streptomyces* development: BldO is a dedicated repressor of whiB. *Molecular Microbiology*. Vol.104(5):700-711 https://doi.org/10.1111/mmi.13663

Bush M.J., Gallagher K.A., Chandra G., Findlay K.C., Schlimpert S., (2022). Hyphal compartmentalization and sporulation in *Streptomyces* require the conserved cell division protein SepX. *Nature Communications*. Vol.13:71 https://doi.org/10.1038%2Fs41467-021-27638-1

Buttner M.J., Chater K.F., Bibb M.J., (1990). Cloning, disruption, and transcriptional analysis of three RNA polymerase sigma factor genes of Streptomyces coelicolor A3(2). *Journal of Bacteriology*. Vol.172(6):3367-3378 https://doi.org/10.1128/jb.172.6.3367-3378.1990

Campbell W.H., Kinghorn J.R., (1990). Functional domains of assimilatory nitrate reductases and nitrite reductases. *Trends in Biochemical Sciences.* Vol.15(8):315-319 https://doi.org/10.1016/0968-0004(90)90021-3

Cantlay S., Sen B.K., Flärdh K., McCormick J.R., (2021). Influence of core divisome proteins on cell division in *Streptomyces venezuelae* ATCC 10712. Microbiology. Vol.167(2):001015 https://doi.org/10.1099%2Fmic.0.001015

Casonato S., Sánchez A.C., Haruki H., González M.R., Provvedi R., Dainese E., Jaouen T., Gola S., Bini E., Vincente M., Johnsson K., Ghisotti D., Palù G., Hernández-Pando R., Manganelli R., (2012). WhiB5, a transcriptional regulator that contributes to *Mycobacterium tuberculosis* virulence and reactivation. *Infection and Immunity*. Vol.80(9):3132-3144 https://doi.org/10.1128%2FIAI.06328-11

Cerny O., Kamanova J., Masin J., Bibova I., Skopova K., Sebo P., (2015). *Bordetella pertussis* adenylate cyclase toxin blocks induction of bactericidal nitric oxide in macrophages through cAMP-dependent activation of the SHP-1 phosphatase. *Journal of Immunology.* Vol.194(10):4901-4903. https://doi.org/10.4049/jimmunol.1402941

Chandra G., Chater K.F., (2014). Developmental biology of *Streptomyces* from the perspective of 100 actinobacterial genome sequences. *FEMS Microbiology Reviews*. Vol.38(3):345-379 https://doi.org/10.1111%2F1574-6976.12047

Chang Z., Sun Y., He J., Vining L.C., (2001). p-Aminobenzoic acid and chloramphenicol biosynthesis in *Streptomyces venezuelae*: gene sets for a key enzyme, 4-amino-4-deoxychorismate synthase. *Microbiology*. Vol.147(8):2113-2126 https://doi.org/10.1099/00221287-147-8-2113

Chater K., (1972). A morphological and genetic mapping study of white colony mutants of *Streptomyces coelicolor*. *Microbiology*. Vol.72(1):9-28 https://doi.org/10.1099/00221287-72-1-9

Chater K.F., (2016). Recent advances in understanding *Streptomyces*. *F1000Res*. Vol.5:2795 https://doi.org/10.12688%2Ff1000research.9534.1

Chater K.F., Biró S., Lee K.J., Palmer T., Hildgund S., (2010). The complex extracellular biology of *Streptomyces*. *FEMS Microbiology Letters*. Vol.34(2):171-198 https://doi.org/10.1111/j.1574-6976.2009.00206.x

Chater KF., Bruton C.J., Plaskitt K.A., Buttner M.J., Méndez C., Helmann J.D., (1989). The developmental fate of *S. coelicolor* hyphae depends upon a gene product homologous with the motility σ factor of *B. subtilis*. *Cell*. Vol.59(1):133-143. https://doi.org/10.1016/0092-8674(89)90876-3

Chawla M., Mishra S., Anand K., Parikh P., Mehta M., Vij M., Verma T., Singh P., Jakkala K., Verma H.N., AjitKumar P., Ganguli M., Seshasayee A.S.N., Singh A., (2018). Redox-dependent condensation of the mycobacterial nucleoid by WhiB4. *Redox Biology*. Vol.19:116-133 https://doi.org/10.1016/j.redox.2018.08.006

Chawla M., Parikh P., Saxena A., Munshi M., Mehta M., Mai D., Srivastava A.K., Narasimhulu K.V., Redding K.E., Vashi N., Kumar D., Steyn A.J.C., Singh A., (2012). *Mycobacterium tuberculosis* WhiB4 regulates oxidative stress response to modulate survival and dissemination in vivo. Molecular Microbiology. Vol.85(6):1148-1165 https://doi.org/10.1111/j.1365-2958.2012.08165.x

Chen J.M., Boy-Röttger S., Dhar N., Sweeney N., Buxton R.S., Pojer F., Rosenkrands I., Cole S.T., (2012) EspD is critical for the virulence-mediating ESX-1 secretion system in *Mycobacterium tuberculosis*. *Journal of Bacteriology*. Vol.194(4):884-893 https://doi.org/10.1128%2FJB.06417-11

Chen Z., Hu Y., Cumming B.M., Lu P., Feng L., Deng J., Steyn A.J.C., Chen S., (2016). Mycobacterial whiB6 differentially regulates ESX-1 and the Dos regulon to modulate granuloma formation and virulence in zebrafish. *Cell Reports.* Vol.16(9):2512-2524 https://doi.org/10.1016/j.celrep.2016.07.080

Cheng Y., Lyu M., Yang R., Wen Y., Song Y., Li J., Chen Z., (2020). SufR, a [4Fe-4S] cluster-containing transcription factor, represses the sufRBDCSU operon in *Streptomyces avermitilis* iron-sulfur cluster assembly. *Applied and Environmental Microbiology*. Vol.86(18):e01523-20 https://doi.org/10.1128%2FAEM.01523-20

Claessen D., de Jong W., Dijkhuizen L., Wösten H.A.B., (2006). Regulation of *Streptomyces* development: reach for the sky! *Trends in Microbiology*. Vol.14(7):313-319 https://doi.org/10.1016/j.tim.2006.05.008

Cobb R.E., Wang Y., Zhao H., (2015). High-efficiency multiplex genome editing of *Streptomyces* species using an engineered CRISPR/Cas system. *ACS Synthetic Biology.* Vol.4(6):723-738. https://doi.org/10.1021/sb500351f

Compton C.L., Fernandopulle M.S., Nagari R.T., Sello J.K., (2015). Genetic and proteomic analyses of pupylation in *Streptomyces coelicolor*. *Journal of Bacteriology*. Vol.197(17):2747-2753 https://doi.org/10.1128/jb.00302-15

Cooper L.E., Fedoseyenko D., Abdelwahed S.H., Kim S.H., Dairi T., Begley T.P., (2013) In vitro reconstitution of the radical S-adenosylmethionine enzyme MqnC involved in the biosynthesis of futalosine-derived menaquinone. *Biochemistry*. Vol.52(27):4592-4594 https://doi.org/10.1021/bi400498d

Crack J.C., den Hengst C.D., Jakimowicz P., Subramanian S., Johnson M.K., Buttner M.J., Thomson A.J., Le Brun N.E., (2009). Characterization of [4Fe-4S]-containing and cluster-free forms of *Streptomyces* WhiD. Vol.48(51):12252-12264 https://doi.org/10.1021/bi901498v

Crack J.C., Green J., Thomson A.J., Le Brun N.E., (2014). Techniques for the production, isolation, and analysis of iron–sulfur proteins. *Metalloproteins*. Vol.1122:33-48 https://doi.org/10.1007/978-1-62703-794-5_4

Crack J.C., Le Brun N.E., (2019). Mass spectrometric identification of [4Fe-4S](NO)$_x$ intermediates of nitric oxide sensing by regulatory iron-sulfur cluster proteins. *Chemistry A European Journal*. Vol.25(14):3675-3684 https://dx.doi.org/10.1002/chem.201806113

Crack J.C., Munnoch J., Dodd E.L., et al. (2015) NsrR from *Streptomyces coelicolor* is a nitric oxide-sensing [4Fe-4S] cluster protein with a specialized regulatory function. *Journal of Biological Chemistry*. Vol.290(20):12689-12704 https://doi.org/10.1074%2Fjbc.M115.643072

Crack J.C., Munnoch J., Dodd E.L., Knowles F., Al Bassam M.M., Kamali S., Holland A.A., Cramer S.P., Hamilton C.J., Johnson M.K., Thomson A.J., Hutchings M.I., Le Brun N.E., (2015). NsrR from *Streptomyces coelicolor* is a nitric oxide-sensing [4Fe-4S] cluster protein with a specialized regulatory function. *Journal of Biological Chemistry*. Vol. 290(20):12689-12704 https://doi.org/10.1074/jbc.M115.643072

Crack J.C., Smith L.J., Stapleton M.R., Peck J., Watmough N.J., Buttner M.J., Buxton R.S., Green J., Oganesyan V.S., Thomson A.J., Le Brun N.E., (2010). Mechanistic insight into the nitrosylation of the [4Fe-4S] cluster of WhiB-like proteins. *ACS* Vol.133(4):1112-1121 https://doi.org/10.1021/ja109581t

Crack J.C., Svistunenko D.A., Munnoch J., Thomson A.J., Hutchings M.I., Le Brun N.E., (2016) Differentiated, Promoter-specific Response of [4Fe-4S] NsrR DNA Binding to Reaction with Nitric Oxide. *Journal of Biological Chemistry*. Vol.291(16):8663-8672 https://doi.org/10.1074/jbc.m115.693192

Cronan J.E., (2021). The classical, yet controversial, first enzyme of lipid synthesis: *Escherichia coli* acetyl-CoA carboxylase. *Microbiology and Molecular Biology Reviews.* Vol.85(3):e0003221 https://doi.org/10.1128%2FMMBR.00032-21 *

Cronan J.E., Thomas J., (2009). Chapter 17 Bacterial fatty acid synthesis and its relationships with polyketide synthetic pathways. *Methods in Enzymology*. Vol.459:395-433 https://doi.org/10.1016%2FS0076-6879(09)04617-5

d'Andrea F.B., Poulton N.C., Froom R., Tam K., Campbell E.A., Rock J.M., (2022). The essential *M. tuberculosis* Clp protease is functionally asymmetric in vivo. *Science Advances*. Vol. 8(18):eabn7943 https://doi.org/10.1126%2Fsciadv.abn7943

Dalton K.A., Thibessard A., Hunter J.I.B., Kelemen G.H., (2007). A novel compartment, the 'subapical stem' of the aerial hyphae, is the location of a sigN-dependent, developmentally distinct transcription in *Streptomyces coelicolor*. *Molecular Microbiology*. Vol.64(3):719-737 https://doi.org/10.1111/j.1365-2958.2007.05684.x

Dar D., Shamir M., Mellin J.R., Koutero M., Stern-Ginossar N., Cossart P., Sorek R., (2016). Term-seq reveals abundant ribo-regulation of antibiotics resistance in bacteria. *Science*. Vol.352(6282):aad9822 https://doi.org/10.1126/science.aad9822

Davies J., Spiegelman G.B., Yim G., (2006) The world of subinhibitory antibiotic concentrations. *Current Opinion Microbiology.* Vol.9(5):445-53 https://doi.org/10.1016/j.mib.2006.08.006

Davis N.K., Chater K.F., (1992). The *Streptomyces coelicolor* whiB gene encodes a small transcription factor-like protein dispensable for growth but essential for sporulation. *Molecular & General Genetics*. Vol.232(3):351-358 https://doi.org/10.1007/bf00266237

De Crécy-Lagard V., Servant-Moisson P., Viala J., Grandvalet C., Mazodier P., (2002). Alteration of the synthesis of the Clp ATP-dependent protease affects morphological and physiological differentiation in *Streptomyces*. *Molecular Microbiology*. Vol.32(3):505-517 https://doi.org/10.1046/j.1365-2958.1999.01364.x

De Jong W., Manteca A., Sanchez J., Bucca G., Smith C.P., Dijkhuizen L., Claessen D., Wösten H.A.B., (2009). NepA is a structural cell wall protein involved in maintenance of spore dormancy in *Streptomyces coelicolor*. *Molecular Microbiology*. Vol.71(6):1591-1603 https://doi.org/10.1111/j.1365-2958.2009.06633.x

De Simone G., di Masi A., Ciaccio C., Coletta M., Ascenzi P., (2020b). NO scavenging through reductive nitrosylation of ferric *Mycobacterium tuberculosis* and *Homo sapiens* nitrobindins. *International Journal of Molecular Science*. Vol.21(24):9395 https://doi.org/10.3390/ijms21249395

De Simone G., di Masi A., Vita G.M., Polticelli F., Pesce A., Nardini M., Bolognesi M., Ciaccio C., Coletta M., Turilli E.S., Fasano M., Tognaccini L., Smulevich G., Abbruzzetti S., Viappiani C., Bruno S., Ascenzi P., (2020a). Mycobacterial and human nitrobindins: Structure and function. *Antioxidants and Redox Signaling*. Vol.33(4):229-246 https://doi.org/10.1089/ars.2019.7874

den Hengst C.D., Tran N.T., Bibb M.J., Chandra G., Leskiw B.K., Buttner M.J., (2010). Genes essential for morphological development and antibiotic production in *Streptomyces coelicolor* are targets of BldD during vegetative growth. *Molecular Microbiology*. Vol.78(2):361-379 https://doi.org/10.1111/j.1365-2958.2010.07338.x

Devine R., (2019). *Characterising the production of novel antimicrobials in Streptomyces formicae.* PhD Thesis: University of East Anglia, School of Biological Sciences, Norwich.

Diacovich L., Mitchell D.L., Pham H., Gago G., Melgar M.M., Khosla C., Gramajo H., Tsai S-C., (2004). Crystal structure of the β-Subunit of acyl-CoA carboxylase: Structure-based engineering of substrate specificity. Vol.43(44):14027-14036 https://doi.org/10.1021/bi049065v

Diacovich L., Peirú S., Kurth D., Rodŕiguez E., Podestá F., Khosla C., Gramajo H., (2002). Kinetic and structural analysis of a new group of acyl-CoA carboxylases found in *Streptomyces coelicolor* A3(2). Vol.277(34):31228-31236 https://doi.org/10.1074/jbc.M203263200

Díaz-Talavera A., Montero-Conde C., Leandro-García L.J., Robledo M., (2022). *Biomolecules*. Vol.12(5):693 https://doi.org/10.3390/biom12050693

Ditkowski B., Holmes N.A., Rydzak J., Donczew M., Bezulska M., Ginda K., Kędzierski P., Zakrzewska-Czerwińska J., Kelemen G.H., Jakimowicz D., (2013). Dynamic interplay of ParA with the polarity protein, Scy, coordinates the growth with chromosome segregation in *Streptomyces coelicolor*. *Open Biology*. Vol.3:130006 https://doi.org/10.1098/rsob.130006

Donczew M., Mackiewicz P., Wróbel A., Flärdh K., Zakrzewska-Czerwińska J., Jakimowicz D., (2016) ParA and ParB coordinate chromosome segregation with cell elongation and division during *Streptomyces* sporulation. Open Biology. Vol.6(4):150263 https://doi.org/10.1098%2Frsob.150263

Droste J., Rückert C, Kalinowski J., Hamed M.B, Anné J., Simoens K, Kristel Bernaerts K., Economou A, Busche T., (2021). Extensive reannotation of the genome of the model streptomycete *Streptomyces lividans* TK24 based on transcriptome and proteome information. *Frontiers in Microbiology*. Vol.12:604034 https://doi.org/10.3389/fmicb.2021.604034

Dubendorff J.W., Studier F.W., (1991). Controlling basal expression in an inducible T7 expression system by blocking the target T7 promoter with lac repressor. *Journal of Molecular Biology.* Vol.219(1):45-49 https://doi.org/10.1016/0022-2836(91)90856-2

Dupuy E., Van der Verren S.E., Lin J., Wilson M.A., Dachsbeck A.V., Viela F., Latour E., Gennaris A., Vertommen D., Dufrêne Y.F., Iorga B.I., Goemans C.V., Remaut H., Collet J-F., (2023). A molecular device for the redox quality control of GroEL/ES substrates. *Cell*. Vol.186(5):1039-1049.e17 https://doi.org/10.1016/j.cell.2023.01.013

Eastman K.A.S., Jochimsen A.S., Bandarian V., (2023). Intermolecular electron transfer in radical SAM enzymes as a new paradigm for reductive activation. *Journal of Biological Chemistry*. Vol.299(9):105058 https://doi.org/10.1016/j.jbc.2023.105058

Ehrlich J., Bartz Q.R., Smith R.M., Joslyn D.A., Burkholder P.R., (1947). Chloromycetin, a new antibiotic from a soil Actinomycete. *Science.* Vol.106(2757):417 https://doi.org/10.1126/science.106.2757.417

Ehrlich J., Gottlieb D., Burkholder P.R., Anderson L.E., Pridham T.G., (1948). *Streptomyces venezuelae*, n. sp., the source of chloromycetin. *Journal of Bacteriology*. Vol.56(4):467-77 https://doi.org/10.1128/jb.56.4.467-477.1948

Einsle O., Rees D.C., (2021). Structural enzymology of nitrogenase enzymes. *Chemical Reviews*. Vol120(12):4969-5004 https://doi.org/10.1021/acs.chemrev.0c00067

Elgrably-Weiss M., Schlosser-Silverman E., Rosenshine I., Altuvia S., (2006). DeoT, a DeoR-type transcriptional regulator of multiple target genes. *FEMS Microbiology Letters*. Vol.254(1):141-148 https://doi.org/10.1111/j.1574-6968.2005.00020.x

Elliot M.A., Bibb M.J., Buttner M.J., Leskiw B.K., (2001). BldD is a direct regulator of key developmental genes in *Streptomyces coelicolor* A3(2). *Molecular Microbiology*. Vol.40(1):257-269 https://doi.org/10.1046/j.1365-2958.2001.02387.x

Empadinhas N., da Costa M.S., (2011) Diversity, biological roles and biosynthetic pathways for sugar-glycerate containing compatible solutes in bacteria and archaea. *Environmental Microbiology*. Vol.13(8):2056-2077 https://doi.org/10.1111/j.1462-2920.2010.02390.x

Engels V., Wendisch V.F., (2007). The DeoR-Type Regulator SugR represses expression of ptsG in *Corynebacterium glutamicum*. *Journal of Bacteriology*. Vol189(8):2955-2966 https://doi.org/10.1128/jb.01596-06

Feng L., Chen S., Hu Y., (2018). PhoPR positively regulates whib3 expression in response to low pH in pathogenic mycobacteria. *Journal of Bacteriology*. Vol.200(8):e00766-17 https://doi.org/10.1128/JB.00766-17

Fernández-Martínez L., Borsetto C., Gomez-Escribano J.P., (2014). New insights into chloramphenicol biosynthesis in *Streptomyces venezuelae* ATCC 10712. *Antimicrobial Agents and Chemotherapy*. Vol.58(12):7441-7450 http://dx.doi.org/10.1128/AAC.04272-14

Fischer F., Raimondi D., Aliverti A., Zanetti G., (2002). *Mycobacterium tuberculosis* FprA, a novel bacterial NADPH-ferredoxin reductase. *European Journal of Biochemistry*. Vol.269(12):3005-3013. https://doi.org/10.1046/j.1432-1033.2002.02989.x.

Fischer M., Falke D., Pawlik T., Sawers G.R., (2014). Oxygen-dependent control of respiratory nitrate reduction in mycelium of *Streptomyces coelicolor* A3(2). *Journal of Bacteriology*. Vol.196(23):4152-4162 https://doi.org/10.1128/JB.02202-14

Fischer M., Falke D., Rönitz J., Haase A., Damelang T., Pawlik T., Sawers R.G., (2019). Hypoxia-induced synthesis of respiratory nitrate reductase 2 of *Streptomyces coelicolor* A3(2) depends on the histidine kinase OsdK in mycelium but not in spores. *Microbiology*. Vol.165(8):905–916 https://doi.org/10.1099/mic.0.000829

Fischer M., Schmidt C., Falke D., Sawers R.G., (2012). Terminal reduction reactions of nitrate and sulfate assimilation in *Streptomyces coelicolor* A3(2): identification of genes encoding nitrite and sulfite reductases. *Research in Microbiology*. Vol.163(5):340-348 https://doi.org/10.1016/j.resmic.2012.05.004

Flärdh K., (2003). Essential role of DivIVA in polar growth and morphogenesis in *Streptomyces coelicolor* A3(2). *Molecular Microbiology*. Vol.49(6):1523–1536. https://doi.org/10.1046/j.1365-2958.2003.03660.x

Flärdh K., Buttner M.J., (2009). *Streptomyces* morphogenetics: dissecting differentiation in a filamentous bacterium. *Nature Reviews Microbiology*. Vol.7(1):36-49 https://doi.org/10.1038/nrmicro1968

Flärdh K., Findlay K.C., Chater K.F., (1999). Association of early sporulation genes with suggested developmental decision points in *Streptomyces coelicolor* A3(2). *Microbiology*. Vol.145(9):2229–2243. https://doi.org/10.1099/00221287-145-9-2229

Fol. M., Chauhan A., Nair N.K., Maloney E., Moomey M., Jagannath C., Madijaru M.V., Rajagopalan M., (2006). Modulation of *Mycobacterium tuberculosis* proliferation by MtrA, an essential two-component response regulator. *Molecular Microbiology*. Vol.60(3):643-657 https://doi.org/10.1111/j.1365-2958.2006.05137.x

Fontecave M., de Choudens S.O., Py B., Barras F., (2005). Mechanisms of iron-sulfur cluster assembly: the SUF machinery. *Journal of Biological Inorganic Chemistry*. Vol.10(7):713-721. https://doi.org/10.1007/s00775-005-0025-1

Fowler-Goldsworthy K., Gust B., Mouz S., Chandra G., Findlay K.C., Chater K.F., (2011). The Actinobacteria-specific gene wblA controls major developmental transitions in *Streptomyces coelicolor* A3(2). *Microbiology*. Vol.157(Pt.5):1312-1328 https://doi.org/10.1099/mic.0.047555-0

Fuchino K., Bagchi S., Cantlay S., Sandblad L., Wu D., Bergman J., Kamali-Moghaddam M., Flärdh K., Ausmees N., (2013). Dynamic gradients of an intermediate filament-like cytoskeleton are recruited by a polarity landmark during apical growth. *PNAS USA*. Vol.110(21):E1889–E1897 https://doi.org/10.1073/pnas.1305358110

Fyans J.K., bignell D., Loria R., Toth I., Palmer T., (2013). The ESX/type VII secretion system modulates development, but not virulence, of the plant pathogen *Streptomyces scabies*. *Molecular Plant Pathology*. Vol.14(2):119-130 https://doi.org/10.1111%2Fj.1364-3703.2012.00835.x

Gabaldón T., Huynen M.A., (2004). Prediction of protein function and pathways in the genome era. *Cellular and Molecular Life Sciences*. Vol.61(7-8):930-944 https://doi.org/10.1007/s00018-003-3387-y

Gago G., Kurth D., Diacovich L., Tsai S-C., Gramajo H., (2006). Biochemical and structural characterization of an essential acyl coenzyme A carboxylase from *Mycobacterium tuberculosis*. Vol.188(2):477-486 https://doi.org/10.1128%2FJB.188.2.477-486.2006

Gaigalat L., Schlüter J-P., Hartmann M., Mormann S., Tauch A., Pühler A., Kalinowski J., (2007). The DeoR-type transcriptional regulator SugR acts as a repressor for genes encoding the phosphoenolpyruvate:sugar phosphotransferase system (PTS) in *Corynebacterium glutamicum*. *BMC Molecular Biology*. Vol.8:104 https://doi.org/10.1186/1471-2199-8-104

Gallagher K.A., Schumacher M.A., Bush M.J., Bibb M.J., Chandra G., Holmes N.A., Zeng W., Henderson M., Zhang H., Findlay K.C., Brennan R.G., Buttner M.J., (2020). c-di-GMP arms an anti-σ to control progression of multicellular differentiation in Streptomyces. *Molecular Cell*. Vol.77(3):586-599 https://doi.org/10.1016/j.molcel.2019.11.006

Garces A., Atmakuri K., Chase M.R., Woodworth J.S., Krastins B., Rothchild A.C., Ramsdell T.L., Lopez M.F., Behar S.M., Sarracino D.A., Fortune S.M. (2010). EspA acts as a critical mediator of ESX1-dependent virulence in *Mycobacterium tuberculosis* by affecting bacterial cell wall integrity. *PLOS Pathogens*. Vol.6(6):e1000957 https://doi.org/10.1371/journal.ppat.1000957

García-Quintans N., Baquedano I., Blesa A., Verdú C., Berenguer J. Mencía M., (2020). A thermostable DNA primase-polymerase from a mobile genetic element involved in defence against environmental DNA. *Environmental Microbiology*. Vol.22(11):4647-4657 https://doi.org/10.1111%2F1462-2920.15207

Garg S.K., Alam S., Bajpai R., Kishan K.V.R., Agrawal P., (2009). Redox biology of *Mycobacterium tuberculosis* H37Rv: protein-protein interaction between GlgB and WhiB1 involves exchange of thiol-disulfide. *BMC Biochemistry*. Vol.10:1 https://doi.org/10.1186%2F1471-2091-10-1

Garg S.K., Alam S., Soni V., Kishan K.V.R., Agrawal P., (2007). Characterization of *Mycobacterium tuberculosis* WhiB1/Rv3219 as a protein disulfide reductase. *Protein Expression and Purification*. Vol.52(2):422-432 https://doi.org/10.1016/j.pep.2006.10.015

Gavriilidou A., Kautsar S.A., Zaburannyi N., Krug D., Müller R., Medema M.H., Ziemert N., (2022). Compendium of specialized metabolite biosynthetic diversity encoded in bacterial genomes. *Nature Microbiology*. Vol.7(5):726-735 https://doi.org/10.1038/s41564-022-01110-2

Geiman D.E., Raghunand T.R., Agarwal N., Bishai W.R., (2006). Differential gene expression in response to exposure to antimycobacterial agents and other stress conditions among seven *Mycobacterium tuberculosis* whiB-like genes. *Antimicrobial Agents and Chemotherapy.* Vol.50(8):10.1128/aac.00295-06 https://doi.org/10.1128/aac.00295-06

Geoghegan K.F., Dixon H.B.F., Rosner P.J., Hoth L.R., Lanzetti A.J., Borzilleri K.A., Marr E.S., Pezzullo L.H., Martin L.B., LeMotte P.K., McColl A.S., Kamath A.V., Stroh J.G., (1999). Spontaneous α-N-6-phosphogluconoylation of a "His-tag" in *Escherichia coli*: The cause of extra mass of 258 or 178 Da in fusion proteins. *Analytical Biochemistry*. Vol.267(1):169-184 https://doi.org/10.1006/abio.1998.2990

Glazebrook M.A., Doull J.L., Stuttard C., Vining L.C., (1990). Sporulation of *Streptomyces venezuelae* in submerged cultures. *Microbiology*. Vol.136(3):581-588 https://doi.org/10.1099/00221287-136-3-581

Godber B.L.J., Doel J.J., Sapkota G.P., Blake D.R., Stevens C.R., Eisenthal R., Harrison R., (2000). Reduction of nitrite to nitric oxide catalyzed by xanthine oxidoreductase. Journal of Biological Chemistry, Vol.11(275):7757-7763. https://doi.org/10.1074/jbc.275.11.7757

Goemans C.V., Beaufay F., Arts I.S., Agrebi R., Vertommen D., Collet J-F., (2018b). The chaperone and redox properties of CnoX chaperedoxins are tailored to the proteostatic needs of bacterial species. *mBio*. Vol.9(6):e01541-18 https://doi.org/10.1128/mbio.01541-18.

Goemans C.V., Vertommen D., Agrebi R., Collet J-F., (2018a). CnoX is a chaperedoxin: A holdase that protects its substrates from irreversible oxidation. *Molecular Cell*. Vol.70(4):614-627.e7 https://doi.org/10.1016/j.molcel.2018.04.002

Gomez J.E., Bishai W.R., (2000). whmD is an essential mycobacterial gene required for proper septation and cell division. *Proc. Natl. Acad. Sci. USA.* Vol. 97(15):8554-8559 https://doi.org/10.1073/pnas.140225297

Gomez-Escribano J.P., Holmes N.A., Schlimpert S., Bibb M.J., Chandra G., Wilkinson B., Buttner M.J., Bibb M.J., (2021). *Streptomyces venezuelae* NRRL B-65442 : genome sequence of a model strain used to study morphological differentiation in filamentous actinobacteria. *Journal of Industrial Microbiology and Biotechnology*. Vol.48(9-10):kuab035 https://doi.org/10.1093/jimb/kuab035

Gregory M.A., Smith M.C.M., Till R., (2003). Integration site for *Streptomyces* phage phiBT1 and development of site-specific integrating vectors. *Journal of Bacteriology*. Vol.185(17):5320-5323 https://doi.org/10.1128/jb.185.17.5320-5323.2003

Gupta V., Sendra M., Naik S.G., Chahal H.K., Huynh B.H., Outten F.W., Fontecave M., Ollagnier-de Choudens S., (2009). Native *Escherichia coli* SufA, coexpressed with SufBCDSE, purifies as a [2Fe-2S] protein acts as an Fe-S transporter to Fe-S target enzymes. *Journal of the American Chemical Society*. Vol.131(17):6149-6153 https://doi.org/10.1021/ja807551e

Gusarov I., Starodubtseva M., Wang Z-Q., McQuade L., Lippard S.J., Stuehr D.J., Nudler E., (2008). Bacterial nitric-oxide synthases operate without a dedicated redox partner. *Journal of Biological Chemistry*. Vol.283(19):13140-13147 https://doi.org/10.1074%2Fjbc.M710178200

Gust B., Chandra G., Jakimowicz D., Yuqing T., Bruton C.J., Chater K.F., (2004). λ Red-mediated genetic manipulation of antibiotic-producing *Streptomyces*. *Advances in Applied Microbiology*. Vol.54:107-128 https://doi.org/10.1016/s0065-2164(04)54004-2

Guyet A., Benaroudj N., Proux C., Gominet M., Coppée J-Y., Mazodier P., (2014). Identified members of the *Streptomyces lividans* AdpA regulon involved in differentiation and secondary metabolism. *BMC Microbiology*. Vol.14:81. https://doi.org/10.1186/1471-2180-14-81

Haiser, H. J., Yousef, M. R., and Elliot, M. A. (2009). Cell wall hydrolases affect germination, vegetative growth, and sporulation in *Streptomyces coelicolor*. *Journal of Bacteriology*. Vol.191:6501–6512. https://doi.org/10.1128/JB.00767-09

Hammond L.R., White M.L., Eswara P.J., (2019). ¡vIVA la DivIVA! *Journal of Bacteriology.* Vol.201(21):e00245-19 https://doi.org/10.1128/jb.00245-19

Hardisson C., Manzanal M. B., Salas J. A., Suarez, J. E., (1978). Fine structure, physiology and biochemistry of arthrospore germination in *Streptomyces antibioticus*. *Microbiology*. Vol.105(2):203–214. https://doi.org/10.1099/00221287-105-2-203

Hausladen A., Gow A., Stamler J.S., (2001). Flavohaemoglobin denitrosylase catalyzes the reaction of a nitroxyl equivalent with molecular oxygen. *PNAS USA*. Vol.98(18):10108-10112 https://doi.org/10.1073%2Fpnas.181199698

Hempel A.M., Cantlay S., Molle V., Flärdh K., (2012). The Ser/Thr protein kinase AfsK regulates polar growth and hyphal branching in the filamentous bacteria *Streptomyces*. *PNAS USA*. Vol.109(35):E2371-2379 https://doi.org/10.1073/pnas.1207409109

Hempel A.M., Wang S.B., Letek M., Gil J.A., Flardh K., (2008). Assemblies of DivIVA mark sites for hyphal branching and can establish new zones of cell wall growth in *Streptomyces coelicolor*. Journal of Bacteriology. Vol.190(22):7579–7583. https://doi.org/10.1128/jb.00839-08

Higo A., Horinouchi S., Ohnishi Y., (2011). Strict regulation of morphological differentiation and secondary metabolism by a positive feedback loop between two global regulators AdpA and BldA in *Streptomyces griseus*. *Molecular Microbiology.* Vol.81(6):1607-22 https://doi.org/10.1111/j.1365-2958.2011.07795.x

Hiraga K., Seeram S.S., Tate S., Tanaka N., Kainosho M., Oda K., (1999). Mutational analysis of the reactive site loop of *Streptomyces* metalloproteinase inhibitor. *The Journal of Biochemistry*. Vol.125(1):202-209 https://doi.org/10.1093/oxfordjournals.jbchem.a022260

Hirano S., Kato J-Y., Ohnishi Y., Sueharu H., (2006). Control of the *Streptomyces* subtilisin inhibitor gene by AdpA in the A-factor regulatory cascade in *Streptomyces griseus*. *Journal of Bacteriology*. Vol. 188(17):6207-6216 http://www.ncbi.nlm.nih.gov/pmc/articles/pmc1595390/

Hiratsuka T., Furihata K., Ishikawa J., Yamashita H., Itoh N., Seto H., Dairi T., (2008) An alternative menaquinone biosynthetic pathway operating in microorganisms. *Science*. Vol.321(5896):1670-1673 https://doi.org/10.1126/science.1160446

Ho J.W., Bishop E., Karchenko P.V., Nègre N., White K.P., Park P.J., (2011). ChIP-chip versus ChIP-seq: Lessons for experimental design and data analysis. *BMC Genomics* Vol.12:134 (2011). https://doi.org/10.1186/1471-2164-12-134

Homerová D, Sevcíková J, Kormanec J., (2003). Characterization of the *Streptomyces coelicolor* A3(2) wblE gene, encoding a homologue of the sporulation transcription factor. *Folia Microbiologica*. Vol.48(4):489-495 https://doi.org/10.1007/bf02931330

Honma S., Ito S., Yajima S., Sasaki Y., (2021). Nitric oxide signaling for actinorhodin production in *Streptomyces coelicolor* A3(2) via the DevS/R two-component system. *Applied Environmental Microbiology*. Vol.87(14):e00480-21 https://doi.org/10.1128%2FAEM.00480-21

Honma S., Ito S., Yajima S., Sasaki Y., (2022). Nitric oxide signaling for aerial mycelium formation in *Streptomyces coelicolor* A3(2) M145. *Applied Environmental Microbiology*. Vol.88(23):e01222-22 https://doi.org/10.1128%2Faem.01222-22

Hopwood D.A., (1967). Genetic analysis and genome structure in *Streptomyces coelicolor*. *Bacteriological Reviews*. Vol.31(4):373-403 https://doi.org/10.1128%2Fbr.31.4.373-403.1967

Hoskisson P.A., Seipke R.F., (2020). Cryptic or silent? the known unknowns, unknown knowns, and unknown unknowns of secondary metabolism. *mBio*. Vol.11(5):e02642-20 https://doi.org/10.1128/mbio.02642-20

Hu Y., Ribbe M.W., (2013). Biosynthesis of the iron-molybdenum cofactor of nitrogenase. *Journal of Biological Chemistry*. Vol.288(19):13173-7 https://doi.org/10.1074/jbc.r113.454041

Huang H., Hou L., Li H., Qiu Y., Ju J., Li W., (2016). Activation of a plasmid-situated type III PKS gene cluster by deletion of a wbl gene in deepsea-derived *Streptomyces somaliensis* SCSIO ZH66. *Microbial Cell Factories*. Vol.15:116 https://doi.org/10.1186/s12934-016-0515-6

Huang T-W., Chen C.W., (2006). A recA null mutation may be generated in *Streptomyces coelicolor*. *Journal of Bacteriology*. Vol.188(19):6771-6779 https://doi.org/10.1128/jb.00951-06

Huang T-W., Hsu C-C., Yang H-Y., Chen C.W., (2013). Topoisomerase IV is required for partitioning of circular chromosomes but not linear chromosomes in *Streptomyces*. *Nucleic Acids Research*. Vol.41(22):10403-13. https://doi.org/10.1093/nar/gkt757

Huang X., Ma T., Tian J., Shen L., Zuo H., Hu C., Liao G., (2017). wblA, a pleiotropic regulatory gene modulating morphogenesis and daptomycin production in *Streptomyces roseosporus*. https://doi.org/10.1111/jam.13512

Huet G., Daffé M., Saves I., (2005). Identification of the *Mycobacterium tuberculosis* SUF machinery as the exclusive Mycobacterial system of [Fe-S] cluster assembly: evidence for its implication in the pathogen's survival. *Journal of Bacteriology*. Vol.187(17):6137-6146 https://doi.org/10.1128%2FJB.187.17.6137-6146.2005

Huh J-H., Kim D-J., Zhao X-Q., Li M., Jo Y-Y., Yoon T-M., Shin S-K., Yong J-H., Ryu Y-W., Yang Y-Y., Suh J-W., (2004). Widespread activation of antibiotic biosynthesis by S-adenosylmethionine in streptomycetes. *FEMS Microbiology Letters*. Vol.238:439-447 https://doi.org/10.1016/j.femsle.2004.08.009

Hull T.D., Ryu M.H., Sullivan M.J., Johnson R.C., Klena N.T., Geiger R.M., Gomelsky M., Bennett J.A., (2012). Cyclic di-GMP phosphodiesterases RmdA and RmdB are involved in regulating colony morphology and development in *Streptomyces coelicolor*. *Journal of Bacteriology*. Vol.194(17):4642-51 https://doi.org/10.1128%2FJB.00157-12

Husain I., Poupard J.A., Norris R.F., (1972). Influence of nutrition on the morphology of a strain of *Bifidobacterium bifidum*. *Journal of Bacteriology*. Vol.111(3):841-844 https://doi.org/10.1128/jb.111.3.841-844.1972

Hwang S., Lee N., Choe D., Lee Y., Kim w., Jeong Y., Cho S., Palsson B.O., Cho B-K., (2021). Elucidating the regulatory elements for transcription termination and posttranscriptional processing in the *Streptomyces clavuligerus* genome. *mSystems*. Vol.6(3):e01013-20 https://doi.org/10.1128%2FmSystems.01013-20

Jakimowicz P., Cheeseman M.R., Bishai W.R., Chater K.F., Thomson A.J., Buttner M.J., (2005). Evidence that the *Streptomyces* developmental protein WhiD, a member of the WhiB family, binds a [4Fe-4S] cluster. *Journal of Biological Chemistry*. Vol.280(9):8309-8315 https://doi.org/10.1074/jbc.M412622200

Jarlier V., Nikaido H., (1994). Mycobacterial cell wall: Structure and role in natural resistance to antibiotics. *FEMS Microbiology Letters*. Vol.123(1-2):11-18 https://doi.org/10.1111/j.1574-6968.1994.tb07194.x

Jenal U., Reinders A., Lori C., (2017). Cyclic di-GMP: second messenger extraordinaire. *Nature Reviews Microbiology*. Vol.15:271-284 https://doi.org/10.1038/nrmicro.2016.190

Jeon J-M, Choi T-R., Lee B-R., Seo J-H., Song H-S., Jung H-R., Yang S-Y., Park J.Y., Kim E-J., Kim B-G., Yang Y-H., (2019). Decreased growth and antibiotic production *in Streptomyces coelicolor* A3(2) by deletion of a highly conserved DeoR family regulator, SCO1463. *Biotechnology and Bioprocess Engineering*. Vol.24:613-621 https://doi.org/10.1007/s12257-019-0084-8

Jeong Y., Kim J-N., Kim M.W., Bucca G., Cho S., Yoon Y.J., Kim B-G., Roe J-H., Kim S.C., Smith C.P., Cho B-K., (2016). The dynamic transcriptional and translational landscape of the model

antibiotic producer *Streptomyces coelicolor* A3(2). *Nature Communications*. Vol.7:11605 https://doi.org/10.1038/ncomms11605

Jiang H., Kendrick K.E., (2000). Characterization of ssfR and ssgA, two genes involved in sporulation of *Streptomyces griseus*. *Journal of Bacteriology.* Vol.182(19).5521-5529 https://doi.org/10.1128/jb.182.19.5521-5529.2000

Johansson P., Hederstedt L., (1999). Organization of genes for tetrapyrrole biosynthesis in gram--positive bacteria. *Microbiology*. Vol.145(pt.3):529-538 https://doi.org/10.1099/13500872-145-3-529

Johnson D.C., Unciuleac M.C., Dean D.R., (2006a). Controlled expression and functional analysis of iron–sulfur cluster biosynthetic components within *Azotobacter vinelandii*. *Journal of Bacteriology*. Vol.188:7551-7561 https://doi.org/10.1128%2FJB.00596-06

Johnson E.G., Sparks J.P., Dzikovski B., Crane B.R., Gibson D.M., Loria R., (2008) Plant-pathogenic *Streptomyces* species produce nitric oxide synthase-derived nitric oxide in response to host signals. *Chemistry and Biology.* Vol.15(1):43-50 https://doi.org/10.1016/j.chembiol.2007.11.014

Johnson K.A., Bhushan S., Stahl A., Hallberg B.M., Frohn A., Glaser E., Eneqvist T., (2006b). The closed structure of presequence protease PreP forms a unique 10,000 $Å^3$ chamber for proteolysis. *EMBO Journal*. Vol.25(9):1977–1986 https://doi.org/10.1038/sj.emboj.7601080

Johnson M. K., (1998). Iron-sulfur proteins: new roles for old clusters. *Current Opinion in Chemical Biology*. Vol.2(2):173–181. https://doi.org/10.1016/s1367-5931(98)80058-6

Jordan S.F., Ioannou I., Rammu H. Halpern A, Bogart L.K, Ahn M., Vasiliadou R., Christodoulou J., Maréchal A., Lane N., (2021). Spontaneous assembly of redox-active iron-sulfur clusters at low concentrations of cysteine. *Nature Communications*. Vol.12:5925 https://doi.org/10.1038/s41467-021-26158-2

Joyce G., Williams K.J., Robb M., Noens E., Tizzano B., Shahrezaei V., Robertson B.D., (2012). Cell division site placement and asymmetric growth in Mycobacteria. *PLOS ONE* 7(9): e44582 https://doi.org/10.1371/journal.pone.0044582

Kaiser B.K., Clifton M.C., Shen B.W., Stoddard B.L., (2009). The structure of a bacterial DUF199/WhiA protein: Domestication of an invasive endonuclease. *Structure*. Vol.17(10):1368-1376 https://doi.org/10.1016/j.str.2009.08.008

Kandolf S., Grishkovskaya I., Belačić K., Bolhuis D.L., Amann S., Foster B., Imre R., Mechtler K., Schleiffer A., Tagare H.D., Zhong E.D., Meinhart A., Brown N.G., Haselbach D., (2022). Cryo-EM structure of the plant 26S proteasome. *Plant Communications*. Vol.3(3):100310 https://doi.org/10.1016%2Fj.xplc.2022.100310

Kang S-H., Huang J., Lee H-N., Hur Y-A., Cohen S.N., Kim E-S., (2007). Interspecies DNA microarray analysis identifies WblA as a pleiotropic down-regulator of antibiotic biosynthesis in *Streptomyces*. *Journal of Bacteriology*. Vol.189(11):4315-4319 https://doi.org/10.1128/jb.01789-06

Karimova G., Pidoux J., Ullmann A., Ladant D., (1998). A bacterial two-hybrid system based on a reconstituted signal transduction pathway. *PNAS.* Vol.95:5752-5756 https://doi.org/10.1073/pnas.95.10.5752

Karimova G., Ullmann A., Ladant D., (2000). A bacterial two-hybrid system that exploits a cAMP signalling cascade in Escherichia coli. *Methods in Enzymology*. Vol.328:59-73 https://doi.org/10.1016/S0076-6879(00)28390-0

Katakayama T., Sekimizu K., (1999) Inactivation of *Escherichia coli* DnaA protein by DNA polymerase III and negative regulations for initiation of chromosomal replication. *Biochimie*. Vol.81(8-9):835-840 https://doi.org/10.1016/s0300-9084(99)00213-8

Kato J., Suzuki A., Yamazaki H., Ohnishi Y., Horinouchi S., (2002). Control by A-factor of a metalloendopeptidase gene involved in aerial mycelium formation in Streptomyces griseus. Journal of Bacteriology. Vol.184(21):6016-6025 https://doi.org/10.1128%2FJB.184.21.6016-6025.2002

Kelemen G.H., Brian P., Flärdh K., Chamberlin L., Chater K.F., Buttner M.J., (1998). Developmental regulation of transcription of whiE, a locus specifying the polyketide spore pigment in *Streptomyces coelicolor* A3(2). *Journal of Bacteriology.* Vol.180(9):2515:2521 https://doi.org/10.1128%2Fjb.180.9.2515-2521.1998

Kelemen G.H., Brown G.L., Kormanec J., Potúcková L., Chater K.F., Buttner M.J., (1996). The positions of the sigma-factor genes, whiG and sigF, in the hierarchy controlling the development of spore chains in the aerial hyphae of *Streptomyces coelicolor* A3(2). *Molecular Microbiology*. Vol.21(3):593-603 https://doi.org/10.1111/j.1365-2958.1996.tb02567.x

Kelemen G.H., Brian P., Flärdh K., Chamberlin L., Chater K.F., Buttner M.J., (1998). Developmental regulation of transcription of whiE, a locus specifying the polyketide spore pigment in *Streptomyces coelicolor* A3(2). *Journal of Bacteriology*. Vol.180(9):2515–2521

Kelly S.M., Jess T.J., Price N.C., (2005). How to study proteins by circular dichroism. *Biochimica et Biophysica Acta*. Vol.1751(2):119-139 https://doi.org/10.1016/j.bbapap.2005.06.005

Kers J.A., Wach M.J., Krasnoff S.B., Widom J., Cameron K.D., Bukhalid R.A., Gibson D.M., Crane B.R., Loria R., (2004) Nitration of a peptide phytotoxin by bacterial nitric oxide synthase. *Nature*. Vol.429:79-82 https://doi.org/10.1038/nature02504

Kieser T., Bibb M.J., Buttner M.J., Chater K.F., Hopwood D.A., (2000). *Practical streptomyces genetics*, [online: https://streptomyces.org.uk/]. John Innes Foundation.

Kim D.W., Hesketh A., Kim E.S., Song J.Y., Lee D.H., Kim I.S., Chater K.F., Lee K.J., (2008). Complex extracellular interactions of proteases and a protease inhibitor influence multicellular development of *Streptomyces coelicolor*. *Molecular Microbiology*. Vol.70(5):1180-1193 https://doi.org/10.1111/j.1365-2958.2008.06471.x

Kim J-S., Lee H-N., Kim P., Lee H-S., Kim E-S., (2012). Negative role of wblA in response to oxidative stress in *Streptomyces coelicolor*. *Journal of Microbiology and Biotechnology*. Vol.22(6):736-741 https://doi.org/10.4014/jmb.1112.12032

Kim J-S., Lee H-N., Lee H-S., Kim P., Kim E-S., (2013). A WblA-binding protein, SpiA, involved in *Streptomyces* oxidative stress response. *Journal of Microbiology and Biotechnology*. Vol.23(10):1365-1371 https://doi.org/10.4014/jmb.1306.06032

Kim M.S., Hahn M.Y., Cho Y., Cho S.N., Roe, J.H., (2009). Positive and negative feedback regulatory loops of thiol-oxidative stress response mediated by an unstable isoform of sigmaR in actinomycetes. *Molecular Microbiology*. Vol.73:815-825 https://doi.org/10.1111/j.1365-2958.2009.06824.x

Kim S.O., Orii Y., Lloyd D., Hughes M.N., Poole R.K., (1999). Anoxic function for *Escherichia coli* flavohaemoglobin (Hmp): reversible binding of nitric oxide and reduction to nitrous oxide. *FEBS Letters.* Vol.445(2-3):389-394 https://doi.org/10.1016/S0014-5793(99)00157-X

Kim T-H., Park J-S., Kim H-J., Kim Y., Kim P., Lee H-S., (2005). The whcE gene of *Corynebacterium glutamicum* is important for survival following heat and oxidative stress. *Biochemical and Biophysical Research Communications*. Vol.337(3):757-764 https://doi.org/10.1016/j.bbrc.2005.09.115

Kirby R., (2011) Chromosome diversity and similarity within the Actinomycetales. *FEMS Microbiology Letters*. Vol.319(1):1-10 https://doi.org/10.1111/j.1574-6968.2011.02242.x

Knappe J., Schacht J., Möckel., Höpner T., Vetter Jr. H., Edenharder R., (1969). Pyruvate formate-lyase reaction in *Escherichia coli*. The enzymatic system converting an inactive form of the lyase into the catalytically active enzyme. *European Journal of Biochemistry*. Vol.11(2):316-327 https://doi.org/10.1111/j.1432-1033.1969.tb00775.x

Kodani S., Hudson M.E., Durrant M.C., Willey J.M., (2004). The SapB morphogen is a lantibiotic-like peptide derived from the product of the developmental gene ramS in *Streptomyces coelicolor*. *PNAS USA*. Vol.101(31):11448-11453 https://doi.org/10.1073/pnas.0404220101

Kodani S., Komaki H., Suzuki M., Koboyakawa F., Hemmi H., (2015). Structure determination of a siderophore peucechelin from *Streptomyces peucetius*. *Biometals*. Vol.28(5):791-801 https://doi.org/10.1007/s10534-015-9866-4

Konar M., Alam S., Arora C., Agrawal P., (2012). WhiB2/Rv3260c, a cell division-associated protein of *Mycobacterium tuberculosis* H37Rv, has properties of a chaperone. *FEBS Journal*. Vol.279:2781-2792 https://doi.org/10.1111/j.1742-4658.2012.08662.x

Konermann L., (2017). Addressing a common misconception: Ammonium acetate as neutral pH "buffer" for native electrospray mass spectrometry. *J. Am. Soc. Mass. Spectrom.* Vol.28(9):1827-1835. https://link.springer.com/article/10.1007/s13361-017-1739-3

König S., Fales H.M., (1998) Formation and decomposition of water clusters as observed in a triple quadrupole mass spectrometer. *J. Am. Soc. Mass.* Vol.9(8):814–822 https://doi.org/10.1016/S1044-0305(98)00044-0

Kormanec J., Ševčíková B., Sprušanský O., Benada O., Kofroňová O., Nováková R., Řežuchová B., Potúčková L., Homérová D., (1998). The *Streptomyces aureofaciens* homologue of the whiB gene is essential for sporulation; its expression correlates with the developmental stage. *Folia Microbiologica*. Vol.43:605-612 https://doi.org/10.1007/bf02816376

Kthiri F., Le H-T., Tagourti J., Kern R., Malki A., Caldas T., Abdallah J., Landoulsi A., Richarme G., (2008). The thioredoxin homolog YbbN functions as a chaperone rather than as an oxidoreductase. *Biochemical and Biophysical Research Communications.* Vol.374(4):668-672 https://doi.org/10.1016/j.bbrc.2008.07.080

Kudhair B.K., Hounslow A.M., Rolfe M.D., Crack J.C., Hunt D.M., Buxton R.S., Le Brun N.E., Williamson M.P., Green J., (2017) Structure of a Wbl protein and implications for NO sensing by *M. tuberculosis*. *Nature Communications*. Vol.8:2280 https://www.nature.com/articles/s41467-017-02418-y

Kwak J., Dharmatilake A.J., Jiang H., Kendrick K.E., (2001). Differential regulation of ftsZ transcription during septation of *Streptomyces griseus*. Vol.183(17): 5092 – 5101 https://doi.org/10.1128/jb.183.17.5092-5101.2001

Larsson C., Luna B., Ammerman N.C., Maiga M., Agarwal N., Bishai W.R., (2012). Gene expression of *Mycobacterium tuberculosis* putative transcription factors whiB1-7 in redox environments. *PLoS ONE*. Vol.7(7):e37516 https://doi.org/10.1371/journal.pone.0037516

Lee J-H., Lee E-J., Roe J-H., (2022). uORF-mediated riboregulation controls transcription of whiB7/wblC antibiotic resistance gene. *Molecular Microbiology*. Vol.117(1):179-192. https://doi.org/10.1111/mmi.14834

Lee J-H., Yoo J-S., Kim Y., Kim J-S., Lee E-J., Roe J-H., (2020). The WblC/WhiB7 transcription factor controls intrinsic resistance to translation-targeting antibiotics by altering ribosome composition. *mBio*. Vol.11(2):e00625-20 https://doi.org/10.1128/mbio.00625-20

Lee J-Y., Kim H-J., Kim E-S., Kim P., Kim Y., Lee H-S., (2013). Regulatory interaction of the *Corynebacterium glutamicum* whc genes in oxidative stress responses. *Journal of Biotechnology.* Vol.168(2):149-154. https://doi.org/10.1016/j.jbiotec.2013.03.017

Lee J-Y., Park J-S., Kim H-J., Kim Y., Lee H-S., (2012). *Corynebacterium glutamicum* whcB, a stationary phase-specific regulatory gene. *FEMS Microbiology Letters*. Vol.327(2):103-109. https://doi.org/10.1111/j.1574-6968.2011.02463.x

Lee Y., Lee N., Jeong Y., Hwang S., Kim W., Cho S., Palsson B.O., Cho B-K., (2019). The transcription unit architecture of *Streptomyces lividans* TK24. *Frontiers in Microbiology*. Vol.10:2074 https://doi.org/10.3389%2Ffmicb.2019.02074

Leskiw B.K., Bibb M.J., Chater K.F., (1991). The use of a rare codon specifically during development? *Molecular Microbiology*. Vol.5(12):2861-2867 https://doi.org/10.1111/j.1365-2958.1991.tb01845.x

Letek M., Ordóñez E., Vaquera J., Margolin W., Flärdh K., Mateos L.M., Gil J.A., (2008). DivIVA is required for polar growth in the MreB-lacking rod-shaped actinomycete *Corynebacterium glutamicum*. *Journal of Bacteriology*. Vol. 190(9):3283-3292. https://doi.org/10.1128%2FJB.01934-07

Levchenko I., Luo L., Baker T.A., (1995). Disassembly of the Mu transposase tetramer by the ClpX chaperone. *Genes & Development*. Vol.9(19):2399-2408 https://doi.org/10.1101/gad.9.19.2399

Li H., Kundu T.K., Zweier J.L., (2009). Characterization of the magnitude and mechanism of aldehyde oxidase-mediated nitric oxide production from nitrite. *Journal of Biological Chemistry*. Vol.49(284):33850-33858. https://doi.org/10.1074/jbc.m109.019125

Li H., Samouilov A., Liu X., Zweier J.L., (2004). Characterization of the effects of oxygen on xanthine oxidase-mediated nitric oxide formation. *Journal of Biological Chemistry*. Vol.17(279):16939-16946. https://doi.org/10.1074/jbc.m314336200

Lilic M., Darst S.A., Campbell E.A., (2021). Structural basis of transcriptional activation by the *Mycobacterium tuberculosis* intrinsic antibiotic-resistance transcription factor WhiB7. *Molecular Cell*. Vol.81(14):2875-2886 https://doi.org/10.1016/j.molcel.2021.05.017

Lilic M., Holmes N.A., Bush M.J., Campbell E.A., (2023). Structural basis of dual activation of cell division by the actinobacterial transcription factors WhiA and WhiB. *PNAS USA*. Vol.120(11):e2220785120 https://doi.org/10.1073/pnas.2220785120

Liu X., Cheng Y., Lyu M., Wen Y., Song Y., Chen Z., Li J., (2017). Redox-sensing regulator Rex regulates aerobic metabolism, morphological differentiation, and avermectin production in *Streptomyces avermitilis*. *Nature Scientific Reports*. Vol.7:44567 https://doi.org/10.1038%2Fsrep44567

Loiseau L., Gerez C., Bekker M., Ollagnier-de-Choudens S., Py B., Sanakis Y., Teixeira-de-Mattos J., Fontecave M., Barras F., (2007). ErpA, an iron–sulfur (Fe-S) protein of the A-type essential for respiratory metabolism in *Escherichia coli*. *Proc. Nat. Acad. Sci. USA*. Vol.104(34):13626-13631 https://doi.org/10.1073/pnas.0705829104

Lovett P.S., (1996). Translation attenuation regulation of chloramphenicol resistance in bacteria – a review. *Gene*. Vol.179(1):157-162 https://doi.org/10.1016/S0378-1119(96)00420-9

Mahanta N., Fedoseyenko D., Dairi T., Begley T.P., (2013). Menaquinone biosynthesis: formation of aminofutalosine requires a unique radical SAM enzyme. *Journal of the American Chemical Society*.Vol.135(:41):15318-15321 https://doi.org/10.1021%2Fja408594p

Mahatha A.C., Mal S., Majumder D., Saha S., Ghosh A., Basu J., Kundu M., (2020). RegX3 activates whiB3 under acid stress and subverts lysosomal trafficking of *Mycobacterium tuberculosis* in a WhiB3-dependent manner. *Frontiers in Microbiology*. Vol.11:572433 https://doi.org/10.3389/fmicb.2020.572433

Manion-Sommerhalter H.R., Fedoseyenko D., Joshi S., Begley T.P., (2021). Menaquinone Biosynthesis: The mechanism of 5,8-dihydroxy-2-naphthoate synthase (MqnD). *Biochemistry* Vol.60(25):1947–1951 https://doi.org/10.1021/acs.biochem.1c00257

Mansy S.S., Xiong Y., Hemann C., Hille R., Sundaralingam M., Cowan J.A., (2002). Crystal structure and stability studies of C77S HiPIP: a serine ligated [4Fe-4S] cluster. *Biochemistry*. Vol.41(4):1195-201 https://doi.org/10.1021/bi011811y

Manteca A., Alvarez R., Salazar N., Yagüe P., Sanchez J., (2008) Mycelium differentiation and antibiotic production in submerged cultures of *Streptomyces coelicolor*. *Applied Environmental* Microbiology. Vol. 74(12):3877-86 https://doi.org/10.1128/aem.02715-07

Manteca A., Fernández M., Sánchez J., (2005) A death round affecting a young compartmentalized mycelium precedes aerial mycelium dismantling in confluent surface cultures of *Streptomyces antibioticus*. Microbiology. Vol.151(11):3689–3697 https://doi.org/10.1099/mic.0.28045-0

Manteca A., Jung H.R., Schwämmle V., Jensen O.N., Sánchez J., (2010). Quantitative proteome analysis of *Streptomyces coelicolor* nonsporulating liquid cultures demonstrates a complex differentiation process comparable to that occurring in sporulating solid cultures. *Journal of Proteome Research.* Vol.9(9):4801-4811 https://doi.org/10.1021/pr100513p

Martinez M.T.P, Martinez A.B., Crack J.C., Holmes J.D., Svistunenko D.A., Johnston A.W.B., Cheesman M.R., Todd J.D., Le Brun N.E., (2017). Sensing iron availability via the fragile [4Fe-4S] cluster of the bacterial transcriptional repressor RirA. *Chemical Science*. Vol. 8(12):8451-8463 https://doi.org/10.1039/C7SC02801F

McCormick J.R., Flärdh K., (2012). Signals and regulators that govern *Streptomyces* development. *FEMS Microbiology Reviews*. Vol.36(1):206-231 https://doi.org/10.1111/j.1574-6976.2011.00317.x

McCormick J.R., Su E.P., Driks A., Losick R., (1994). Growth and viability of *Streptomyces coelicolor* mutant for the cell division gene *ftsZ. Molecular Microbiology*. Vol.14(2):243-254 https://doi.org/10.1111/j.1365-2958.1994.tb01285.x

McLean K.J., Sabri M., Marshall K.R., Lawson R.J., Lewis D.G., Clift D., Balding P.R., Dunford A.J., Warman A.J., McVey J.P., Quinn A-M., Sutcliffe M.J., Scrutton N.S., Munro A.W., (2005). Biodiversity of cytochrome P450 redox systems. *Biochemical Society Transactions* Vol.33(4):796–801 https://doi.org/10.1042/BST0330796

Mendez C., Chater K.F., (1987). Cloning of WhiG, a gene critical for sporulation of *Streptomyces coelicolor* A3(2). *Journal of Bacteriology*. Vol.169(12):5715-5720 https://doi.org/10.1128/jb.169.12.5715-5720.1987

Merrick M.J., (1976). A morphological and genetic mapping study of bald colony mutants of *Streptomyces coelicolor*. Vol.96(2):299-315 https://doi.org/10.1099/00221287-96-2-299

Molle V., Buttner M.J., (2000a). Different alleles of the response regulator gene bldM arrest *Streptomyces coelicolor* development at distinct stages. *Molecular Microbiology*. Vol.36(6):1265:1278 https://doi.org/10.1046/j.1365-2958.2000.01977.x

Molle V., Palframan W.J., Findlay K.C., Buttner M.J., (2000b) WhiD and WhiB, homologous proteins required for different stages of sporulation in *Streptomyces coelicolor* A3(2). *Journal of Bacteriology*. Vol.182(5):1286-1295 https://doi.org/10.1128/JB.182.5.1286-1295.2000

Möller M.N., Rios N., Trujillo M., Radi R., Denicola A., Alvarez B., (2019). Detection and quantification of nitric oxide-derived oxidants in biological systems. *Journal of Biological Chemistry*.Vol.294(40):14776-14802 https://doi.org/10.1074/jbc.rev119.006136

Morris R.P., Nguyen L., Gatfield J., Thompson C.J., (2005). Ancestral antibiotic resistance in *Mycobacterium tuberculosis*. *PNAS*. Vol.102(34):12200-12205 https://doi.org/10.1073/pnas.0505446102

Müller A.U Imkamp F., Weber-Ban E., (2018). The mycobacterial LexA/RecA-independent DNA damage response is controlled by PafBC and the Pup-proteasome system. *Cell Reports*. Vol.23(12):3551-3564 https://doi.org/10.1016/j.celrep.2018.05.073

Müller A.U., Leibundgut M., Ban N., Weber-Ban E., (2019). Structure and functional implications of WYL domain-containing bacterial DNA damage response regulator PafBC. *Nature Communications.* Vol.10, 4653 (2019). https://doi.org/10.1038/s41467-019-12567-x

Muller, A.U., Kummer, E., Schilling, C.M., Ban, N., Weber-Ban, E. (2021a). Transcriptional control of mycobacterial DNA damage response by sigma adaptation. *Science Advances*. Vol.7(49):eabl4064 https://doi.org/10.1126/sciadv.abl4064

Munnoch J., Martinez M., Svistunenko D., Crack J.C., Le Brun N.E., Hutchings M.I., (2016). Characterization of a putative NsrR homologue in *Streptomyces venezuelae* reveals a new member of the Rrf2 superfamily. *Nature Scientific Reports.* Vol.6:31597 https://doi.org/10.1038/srep31597

Munnoch J.T., Martinez M.T.P., Svistunenko D.A., Crack J.C., Le Brun N.E., Hutchings M.I., (2016). Characterization of a putative NsrR homologue in *Streptomyces venezuelae* reveals a new member of the Rrf2 superfamily. *Nature Scientific Reports*. Vol.6:31597 https://doi.org/10.1038/srep31597

Murakami K., Mitchell T., Nishimura J.S., (1972). Nucleotide specificity of *Escherichia coli* succinic thiokinase: Succinyl coenzyme A-stimulated nucleoside diphosphate kinase activity of the enzyme. *Journal of Biological Chemistry*. Vol.247(19):6247-6252 https://doi.org/10.1016/S0021-9258(19)44789-3

Murarka P., Keshav A., Meena B.K., Srivastava P., (2020). Functional characterisation of the transcription regulator WhiB1 from Gordonia sp. IITR100. *Microbiology*. Vol.166(12):1181-1190 https://doi.org/10.1099/mic.0.000985.

Nah J-H., Park S-H., Yoon H-M., Choi S-S., Lee C-H., Kim E-S., (2012). Identification and characterization of wblA-dependent tmcT regulation during tautomycetin biosynthesis in *Streptomyces* sp. CK4412. *Biotechnology Advances*. Vol.30(1):202-209 https://doi.org/10.1016/j.biotechadv.2011.05.004.

Nakajima S., Satoh Y., Yanashima K., Matsui T., Dairi T., (2015). Ergothioneine protects *Streptomyces coelicolor* A3(2) from oxidative stresses. *Journal of Bioscience and Bioengineering*. Vol.120(3):294-298 https://doi.org/10.1016/j.jbiosc.2015.01.013

Nesvizhskii A.I., Vitek O., Aebersold R., (2007). Analysis and validation of proteomic data generated by tandem mass spectrometry. *Nature Methods*. Vol. 4(10):787-97. https://doi.org/10.1038/nmeth1088

Newton G.L., Bewley C.A., Dwyer T.J., Horn R., Aharonoqitz Y., Cohen G., Davies J., Faulkner J., Fahey R.C., (1995). The structure of U17 isolated from *Streptomyces clavuligerus* and its properties as an antioxidant thiol. *European Journal of Biochemistry*. Vol.230(2):821-825 https://doi.org/10.1111/j.1432-1033.1995.0821h.x

Newton G.L., Buchmeier N., Fahey R.C., (2008). Biosynthesis and functions of mycothiol, the unique protective thiol of Actinobacteria. *Microbiology and Molecular Biology Reviews*. Vol.72(3):471-494 https://doi.org/10.1128%2FMMBR.00008-08

Newton G.L., Fahey R.C., Cohen G., Aharonowitz Y., (1993). Low-molecular-weight thiols in streptomycetes and their potential role as antioxidants. *Journal of Bacteriology*. Vol.175(9):2734-2742 https://doi.org/10.1128%2Fjb.175.9.2734-2742.1993

Nodwell J.R., Losick R., (1998). Purification of an extracellular signaling molecule involved in production of aerial mycelium by *Streptomyces coelicolor*. *Journal of Bacteriology*. Vol.180(5):1334-1337 https://doi.org/10.1128%2Fjb.180.5.1334-1337.1998

Nodwell J.R., McGovern K., Losick R., (1996). An oligopeptide permease responsible for the import of an extracellular signal governing aerial mycelium formation in *Streptomyces coelicolor*. *Molecular Microbiology*. Vol.22(5):881-893 https://doi.org/10.1046/j.1365-2958.1996.01540.x

Noh J-H., Kim S-H., Lee H-N., Lee S.Y., Kim E-S., (2010) Isolation and genetic manipulation of the antibiotic down-regulatory gene, wblA ortholog for doxorubicin-producing *Streptomyces* strain improvement. *Applied Microbiology and Biotechnology*. Vol.86:1145-1153 https://doi.org/10.1007/s00253-009-2391-z

O'Donnell V.B., Freeman B.A., (2001). Interactions Between Nitric Oxide and Lipid Oxidation Pathways. *Circulation Research.* Vol.88(1):12-21 https://doi.org/10.1161/01.RES.88.1.12

Oda K., Koyama T., Murao S., (1979). Purification and properties of a proteinaceous metallo-proteinase inhibitor from *Streptomyces nigrescens* TK-23. *Biochimica et Biophysica Acta*. Vol.571(1):147-156 https://doi.org/10.1016/0005-2744(79)90235-3

Okamoto S., Lezhava A., Hosaka T., Okamoto-Hosoya Y., Ochi K., (2003) Enhanced expression of S-adenosylmethionine synthetase causes overproduction of actinorhodin in *Streptomyces coelicolor* A3(2). *Journal of Bacteriology*. Vol.185(2):601-609 https://doi.org/10.1128/jb.185.2.601-609.2003

Olano C., Lombó F., Méndez C., Salas J.A., (2008). Improving production of bioactive secondary metabolites in actinomycetes by metabolic engineering. *Metabolic Engineering*. Vol.10(5):281–292. https://doi.org/10.1016/j.ymben.2008.07.001

Overbeek R., Fonstein M., D'Souza M., Pusch G.D., Maltsev N., (1999). The use of gene clusters to infer functional coupling. *PNASUSA* Vol.96:2896–2901 https://doi.org/10.1073/pnas.96.6.2896

Paget M.S., Kang J.G., Roe J.H., Buttner M.J., (1998). SigmaR, an RNA polymerase sigma factor that modulates expression of the thioredoxin system in response to oxidative stress in *Streptomyces coelicolor* A3(2). *EMBO Journal.* Vol.17(19):5776-82 https://doi.org/10.1093/emboj/17.19.5776

Panigrahi A., O'Malley B.W., (2021). Mechanisms of enhancer action: the known and the unknown. *Genome Biology*. Vol.22(1):108 https://doi.org/10.1186/s13059-021-02322-1

Parashar A, Colvin K.R., Bignell D.R.D., Leskiw B.K., (2009). BldG and SCO3548 interact antagonistically to control key developmental processes in *Streptomyces coelicolor*. *Journal of Bacteriology.* Vol.191(8):2541-2550 https://doi.org/10.1128%2FJB.01695-08

Park H-S., Shin S-K., Yang Y-Y., Kwon H-J., Suh J-W., (2005). Accumulation of S-adenosylmethionine induced oligopeptide transporters including BldK to regulate differentiation events in *Streptomyces coelicolor* M145. *FEMS Microbiology Letters*. Vol.249(2):199-206 https://doi.org/10.1016/j.femsle.2005.05.047

Park J.C., Park J-S., Kim Y., Kim P., Kim E.S., Lee H-S., (2016). SpiE interacts with *Corynebacterium glutamicum* WhcE and is involved in heat and oxidative stress responses. *Applied Microbiology and Biotechnology*. Vol.100(9)4063-4072 https://doi.org/10.1007/s00253-016-7440-9

Park J-H., Lee J-H., Roe J-H., (2019). SigR, a hub of multilayered regulation of redox and antibiotic stress responses. *Molecular Microbiology*. Vol.112(2):420-431 https://doi.org/10.1111/mmi.14341

Pei H-H., Hilal T., Chen Z.A., Huang Y-C., Gao Y., Said N., Loll B., Rappsilber J., Belogurov G.A., Artsimovitch I., Wahl M.C., (2020). The δ subunit and NTPase HelD institute a two-pronged mechanism for RNA polymerase recycling. *Nature Communications*. Vol.11:6418 https://doi.org/10.1038/s41467-020-20159-3

Persson J., Chater K.F., Flärdh K., (2013). Molecular and cytological analysis of the expression of *Streptomyces* sporulation regulatory gene whiH. *FEMS Microbiology Letters*. Vol.341(2):96-105 https://doi.org/10.1111/1574-6968.12099

Piette A., Derouaux A., Gerkens P., Noens E. E., Mazzucchelli G., Vion S., Koerten H.K., Titgemeyer F., De Pauw E., Leprince P., van Wezel G.P., Galleni M., Rigali S., (2005). From dormant to germinating spores of *Streptomyces coelicolor* A3(2): new perspectives from the crp null mutant. *Journal of Proteome Research.* Vol.4(5):1699–1708. https://doi.org/10.1021/pr050155b

Płachetka M., Krawiec M., Zakrzewska-Czerwińska J., Wolański M., (2021). AdpA positively regulates morphological differentiation and chloramphenicol biosynthesis in *Streptomyces venezuelae*. *Microbiology Spectrum*. Vol.9(3):e0198121. https://doi.org/10.1128/spectrum.01981-21

Poole R.K., (2020) Flavohaemoglobin: the pre-eminent nitric oxide–detoxifying machine of microorganisms. *F1000 Research.* Vol.9(F1000 Faculty Rev.):7 https://doi.org/10.12688%2Ff1000research.20563.1

Poralla K., Muth G., Härtner T., (2000). Hopanoids are formed during transition from substrate to aerial hyphae in *Streptomyces coelicolor* A3(2). *FEMS Microbiology Letters*. Vol.189(1):93-95 https://doi.org/10.1111/j.1574-6968.2000.tb09212.x

Pospíšil S., Halada P., Petříček M., Sedmera P., (2007). Glucosylglycerate is an osmotic solute and an extracellular metabolite produced by *Streptomyces caelestis*. *Folia Microbiologica*. Vol.52(5):451-461 https://doi.org/10.1007/bf02932103

Purushotham G., Sarva K.B., Blaszczyk E., Rajagopalan M., Madijaru M.V., (2015). *Mycobacterium tuberculosis* oriC sequestration by MtrA response regulator. *Molecular Microbiology*. Vol.98(3):586-604. https://doi.org/10.1111%2Fmmi.13144

Rabyk M., Ostash B ., Rebets Y., Walker S., Fedorenko V., (2011). *Streptomyces ghanaensis* pleiotropic regulatory gene wblAgh influences morphogenesis and moenomycin production. *Biotechnology Letters*. Vol.33:2481-2486 https://doi.org/10.1007/s10529-011-0728-z

Radi R., (2004). Nitric oxide, oxidants, and protein tyrosine nitration. *PNAS USA.* Vol.101(12):4003-4008 https://doi.org/10.1073/pnas.0307446101

Raffaelle M., Kanin E.I., Vogt J., Burgess R.R., Ansari A.Z., (2005). Holoenzyme switching and stochastic release of sigma factors from RNA polymerase *in vivo*. *Molecular Cell*. Vol.20(3):357-366 https://doi.org/10.1016/j.molcel.2005.10.011

Raghnunand T.R., Bishai W.R., (2006). *Mycobacterium smegmatis* whmD and its homologue *Mycobacterium tuberculosis* whiB2 are functionally equivalent. *Microbiology.* Vol.152(pt.9):2735-2747 https://doi.org/10.1099/mic.0.28911-0

Raju R.M., Jedrychowski M.P., Wei J.R., Pinkham J.T., Park A.S., O'Brien K., Rehren G., Schnappinger D., Gygi S.P., Rubin E.J., (2014). Post-translational regulation via Clp protease is critical for survival of *Mycobacterium tuberculosis*. *PLOS Pathogens*. Vol.10(3):e1003994. https://doi.org/10.1371/journal.ppat.1003994

Ramón-García S., Ng C., Jensen P.R., Dosanjh M., Burian J., Morris R.P., Folcher M., Eltis L.D., Grzesiek S., Nguyen L., Thompson C.J., (2013). WhiB7, an Fe-S-dependent transcription factor that activates species-specific repertoires of drug resistance determinants in Actinobacteria. *Journal of Biological Chemistry*. Vol.288(48):34514-34528 https://doi.org/10.1074%2Fjbc.M113.516385

Rand L., Hinds J., Springer B., Sander P., Buxton R.S., Davis E.O., (2003) The majority of inducible DNA repair genes in *Mycobacterium tuberculosis* are induced independently of RecA. *Molecular Microbiology*. Vol.50(3):1031-1042 https://doi.org/10.1046/j.1365-2958.2003.03765.x

Raney K.D., Byrd A.K., Aarattuthodiyil S., (2012). Structure and mechanisms of SF1 DNA helicases. *Advances in Experimental Medicine and Biology*. Vol.767:17-46 https://doi.org/10.1007/978-1-4614-5037-5_2

Reinhardt L., Thomy D., Lakemeyer M., Westermann L.M., Ortega J., Sieber S.A., Sass P., Brötz-Oesterhelt H., (2022). Antibiotic acyldepsipeptides stimulate the *Streptomyces* Clp-ATPase/ClpP complex for accelerated proteolysis. *mBio*. Vol.13(6):e01413-22 https://doi.org/10.1128/mbio.01413-22

Revill P.W., Bibb M.J., Scheu A-K., Kieser H.J., Hopwood D.A., (2001). β-Ketoacyl acyl carrier protein synthase III (FabH) is essential for fatty acid biosynthesis in *Streptomyces coelicolor* A3(2). *Journal of Bacteriology.* Vol.183(11):3526-3530 https://doi.org/10.1128/jb.183.11.3526-3530.2001

Rhee K.Y., de Carvalho L.P.S., Bryk R., Ehrt S., Marrero J., Park S.W., Schnappinger D., Venugopal A., Nathan C., (2011). Central carbon metabolism in *Mycobacterium tuberculosis*: an unexpected frontier. *Trends in Microbiology*. Vol.19(7):307-314 https://doi.org/10.1016/j.tim.2011.03.008

Ribeiro J.M., Hazzard J.M., Nussenzveig R.H., Champagne D.E., Walker F.A., (1993). Reversible binding of nitric oxide by a salivary heme protein from a bloodsucking insect. *Science*. Vol.260(5107):539-541 https://doi.org/10.1126/science.8386393

Rico S., Santamaria R.I., Yepes A., Rodríguez H., Laing E., Bucca G., Smith C.P., Díaz M., (2014). Deciphering the regulon of *Streptomyces coelicolor* AbrC3, a positive response regulator of antibiotic production. *Applied and Environmental Microbiology*. Vol.80(8):2417-2428 https://doi.org/10.1128%2FAEM.03378-13

Rigali S, Titgemeyer F, Barends S, Mulder S, Thomae AW, Hopwood DA, van Wezel GP., (2008). Feast or famine: the global regulator DasR links nutrient stress to antibiotic production by *Streptomyces*. *EMBO Reports*. Vol.9(7):670-675 https://doi.org/10.1038/embor.2008.83

Rigali S., Nothaft H., Noens E.E., Schlicht M., Colson S., Müller M., Joris B., Koerten H.K., Hopwood D.A., Titgemeyer F., van Wezel G.P., (2006). The sugar phosphotransferase system of *Streptomyces coelicolor* is regulated by the GntR-family regulator DasR and links N-acetylglucosamine metabolism to the control of development. *Molecular Microbiology*. Vol.61(5):1237-1251 https://doi.org/10.1111/j.1365-2958.2006.05319.x

Robinson J.T., Thorvaldsdóttir H., Winckler W., Guttman M., Lander E.S., Getz G., Mesirov J.P., (2011). Integrative Genomics Viewer. *Nature Biotechnology* Vol.29(1):24-26. https://doi.org/10.1038%2Fnbt.1754.

Roche B., Aussel L., Ezraty B., Mandin P., Py B., Barras F., (2013). Iron/sulfur proteins biogenesis in prokaryotes: Formation, regulation and diversity. *BBA – Bioenergetics*. Vol.1827(3):455-469 https://doi.org/10.1016/j.bbabio.2012.12.010

Rodŕiguez E., Banchio C., Diacovich L., Bibb M.J., Gramajo H., (2001). Role of an essential acyl coenzyme A carboxylase in the primary and secondary metabolism of *Streptomyces coelicolor* A3(2). *Applied and Environmental Microbiology*. Vol.67(9):4166-4176 https://doi.org/10.1128/AEM.67.9.4166-4176.2001

Rodŕiguez E., Gramajo H., (1999) Genetic and biochemical characterization of the α and β components of a propionyl-CoA carboxylase complex of *Streptomyces coelicolor* A3(2) . Vol.145(11):3109-3119 https://doi.org/10.1099/00221287-145-11-3109

Rohmer M., Bouvier-Nave P., Ourisson G., (1984). Distribution of hopanoid triterpenes in prokaryotes. *Microbiology*. Vol.130(5):1137-1150 https://doi.org/10.1099/00221287-130-5-1137

Rondon M.R., Trzebiatowski J.R., Escalante-Semerena J.C., (1997). Biochemistry and molecular genetics of cobalamin biosynthesis. *Progress in Nucleic Acid Research and Molecular Biology*. Vol.56:347-384 https://doi.org/10.1016/S0079-6603(08)61010-7

Ruban-Osmialowska B., Jakimowicz D., Smulczyk-Krawczyszyn A., Chater K. F., and Zakrzewska-Czerwinska J. (2006). Replisome localization in vegetative and aerial hyphae of *Streptomyces coelicolor*. *Journal of Bacteriology*. Vol.188(20):7311–7316 https://doi.org/10.1128/jb.00940-06

Rubbo H., Radi R., Trujillo M., Telleri R., Kalyanaraman B., Barnes S., Kirk M., Freeman B.A., (1994). Nitric Oxide regulation of superoxide and peroxynitrite-dependent lipid peroxidation. Formation of novel nitrogen-containing oxidized lipid derivatives. *Journal of Biological Chemistry*. Vol.269(42):26066–26075 https://doi.org/10.1016/S0021-9258(18)47160-8

Russell R.R., Taegtmeyer H., (2013) Editor(s): William J. Lennarz, M. Daniel Lane. *Anaplerosis* in *Encyclopedia of Biological Chemistry* (Second Edition). Academic Press Pages 105-110, ISBN 9780123786319, https://doi.org/10.1016/B978-0-12-378630-2.00395-9

Rybniker J., Nowag A., van Gumpel E., Nissen N., Robinson N., Plum G., Hartmann P., (2010). Insights into the function of the WhiB-like protein of mycobacteriophage TM4--a transcriptional inhibitor of WhiB2. *Molecular Microbiology*. Vol.77(3):642-657 https://doi.org/10.1111/j.1365-2958.2010.07235.x

Ryding N.J., Kelemen G.H., Whatling C.A., Flärdh K., Buttner M.J., Chater K.F., (1998). A developmentally regulated gene encoding a repressor-like protein is essential for sporulation in *Streptomyces coelicolor* A3(2). *Molecular Microbiology*. Vol.29(1):343-357 https://doi.org/10.1046/j.1365-2958.1998.00939.x

Sáenz J.P., Grosser D., Bradley A.S., Simons K., (2012). Hopanoids as functional analogues of cholesterol in bacterial membranes. *PNAS USA*. Vol.112(38):11971-11976 https://doi.org/10.1073/pnas.1515607112

Saini V., Farhana A., Steyn A.J.C., (2012). *Mycobacterium tuberculosis* whiB3: A novel iron–sulfur cluster protein that regulates redox homeostasis and virulence. *Antioxidants and Redox Signalling*. Vol.16(7):687-697 https://doi.org/10.1089%2Fars.2011.4341

San Roman S.A., Facey P.D., Fernández-Martínez L., Rodriguez C., Vallin C., Del Sol R., Dyson P., (2010). A heterodimer of EsxA and EsxB is involved in sporulation and is secreted by a type VII secretion system in *Streptomyces coelicolor*. *Microbiology*. Vol.156(6):1719-1729 https://doi.org/10.1099/mic.0.037069-0

Sandoval-Calderón M., Guan Z., Sohlenkamp C., (2017). Knowns and unknowns of membrane lipid synthesis in streptomycetes. *Biochimie*. Vol.141:21-29 https://doi.org/10.1016%2Fj.biochi.2017.05.008

Santamaría R.I., Sevillano L., Martín J., González I., Díaz M., (2018). The XRE-DUF397 protein pair, Scr1 and Scr2, acts as a strong positive regulator of antibiotic production in *Streptomyces*. *Frontiers in Microbiology*. Vol.9:2791 https://doi.org/10.3389/fmicb.2018.02791

Santos-Beneit F., Roberts D.M., Cantlay S., McCormick J.R., Effrington J., (2014) A mechanism for FtsZ-independent proliferation in *Streptomyces*. *Nature Communicatons*. Vol.8:1378 https://doi.org/10.1038/s41467-017-01596-z

Sasaki Y., Oguchi H., Kobayashi T., Kusama S., Sugiura R., Kenta Moriya K., Hirata T., Yukioka Y., Takaya N., Yajima S., Ito S., Okada K., Ohsawa K., Ikeda H., Takano H., Ueda K., Shoun H., (2016) Nitrogen oxide cycle regulates nitric oxide levels and bacterial cell signaling. *Nature Scientific Reports*. Vol.6:22038 https://doi.org/10.1038/srep22038

Sasaki Y., Takaya N., Morita A., Nakamura A., Shoun H., (2014). Nitrite formation from organic nitrogen by *Streptomyces antibioticus* supporting bacterial cell growth and possible involvement of nitric oxide as an intermediate. *Bioscience Biotechnology Biochemistry*. Vol.78(9):1592–1602 https://doi.org/10.1080/09168451.2014.932665

Schlimpert S., Flärdh K., Buttner M., (2016). Fluorescence time-lapse imaging of the complete *S. venezuelae* life cycle using a microfluidic device. *Journal of Visualised Experiments*. Vol.28(108):53863 https://doi.org/10.3791/53863

Schlimpert S., Wasserstrom S., Chandra G., Bibb M.J., Findlay K.C., Flärdh K., Buttner M., (2017). Two dynamin-like proteins stabilize FtsZ rings during *Streptomyces* sporulation *PNAS USA*. Vol.114(30):E6176-6183 https://doi.org/10.1073/pnas.1704612114

Schumacher M.A., Bush M.J., Bibb M.J., Ramos-León F., Chandra G., Seng W., Buttner M.J., (2018). The crystal structure of the RsbN-σBldN complex from *Streptomyces venezuelae* defines a new structural class of anti-σ factor. *Nucleic Acids Research*. Vol.46(14):7405-7417 https://doi.org/10.1093/nar/gky493

Schumacher M.A., Zeng W., Findlay K.C., Buttner M.J., Brennan R.G., Tschowri N., (2017). The *Streptomyces* master regulator BldD binds c-di-GMP sequentially to create a functional $BldD_2$-$(c\text{-}di\text{-}GMP)_4$ complex. *Nucleic Acids Research*. Vol.45(11):6923-6933 https://doi.org/10.1093/nar/gkx287

Schürmann M., Wübbeler J.H., Grote J., Steinbüchel A., (2011). Novel reaction of succinyl coenzyme A (Succinyl-CoA) synthetase: Activation of 3-Sulfinopropionate to 3-sulfinopropionyl-CoA in *Advenella mimigardefordensis* strain DPN7T during degradation of 3,3′-dithiodipropionic acid. *Journal of Bacteriology*. Vol.193(12):3078-3089 https://doi.org/10.1128%2FJB.00049-11

Seeram S.S., Hiraga K., Oda K., (1997). Resynthesis of reactive site peptide bond and temporary inhibition of *Streptomyces* metalloproteinase inhibitor. *The Journal of Biochemistry.* Vol.122(4):788-794 https://doi.org/10.1093/oxfordjournals.jbchem.a021824

Seipke R.F, Loria R., (2009). Hopanoids are not essential for growth of *Streptomyces scabies* 87-22. *Journal of Bacteriology*. Vol.191(16):5216-23. https://doi.org/10.1128/jb.00390-09

Sevcikova B., Rezuchova B., Homerová D., Kormanec J., (2010) The anti-anti-sigma factor BldG is involved in activation of the stress response sigma factor σH in *Streptomyces coelicolor* A3(2). *Journal of Bacteriology*. Vol.192(21):5674-5681 https://doi.org/10.1128%2FJB.00828-10

Sevcikova B., Rezuchova B., Mazurakova V., Homerová D., Novakova R., Feckova L., Kormanec J., (2021). Cross-recognition of Promoters by the nine sigB homologues present in

Streptomyces coelicolor A3(2). *International Journal of Molecular Sciences*. Vol.22(15):7849 https://doi.org/10.3390/ijms22157849

Sevcikova B., Rezuchova B., Mingyar E., Homerová D., Novakova R., Feckova L., Feckova L., Kormanec J., (2020). Pleiotropic anti-anti-sigma factor BldG is phosphorylated by several anti-sigma factor kinases in the process of activating multiple sigma factors in *Streptomyces coelicolor* A3(2). *Gene*. Vol.755:144883 https://doi.org/10.1016/j.gene.2020.144883

Sharma V., Kaur R., Salwan R., (2021). *Streptomyces*: host for refactoring diverse bioactive secondary metabolites. *Three Biotech*. Vol.11(7):340 https://doi.org/10.1007%2Fs13205-021-02872-y

Shi Y., Chen X., Elsasser S., Stocks B.B., Tian G., Lee B.H., Shi Y., Zhang N., de Poot S.A., Tuebing F, Sun S., Vannoy J., Tarasov S.G., Engen J.R., Finley D., Walters K.J., (2016). Rpn1 provides adjacent receptor sites for substrate binding and deubiquitination by the proteasome. *Science*. Vol.351(6275):aad9421 https://doi.org/10.1126/science.aad9421

Singh A., Crossman D.K., Mai D., Guidry L., Voskuil M.I., Renfrow M.B., Steyn A.J.C., (2009). *Mycobacterium tuberculosis* WhiB3 maintains redox homeostasis by regulating virulence lipid anabolism to modulate macrophage response. https://doi.org/10.1371/journal.ppat.1000545

Singh A., Guidry L., Narasimhulu K.V., Steyn A.J.C., (2007). *Mycobacterium tuberculosis* WhiB3 responds to O_2 and nitric oxide via its [4Fe-4S] cluster and is essential for nutrient starvation survival. *PNAS*. Vol.104(28):11562-11567 https://doi.org/10.1073/pnas.0700490104

Singh R., Reynolds K.A., (2015). Characterization of FabG and FabI of the *Streptomyces coelicolor* dissociated fatty acid synthase. *ChemBioChem*. Vol.16(4):631-640 https://doi.org/10.1002/cbic.201402670

Smadel J.E., Woodward T.E., Ley Jr. H.L., Lewthwaite R., (1949). Chloramphenicol (chloromycetin) in the treatment of tsutsugamushi disease (scrub typhus). *Journal of Clinical Investigation.* Vol.5(Pt.2):1196-1215 https://doi.org/10.1172%2FJCI102154

Šmídová K., Ziková A., Pospíšil J., Schwarz M., Bobek J., Vohradsky J., (2018). DNA mapping and kinetic modeling of the HrdB regulon in *Streptomyces coelicolor*. *Nucleic Acids Research.* Vol.47(2):621-633 https://doi.org/10.1093/nar/gky1018

Smith L., (2012). *Characterisation of the essential transcription factor, WhiB1, from Mycobacterium tuberculosis*. PhD Thesis: The University of Sheffield, School of Biosciences, Sheffield.

Smith L.J., Stapleton M.R., Buxton R.S., Green J., (2012). Structure-function relationships of the *Mycobacterium tuberculosis* transcription factor WhiB1. *PLOS ONE.* Vol.7(7):e40407 https://doi.org/10.1371/journal.pone.0040407

Smith L.J., Stapleton M.R., Fullstone G.J.M., Crack J.C., Thomson A.J., Le Brun N.E., Hunt D.M., Harvey E., Adinolfi S., Buxton R.S., Green J., (2010). *Mycobacterium tuberculosis* WhiB1 is an essential DNA-binding protein with a nitric oxide-sensitive iron-sulfur cluster. *Journal of Biochemistry*. Vol.432(3):417-427 https://doi.org/10.1042/bj20101440

Soliveri J.A., Gomez J., Bishai W.R., Chater K.F., (2000). Multiple paralogous genes related to the *Streptomyces coelicolor* developmental regulatory gene whiB are present in *Streptomyces* and other actinomycetes. *Microbiology.* Vol.146(Pt.2):333-343 https://doi.org/10.1099/00221287-146-2-333

Som N., (2016) MtrAB-LpqB: a conserved pathway regulating cell division in the phylum Actinobacteria? PhD Thesis: University of East Anglia, School of Biological Sciences, Norwich.

Som N.F., Heine D., Holmes N., Knowles F., Chandra G., Seipke R.F., Hoskisson P.A., Wilkinson B., Hutchings M.I., (2017b). The MtrAB two-component system controls antibiotic production in *Streptomyces coelicolor* A3(2). *Microbiology*. Vol.163(10):1415-1419 https://doi.org/10.1099%2Fmic.0.000524

Som N.F., Heine D., Holmes N.A., Munnoch J.T., Chandra G., Seipke R.F., Hoskisson P.A., Wilkinson B., Hutchings M.I., (2017a). The conserved actinobacterial two-component system MtrAB coordinates chloramphenicol production with sporulation in *Streptomyces venezuelae* NRRL B-65442. *Frontiers in Microbiology*. Vol.8:1145 https://doi.org/10.3389/fmicb.2017.01145

Sorsby A., Ungar J., Crick R.P., (1953). Aureomycin, chloramphenicol, and terramycin in ophthalmology. *British Medical Journal*. Vol.2(4831):301-304 https://doi.org/10.1136/bmj.2.4831.301

Sparacino-Watkins C.E., Tejero J., Sun B., Gauthier M.C., Thomas J., Ragireddy V., Merchant B.A., Wang J., Azarov I., Basu P., Gladwin M.T., (2014). Nitrite reductase and nitric-oxide synthase activity of the mitochondrial molybdopterin enzymes mARC1 and mARC2. *Journal of Biological Chemistry*. Vol.289(15):10345-10358 https://doi.org/10.1074%2Fjbc.M114.555177

Stallings C.L., Stephanou N.C., Chu L., Hochschild A., Nickels B.E., Glickman M.S., (2009). CarD is an essential regulator of rRNA transcription required for *Mycobacterium tuberculosis* persistence. *Cell*. Vol.138(1):146-159 https://doi.org/10.1016%2Fj.cell.2009.04.041

Stapleton M.R., Smith L.J., Hunt D.M., Buxton R.S., Green J., (2012). *Mycobacterium tuberculosis* WhiB1 represses transcription of the essential chaperonin GroEL2. *Tuberculosis*. Vol.92(4):328-332 https://doi.org/10.1016%2Fj.tube.2012.03.001

Starr B.D., Hawley D.K., (1991). TFIID binds in the minor groove of the TATA box. *Cell*. Vol.67(6):1231-1240 https://doi.org/10.1016/0092-8674(91)90299-E

Stevenson C.E.M., Assaad A., Chandra G., Le T.B.K., Greive S.J., Bibb M.J., Lawson D.M., (2013). Investigation of DNA sequence recognition by a streptomycete MarR family transcriptional regulator through surface plasmon resonance and X-ray crystallography. *Nucleic Acids Research*. Vol.41(14):7009-7022 https://doi.org/10.1093%2Fnar%2Fgkt523

Stevenson C.E.M., Lawson D.M., (2021). Analysis of protein-DNA interactions using surface plasmon resonance and a ReDCaT chip. *Protein-Ligand Interactions.* Vol.2263:369-379 https://doi.org/10.1007/978-1-0716-1197-5_17

Stewart M.Y.Y., Bush M.J., Crack J.C., Buttner M.J., Le Brun N.E., (2020) Interaction of the *Streptomyces* Wbl protein WhiD with the principal sigma factor σ^{HrdB} depends on the WhiD [4Fe-4S] cluster. *Journal of Biological Chemistry.* Vol.295(28): 9752-9765 https://www.jbc.org/article/S0021-9258(17)48988-5/fulltext

Stojanovski B.M., Hunter G.A., Na I., Uversky V.N., Jiang R.H.Y., Ferreira G.C., (2009). 5-aminolevulinate synthase catalysis: The catcher in heme biosynthesis. *Molecular Genetics and Metabolism.* Vol.55(1):102-110 https://doi.org/10.1016/j.ymgme.2019.06.003

Strakova E., Bobek J., Zikova A., Vohradsky J., (2013b). Global features of gene expression on the proteome and transcriptome levels in *S. coelicolor* during germination. *PLoS ONE* Vol.8(9):e72842 https://doi.org/10.1371/journal.pone.0072842

Strakova, E., Bobek, J., Zikova, A., Rehulka, P., Benada, O., Rehulkova, H., Kofronova O., Vohradsky J., (2013a). Systems insight into the spore germination of *Streptomyces coelicolor*. *Journal of Proteome Research*. Vol.12(1):525–536 https://doi.org/10.1021/pr300980v

Stratton K.J., Bush M.J., Chandra G., Stevenson C.E.M., Findlay K.C., Schlimpert S., (2022). Genome-wide identification of the LexA-mediated DNA damage response in *Streptomyces venezuelae*. *Journal of Bacteriology*. Vol.204(8):e0010822 https://doi.org/10.1128/jb.00108-22

Sugimoto S., Yamanaka K., Nishikori S., Miyagi A., Ando T., Ogura T., (2010). AAA+ Chaperone ClpX regulates dynamics of prokaryotic cytoskeletal protein FtsZ. *Journal of Biological Chemistry*. Vol.285(9):6648-6657 https://doi.org/10.1074/jbc.M109.080739

Suzuki M., Taguchi S., Yamada S., Kojima S., Miura K.I., Momose H., (1997). A novel member of the subtilisin-like protease family from *Streptomyces albogriseolus*. *Journal of Bacteriology*. Vol.179(2):430-438 https://doi.org/10.1128/jb.179.2.430-438.1997

Tabib-Salazar A., Liu B., Doughty P., Lewis R.A., Ghosh S., Parsy M.L., Simpson P.J., O'Dwyer K., Matthews S.J., Paget M.S., (2013). The actinobacterial transcription factor RbpA binds to the principal sigma subunit of RNA polymerase. *Nucleic Acids Research*. Vol.41:5679–5691 https://doi.org/10.1093/nar/gkt277

Takano E., Tao M., Long F., Bibb M.J., Wang L., Li W., Buttner M.J., Bibb M.J., Deng Z.X., Chater K.F., (2003). A rare leucine codon in adpA is implicated in the morphological defect of bldA mutants of *Streptomyces coelicolor*. *Molecular Microbiology*. Vol.50(2):475-86 https://doi.org/10.1046/j.1365-2958.2003.03728.x

Takano H., Fujimoto M., Urano H., Beppu T., Ueda K., (2011). Cross-interaction of anti-σH factor RshA with BldG, an anti-sigma factor antagonist in *Streptomyces griseus*. *FEMS Microbiology Letters*. Vol.314(2):158-163 https://doi.org/10.1111/j.1574-6968.2010.02155.x

Tan M.P., Sequeira P., Lin W.W., Phong W.Y., Cliff P., Ng S.H., Lee B.H., Camacho L., Schnappinger D., Ehrt S., Dick T., Pethe K., Alonso S., (2010). Nitrate respiration protects hypoxic *Mycobacterium tuberculosis* against acid- and reactive nitrogen species stresses. *PLOS ONE*. Vol.5(10):e13356 https://doi.org/10.1371/journal.pone.0013356

Telkov M. V., Demina G. R., Voloshin S. A., Salina E. G., Dudik T. V., Stekhanova T. N., Mukamolova G.V., Kazaryan K.A., Goncharenko A.V., Young M., Kaprelyants A.S., (2006). Proteins of the Rpf (resuscitation promoting factor) family are peptidoglycan hydrolases. *Biochemistry*. Vol.71(4):414–422. https://doi.org/10.1134/s0006297906040092

Teo G., Liu G., Zhang J., Nesvizhskii A.I., Gingras A-C., Choi H., (2014). SAINTexpress: improvements and additional features in significance analysis of interactome software. *Journal of Proteomics*. Vol.100:37-43 https://doi.org/10.1016%2Fj.jprot.2013.10.023

Teufel F., Armenteros J.J.A., Johansen A.R., Gíslason M.H., Pihl S.I., Tsirigos K.D., Winther O., Brunak S., von Heijne G., Nielsen H., (2022). SignalP 6.0 predicts all five types of signal peptides using protein language models. *Nature Biotechnology*. Vol.40:1023-1025 https://doi.org/10.1038/s41587-021-01156-3

Thanapipatsiri A., Gomez-Escribano J.P., Song L., Bibb M.J., Al-Bassam M., Chandra G., Thamchaipenet A., Challis G.L., Bibb M.J., (2016). Discovery of unusual biaryl polyketides by activation of a silent *Streptomyces venezuelae* biosynthetic gene cluster. *Chembiochem*. Vol.17(`22):2189-2198 https://doi.org/10.1002/cbic.201600396

Tian J., Bryk R., Shi S., Erdjument-Bromage H., Tempst P., Nathan C., (2005). *Mycobacterium tuberculosis* appears to lack α-ketoglutarate dehydrogenase and encodes pyruvate dehydrogenase in widely separated genes. *Molecular Microbiology*. Vol.57(3):859-868 https://doi.org/10.1111/j.1365-2958.2005.04741.x

Tian Y., Fowler K., Findlay K., Tan H., Chater K.F., (2007). An unusual response regulator influences sporulation at early and late stages in *Streptomyces coelicolor*. *Journal of Bacteriology*. Vol.189(7):2873-85 https://doi.org/10.1128/jb.01615-06

Tillotson R.D., Wösten, H.A.B., Richter M., Willey J.M., (1998). A surface active protein involved in aerial hyphae formation in the filamentous fungus *Schizophillum* commune restores the capacity of a bald mutant of the filamentous bacterium *Streptomyces coelicolor* to erect aerial

structures. *Molecular Microbiology*. Vol.30(3):595-602 https://doi.org/10.1046/j.1365-2958.1998.01093.x

Tiwari P., Kauila P., Guptasarma P., (2019). Understanding anomalous mobility of proteins on SDS-PAGE with special reference to the highly acidic extracellular domains of human E- and N-cadherins. *Electrophoresis*. Vol.40(9):1273-1281 https://doi.org/10.1002/elps.201800219

Traag B.A., Kelemen G.H., van Wezel G.P., (2004). Transcription of the sporulation gene ssgA is activated by the IclR-type regulator SsgR in a whi-independent manner in *Streptomyces coelicolor* A3(2). *Molecular Microbiology*. Vol.53(3):985-1000 https://doi.org/10.1111/j.1365-2958.2004.04186.x

Tramonti A., Nardella C., di Salvo M.L., Pascarella S., Contestabile R., (2018). The MocR-like transcription factors: pyridoxal 5′-phosphate-dependent regulators of bacterial metabolism https://doi.org/10.1111/febs.14599

Tripathi A., Anand K., Das M., O'Niel R.A., Sabarinath P.S., Thakur C., Reddy R.R.L., Rajmani R.S., Chandra N., Laxman S., Singh A., (2022). *Mycobacterium tuberculosis* requires SufT for Fe-S cluster maturation, metabolism, and survival in vivo. *PLOS Pathogens*. Vol.18(4):e1010475 https://doi.org/10.1371/journal.ppat.1010475

Tsai H-H., Huang C-H., Tessmer I., Erie D.A., Chen C.W., (2011). Linear Streptomyces plasmids form superhelical circles through interactions between their terminal proteins. *Nucleic Acids Research*. Vol.39(6):2165-2174 https://doi.org/10.1093/nar/gkq1204

Tschowri N., Schumacher M.A., Schlimpert S., Findlay K.C., Brennan R.G., (2014). Tetrameric c-di-GMP mediates effective transcription factor dimerization to control *Streptomyces* development. *Cell*. Vol.158(5):1136-1147 https://doi.org/10.1016%2Fj.cell.2014.07.022

Ugalde S.O., de Koning C.P., Wallraven K., Bruyneel B., Vermeulen N.P.E., Grossmann T.N., Bitter W., Commandeur J.N.M., Vos J.C., (2018). Linking cytochrome P450 enzymes from *Mycobacterium tuberculosis* to their cognate ferredoxin partners. *Applied Microbiology and Biotechnology.* Vol.102:9231-9242 https://doi.org/10.1007%2Fs00253-018-9299-4

Uplekar S., Rougemont J., Cole S.T., Sala C., (2013). High-resolution transcriptome and genome-wide dynamics of RNA polymerase and NusA in *Mycobacterium tuberculosis*. *Nucleic Acids Research*. Vol.41(2):961-977 https://doi.org/10.1093%2Fnar%2Fgks1260

Urem M., van Rossum T., Bucca G., Moolenar G.F., Laing E., Świątek-Połatyńska M.A., Willemse J., Tenconi E., Rigali S., Goosen N., Smith C.P., van Wezel G.P., (2016). OsdR of *Streptomyces coelicolor* and the dormancy regulator DevR of *Mycobacterium tuberculosis* control overlapping regulons. *mSystems* Vol.1(3):e00014-16 https://doi.org/10.1128/msystems.00014-16

van Wezel G.P., Bibb M.J., (1996) A novel plasmid vector that uses glucose kinase gene (glkA) for the positive selection of stable gene disruptants in *Streptomyces*. *Gene*. Vol.182(1-2):229–230 https://doi.org/10.1016/s0378-1119(96)00563-x

Vargas D., Hageman S., Gulati M., Nobile C.J., Rawat M., (2016). S-nitrosomycothiol reductase and mycothiol are required for survival under aldehyde stress and biofilm formation in *Mycobacterium smegmatis*. *IUBMB Life*. Vol.68(8):621-628 https://doi.org/10.1002/iub.1524

Vine C.E., Cole V., (2011) Nitrosative stress in *Escherichia coli*: reduction of nitric oxide. *Biochemical Society Transactions*. Vol.39(1):213-215 https://doi.org/10.1042/bst0390213

Vinella D., Brochier-Armanet C., Loiseau L., Talla E., Barras F., (2009). Iron–sulfur (Fe/S) protein biogenesis: phylogenomic and genetic studies of A-type carriers. *PLoS Genetics*. Vol.5(5):e1000497 https://doi.org/10.1371/journal.pgen.1000497

Voelker U., Dufour A., Haldenwang W.G., (1995). The *Bacillus subtilis* rsbU gene product is necessary for RsbX-dependent regulation of σ^B. *Journal of Bacteriology*. Vol.177(1):114-122 https://doi.org/10.1128/jb.177.1.114-122.1995

Vogt R.N., Steenkamp D.J., Zheng R., Blanchard J.S., (2003). The metabolism of nitrosothiols in the Mycobacteria: identification and characterization of S-nitrosomycothiol reductase. *The Biochemical Journal*. Vol.374(Pt3):657-666 https://doi.org/10.1042/bj20030642

Vollmer B., Steblau N., Ladwig N., Mayer C., Macek B., Mitousis L., Sigle S., Walter A., Wohlleben W., Muth G., (2019). Role of the *Streptomyces* spore wall synthesizing complex SSSC in differentiation of Streptomyces coelicolor A3(2). *International Journal of Medical Microbiology*. Vol.309(6):151327 https://doi.org/10.1016/j.ijmm.2019.07.001

Wan T., Li S., Beltran D.G., Schacht A., Zhang L., Becker D.F., Zhang L., (2020). Structural basis of non-canonical transcriptional regulation by the σ^A-bound iron-sulfur protein WhiB1 in *M. tuberculosis*. *Nucleic Acids Research*. Vol.48(2):501-516 https://doi.org/10.1093/nar/gkz1133

Wang J., Krizowski S., Fischer-Schrader K., Niks D., Tejero J., Sparacino-Watkins C., Wang L., Ragireddy V., Frizzell S., Kelley E.E., Zhang Y., Basu P., Hille R., Schwarz G., Gladwin M.T., (2015). Sulfite Oxidase Catalyzes Single-Electron Transfer at Molybdenum Domain to Reduce Nitrite to Nitric Oxide. Antioxidants & Redox Signaling, Vol.4(23):283-294. https://doi.org/10.1089/ars.2013.5397

Wang J., Zhao G-P., (2009). GlnR positively regulates nasA transcription in *Streptomyces coelicolor*. *Biochemical and Biophysical Research Communications.* Vol.386(1):77-81 https://doi.org/10.1016/j.bbrc.2009.05.147

Wang X.J., Guo S.L., Guo W.Q., Xi D., Xiang W-S., (2009). Role of nsdA in negative regulation of antibiotic production and morphological differentiation in *Streptomyces bingchengensis*. *Journal of Antibiotics*. Vol.62:309-313. https://doi.org/10.1038/ja.2009.33

Wang Y., Cui T., Zhang C., Yang M., Huang Y., Li W., Zhang L., Gao C., He Y., Li Y., Huang F., Zeng J., Huang C., Yang Q., Tian Y., Zhao C., Chen H., Zhang H., He Z-G., (2010). Global protein−protein interaction network in the human pathogen *Mycobacterium tuberculosis* H37Rv. *Journal of Proteome Research*. Vol.9(12):6665-6677 https://doi.org/10.1021/pr100808n

Wawrzynow A., Wojtkowiak D., Marszalek J., Banecki B., Jonsen M., Graves B., Georgopoulos C., Zylicz M., (1995). The ClpX heat-shock protein of *Escherichia coli*, the ATP-dependent substrate specificity component of the ClpP-ClpX protease, is a novel molecular chaperone. *EMBO Journal.* Vol.14(9):1867-1877 https://doi.org/10.1002%2Fj.1460-2075.1995.tb07179.x

Weber-Ban E.U., Reid B.G., Miranker A.D., Horwich A.L., (1999). Global unfolding of a substrate protein by the Hsp100 chaperone ClpA. *Nature*. Vol.401:90-93 https://doi.org/10.1038/43481

Wei J., He L., Niu G., (2018). Regulation of antibiotic biosynthesis in actinomycetes: Perspectives and challenges. *Synthetic and Systems Biotechnology*. Vol3(4):229-235 https://doi.org/10.1016/j.synbio.2018.10.005

Weichsel A., Andersen J.F., Champagne D.E., Walker F.A., Montfort W.R., (1998). Crystal structures of a nitric oxide transport protein from a blood-sucking insect. *Nature Structural and Molecular Biology*. Vol.5:304-309 https://doi.org/10.1038/nsb0498-304

Wiedermannová J., Sudzinová P., Koval' T., Rabatinová A., Šanderova H., Rittich Š., Dohnálek J., Fu Z., Halada P., Lewis P., Krásny L., (2014). Characterization of HelD, an interacting partner of RNA polymerase from *Bacillus subtilis*. *Nucleic Acids Research*. Vol.42(8):5151-5163 https://doi.org/10.1093/nar/gku113

Willemse D., Weber B., Masino L., Warren R.M., Adinolfi S., Pastor A., Williams M.J, (2018). Rv1460, a SufR homologue, is a repressor of the suf operon in *Mycobacterium tuberculosis*. *PLOS One*. Vol.13(7):e0200145 https://doi.org/10.1371/journal.pone.0200145

Willemse J., Borst J.W., de Waal E., Bisseling T., van Wezel G.P., (2011). Positive control of cell division: FtsZ is recruited by SsgB during sporulation of *Streptomyces*. *Genes and Development*. Vol.25(1):89-99 https://doi.org/10.1101/gad.600211

Willey J.M., Schwedock J., Losick R., (1993). Multiple extracellular signals govern the production of a morphogenetic protein involved in aerial mycelium formation by *Streptomyces coelicolor*. *Genes and Development*. Vol.7:895-903 https://doi.org/10.1101/gad.7.5.895

Wolański M., Donczew R., Ostrowska-Kois A., Masiewicz P., Jakimowicz D., Zakrzewska-Czerwinska J., (2011b). The Level of AdpA Directly Affects Expression of Developmental Genes in *Streptomyces coelicolor*. *Journal of Bacteriology*. Vol.192(22):6358-6365 https://doi.org/10.1128/jb.05734-11

Wolański M., Jakimowicz D., Zakrzewska-Czerwińska J., (2012). AdpA, key regulator for morphological differentiation regulates bacterial chromosome replication. *Open Biology.* Vol.2(7):120097 https://doi.org/10.1098/rsob.120097

Wolański M., Wali R., Tilley E., Jakimowicz D., Zakrzewska-Czerwinska J., and Herron P., (2011a). Replisome trafficking in growing vegetative hyphae of *Streptomyces coelicolor* A3(2). *Journal of Bacteriology*. Vol.193(5):1273–1275 https://doi.org/10.1128/jb.01326-10

Wright M. M., Schopfer F.J., Baker P.R.S., Vidyasagar V., Powell P., Chumley P., Iles K.E., Freeman B.A., Agarwal A., (2006) Fatty acid transduction of NO signaling: nitrolinoleic acid potently activates endothelial heme oxygenase 1 expression. *PNAS USA.* Vol.103(11):4299–4304 https://doi.org/10.1073/pnas.0506541103

Wu M., Tao Y., Liu X., Zang J., (2013). Structural basis for phosphorylated autoinducer-2 modulation of the oligomerization state of the global transcription regulator LsrR from *Escherichia coli*. *Journal of Biological Chemistry*. Vol.288(22):15878-15887 https://doi.org/10.1074/jbc.M112.417634

Wu M-L., Gengenbacher M., Chung J.C.S., Chen S.L., Mollenkopf H-J., Kaufmann S.H.E., Dick T., (2016). Developmental transcriptome of resting cell formation in *Mycobacterium smegmatis*. *BMC Genomics.* Vol.17:837 https://doi.org/10.1186/s12864-016-3190-4

Xu D., Kwon H.J., Suh J.W., (2008). S-adenosylmethionine induces bldH and activates secondary metabolism by involving the TTA-codon control of bldH expression in *Streptomyces lividans*. *Archives of microbiology*. Vol.189(4):419-26. https://doi.org/10.1007/s00203-007-0336-4

Xu Z., Wang Y., Chater K.F., Ou H-Y., Xu H.H., Deng Z., Tao M., (2017). Large-scale transposition mutagenesis of *Streptomyces coelicolor* identifies hundreds of genes influencing antibiotic biosynthesis. *Applied and Environmental Microbiology*. Vol.83(6):e02889-16 https://doi.org/10.1128%2FAEM.02889-16

Yagüe P., Lopez-Garcia M.T., Rioseras B., Sanchez J., Manteca A., (2012) New insights on the development of *Streptomyces* and their relationships with secondary metabolite production. *Current Trends Microbiology*. Vol.8:65-73

Yagüe P., Rodríguez-García A., López-García M.T., Martín J.F., Rioseras B., Sánchez J., Manteca A., (2013) Transcriptomic Analysis of *Streptomyces coelicolor* Differentiation in Solid Sporulating Cultures: First Compartmentalized and Second Multinucleated Mycelia Have Different and Distinctive Transcriptomes. *PLOS ONE* Vol.8(3): e60665. https://doi.org/10.1371/journal.pone.0060665

Yan H., Lu X., Sun D., Zhuang S., Chen Q., Chen Z., Li J., Wen Y., (2019). BldD, a master developmental repressor, activates antibiotic production in two *Streptomyces* species. Vol.113(1):123-142 https://doi.org/10.1111/mmi.14405

Yanofsky C., (1981). Attenuation in the control of expression of bacterial operons. *Nature*. Vol.289:751-758 https://doi.org/10.1038/289751a0

Yoo J.S., Oh G.S., Ryoo S., Roe J.H., (2016). Induction of a stable sigma factor SigR by translation-inhibiting antibiotics confers resistance to antibiotics. *Nature Scientific Reports.* Vol.6:28628. https://doi.org/10.1038/srep28628

You, D., Xu, Y., Yin, B. C., and Ye, B. C. (2019). Nitrogen regulator GlnR controls redox sensing and lipids anabolism by directly activating the whiB3 in *Mycobacterium smegmatis*. *Frontiers in Microbiology*. Vol.10:74 https://doi.org/10.3389/fmicb.2019.00074

Yu P., Liu S-P., Bu Q-T., Zhou Z-X., Zhu Z-H., Huang F-L., Li Y-Q., (2014). $WblA_{ch}$, a pivotal activator of natamycin biosynthesis and morphological differentiation in *Streptomyces chattanoogensis* L10, is positively regulated by $AdpA_{ch}$. Vol.80(22):6879:6887 https://doi.org/10.1128/AEM.01849-14

Yu T.W., Hopwood D.A.Y. (1995). Ectopic expression of the *Streptomyces coelicolor* whiE genes for polyketide spore pigment synthesis and their interaction with the act genes for actinorhodin biosynthesis. *Microbiology*. Vol.141(11):2779–2791. https://doi.org/10.1099/13500872-141-11-2779

Yukioka Y., Tanahashi T., Shida K., Oguchi H., Ogawa S., Saita C., Yajima S., Ito S., Ohsawa K., Shoun H., Sasaki Y., (2017). A role of nitrite reductase (NirBD) for NO homeostatic regulation in *Streptomyces coelicolor* A3(2). *FEMS Microbiology Letters*. Vol.364(1):fnw241 https://doi.org/10.1093/femsle/fnw241

Zhai Q., Duan B., Lin C., Liu J., Zhang L., Xia B., (2022). DNA binding mechanism of WhiB4 from *Mycobacterium tuberculosis*. *Magnetic Resonance Letters*. Vol.2(1):17-27 https://doi.org/10.1016/j.mrl.2021.100010

Zhang P., Wu L., Zhu Y., Liu M., Wang Y., Cao G., Chen X-L., Tao M., Pang X., (2017) Deletion of MtrA inhibits cellular development of *Streptomyces coelicolor* and alters expression of developmental regulatory genes. *Frontiers in Microbiology.* Vol.8:2013 https://doi.org/10.3389/fmicb.2017.02013

Zheng W., Zhang C., Li Y., Pearce R., Bell E.W., Zhang Y., (2021). Folding non-homologous proteins by coupling deep-learning contact maps with I-TASSER assembly simulations. *Cell Reports Methods*. 1(3):100014 https://doi.org/10.1016/j.crmeth.2021.100014

Zhi X-Y., Yao J-C., Tang S-K., Huang Y., Li H-W., Li W-J., (2014). The futalosine pathway played an important role in menaquinone biosynthesis during early prokaryote evolution. *Genome Biology and Evolution*. Vol.6(1):149-160 https://doi.org/10.1093%2Fgbe%2Fevu007

Zhu Y., Wang J., Wenya S., Lu T., Li A., Pang X., (2022). Effects of dual deletion of glnR and mtrA on expression of nitrogen metabolism genes in *Streptomyces venezuelae*. *Microbial Biotechnology*. Vol.15(6):1795-1810 https://doi.org/10.1111/1751-7915.14016

Zhu Y., Zhang P., Zhang J., Xu W., Wang X., Wu L., Sheng D., Ma W., Cao G., Chen X-L, Lu Y., Zhang Y-Z, Pang X., (2019). The developmental regulator MtrA binds GlnR boxes and represses nitrogen metabolism genes in *Streptomyces coelicolor*. *Molecular Microbiology*. Vol.112(1):29-45 https://doi.org/10.1111/mmi.14252

Appendices

Table A.1. Primers used in this thesis, their respective orientations and brief descriptions of their uses.

Primer	Ori	Description of Target/Function	Sequence
LBc004	F	*S.coelicolor wblE* amplification	**CCTAGAGAGGTAGCAGCC** ATGGACTGGCGTCACCGCG
LBc002	R	*S.coelicolor wblE* amplification	**gataagtttatc aagctt *TCA***GGCGGAGGCCTGACGA
LB007	F	wblE multiple use / diagnostic primer 1	AGCGTTCACATTCACAAGCA
LB008	R	wblE multiple use / diagnostic primer 2	TTGGCTTCCTCGATCTGCA
LB009	R	wblE multiple use / diagnostic primer 3	GCTCGAATGCTGTGGGTTAC
LB010	R	wblE multiple use / diagnostic primer 4	GTTCACCGCCCCTTTATTCC
LB011	F	*vnz_24260*-situated sgRNA (a)	**ACGC** CCACCGCCGGAGTGGAAAGA
LB012	R	*vnz_24260*-situated sgRNA (a)	**AAAC** TCTTTCCACTCCGGCGGTGG
LB013	F	*wblE* KO HRT 5' primer	ttgccgccgggcgtttttta tctaga GGCGTCCACCAACATGTACAC
LB013ex	F	*vnz_24260* KO HRT 5' primer	ttgccgccgggcgtttttta tctaga ATCAAGCGCCACTTCCGTGACAAG
LB014a	R	(a)sgRNA PAM mutation	CG**A**CGCAGTCCGAGCACGTC GAGCGCCGTTTCGAAGGAC
LB015a	F	(a)sgRNA PAM mutation	GACGTGCTCGGACTGCG**T**CG TCTTTCCACTCCGGCGGT
LB016	R	*wblE* KO HRT central primer	GGTGAATGCATACGCGATGTATGC AAGCTGGTTGCTTGTGAATGTGAAC
LB017	F	*wblE* KO HRT central primer	GTTCACATTCACAAGCAACCAGCTT GCATACATCGCGTATGCATTCACC
LB018	R	*wblE* KO HRT 3' terminal primer (short)	ccttttacggttcctggcctctagaGATGGTCCTCACCGAGATCCT
LB021	R	*vnz_24260* KO HRT 3' terminal primer	ccttttacggttcctggcctctagaACGAAGGTGGTCCTCGACATT
gRNA-test	F	pCRISPomyces-2 gRNA test primer	ATACGGCTGCCAGATAAGGC
LB032	F	ptasRNAi #2 2xNdeI o/h F	ggattccatatgCAGTGGTGGTGGTGGTGGTGCgcatgcCCGGTGTTGCCGATGGGGAAG
LB033	R	ptasRNAi #2 2xNdeI o/h R	ggattccatatgCAGTGGTGGTGGTGGTGGTGCctgcagGGGATTCGTGAAAGCGTTCAC
LB034	R	NFLAG tag genome-to-flag o/l	CCGTCGTGGTCCTTGTAGTC CATGGCTGCTACCTCTCTAGGGT
LB035	F	NFLAG-tag with 034 genomic o/l	ACCCTAGAGAGGTAGCAGCCATG GACTACAAGGACCACGACGG
LB036	R	NFLAG-tag wblE with genomic o/l	GGCGTTGTGACGCCAGTCCAT actaccgccaccgccaga
LB037	F	NFLAG-tag wblE with flag o/l	tctggcggtggcggtagt ATGGACTGGCGTCACAACGC
LB038	F	F-test upstream of PAM in vnz_24260	TTTCGACGCGAGTGTCATCGG

LB040	F	R-test outside LB018/ LB021 KO terminal primers	GGAGTTCGACGAGATCGCCGA
LB041*	F	*wblE* amplification only.	GTGGAAGGGCCCAAAGTCCTTTC
LB041	F	*wblE* – AvrII	ggattc CCTAGG GTGGAAGGGCCCAAAGTCCTTTC
LB041hf	F	*wblE* – AvrII, pSS170 overlap	ctcgagagatgtaca CCTAGG GTGGAAGGGCCCAAAGTCCTTTC
LB042	R	*wblE* - HindIII	ggattc AAGCTT GCGGTGAATGCATACGCGATGTAT
LB042hf	R	*wblE* - HindIII, pSS170 overlap	gataagtttatc AAGCTT tcaGGCGCTGGCGTTACGC
LB043	F	*wblE* – NdeI	ggattc CATATG GACTGGCGTCACAACGC
LB046	F	*wblE* internal sgRNA	ACGC GGGGTCTTCCTCACGACAAA
LB047	R	*wblE* internal sgRNA	AAAC TTTGTCGTGAGGAAGACCCC
LB048	R	vnz_24260 KO HRT central Rev	TCAATTGACCACGAGAAGTGCGCG CATGAGCGCCAGGGTACCTACC
LB049	F	vnz_24260 KO HRT central Fwd	ATGCGCGCACTTCTCGTGGTCAATTGA GTGGAAGGGCCCAAAGTCCTTT
LB050	R	*wblE snt* introducing Rev	CCGCGTTGTGACGCCAGTCCATGGCTGCTACCTCTCTAGGGTGTTA
LB051	F	*wblE snt* introducing Fwd	*CAGCCATGGACTGGCGTCACAACGCGG* TTTGTCGTGAGGAAGACCCCGAG
LB071	R	*wblE*p reverse, overlap with LBc004	GTGACGCCAGTCCAT GGCTGCTACCTCTCTAGGGTGTTACA
LB072	F	*wblE*-NdeI incorporating (pCi)*snt* (pIJ24255$_{SNT}$)	gctg cat ATGGACTGGCGTCACAACGCGG TTTGTCGTGAGGAAGACCCCGAG
LB082n	F	WblE c.o. Fwd amplification NdeI	ctgatcc catatg GACTGGCGTCATAATGCGGTGT
LB083t	R	*WblEc.o.* Rev with no TGA HindIII pET29b o/l	ggaaccgcgtggcag aagctt CGCGCTCGCATTACGCG
LB083ut	R	*WblEc.o.* Rev with TGA-stop HindIII	*ggaaccgcgtggcag aagctt TCACGCGCTCGCATTACGCG*
LB088	F	C9; 37; 40; 46S; D13A fragment adaptor	CAGCCATGGACTGGCGTCAC
LB089	F	CFLAG (Genewiz™) fragment adaptor	TCGC AACCGGGCGCGTAACGC
LB108	F	pKT25 dgkE Fwd	acgcggcgggctgcagggtcgac TCTAGA GATG CGTGCGCTGCTGGTTGTGAA
LB109	R	pKT25 dgkE Rev	acggccgaattcttagttactta GGTACC CG AACGATCACACGCAGCGCAC
LB110	F	pUT18c dgkE Fwd	tggaacgccactgcaggtcgac TCTAGA GATG CGTGCGCTGCTGGTTGTGAA
LB111	R	pUT18c dgkE Rev	ttatatcgatgaattcgagctc GGTACC CG AACGATCACACGCAGCGCAC
LB112	F	pKNT25 & pUT18 *hrdB-trunc*$_{c.o.}$	gcttgcatgcctgcaggtcgac TCTAGA GATG CCGGCGGATGCGGTGAG
LB113	R	pKNT25 *hrdB-trunc*$_{c.o.}$	catggtcattgaattcgagctc GGTACC CG TTAATCCAGATAGTCACGCAGCACTTG
LB114	R	pUT18 *hrdB-trunc*$_{c.o.}$	cgctggcggctgaattcgagctc GGTACC CG TTAATCCAGATAGTCACGCAGCACTTG
LB115	F	pKT25 *hrdB-trunc*$_{c.o.}$	acgcggcgggctgcagggtcgac TCTAGA GATG CCGGCGGATGCGGTGAG

LB116	R	pKT25 *hrdB-trunc*$_{c.o.}$	acggccgaattcttagttactta GGTACC CG TTAATCCAGATAGTCACGCAGCACTTG
LB117	F	pUT18c *hrdB-trunc*$_{c.o.}$	tggaacgccactgcaggtcgac TCTAGA GATG CCGGCGGATGCGGTGAG
LB118	R	pUT18c *hrdB*$_{trunc\text{-}c.o.}$	ttatatcgatgaattcgagctc GGTACC CG TTAATCCAGATAGTCACGCAGCACTTG
LB119	F	pKNT25 & pUT18 *wblE*$_{c.o.}$	gcttgcatgcctgcaggtcgac TCTAGA *GATG* GACTGGCGTCATAATGCGGTGT
LB120	R	pKNT25 *wblE*$_{c.o.}$	catggtcattgaattcgagctc GGTACC *CG* CGCGCTCGCATTACGCG
LB121	R	pUT18 *wblE*$_{c.o.}$	cgctggcggctgaattcgagctc GGTACC CG CGCGCTCGCATTACGCG
LB122	F	pKT25 *wblE*$_{c.o.}$	acgcggcgggctgcagggtcgac TCTAGA GATG GACTGGCGTCATAATGCGGTGT
LB123	R	pKT25 *wblE*$_{c.o.}$	acggccgaattcttagttactta GGTACC *CG* CGCGCTCGCATTACGCG
LB124	F	pUT18c *wblE*$_{c.o.}$	tggaacgccactgcaggtcgac TCTAGA GATG GACTGGCGTCATAATGCGGTGT
LB125	R	pUT18c *wblE*$_{c.o.}$	ttatatcgatgaattcgagctc GGTACC CG CGCGCTCGCATTACGCG
LB126	R	*wblE* 24255CT-*trunc*	aaaaggggatgataagtttatcaagctt TCA CTCGTCCTCGCTGAGGCCA
LB127	F	*hrdB*$_{c.o.}$*-trunc,* EcoRI	ggatccgaattcgatgccggcggatgcggtgagcttc
LB128	R	*hrdB*$_{c.o.}$*-trunc,* HindIII	ggccgcaagcttttaatccagatagtcacgcagcacttg
LBx2.1F	F	*vnz_07310* (N-terminus or Full length); GTG to ATG	ggtcgac TCTAGA gatg ACGACCCGGCGCACC
LBx2.2F	F	*vnz_07310* N-terminus	ggtcgac TCTAGA gatg AAGCTGGAGCAGATCTGCGTC
LBx2.1R	R	*vnz_07310* C-terminus	ggtcgac GGTACC cg GACGCAGATCTGCTCCAGCTT
LBx2.2R	R	*vnz_07310* C-terminus or Full length	ggtcgac GGTACC cg CGCTCC CCCGGTGTGCACCTGGAA
LBx4.1F	F	*S. venezuelae clpX* BTH	ggtcgac TCTAGA g GTG GCACGCATCGGTGATGG
LBx4.1R	R	*S. venezuelae clpX* BTH	ggtcgac GGTACC cg CGCCGACTTCTCGTGCCTG
LBx5.1F	F	*S. venezuelae mqnC* BTH	ggtcgac TCTAGA g GTGACCGAGAAGGCCGAACTC
LBx5.1R	R	*S. venezuelae mqnC* BTH	ggtcgac GGTACC cg GTTCGCGTCGAGGAGCTTCAG
pSS-F	F	pSS170 and pIJ10257 MCS test primer	gccagtggtatttatgtcaacaccgc
pSS-R	R	pSS170 MCS test primer	cagctccatcagcaaaaggggat
pIJ-R	R	pIJ10257 MCS test primer	ccaacgtcatctcgttctccgctc
pCRISP-t	F	pCRISPomyces-2 HRT XbaI test primer	AGGCTAGTCCGTTATCAACTTGAAA
pCRISP-t	R	pCRISPomyces-2 HRT XbaI test primer	TCGCCACCTCTGACTTGAGCGTCGA
BAC2HF	F	Bacterial 2 Hybrid vector MCS test	tgttgtgtggaattgtgagcgga
HNA185	R	ReDirect *aac(3)IV* confirmation	gagctgcacatgaacccatt
HNA397	F	ReDirect *wblE* confirmation	gcccaaagtcctttcactcg
HNA398	R	ReDirect *wblE* confirmation	Ggcactgctccatgacgg

Table A.2. Commercially synthesised gene fragments.

Fragment	Features	Source	Sequence
C9S	partial *wblE (snt)*, C9S	IDT® gBlock™	CAGCCATGGACTGGCGTCACAACGCGGTTTCGCGTGAGGAAGACCCCGAGCTGTTCTTCCCCATCGGCAAC ACCGGTCCTGCGCTGCTGCAGATCGAGGAAGCCAAGGCCGTCTGTCGCCGCTGCCCCGTCATGGAGCAGTG CCTGCAGTGGGCGCTCGAGTCCGGCCAGGACTCCGGCGTCTGGGGTGGCCTCAGCGAGGACGAGCGCCGCG CGATGAAGCGCCGCGCCGCTCGCAACCGGGCGCGTAACGCCAGCGCCTGAaagcttgataaacttatc
C37S	partial *wblE (snt)*, C37S codon change	IDT® gBlock™	CAGCCATGGACTGGCGTCACAACGCGGTTTGTCGTGAGGAAGACCCCGAGCTGTTCTTCCCCATCGGCAAC ACCGGTCCTGCGCTGCTGCAGATCGAGGAAGCCAAGGCCGTCTCGCGCCGCTGCCCCGTCATGGAGCAGTG CCTGCAGTGGGCGCTCGAGTCCGGCCAGGACTCCGGCGTCTGGGGTGGCCTCAGCGAGGACGAGCGCCGCG CGATGAAGCGCCGCGCCGCTCGCAACCGGGCGCGTAACGCCAGCGCCTGAaagcttgataaacttatc
C40S	partial *wblE (snt)*, C40S codon change	IDT® gBlock™	CAGCCATGGACTGGCGTCACAACGCGGTTTGTCGTGAGGAAGACCCCGAGCTGTTCTTCCCCATCGGCAAC ACCGGTCCTGCGCTGCTGCAGATCGAGGAAGCCAAGGCCGTCTGTCGCCGCTCCCCCGTCATGGAGCAGTG CCTGCAGTGGGCGCTCGAGTCCGGCCAGGACTCCGGCGTCTGGGGTGGCCTCAGCGAGGACGAGCGCCGCG CGATGAAGCGCCGCGCCGCTCGCAACCGGGCGCGTAACGCCAGCGCCTGAaagcttgataaacttatc
C46S	partial *wblE* (*snt*), C46S codon change	IDT® gBlock™	CAGCCATGGACTGGCGTCACAACGCGGTTTGTCGTGAGGAAGACCCCGAGCTGTTCTTCCCCATCGGCAAC ACCGGTCCTGCGCTGCTGCAGATCGAGGAAGCCAAGGCCGTCTGTCGCCGCTGCCCCGTCATGGAGCAGTC CCTGCAGTGGGCGCTCGAGTCCGGCCAGGACTCCGGCGTCTGGGGTGGCCTCAGCGAGGACGAGCGCCGCG CGATGAAGCGCCGCGCCGCTCGCAACCGGGCGCGTAACGCCAGCGCCTGAaagcttgataaacttatc
D13A	partial *wblE* (*snt*), D13A codon change	Genewiz	CAGCCATGGACTGGCGTCACAACGCGGTTTGTCGTGAGGAAGCGCCCGAGCTGTTCTTCCCCATCGGCAAC ACCGGTCCTGCGCTGCTGCAGATCGAGGAAGCCAAGGCCGTCTGTCGCCGCTGCCCCGTCATGGAGCAGTG CCTGCAGTGGGCGCTCGAGTCCGGCCAGGACTCCGGCGTCTGGGGTGGCCTCAGCGAGGACGAGCGCCGCG CGATGAAGCGCCGCGCCGCTCGCAACCGGGCGCGTAACGCCAGCGCCTGAaagcttgataaacttatc
CFLAG	3xFLAG-tag sequence, codon-optimised for *Streptomyces*	IDT® Megamer™	CAACCGGGCGCGTAACGCCAGCGCCGACTACAAGGACCACGACGGCGACTACAAGGACCACGACATCGACT ACAAGGACGATGACGACAAGTGAaagcttgataaacttatcatccccttttgctgatggagctgcaca

Table A.3. Plasmid backbones and derivatives generated in this thesis. The first two rows of this table show how this table is laid out.

Plasmid Backbone	**Genotype and Features**	**Sources**
Derivative(s)		
pSS170	pMS82 derivative*, oriT*, ΦBT1 *attB-int,* Hyg^R	Dr S. Schlimpert, John Innes Centre, Norwich, UK
$pSS24255_{WT}$	*wblE*p, native *wblE* cds.	This work
$pSS24255_{SNT}$	*wblE*p, *wblE* with Cas9-silencing PAM mutation (*snt*),	This work
$pSS24255CF_{SNT}$	*wblE*p*, wblE* (SNT), C-terminal 3xFLAG-tag	This work
pSSVP5240	*S. ven wblE*p and *S. coelicolor wblE* cds	This work
$pSS24255C9S_{SNT}$	*wblE*p and *wblE* (SNT) C9S mutant cds	This work
$pSS24255C37S_{SNT}$	*wblE*p and *wblE* (SNT) C37S mutant cds	This work
$pSS24255C40S_{SNT}$	*wblE*p and *wblE* (SNT) C40S mutant cds	This work
$pSS24255C46S_{SNT}$	*wblE*p and *wblE* (SNT) C46S mutant cds	This work
pIJ10257	pMS82 derivative, *oriT*, ΦBT1 *attB-int*, *ermE*p*, Hyg^R	Hong *et al.*, 2005
$pIJ24255_{WT}$	Native *wblE* cds	This work
$pIJ24255_{SNT}$	Native *wblE* cds with Cas9-silencing PAM mutation (*snt*)	This work
pCRISPomyces-2	*oriT*, *rep-pSG5*(ts), *colE1*, *S. py cas9*, *sgRNA-tracrRNA* cassette, Apr^R	Cobb *et al.*, 2015
pCa24255KO	sgRNA targeting *vnz_24260*, *wblE* (vnz_24255) KO HRT	This work
pCa24255C40S	sgRNA targeting *vnz_24260*, *wblE* (vnz_24255) C40S HRT	This work
pCa24255NF	sgRNA targeting *vnz_24260*, *wblE* (vnz_24255) 3xNFLAG	This work
pCa24260KO	sgRNA targeting *vnz_24260, vnz_24260* KO HRT leaving 8 codons.	This work
pCi24255KO	sgRNA targeting *wblE, wblE* KO HRT	This work
pET28a(+)	KanR, N-terminal 6xHis-tag	Dubendorff & Studier, 1991
pET28a-NWblE	Codon optimised (NdeI-HindIII)	Genscript®
pET29b(+)	KanR, C-terminal 6xHis-tag	Dubendorff & Studier, 1991
pET29b-CWblE	Codon optimised *wblE* with C-terminal 6xHis-tag (NdeI-XhoI)	This work
pUZ8002	RK2 derivative with a mutation in *oriT*, Kan^R	Keiser *et al*., 2000
-	-	-
pKT25	KanR, o*ri*-p15A, 3' MCS in *cyaAT25*, *T17*p	Karimova *et al*., 1998 & 2000
pKT25-*wblE*	Codon optimised *wblE* cds (XbaI-KpnI)	This work
pKT25-*hrdB*	Codon optimised *hrdB4.2* cds (XbaI-KpnI)	This work

pKT25-*clpX*	Native *S.ven clpX* cds (XbaI-KpnI)	This work
pKT25-*mqnC*	Native *S.ven mqnC* cds (XbaI-KpnI)	This work
pKT25-*mtrA*	Codon optimised *S.ven mtrA* cds (XbaI-KpnI)	Dr. Neil Holmes, John Innes Centre, UK
pKT25-*scy*	Native *S.ven scy* cds (XbaI-KpnI)	Dr. Neil Holmes, John Innes Centre, UK
pKT25-*zip*	Codon optimised GCN4 bZip (positive control)	Euromedex™
pKNT25	KanR, p15A o*ri*, 5' MCS in *cyaAT25*, *T17*p	(Karimova et al., 1998 & 2000)
pKNT25-*wblE*	Codon optimised *wblE* cds (XbaI-KpnI)	This work
pKNT25-*hrdB*	Codon optimised *hrdB4.2* cds (XbaI-KpnI)	This work
pKNT25-*clpX*	Native *S.ven clpX* cds (XbaI-KpnI)	This work
pKNT25-*mqnC*	Native *S.ven mqnC* cds (XbaI-KpnI)	This work
pKNT25-*mtrA*	Codon optimised *S.ven mtrA* cds (XbaI-KpnI)	Dr. Neil Holmes, John Innes Centre, UK
pKNT25-*scy*	Native *S.ven scy* cds (XbaI-KpnI)	Dr. Neil Holmes, John Innes Centre, UK
pUT18	AmpR, *oriC*, 5' MCS in *cyaAT18*, *T17*p	(Karimova et al., 1998 & 2000)
pUT18-*wblE*	Codon optimised *wblE* cds (XbaI-KpnI)	This work
pUT18-*hrdB*	Codon optimised *hrdB4.2* cds (XbaI-KpnI)	This work
pUT18-*07310N*	Native *S.ven* vnz_*07310* N-terminus cds (XbaI-KpnI)	This work
pUT18-*07310C*	Native *S.ven* vnz_*07310* C-terminus cds (XbaI-KpnI)	This work
pUT18-*scy*	Native *S.ven scy* cds (XbaI-KpnI)	Dr. Neil Holmes, John Innes Centre, UK
pUT18c	AmpR, *oriC*, 3' MCS in *cyaAT18*, *T17*p	(Karimova et al., 1998 & 2000)
pUT18c-*wblE*	Codon optimised *wblE* cds (XbaI-KpnI)	This work
pUT18c-*hrdB*	Codon optimised *hrdB4.2* cds (XbaI-KpnI)	This work
pUT18c-*mqnC*	Native *S.ven mqnC* cds (XbaI-KpnI)	This work
pUT18c-*07310N*	Native *S.ven* vnz_*07310* N-terminus (aa 1-254) cds (XbaI-KpnI)	This work
pUT18c-*07310C*	Native *S.ven* vnz_*07310* C-terminus (aa 247-448) cds (XbaI-KpnI)	This work
pUT18c-*scy*	Native *S.ven scy* cds (XbaI-KpnI)	Dr. Neil Holmes, John Innes Centre, UK
pUT18c-*zip*	Codon optimised GCN4 bZip (positive control)	Euromedex™

Table A.4. (a) Oligonucleotides used for *wblE* promoter SPR with the ssDNA ReDCaT-linker region in lower case

Oligo.	Sequence (5'-3')	Probe (/16)
wblEpFor_1	TAGGTGGACGACGAGGAGCGGGCGACCGGCCCGGCGCCCT	*wblE*p-f1
wblEpRev_1	AGGGCGCCGGGCCGGTCGCCCGCTCCTCGTCGTCCACCTAcctaccctacgtcctcctgc	
wblEpFor_2	GTGAGTGGAAGGGCCCAAAGTCCTTTCACTCGAACGTTTA	*wblE*p-f2
wblEpRev_2	TAAACGTTCGAGTGAAAGGACTTTGGGCCCTTCCACTCACcctaccctacgtcctcctgc	
wblEpFor_3	TCACTCGAACGTTTAGGCGCGCATCCACCCCTTAGAAGTA	*wblE*p-f3
wblEpRev_3	TACTTCTAAGGGGTGGATGCGCGCCTAAACGTTCGAGTGAcctaccctacgtcctcctgc	
wblEpFor_4	CACCCCTTAGAAGTACGGCTGTGACCTAGCCGACACCGAG	*wblE*p-f4
wblEpRev_4	CTCGGTGTCGGCTAGGTCACAGCCGTACTTCTAAGGGGTGcctaccctacgtcctcctgc	
wblEpFor_5	CTAGCCGACACCGAGGAATCAAAAAAAACTTTCCGGAAGG	*wblE*p-f5
wblEpRev_5	CCTTCCGGAAAGTTTTTTTTGATTCCTCGGTGTCGGCTAGcctaccctacgtcctcctgc	
wblEpFor_6	AAACTTTCCGGAAGGGGTTGTATCCGTTGCTGGGGTTTGG	*wblE*p-f6
wblEpRev_6	CCAAACCCCAGCAACGGATACAACCCCTTCCGGAAAGTTTcctaccctacgtcctcctgc	
wblEpFor_7	GTTGCTGGGGTTTGGGAGTCTCTTCTTGGCGATCGGGACG	*wblE*p-f7
wblEpRev_7	CGTCCCGATCGCCAAGAAGAGACTCCCAAACCCCAGCAACcctaccctacgtcctcctgc	
wblEpFor_8	TTGGCGATCGGGACGGCCCGCAACACCGGCCTCCACTGAG	*wblE*p-f8
wblEpRev_8	CTCAGTGGAGGCCGGTGTTGCGGGCCGTCCCGATCGCCAAcctaccctacgtcctcctgc	
wblEpFor_9	CCGGCCTCCACTGAGAGCCAGAACCCCTCCTCAGTCTTAG	*wblE*p-f9
wblEpRev_9	CTAAGACTGAGGAGGGGTTCTGGCTCTCAGTGGAGGCCGGcctaccctacgtcctcctgc	
wblEpFor_10	CCTCCTCAGTCTTAGGACCACACCAGTTGATCTGGCAGTC	*wblE*p-f10
wblEpRev_10	GACTGCCAGATCAACTGGTGTGGTCCTAAGACTGAGGAGGcctaccctacgtcctcctgc	
wblEpFor_11	GTTGATCTGGCAGTCGGCCCTTCCCTTGCGGGGGGATTCG	*wblE*p-f11
wblEpRev_11	CGAATCCCCCCGCAAGGGAAGGGCCGACTGCCAGATCAACcctaccctacgtcctcctgc	
wblEpFor_12	TTGCGGGGGGATTCGTGAAAGCGTTCACATTCACAAGCAA	*wblE*p-f12
wblEpRev_12	TTGCTTGTGAATGTGAACGCTTTCACGAATCCCCCCGCAAcctaccctacgtcctcctgc	
wblEpFor_13	CACATTCACAAGCAACCAGCTTGTAACACCCTAGAGAGGT	*wblE*p-f13
wblEpRev_13	ACCTCTCTAGGGTGTTACAAGCTGGTTGCTTGTGAATGTGcctaccctacgtcctcctgc	
wblEpFor_14	ACACCCTAGAGAGGTAGCAGCCATGGACTGGCGTCACAAC	*wblE*p-f14
wblEpRev_14	GTTGTGACGCCAGTCCATGGCTGCTACCTCTCTAGGGTGTcctaccctacgtcctcctgc	
wblEpFor_15	GACTGGCGTCACAACGCCGTTTGTCGTGAGGAAGACCCCG	*wblE*p-f15
wblEpRev_15	CGGGGTCTTCCTCACGACAAACGGCGTTGTGACGCCAGTCcctaccctacgtcctcctgc	
wblEpFor_16	GTGAGGAAGACCCCGAGCTGTTCTT	*wblE*p-f16
wblEpRev_16	AAGAACAGCTCGGGGTCTTCCTCACcctaccctacgtcctcctgc	

(b) Oligonucleotides used for *dnaA* promoter SPR and ssDNA ReDCaT-linker region in lower case.

Oligo.	Sequence	Probe (/27)
dnaApFor_1	TAGGTGGACGACGAGGAGCGGGCGACCGGCCCGGCGCCCT	*dnaA*p-f1
dnaApRev_1	AGGGCGCCGGGCCGGTCGCCCGCTCCTCGTCGTCCACCTAcctaccctacgtcctcctgc	
dnaApFor_2	CCGGCCCGGCGCCCTCGGCGTACCGCGGTTGCGAAGTCCT	*dnaA*p-f2
dnaApRev_2	AGGACTTCGCAACCGCGGTACGCCGAGGGCGCCGGGCCGGcctaccctacgtcctcctgc	
dnaApFor_3	CGGTTGCGAAGTCCTCGCGCCGCCTCAGCCGATTGTCGGT	*dnaA*p-f3
dnaApRev_3	ACCGACAATCGGCTGAGGCGGCGCGAGGACTTCGCAACCGcctaccctacgtcctcctgc	
dnaApFor_4	CAGCCGATTGTCGGTAGGCAGCACGTCATGACCCGTTTAG	*dnaA*p-f4
dnaApRev_4	CTAAACGGGTCATGACGTGCTGCCTACCGACAATCGGCTGcctaccctacgtcctcctgc	
dnaApFor_5	TCATGACCCGTTTAGCGGATCAGGCGGACAGCTCAGAGCG	*dnaA*p-f5
dnaApRev_5	CGCTCTGAGCTGTCCGCCTGATCCGCTAAACGGGTCATGAcctaccctacgtcctcctgc	
dnaApFor_6	GGACAGCTCAGAGCGACCCTTGGAACGACGGTTCGCAAGG	*dnaA*p-f6
dnaApRev_6	CCTTGCGAACCGTCGTTCCAAGGGTCGCTCTGAGCTGTCCcctaccctacgtcctcctgc	
dnaApFor_7	CGACGGTTCGCAAGGATGGCTCGGCCGGCACGCGTACGCA	*dnaA*p-f7
dnaApRev_7	TGCGTACGCGTGCCGGCCGAGCCATCCTTGCGAACCGTCGcctaccctacgtcctcctgc	
dnaApFor_8	CGGCACGCGTACGCATCCGCAGGCGGAAGCCGTGGGTCTT	*dnaA*p-f8
dnaApRev_8	AAGACCCACGGCTTCCGCCTGCGGATGCGTACGCGTGCCGcctaccctacgtcctcctgc	
dnaApFor_9	GAAGCCGTGGGTCTTGGCGCGACGACGGTTGTTCGGCTGG	*dnaA*p-f9

dnaApRev_9	CCAGCCGAACAACCGTCGTCGCGCCAAGACCCACGGCTTCcctaccctacgtcctcctgc	
dnaApFor_10 dnaApRev_10	CGGTTGTTCGGCTGGAAGGTGCGCTTGCTCACTCGGGGGC GCCCCCGAGTGAGCAAGCGCACCTTCCAGCCGAACAACCGcctaccctacgtcctcctgc	*dnaA*p-f10
dnaApFor_11 dnaApRev_11	TGCTCACTCGGGGGCTCCAGAAATGATTCGTAGATGGCGG CCGCCATCTACGAATCATTTCTGGAGCCCCCGAGTGAGCAcctaccctacgtcctcctgc	*dnaA*p-f11
dnaApFor_12 dnaApRev_12	ATTCGTAGATGGCGGGACATCGCCTGGCTGTCACCGTGCG CGCACGGTGACAGCCAGGCGATGTCCCGCCATCTACGAATcctaccctacgtcctcctgc	*dnaA*p-f12
dnaApFor_13 dnaApRev_13	GGCTGTCACCGTGCGCCCACGAGTAGCTCGCAATACGCCC GGGCGTATTGCGAGCTACTCGTGGGCGCACGGTGACAGCCcctaccctacgtcctcctgc	*dnaA*p-f13
dnaApFor_14 dnaApRev_14	GCTCGCAATACGCCCGAGTGCACCGCTTCACGATCACTGA TCAGTGATCGTGAAGCGGTGCACTCGGGCGTATTGCGAGCcctaccctacgtcctcctgc	*dnaA*p-f14
dnaApFor_15 dnaApRev_15	CTTCACGATCACTGACCGTGATCTTTGCCCATCGGAGGCA TGCCTCCGATGGGCAAAGATCACGGTCAGTGATCGTGAAGcctaccctacgtcctcctgc	*dnaA*p-f15
dnaApFor_16 dnaApRev_16	TGCCCATCGGAGGCAGGCGGCAGCAGCCATCGACAACTCG CGAGTTGTCGATGGCTGCTGCCGCCTGCCTCCGATGGGCAcctaccctacgtcctcctgc	*dnaA*p-f16
dnaApFor_17 dnaApRev_17	GCCATCGACAACTCGACCTGGTTACGGTACGCGCGGCTAC GTAGCCGCGCGTACCGTAACCAGGTCGAGTTGTCGATGGCcctaccctacgtcctcctgc	*dnaA*p-f17
dnaApFor_18 dnaApRev_18	GGTACGCGCGGCTACGCCATCCGGTCAAACCGACCTGTCG CGACAGGTCGGTTTGACCGGATGGCGTAGCCGCGCGTACCcctaccctacgtcctcctgc	*dnaA*p-f18
dnaApFor_19 dnaApRev_19	CAAACCGACCTGTCGCCACCCCCCATTGTGCACAGGCTGT ACAGCCTGTGCACAATGGGGGGTGGCGACAGGTCGGTTTGcctaccctacgtcctcctgc	*dnaA*p-f19
dnaApFor_20 dnaApRev_20	TTGTGCACAGGCTGTGGACAACAACTTGAACCACGTCATC GATGACGTGGTTCAAGTTGTTGTCCACAGCCTGTGCACAAcctaccctacgtcctcctgc	*dnaA*p-f20
dnaApFor_21 dnaApRev_21	TTGAACCACGTCATCCGGCGCGACTACCGTGGATGGACTC GAGTCCATCCACGGTAGTCGCGCCGGATGACGTGGTTCAAcctaccctacgtcctcctgc	*dnaA*p-f21
dnaApFor_22 dnaApRev_22	ACCGTGGATGGACTCCACAATCTTTTCCGTTCTGTCCTTA TAAGGACAGAACGGAAAAGATTGTGGAGTCCATCCACGGTcctaccctacgtcctcctgc	*dnaA*p-f22
dnaApFor_23 dnaApRev_23	TCCGTTCTGTCCTTACCTGTCCTCACGGGTTCTGTCCTCA TGAGGACAGAACCCGTGAGGACAGGTAAGGACAGAACGGAcctaccctacgtcctcctgc	*dnaA*p-f23
dnaApFor_24 dnaApRev_24	CGGGTTCTGTCCTCACGGACATCGACCCACCGTCCCCGAG CTCGGGGACGGTGGGTCGATGTCCGTGAGGACAGAACCCGcctaccctacgtcctcctgc	*dnaA*p-f24
dnaApFor_25 dnaApRev_25	CCCACCGTCCCCGAGAACCACACCATCAGGGGACCTGCGA TCGCAGGTCCCCTGATGGTGTGGTTCTCGGGGACGGTGGGcctaccctacgtcctcctgc	*dnaA*p-f25
dnaApFor_26 dnaApRev_26	TCAGGGGACCTGCGAGAAAGCGTGCCCTGTGGCTGACGTT AACGTCAGCCACAGGGCACGCTTTCTCGCAGGTCCCCTGAcctaccctacgtcctcctgc	*dnaA*p-f26
dnaApFor_27 dnaApRev_27	CCTGTGGCTGACGTTCCTGCTGATCTTGCCGCAG CTGCGGCAAGATCAGCAGGAACGTCAGCCACAGGcctaccctacgtcctcctgc	*dnaA*p-f27

Table A.5. Bacterial species and strains, and derivatives generated in this thesis.

Bacterial strain	**Genotype and Features**	**Source / Reference**
Derivative strain		
S. venezuelae NRRL B-65442	Wild-type strain	Gomez-Escribano *et al.,* 2021
24255WT	NRRL B-65442 :: ΦBT1 *attB* pSS24255$_{WT}$, Hyg^{R}	This work
24255SNT	NRRL B-65442 :: ΦBT1 *attB* pSS24255$_{SNT}$, Hyg^{R}	
O24255WT	NRRL B-65442 :: ΦBT1 *attB* pIJ24255$_{WT}$, Hyg^{R}	
O24255SNT	NRRL B-65442 :: ΦBT1 *attB* pIJ24255$_{SNT}$, Hyg^{R}	
24255CF	NRRL B-65442 :: ΦBT1 *attB* pSS24255CF$_{SNT}$, 3xFLAG-tag (CT), Hyg^{R}	
VP5240	NRRL B-65442 :: ΦBT1 *attB* pSSvp5240, Hyg^{R}	
Δ24255SNT	NRRL B-65442 Δ*wblE* :: ΦBT1 *attB* pSS24255$_{SNT}$, Hyg^{R}	
ΔO24255SNT	NRRL B-65442 Δ*wblE* :: ΦBT1 *attB* pIJ24255$_{SNT}$, Hyg^{R}	
Δ24255CF	NRRL B-65442 Δ*wblE* :: ΦBT1 *attB* pSS24255CF$_{SNT}$, Hyg^{R}	
Δ24255D13A	NRRL B-65442 Δ*wblE* :: ΦBT1 *attB* pSS24255D13A$_{SNT}$, Hyg^{R}	
ΔVP5240	NRRL B-65442 Δ*wblE* :: ΦBT1 *attB* pSSvp5240, Hyg^{R}	
E. coli NEB5α	*F-, fhuA2*Δ(*argF-lacZ*)U169 *phoA glnV44* Φ80Δ(*lacZ*)M15 *gyrA96 recA1 relA1 endA1 thi-1 hsdR17*	New England Biolabs®
All BAC2H vectors pCi derivative vectors		
E. coli Top10	*F-*, *mcrA* Δ(*mrr-hsd*RMS-*mcr*BC) Φ80*lac*ZΔM15 Δ*lacX74 recA1 araD139* Δ(*ara leu*) 7697 *galU galK rpsL* (Str^{R}) *endA1 nupG*	Laboratory stock
pET28a vectors pCa derivative Vectors		
E. coli ET12567	*dam^{-} dcm^{-} hsdS^{-}*, Cap^{R}	MacNeil *et al*., 1992; Keiser *et al*., 2000
-pCa24255KO	Carrying pCa24255KO plasmid	This work
-pCa24260KO	Carrying pCa24260KO plasmid	" "
-pCi24255KO	Carrying pCi24255KO plasmid	" "
-pIJ24255$_{WT}$	Carrying pIJ24255 - native *wblE* cds	" "
-pIJ24255$_{SNT}$	Carrying pIJ24255 - *wblE* (*snt*) cds	" "
-pSS24255$_{WT}$	Carrying pSS24255 - native *wblE* cds	" "

-pSS24255$_{SNT}$	Carrying pSS24255 - *wblE* (*snt*) cds	“ ”
-pSS24255C9S	Carrying pSS24255C9S - *wblE* (*snt*) C9S cds	“ ”
-pSS24255C37S	Carrying pSS24255C9S - *wblE* (*snt*) C37S cds	“ ”
-pSS24255C40S	Carrying pSS24255C9S - *wblE* (*snt*) C40S cds	“ ”
-pSS24255C46S	Carrying pSS24255C9S - *wblE* (*snt*) C46S cds	“ ”
-pSS24255D13A	Carrying pSS24255D13A - *wblE* (*snt*) D13A cds	“ ”
-pSSVP5240	Carrying pSSVP5240 – *wblE*p (*S.ven*) / *wblE* cds (*S.coe*) (N6R; N82Q)	“ ”
E. coli BL21 λDE3	*F-, fhuA2 [lon] ompT gal (λ DE3) [dcm] ΔhsdS λ DE3 = λ sBamHIo ΔEcoRI-B int::(lacI::PlacUV5::T7 gene1) i21 Δnin5*	New England Biolabs®
BL21-pET28a-NWblE	codon optimised *wblE*-6xHis(NT), cleavable	This work
BL21-pET29b-CWblE	codon optimised *wblE*-6xHis(CT)	“ ”
E. coli BTH101	F-, *cya-99*, *araD139*, *galE15*, *galK16*, *rpsL1* (Str^{R}), *hsdR2*, *mcrA1*, *mcrB1*	Euromedex™, Karimova *et al.,* 1998; 2000; 2005
BTH1(-)	pKT25- & pUT18c-	This work
BTH2(+)	pKT25-*zip* & pUT18c-*zip*	“ ”
BTHF1	pUT18-*wblE* & pKT25-	“ ”
BTHF2	pUT18c-*wblE* & pKT25-	“ ”
BTHF3	pKNT25-*wblE* & pUT18-	“ ”
BTHF4	pKT25-*wblE* & pUT18-	“ ”
BTHF9	pUT18-*hrdB* & pKT25-	“ ”
BTHF10	pUT18c-*hrdB* & pKT25-	“ ”
BTHF11	pKNT25-*hrdB* & pUT18-	“ ”
BTHF12	pKT25-hrdB & pUT18-	“ ”
BTHLB1	pUT18-*wblE* & pKNT25-*wblE*	“ ”
BTHLB2	pUT18-*wblE* & pKT25-*wblE*	“ ”
BTHLB3	pUT18-*wblE* & pKNT25-*hrdB*	“ ”
BTHLB4	pUT18-*wblE* & pKT25-*hrdB*	“ ”
BTHLB7	pUT18c-*wblE* & pKNT25-*wblE*	“ ”
BTHLB8	pUT18c-*wblE* & pKT25-*wblE*	“ ”
BTHLB9	pUT18c-*wblE* & pKNT25-*hrdB*	“ ”
BTHLB10	pUT18c-*wblE* & pKT25-*hrdB*	“ ”

BTHLB15	pKNT25-*wblE* & pUT18-*hrdB*	“ ”
BTHLB16	pKNT25-*wblE* & pUT18c-*hrdB*	“ ”
BTHLB21	pKT25-*wblE* & pUT18-*hrdB*	“ ”
BTHLB22	pKT25-*wblE* & pUT18c-*hrdB*	“ ”
BTHA1F	pKT25-*mtrA* & pUT18-	“ ”
BTHA2F	pKNT25-*mtrA* & pUT18-	“ ”
BTHA3F	pUT18-*mtrA* & pKT25-	“ ”
BTHA4F	pUT18c-*mtrA* & pKT25-	“ ”
BTHA1	pKNT25-*mtrA* & pUT18-*wblE*	“ ”
BTHA2	pKNT25-*mtrA* & pUT18c-*wblE*	“ ”
BTHA3	pKT25-*mtrA* & pUT18-*wblE*	“ ”
BTHA4	pKT25-*mtrA* & pUT18c-*wblE*	“ ”
BTHC1F	pKT25-*mqnC* & pUT18-	“ ”
BTHC2F	pKNT25-*mqnC* & pUT18-	“ ”
BTHC4F	pUT18c-*mqnC* & pKT25-	“ ”
BTHC1	pKNT25-*mqnC* & pUT18-wblE	“ ”
BTHC2	pKNT25-*mqnC* & pUT18c-wblE	“ ”
BTHC3	pKT25-*mqnC* & pUT18-wblE	“ ”
BTHC4	pKT25-*mqnC* & pUT18c-wblE	“ ”
BTHC7	pUT18c-*mqnC* & pKNT25-*wblE*	“ ”
BTHC8	pUT18c-*mqnC* & pKT25-*wblE*	“ ”
BTHX1F	pKT25-*clpX* & pUT18-	“ ”
BTHX2F	pKNT25-*clpX* & pUT18-	“ ”
BTHX3F	pUT18-*clpX* & pKT25-	“ ”
BTHX4F	pUT18c-*clpX* & pKT25-	“ ”
BTHX1	pKNT25-*clpX* & pUT18-*wblE*	“ ”
BTHX2	pKNT25-*clpX* & pUT18c-*wblE*	“ ”
BTHX3	pKT25-*clpX* & pUT18-*wblE*	“ ”
BTHX4	pKT25-*clpX* & pUT18c-*wblE*	“ ”
BTHHN5	pUT18-*07310N &* pKNT25-*wblE*	“ ”
BTHHN6	pUT18-*07310N* & pKT25-*wblE*	“ ”

BTHHN7	pUT18c-*07310N* & pKNT25-*wblE*	“ ”
BTHHN8	pUT18c-*07310N* & pKT25-*wblE*	“ ”
BTHHC5	pUT18-*07310C* & pKNT25-*wblE*	“ ”
BTHHC6	pUT18-*07310C* & pKT25-*wblE*	“ ”
BTHHC7	pUT18c-*07310C* & pKNT25-*wblE*	“ ”
BTHHC8	pUT18c-*07310C* & pKT25-*wblE*	“ ”
BTHS1+	pKT25-*scy* & pUT18-*scy*	“ ”
BTHS2+	pKT25-*scy* & pUT18c-*scy*	“ ”
BTHS1	pKNT25-*scy* & pUT18-*wblE*	“ ”
BTHS2	pKNT25-*scy* & pUT18c-*wblE*	“ ”
BTHS3	pKT25-*scy* & pUT18-*wblE*	“ ”
BTHS4	pKT25-*scy* & pUT18c-*wblE*	“ ”
BTHS5	pUT18-*scy* & pKNT25-*wblE*	“ ”
BTHS6	pUT18-*scy* & pKT25-*wblE*	“ ”
BTHS7	pUT18c-*scy* & pKNT25-*wblE*	“ ”
BTHS8	pUT18c-*scy* & pKT25-*wblE*	“ ”

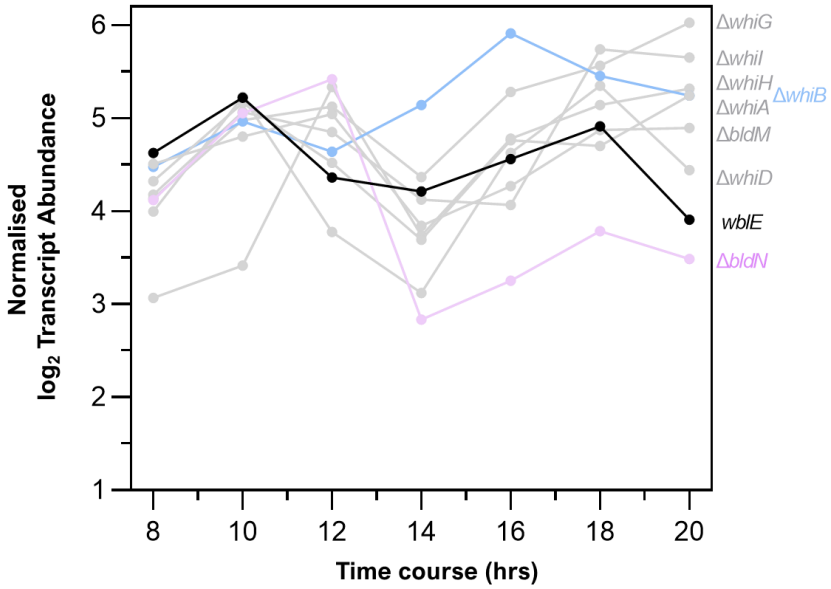

Figure A.1 The *wblE* transcript expression profile in wild-type *S. venezuelae* (black), plotted against *wblE* expression profiles in the Δ*bldM,* Δ*whiA,* Δ*whiD,* Δ*whiG,* Δ*whiH,* Δ*whiI S. venezuelae* developmental mutants (all grey). The expression profiles for the Δ*bldN* (lilac) and Δ*whiB* (blue) mutants described in Chapter 5.6 are highlighted. Log_2 transcript abundances were normalized to the median of the data. Endpoint measurements are labelled with the associated mutant.

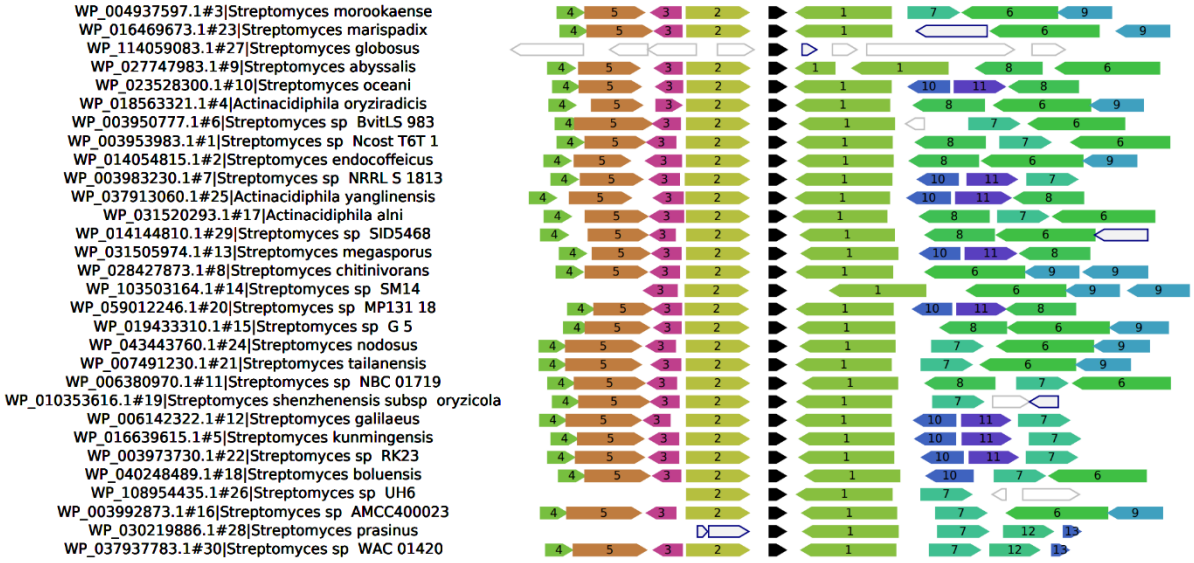

no.	*Streptomyces* spp.	*Mycobacterium* spp.	*Corynebacterium* spp.	*Bifidobacterium* spp.
1.	PAS-domain histidine kinase	Hypothetical protein	Hypothetical Protein	TagU-family protein
2.	Diacylglycerol kinase	PAS-domain histidine kinase	Anti-σ^H (RshA)	PAS-domain histidine kinase
3.	Anti-σ^H (UshX)	Diacylglycerol kinase	Hypothetical (β-propellor)	FtsK/SpoIIIE domain protein
4.	Hypothetical protein	Putative lipoyl carrier protein	ECF Sigma Factor (σ^H)	Hemolysin III family protein
5.	ECF sigma factor (σ^H)	Isochorismate synthase (MenF)	DEAD-box helicase	Elongation Factor GreA
6.	GlcN-6-P deaminase (NagB)	Anti-σ^H (RshA)	DUF3107 protein	FKBP-type cochaperone
7.	Putative sugar isomerase	GNAT *N*-acetyltransferase	SOS-associated peptidase	WhiB-like (WhiB)
8.	GH3 family protein (DasD)	ECF Sigma Factor (σ^H)	Cys-tRNA(Pro) deacylase	Family 2 Glycosyltransferase
9.	TetR family regulator	Hypothetical protein	3-Phosphoshikimate 1-CVT	Serine hydrolase
10.	SDR family oxidoreductase	Putative acid phosphatase	DUF4288 protein	DUF5719 protein

Figure A.2. WebFlaGs analysis for the *wblE* (*whiB1*) genetic neighbourhood in *Streptomyces*, *Mycobacterium*, *Corynebacterium*, and *Bifidobacterium* spp. The *Streptomyces* gene arrangement over 30 species is shown, and a comparison of the top 10 hits is shown below in the table, with homologous or functionally related proteins conserved across genera highlighted in the same colour. Details for WebFlaGs query submission and BLASTp parameters can be found in Chapter 2.32.3.

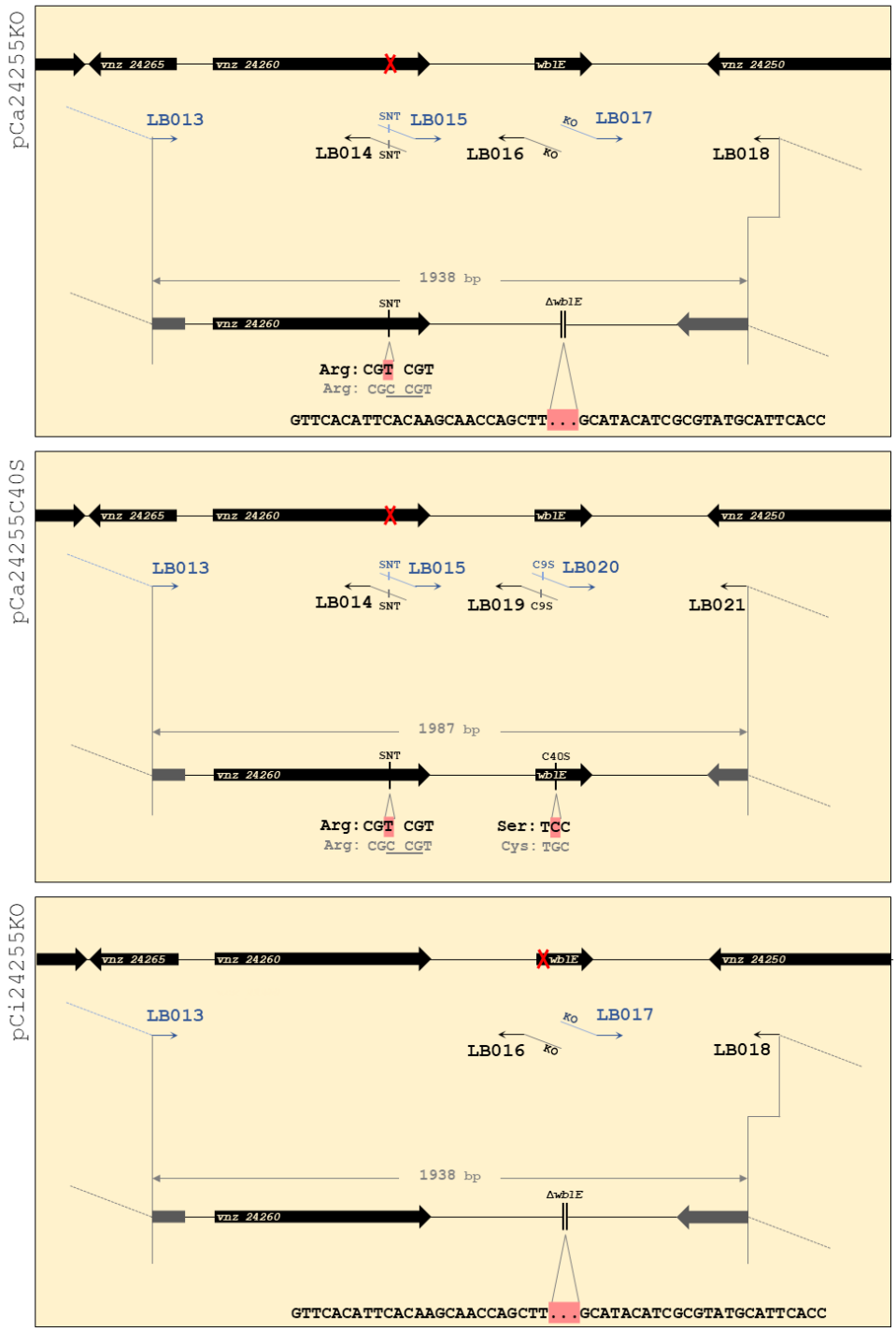

Figure A.3. Schematics for the PCR amplification and Gibson assembly of homologous repair templates. Arrows represent primers with forward primers in red and reverse primers in black. Diagonal extensions represent complementary overhangs; the longer, external (dashed) lines represent regions with complementarity to the XbaI-cut pCRISPomyces-2 backbone. Double line breaks in pCa24255KO and pCi24255KO schematics represent the boundaries of the Δ*wblE* sequence, specified by LB016-LB017 and shown in more detail beneath KO HRT constructs. Single line breaks represent single nucleotide changes and are labelled SNT (Cas9-silencing) and C9S (Cysteine mutation) with respect to their mutations. Red crosses within genes represent the active PAM-site, targeted by the sgRNAs (chapter 4).